

厚生労働科学研究費補助金

難治性疾患政策研究事業

網膜脈絡膜・視神経萎縮症に関する調査研究

令和6年度 総括・分担研究報告書

研究代表者 近藤 峰生

令和7年 2025年 3月

目 次

I. 総括研究報告

- 網膜脈絡膜・視神経萎縮症に関する調査研究に関する調査研究 ----- 1
近藤 峰生

II. 分担研究報告

1. 萎縮型加齢黄斑変性に関する研究 ----- 8
辻川 明孝
(資料1) パキコロイド型と従来型の地図状萎縮 (GA) の特徴と進行 -----11
2. 網膜色素変性に関する研究 ----- 20
池田 康博
(資料2) 網膜色素変性症および関連疾患の日本人患者2325人の遺伝的所見 ----- 25
(資料3) 同心円状周辺視野欠損患者における装着型暗視装置の有効性 ----- 33
3. 黄斑ジストロフィに関する研究 ----- 39
角田 和繁
(資料4) 日本人IRD患者におけるRPGRIPI1変異と杆体一色覚 ----- 43
(資料5) 日本におけるスタルガルト病の遺伝子バリエーションと臨床像 ----- 55
4. 近視性脈絡膜萎縮に関する研究 ----- 63
大野 京子
(資料6) 近視性黄斑部新生血管の診療ガイドライン ----- 66
(資料7) 強度近視の後方強膜における渦状コラーゲン線維の配列 ----- 77
5. 家族性滲出性硝子体網膜症に関する研究 ----- 90
近藤 寛之
(資料8) 血管造影によるFEVRの牽引性網膜剥離の手術結果を予測 ----- 93
(資料9) AD遺伝が確認された軽症FEVRの血管造影特性 ----- 101
6. 特発性傍中心窩毛細血管拡張症に関する研究 ----- 108
飯田 知弘
7. 杆体一色覚に関する研究 ----- 111
上野 真治
(資料10) 杆体一色覚の診断基準および全国調査票 ----- 114
(資料11) 日本における杆体一色覚の遺伝学的および臨床的特性 ----- 117
8. 全国視覚障害認定の実態疫学調査に関する研究 ----- 126
森實 祐基
9. 難治性視神経症に関する研究 ----- 128
中村 誠
(資料13) レーベル遺伝性視神経症の疫学調査 (学会発表スライド) ----- 131
(資料14) LHON「Plus」とm.14487 T>C変異が片側性ジストニアの原因 ----- 156
10. 自己免疫網膜症に関する研究 ----- 163
園田 康平
11. 日本における遺伝性網膜ジストロフィに対する遺伝学的検査および遺伝子治療の運用体制構築に関する研究 ----- 166

西口 康二	
(資料15) Specification of Variant Interpretation Guidelines for Inherited Retinal Dystrophy in Japan -----	170
(資料16) IRDの原因遺伝子のバリエーションリスト-----	181
III. 研究成果の刊行に関する一覧表 -----	198

厚生労働科学研究費補助金（難治性疾患政策研究事業）
総括研究報告書

網膜脈絡膜・視神経萎縮症に関する調査研究

研究代表者

三重大学大学・医学系研究科・教授 近藤 峰生

研究要旨

各疾患あるいはプロジェクト毎に 11 のグループ(G)を作り、各グループが目的と進捗状況に沿って研究を進めた。G1 の萎縮型加齢黄斑変性では、日本と海外の地図状萎縮の特徴の違いを明らかにした。G2 の網膜色素変性は、10 年ぶりに診療ガイドラインの改訂を開始した。G3 の黄斑ジストロフィは、希少なタイプの実態調査を行なった。G4 の近視性網膜脈絡膜萎縮は、後部ぶどう腫を伴う患者の遺伝子を解析した。G5 の家族性滲出性硝子体網膜症は、軽症患者の広角血管造影の特性を明らかにした。G6 の特発性傍中心窩毛細血管拡張症は、鑑別診断に重要な疾患群を示した。G7 の杆体一色覚は、診断基準を作成して全国患者数調査を開始した。G8 の視覚障害の実態疫学調査では、今後必要な追加情報が話し合われた。G9 の難治性視神経症では、データベースにより得られた LHON の患者の実態調査をまとめた。G10 の自己免疫網膜症では、全国 90 施設に送付したアンケート調査の結果をまとめた。G11 では、日本における遺伝性網膜ジストロフィの遺伝学的検査解釈のガイドラインを作成し、遺伝子治療の報告会を開催した。全てのグループが関連学会や関連研究班（AMED など）と連携を進めるとともに、医療従事者、国民、患者やその家族へ情報の提供を積極的に行い、本研究班独自の HP も作成された (<https://rcona.jp/>)。

研究分担者

東京女子医科大学・医学部・教授 飯田 知弘
宮崎大学・医学部・教授 池田 康博
弘前大学・医学研究科・教授 上野 真治
東京医科歯科大学・医歯学総合研究科・教授 大野 京子
琉球大学・医学研究科・教授 古泉 英貴
産業医科大学・医学部・教授 近藤 寛之
鹿児島大学・医歯学総合研究科・教授 坂本 泰二
九州大学・医学研究院・教授 園田 康平
京都大学・医学研究科・教授 辻川 明孝
国立病院機構東京医療センター・視覚研究部・部長 角田 和繁
神戸大学・医学研究科・教授 中村 誠
名古屋大学・医学系研究科・教授 西口 康二
岡山大学・医歯薬学総合研究科・教授 森實 祐基

A. 研究目的

網膜脈絡膜・視神経萎縮症は、眼科で最も難病患者数が多い領域である。これまで我々は、各疾患あるいはプロジェクト毎に11のグループに分かれ、それぞれのグループの目的と進捗状況に沿って調査研究を推進してきた。特に今回は、以下の3つの項目を重要な目的とする。

(1) 杆体一色覚(G7)と自己免疫網膜症(G10)という新たな難病候補疾患に関しては、専門家で協議を行なった後で、診断ガイドラインを作成し、全国にアンケートを送付して患者数調査を行い、難病に相当すると判断された場合には指定難病に申請手続きを行う。

(2) 診療ガイドラインの見直しが必要な網膜色素変性(G2)では、Minds形式に従ってガイドラインの改訂を進める。また遺伝性網膜ジストロフィに対する遺伝学的検査においては国際的なACMGガイドラインのみでは不十分な部分があるため、日本における遺伝性網膜ジストロフィの実情にあった独自のガイドラインを作成し、同時にバリアントリストを更新することで、遺伝子検査の質の向上と均てん化を推進する。

(3) 関連学会や関連研究班(AMEDなど)、患者会(JRPSなど)との連携を推進し、医療従事者、国民、患者やその家族へ正しい疾患情報の提供を推進する。これらにより、「網膜脈絡膜・視神経萎縮症」の難病患者に対する医療の質向上に役立てる。また、令和6年度に本研究班独自のホームページを立ち上げ、研究成果もHP上に公表する。

B. 研究方法

研究方法については、G1-G11のグループ毎

に異なるため、それぞれの分担研究報告書内の研究方法に記載した。

(倫理面への配慮)

今回の調査研究に関しては、患者の個人情報に含まれなかった。しかし倫理面には十分配慮して行った。

C. 研究結果

(各グループ毎に結果のサマリーを記載)

グループ1(G1)：萎縮型加齢黄斑変性

萎縮型加齢黄斑変性にみられる境界明瞭な萎縮病巣は、地図状萎縮(geographic atrophy: GA)と呼ばれる。今回G1において、日本人のGA患者群を詳細に検討した結果、日本人におけるGAのいくつかの特徴は白人集団におけるGAの特徴とは異なっており、これは集団の中にパキコロイドによるGAが含まれていることに起因していることを明らかにし、この結果を英文誌に発表した(Sato et al. Ophthalmol Sci. 2024)。

グループ2(G2)：網膜色素変性

網膜色素変性(指定難病:90)班では患者レジストリを進めており、得られたデータを臨床研究や新規治療法開発に活用する試みを行なっている。現在さらなる登録数増加に向けて参加施設数を増やすなどを検討している。また、10年前に作成された「網膜色素変性の診療ガイドライン」は追加・修正は必要になってきており、改訂を開始した。さらに、全国および支部の患者会(JRPS)で患者やその家族に疾患に関する情報提供を行った。

グループ3(G3)：黄斑ジストロフィ

黄斑ジストロフィ(指定難病:301)は典型的な6つの病型とその他の病型に分けら

れるが、国内で発症数や病態が十分に解明されていない7つのタイプの「全身疾患に伴う希少な黄斑ジストロフィ」について調査を行なった。その結果、これら全てのタイプの希少な黄斑ジストロフィの患者数が10例以下であり、全国でもこれらの黄斑ジストロフィの患者数が極めて少ないことがわかった。

グループ4 (G4) : 近視性網膜脈絡膜萎縮

強度近視の中でも後部ぶどう腫を伴う患者は特に重度の視機能障害をきたしやすい。現在G4では、後部ぶどう腫を伴う強度近視の患者からDNAサンプルを採取して、後部ぶどう腫を伴う強度近視に関連する遺伝子群を探索する研究が進行中である。

また日本眼科学会、日本眼科医会、日本近視学会、日本小児眼科学会などと連携し、国民、近視患者やその家族に対して近視の進行予防や治療に関する正しい情報を提供する啓発活動を行っている。

グループ5 (G5) : FEVR

FEVR (家族性滲出性硝子体網膜症) の常染色体顕性(AD) 遺伝子の病原性変異を有することが確認された軽症患者の超広角フルオレセイン血管造影(UWFA) の特性を研究した。その結果、V字型血管ノッチ、ブラシ状血管端、血管外網膜の組み合わせは、Norrin/ β -Catenin 遺伝子の病原性変異体を有するAD-FEVR患者のバイオマーカーとして有用であることが示唆された。

グループ6 (G6) : MacTel 2型

特発性傍中心窩毛細血管拡張症(MacTel) の2型は眼科専門医であっても診断が難しい。そこで、眼科医にとって診断が難しいMacTel 2型と鑑別を有する疾患について専門家で話し合いを行なった。その結果、特に

陳旧性網膜静脈分枝閉塞症、放射線網膜症、滲出型加齢黄斑変性(特にRAP)、タモキシフェン網膜症などとの鑑別が重要であると考えられた。鑑別の際の注意点も示された。

グループ7 (G7) : 杆体一色覚 (ACHM)

指定難病に申請するために専門家によりACHMの診断基準を作成し、また患者数を調査するために全国の156施設にアンケート形式で調査票を送付した。診断基準としては、①眼底所見、②臨床症状、③全視野ERG所見、④遺伝形式を項目として挙げ、鑑別すべき疾患群も示した。

グループ8 (G8) : 視覚障害者の疫学調査

今回我々は、今後の全国視覚障害認定の実態疫学調査に関する具体的な調査内容について、どのような追加情報が必要であるかを話し合った。その結果、「黄斑変性」という病名の場合、これが加齢黄斑変性なのか、近視による黄斑症なのか、黄斑ジストロフィのような遺伝性疾患であるのかが不明であり、今後このような具体的な病名を加えることにより国民にも有用な正しい情報提供ができると考えられた。

グループ9 (G9) : 難治性視神経症

レーベル遺伝性視神経症(指定難病302: LHON)の症例データベースを利用して、患者の詳細な臨床情報を調査した。326例の症例(男性87.2%、女性12.8%)が登録された。重回帰分析の結果では、視力予後の悪化を規定する因子として、高齢およびmt11778G>Aバリエーションが抽出された。データベースシステム構築によりLHONの患者の疫学的な実態がより詳細に把握できるようになった。

グループ10 (G10) : 自己免疫網膜症

本年度は、診断基準を確立するために全国に送付したAIRに関するアンケート調査

の結果をまとめた。診断基準案の4項目を全て満たしたのは121名(65.4%)であった。診断に必須と考える項目の上位2位は、B:網膜電図異常、C:視覚機能異常を引き起こす明らかな原因がないことであり、抗網膜抗体の有無の結果は参考程度に捉える施設が多いという結果であった。

グループ11 (G10): 遺伝子検査・治療

遺伝性網膜ジストロフィおよび日本人患者の特性を考慮した遺伝学的検査解釈のガイドライン「Specification of variant interpretation guidelines for inherited retinal dystrophy in Japan」を作成し、バリエーションリストの内容を更新する会議を月1回程度行った。また、ルクスターナによる遺伝子治療に関しては、これまで行われた治療症例に対して治療内容と経過について報告および検討会を開催した。

D. 考察

1) 診療ガイドライン・診断基準・重症度作成による難病の診断技術の向上

G2では古くなった診療ガイドラインを部分的に改訂する作業が開始された。G7とG10では新たな診療ガイドラインと診断基準、重症度作成を進め、全国患者数の推定を進める。もしも該当するようであれば難病申請の準備を開始する予定である。G11では日本の遺伝性網膜ジストロフィの実情に即した遺伝学的結果の解釈ガイドラインを作成したが、これは遺伝学的検査の質の向上に寄与すると考えられた。

2) 全国調査による患者数推定

G8で継続的に行われている全国視覚障害者調査では、日本における最新の視覚障害者数と原因疾患の割合が明らかにされ、こ

の成果は医療政策に広く活用されるとともに国民への疾病予防や啓発にも役立っている。今回は特に今後の調査に有用な追加情報について話し合われた。また、G7, G10の疾患では全国患者数や重症者数の推定も行われており、新たな指定難病候補の評価に役立つと考えられた。

3) 患者データベースの構築と、他の研究班との横断的連携、および新規治療法開発
G2, G3, G9の疾患では患者のデータベース構築が進められた。特にG2では登録患者数が5000名を超えている。これらのデータベースを活用して日本における疾患の臨床的特徴の研究が進められるとともに、原因遺伝子と臨床像の関連が明らかにされる。これらのデータベースは、難病プラットフォームやAMEDとのデータベースと横断的な連携にも利用されており、国内企業との新規治療法開発の共同研究や治験にも利用が可能で、希少難病に対する日本発の新規治療の開発が期待される。

4) 調査結果の公表、医療従事者、患者、および国民に対する啓発活動

全体を通じて得られた網脈絡膜疾患の病態、疫学、遺伝情報、予防、新たな治療法に関する研究などを論文、学会、医師向けの講習会、市民公開講座、難病HPなどを通じて公表することで、これらの疾患の啓発が推進される。令和6年度は新たに本研究班独自のHPも作成した(<https://rcona.jp/>)。

5) 眼科における遺伝子検査および遺伝子治療の円滑な運用体制の構築

2023年に日本で初めて眼科における遺伝学的検査および遺伝子治療が承認され、保険収載された。本研究班のG11が中心となり、遺伝子検査および治療が日本において

円滑に運用されるように、会議を繰り返し、適切なガイドラインや手引きを作成し、その運用体制の構築と確認を行なっている。

E. 結論

G1-G11 のグループそれぞれが当初の計画を概ね達成することができた。本年度において特に着目すべき成果は、網膜色素変性の診療ガイドラインの改訂開始 (G2)、黄斑

ジストロフィの希少タイプの実態調査 (G3)、G7 および G9 で難病候補の全国調査を開始、最新の視覚障害者の結果公表 (G8)、日本独自の遺伝学的検査解釈のガイドラインを発売したこと (G11) である。

F. 健康危険情報

なし

G. 研究発表

1. 論文発表 (特に重要なもの 15 編を選定した)

- 1) Ueno S, Hayashi T, Tsunoda K, Aoki T, Kondo M. Nationwide epidemiologic survey on incidence of macular dystrophy in Japan. Jpn J Ophthalmol. 2024 May;68(3):167-173.
- 2) Mizobuchi K, Hayashi T, Tanaka K, Kuniyoshi K, Murakami Y, Nakamura N, Torii K, Mizota A, Sakai D, Maeda A, Kominami T, Ueno S, Kusaka S, Nishiguchi KM, Ikeda Y, Kondo M, Tsunoda K, Hotta Y, Nakano T. Genetic and Clinical Features of ABCA4-Associated Retinopathy in a Japanese Nationwide Cohort. Am J Ophthalmol. 2024 Aug;264:36-43.
- 3) Suga A, Mizobuchi K, Inooka T, Yoshitake K, Minematsu N, Tsunoda K, Kuniyoshi K, Kawai Y, Omae Y, Tokunaga K; NCBN Controls WGS Consortium; Hayashi T, Ueno S, Iwata T. A homozygous structural variant of RPGRIP1 is frequently associated with achromatopsia in Japanese patients with IRD. Genet Med Open. 2024 Mar 26;2:101843.
- 4) Goto K, Koyanagi Y, Akiyama M, Murakami Y, Fukushima M, Fujiwara K, Iijima H, Yamaguchi M, Endo M, Hashimoto K, Ishizu M, Hirakata T, Mizobuchi K, Takayama M, Ota J, Sajiki AF, Kominami T, Ushida H, Fujita K, Kaneko H, Ueno S, Hayashi T, Terao C, Hotta Y, Murakami A, Kuniyoshi K, Kusaka S, Wada Y, Abe T, Nakazawa T, Ikeda Y, Momozawa Y, Sonoda KH, Nishiguchi KM. Disease-specific variant interpretation highlighted the genetic findings in 2325 Japanese patients with retinitis pigmentosa and allied diseases. J Med Genet. 2024 Jun 20;61(7):613-620.
- 5) 上田奈央子, 辻川明孝. 総論：日本人の萎縮型加齢黄斑変性の特徴. 眼科 66(7)625-63, 2024.
- 6) Sato Y, Ueda-Arakawa N, Takahashi A, Miyake M, Mori Y, Miyara Y, Hara C, Kitajima

- Y, Maruko R, Kawai M, Takahashi H, Koizumi H, Maruyama-Inoue M, Yanagi Y, Iida T, Takahashi K, Sakamoto T, Tsujikawa A. Clinical Characteristics and Progression of Pachychoroid and Conventional Geographic Atrophy. *Ophthalmol Sci*. 2024 Apr 10;4(5):100528.
- 7) Murakami Y, Hisai T, Shimokawa S, Fukushima M, Fujiwara K, Hirata A, Takada A, Miyahara F, Nakashima N, Kobayakawa Y, Arima M, Mawatari G, Ishizu M, Kaida T, Miyata K, Ikeda Y, Sonoda KH. Study protocol for a prospective natural history registry investigating the relationships between inflammatory markers and disease progression in retinitis pigmentosa: the RP-PRIMARY study. *Jpn J Ophthalmol*. 2025 Online ahead of print.
- 8) Hiraoka M, Urakawa Y, Kawai K, Yoshida A, Hosakawa J, Takazawa M, Inaba A, Yokota S, Hirami Y, Takahashi M, Ohara O, Kurimoto Y, Maeda A. Copy number variant detection using next-generation sequencing in EYS-associated retinitis pigmentosa. *PLoS One*. 2024 Jun 24;19(6):e0305812.
- 9) Higa N, Hayashi T, Mizobuchi K, Iwasa M, Kubota S, Kuniyoshi K, Kameya S, Kondo H, Kondo M, Nakano T. A novel RPE65 variant p.(Ala391Asp) in Leber congenital amaurosis: a case report and literature review in Japan. *Front Med (Lausanne)*. 2024 Sep 18;11:1442107.
- 10) 大野京子、三宅正裕、柳靖雄、白澤誠、近藤峰生、生野恭司. 近視性黄斑部新生血管の診療ガイドライン. *日本眼科学会雑誌*. 128:719-729, 2024.
- 11) Okamoto M, Matsushita I, Nagata T, Fujino Y, Kondo H. Angiographic Characteristics in Mild Familial Exudative Vitreoretinopathy with Genetically Confirmed Autosomal Dominant Inheritance. *Ophthalmol Retina*. 2025 Feb;9(2):187-193.
- 12) Cheung CMG, Dansingani KK, Koizumi H, Lai TYY, Sivaprasad S, Boon CJF, Van Dijk EHC, Chhablani J, Lee WK, Freund KB. Pachychoroid disease: review and update. *Eye (Lond)*. 2025 Apr;39(5):819-834.
- 13) Takano F, Ueda K, Chihara N, Arai M, Sakamoto M, Kurimoto T, Yamada-Nakanishi Y, Nakamura M. Leber Hereditary Optic Neuropathy "Plus" with the m.14487 T>C Mutation as the Causality of Hemidystonia: A Case Report. *Case Rep Ophthalmol*. 2024 Nov 13;15(1):852-858.
- 14) Takano F, Ueda K, Kurimoto T, Arai M, Nagai T, Yamada-Nakanishi Y, Nakamura M. An exploratory study to evaluate efficacy and safety of frequent Transcutaneous Electrical Stimulation for Leber Hereditary Optic Neuropathy. *Sci Rep*. 2025 Feb 9;15(1):4829.
- 15) Fujinami K, Nishiguchi KM, Oishi A, Akiyama M, Ikeda Y; Research Group on

Rare, Intractable Diseases (Ministry of Health, Labour, Welfare of Japan).
Specification of variant interpretation guidelines for inherited retinal
dystrophy in Japan. Jpn J Ophthalmol. 2024 Jul;68(4):389-399.

2. 学会発表

- 1) 近藤峰生、高橋政代、角田和繁、不二門 尚、山本修一：「遺伝性網膜疾患診療における課題と展望」．日本網膜色素変性症協会（JRPS）創立30周年記念 第19回網脈絡膜フォーラム．10月14日 2024年．東京．
- 2) 上田奈央子、佐藤有紀子、宮良安宣、原千佳子、北嶋瑤子、丸子留佳、河合萌子、高橋元、高橋綾子、三宅正裕、森雄貴、近藤峰生、辻川明孝．日本人の萎縮型加齢黄斑変性における reticular pseudodrusen の検討（多施設研究）．第128回日本眼科学会総会、2024年4月18～21日、東京．
- 3) Ohno-Matsui K, Lu H, Yamanari M. Novel whorl-like collagen fiber arrangement around emissary canals in the posterior sclera. Macula Society. Feb. 13, Charlotte Harbor, Florida, USA, 2025.
- 4) Ueno S, Inooka T, Tsunoda K, Kuniyoshi K, Kondo H, Mizobuchi K, Suga A, Iwata T, Yoshitake K, Kondo M, Kominami T, Nishiguchi KM, Hayashi T. Fujiretina. March. 28-30, Tokyo, Japan, 2025.
- 5) Matoba R, Morimoto N, Kawasaki R, Fujiwara M, Kanenaga K, Yamashita H, Sakamoto T, Morizane Y. A nationwide survey of newly certified visually impaired individuals in Japan for the fiscal year 2019: impact of the revision of criteria for visual impairment certification. Jpn J Ophthalmol. 2023 May;67(3):346-352.
- 6) 上田香織、山上明子、石川裕人、中馬秀樹、石川均、池田康博、近藤峰生、中村誠．レーベル遺伝性視神経症に関する患者データベースに基づく疫学調査．日本眼科学会総会．2025年4月18日．東京．
- 7) 安藤亮、長谷川英一、楠原仙太郎、園田康平、近藤峰生．自己免疫網膜症に関する日本国内調査：アンケート結果報告．第78回日本臨床眼科学会．11月16日 2024年，京都．
- 8) Nishiguchi KM. Future of genomic medicine for inherited retinal degeneration. Fuji Retina. Tokyo, March 30, 2025.

H. 知的財産権の出願・登録状況

1. 特許取得 なし
2. 実用新案登録 なし
3. その他 なし

厚生労働科学研究費補助金（難治性疾患政策研究事業）

分担研究報告書

萎縮型加齢黄斑変性に関する研究

研究分担者	京都大学・医学研究科・教授 辻川 明孝 東京女子医科大学・医学部・教授 飯田 知弘 琉球大学・医学研究科・教授 古泉 英貴
研究協力者	横浜市立大学・医学部・客員教授 柳 靖雄 三重大学・医学系研究科・病院准教授 松原 央

加齢黄斑変性（AMD）は、新生血管型（neovascular）と萎縮型（atrophic）に分類される。萎縮型 AMD にみられる網膜外層、網膜色素上皮（RPE）、および脈絡毛細血管板の境界明瞭な萎縮病巣は、「地図状萎縮（geographic atrophy: GA）」とよばれる。今回我々は、日本人の GA 患者群をさらに研究し、アジア人 GA に特有の臨床的特徴をパキコロイド GA で説明できるかどうかを研究した。その結果、人口統計学および眼科的特徴は、パキコロイド型 GA と従来型 GA の間で異なっていた。年齢とベースラインの GA 面積で調整したパキコロイド型 GA の進行率は、従来型 GA よりも有意に遅いことがわかった。従来型 GA を有する日本人患者は、白人集団と同様の特徴と進行率を示した。以上の結果から、日本人における GA のいくつかの特徴は白人集団における GA の特徴とは異なっており、これはパキコロイドによる GA が含まれていることに起因している可能性があると考えられた。

A. 研究目的

加齢黄斑変性（AMD）は、新生血管型（neovascular）と萎縮型（atrophic）に分類される。萎縮型 AMD にみられる網膜外層、網膜色素上皮（RPE）、および脈絡毛細血管板の境界明瞭な萎縮病巣は「地図状萎縮（geographic atrophy: GA）」とよばれる。

令和 5 年度に本研究班は、アジア人における AMD の臨床的特徴と GA 進行率を明らかにした（Sato et al. Ophthalmol Retina. 2023）。令和 6 年度は、日本人の GA コホートをさらに研究し、アジア人 GA に特有の臨床的特徴をパキコロイド GA で説明できるかどうかを明らかにするとともに、ドルー

ゼンに関連した日本人の従来型 GA が白人集団の GA と同じ特徴を持つかどうかを研究した。

B. 研究方法

日本国内の 6 つの大学病院で診断された 173 人の患者、合計 173 眼（パキコロイド GA 38 眼、従来型 GA 135 眼）を対象とした。患者はすべて日本人で、眼底自発蛍光画像は解析可能な画質であった。さらに、101 眼（パキコロイド GA 22 眼、従来型 GA 79 眼）が経過観察グループとされた。

研究対象眼は、パキコロイド GA と従来型 GA に分類された。前者は、パキコロイドの

特徴がありドルーゼンがない場合に診断された。多変量線形回帰分析を用いて、GAの進行率とGAのサブタイプとの関連を検討した。

(倫理面への配慮)

今回の研究に関しては患者の個人情報は全て匿名化し、倫理面に十分配慮して行った。

C. 研究結果

パキコロイドGA群は有意に若く(70.3歳 vs 78.7歳; $P < 0.001$)、男性優位であり(89.5 vs 55.6%; $P < 0.001$)、最高矯正視力は良好で(logMAR 0.15 vs 0.40; $P < 0.002$)、脈絡膜が厚く($312.4 \mu\text{m}$ vs. $161.6 \mu\text{m}$; $P < 0.001$)、単一GA型の割合が高く(94.7 vs. 49.6%; $P < 0.001$)、またGA面積が小さかった(0.59 mm^2 vs. 3.76 mm^2 ; $P < 0.001$)。

経過観察できたグループをみると、GAの平均進行率(平方根変換)は、従来のGA群よりもパキコロイドGA群で有意に遅かつ

た(0.11 mm/年 vs. 0.27 mm/年 ; $P < 0.001$)。

D. 考察

人口統計学のおよび眼科的特徴は、パキコロイド型GAと従来型GAの間に異なっていた。年齢とベースラインのGA面積で調整したパキコロイド型GAの進行率は、従来型GAよりも有意に遅いことがわかった。従来型GAを有する日本人患者は、白人集団と同様の特徴と進行率を示した。日本人におけるGAのいくつかの特徴は、白人集団におけるGAの特徴とは異なっており、これはパキコロイドによるGAが含まれていることに起因している可能性がある。

E. 結論

今回の研究により、日本人のGAの臨床的特徴とGA進行率がより詳細に明らかになった。日本人においてGAを研究および治療する際には、パキコロイドGAなのか通常型GAなのか評価した上で行う必要があると考えられた。

F. 健康危険情報：なし

G. 研究発表

1. 論文発表

- 1) Cheung CMG, Chen Y, Holz F, Tsujikawa A, Sadda S. Geographic atrophy in Asia. Graefes Arch Clin Exp Ophthalmol. 2025. Online ahead of print.
- 2) Sato Y, Ueda-Arakawa N, Takahashi A, Miyake M, Mori Y, Miyara Y, Hara C, Kitajima Y, Maruko R, Kawai M, Takahashi H, Koizumi H, Maruyama-Inoue M, Yanagi Y, Iida T, Takahashi K, Sakamoto T, Tsujikawa A. Clinical Characteristics and Progression of Pachychoroid and Conventional Geographic Atrophy. Ophthalmol Sci. 2024 Apr 10;4(5):100528.
- 3) Kogo T, Muraoka Y, Hata M, Ishikura M, Nishigori N, Akiyama Y, Ueda-Arakawa N, Miyata M, Ooto S, Takahashi A, Miyake M, Tsujikawa A. Preferential Locations of Polypoidal Lesions and Adjacent Pigment Epithelium Detachments in Polypoidal

Choroidal Vasculopathy in a Japanese Population. Invest Ophthalmol Vis Sci. 2025 Feb 3;66(2):70.

- 4) Maruko I, Maruko R, Kawano T, Iida T. Comparisons of choroidal thickness and volume in eyes with central serous chorioretinopathy to that of control eyes determined by ultra-widefield optical coherence tomography. Graefes Arch Clin Exp Ophthalmol. 2024
- 5) Cheung CMG, Dansingani KK, Koizumi H, Lai TYY, Sivaprasad S, Boon CJF, Van Dijk EHC, Chhablani J, Lee WK, Freund KB. Pachychoroid disease: review and update. Eye (Lond). 2025 Apr;39(5):819-834.
- 6) Yanagi Y, Takahashi K, Iida T, Gomi F, Onishi H, Morii J, Sakamoto T. Cost-effectiveness Analysis of Ranibizumab Biosimilar for Neovascular Age-Related Macular Degeneration and its Subtypes from the Societal and Patient Perspectives in Japan. Ophthalmol Ther. 2024 Oct;13(10):2629-2644.
- 7) Chujo S, Matsubara H, Mase Y, Kato K, Kondo M. Recurrence Rate during 5-Year Period after Suspension of Anti-Vascular Endothelial Growth Factor Treatment for Neovascular Age-Related Macular Degeneration. J Clin Med. 2024 Jul 24;13(15):4317.
- 8) 上田奈央子, 辻川明孝. 総論：日本人の萎縮型加齢黄斑変性の特徴. 眼科 66(7)625-63, 2024.

2. 学会発表

- 1) 上田奈央子、畑 匡侑、佐藤有紀子、高橋綾子、大音壮太郎、田村寛、宮田学、三宅正裕、木戸愛、辻川明孝. 萎縮型 AMD における pseudodrusen. 第 130 回京都眼科学会、2024 年 6 月 16 日、京都市.
- 2) 上田奈央子、佐藤有紀子、宮良安宣、原千佳子、北嶋瑤子、丸子留佳、河合萌子、高橋元、高橋綾子、三宅正裕、森雄貴、近藤峰生、辻川明孝. 日本人の萎縮型加齢黄斑変性における reticular pseudodrusen の検討（多施設研究）. 第 128 回日本眼科学会総会、2024 年 4 月 18～21 日、東京.

H. 知的財産権の出願・登録状況

1. 特許取得 なし
2. 実用新案登録 なし
3. その他 なし

Clinical Characteristics and Progression of Pachychoroid and Conventional Geographic Atrophy

Yukiko Sato, MD,¹ Naoko Ueda-Arakawa, MD, PhD,¹ Ayako Takahashi, MD, PhD,¹ Masahiro Miyake, MD, PhD,¹ Yuki Mori, MD, PhD,¹ Yasunori Miyara, MD,² Chikako Hara, MD, PhD,³ Yoko Kitajima, MD,⁴ Ruka Maruko, MD, PhD,⁵ Moeko Kawai, MD,⁵ Hajime Takahashi, MD, PhD,⁶ Hideki Koizumi, MD, PhD,² Maiko Maruyama-Inoue, MD, PhD,⁴ Yasuo Yanagi, MD, PhD,⁷ Tomohiro Iida, MD, PhD,⁵ Kanji Takahashi, MD, PhD,⁶ Taiji Sakamoto, MD, PhD,⁸ Akitaka Tsujikawa, MD, PhD¹

Purpose: To elucidate the clinical characteristics and progression rates of pachychoroid and conventional geographic atrophy (GA).

Design: Retrospective, multicenter, observational study.

Participants: A total of 173 eyes from 173 patients (38 eyes with pachychoroid GA and 135 with conventional GA) from 6 university hospitals in Japan were included. All patients were Japanese, aged ≥ 50 years and with fundus autofluorescence images having analyzable image quality. A total of 101 eyes (22 with pachychoroid GA and 79 with conventional GA) were included in the follow-up group.

Methods: The studied eyes were classified as having pachychoroid or conventional GA; the former was diagnosed if the eye had features of pachychoroid and no drusen. The GA area was semiautomatically measured on fundus autofluorescence images, and the GA progression rate was calculated for the follow-up group. Multivariable linear regression analysis was used to determine whether the rate of GA progression was associated with GA subtype.

Main Outcome Measures: Clinical characteristics and progression rates of pachychoroid and conventional GA.

Results: The pachychoroid GA group was significantly younger (70.3 vs. 78.7 years; $P < 0.001$), more male-dominant (89.5 vs. 55.6%; $P < 0.001$), and had better best-corrected visual acuity (0.15 vs. 0.40 in logarithm of the minimum angle of resolution; $P = 0.002$), thicker choroid (312.4 vs. 161.6 μm ; $P < 0.001$), higher rate of unifocal GA type (94.7 vs. 49.6%; $P < 0.001$), and smaller GA area (0.59 vs. 3.76 mm^2 ; $P < 0.001$) than the conventional GA group. In the follow-up group, the mean GA progression rate (square-root transformation) was significantly lower in the pachychoroid GA group than in the conventional GA group (0.11 vs. 0.27 mm/year ; $P < 0.001$).

Conclusions: Demographic and ocular characteristics differed between GA subtypes. The progression rate of pachychoroid GA, adjusted for age and baseline GA area, was significantly lower than that of conventional GA. Japanese patients with conventional GA showed characteristics and progression rates similar to those in White populations. Some characteristics of GA in Japanese population differ from those in Caucasian populations, which may be due to the inclusion of pachychoroid GA.

Financial Disclosure(s): Proprietary or commercial disclosure may be found in the Footnotes and Disclosures at the end of this article. *Ophthalmology Science* 2024;4:100528 © 2024 by the American Academy of Ophthalmology. This is an open access article under the CC BY-NC-ND license (<http://creativecommons.org/licenses/by-nc-nd/4.0/>).

Geographic atrophy (GA) is recognized as a leading cause of visual impairment in elderly people in developed countries.¹ In recent years, evidence regarding on its prevalence, risk factors, and clinical characteristics in White populations has been growing. Moreover, in these populations, reticular pseudodrusen, banded or diffuse trickling fundus autofluorescence (FAF) pattern, multifocal GA, noncentral GA, and bilateral GA have been reported as markers of

rapid progression.² Ethnic differences have been suggested in the clinical features of GA, especially, its low prevalence in Asian populations.³ However, it remains unclear whether the GA progression rate and risk factors for progression in White populations are also applicable to Asian populations.

Geographic atrophy affects approximately 5 million people worldwide.⁴ Currently, its prevalence remains low in

Asian countries; however, with the rapid aging of the population, effective treatment for GA is becoming an urgent medical need. Numerous previous studies have examined potential treatments for GA, and a series of suitable treatments have been recently approved in the United States.^{5,6} Nevertheless, previous clinical trials have not considered the impact of GA subtypes, and it has not been discussed whether ethnic differences should be considered in the application of these treatment methods.

Our recent study examined 173 Japanese patients with GA, showing differences between the Japanese and White population samples.⁷ We revealed that Japanese patients with GA were male dominant and had small lesions, thick choroids, and slow GA progression rates. Moreover, some patients presented with GA without drusen but with features of pachychoroid, known as pachychoroid GA. Although Asian population sometimes presents with pachychoroid GA, which differs from drusen-related conventional GA, the characteristics of these 2 subtypes remain unclear.

In this study, we further examined a Japanese cohort with GA to elucidate whether pachychoroid GA can account for the unique clinical characteristics of Asian GA and clarify whether drusen-related conventional GA has the same features as GA in White populations.

Methods

Ethics Statement

This study adhered to the principles of the Declaration of Helsinki and was approved by the institutional review board and Ethics Committee of Kyoto University Graduate School of Medicine. The requirement for written informed consent was waived because this was a retrospective study and only anonymized data were used for analysis.

Participants

The design of this retrospective multicenter study is described elsewhere.⁷ Briefly, consecutive patients diagnosed with GA at 6 university hospitals in Japan (Kyoto University Hospital, Tokyo Women's Medical University Hospital, University of the Ryukyus Hospital, Osaka University Hospital, Yokohama City University Medical Center, and Kansai Medical University Hospital) between January 2009 and December 2021 were enrolled. The inclusion criteria were Japanese ethnicity, age ≥ 50 years, and definite GA in at least 1 eye. The diagnosis of GA was based on the diagnostic criteria for GA in the Japanese people, described in detail elsewhere.^{8,9} Briefly, GA diagnosis required the following ocular findings: (1) at least 250 μm in diameter, (2) round/oval/cluster-like or geographic in shape, (3) sharp delineation, (4) hypopigmentation or depigmentation in retinal pigment epithelium, and (5) clear visualization of large and medium choroidal vessels, without any history of inherited diseases, high myopia, chronic central serous chorioretinopathy (CSC), traumatic injury, retinal epithelial tear, history of laser photocoagulation, or macular neovascularization. Macular dystrophies and genetic causes of macular atrophy were excluded based on clinical presentation such as age of onset, symmetry of the right and left eyes and findings of FAF (such as flecks in Stargardt disease). In the cases where inherited diseases were suspected, electroretinography and genetic tests, if possible, were performed. Otherwise, suspicious cases were excluded. Eyes without FAF

images and those with poor image quality were excluded. If both eyes met the inclusion criteria, only the right eye was included in the study. Smoking status was confirmed using medical records.

Eyes with FAF images acquired at an interval of more than 6 months were included in the follow-up group. The dates of the first and last FAF assessments were defined as the baseline and final visits, respectively.

Multimodal Imaging Methods

All patients underwent a comprehensive ophthalmologic examination, which included assessments such as best-corrected visual acuity (BCVA), slit-lamp biomicroscopy using a noncontact lens, axial length, FAF, color fundus photography (CFP) (TRC50DX, Topcon, Tokyo, Japan; TRCNW6S, Topcon; TRCNW8F, Topcon), and either spectral-domain (SD) OCT (OCT3000, Carl Zeiss; HRA, Heidelberg Engineering; Avanti, Optovue.) or swept-source (SS) OCT (Atlantis, Topcon; Triton, Topcon). Fundus autofluorescence images were obtained using a confocal scanning laser ophthalmoscope (HRA Heidelberg Engineering) with a $30^\circ \times 30^\circ$ field of view centered on the fovea. The SD/SS-OCT images included horizontal and vertical line scans through the foveal center. Enhanced depth imaging OCT¹⁰ scans were also taken.

Image Analysis

Image analysis details are described elsewhere.⁷ Briefly, drusen were diagnosed based on CFP and SD/SS-OCT, and reticular pseudodrusen were diagnosed based on multimodal imaging findings, including CFP, SD/SS-OCT, and FAF. Central macular thickness and subfoveal choroidal thickness (SFCT) were measured manually on SD/SS-OCT images obtained by the vertical and horizontal scans through the foveal center, and the values were averaged. The SFCT was measured using either SS or Enhanced depth imaging -OCT.

The GA location (central or non-central), GA pattern (unifocal or multifocal), and measurements of central macular thickness and SFCT were performed at each research institute. All CFP, FAF, and SD/SS-OCT images were gathered at a single institute (Kyoto University Hospital), and the study eyes were classified as having conventional or pachychoroid GA. Pachychoroid GA was diagnosed when the following conditions were fulfilled: (1) clinical and anatomical features of the pachychoroid phenotype were identified, including reduced fundus tessellation on CFP and dilated outer choroidal vessels on OCT and (2) no drusen were observed (Fig 1).¹¹ The classification of GA was independently performed by 2 retinal specialists (Y.S. and N.U.A.). In cases of disagreement, a third retinal specialist (A.Takahashi) was consulted. The areas of GA were measured on FAF images by a single assessor (Y.S.) using the Region Finder software, version 1.10.2.0 (Heidelberg Engineering). Reproducibility was confirmed by another assessor, as previously reported.⁷

The GA progression rate was calculated as the difference in the GA area between the baseline and final visit on FAF images, divided by follow-up duration (mm^2/year). The square root transformation (SQRT) method¹² was used to analyze the GA progression rate to eliminate the dependence of GA progression rate on the baseline GA area (mm^2/year).

Statistical Analysis

Statistical analysis was performed using JMP software (version 16.2; SAS Institute, Inc). All values are presented as the mean \pm standard deviation or counts. BCVA was assessed using a Landolt chart and converted to the logarithm of the minimum angle of resolution (logMAR) for the statistical analysis. Continuous variables were compared using the Mann-Whitney U test. Each

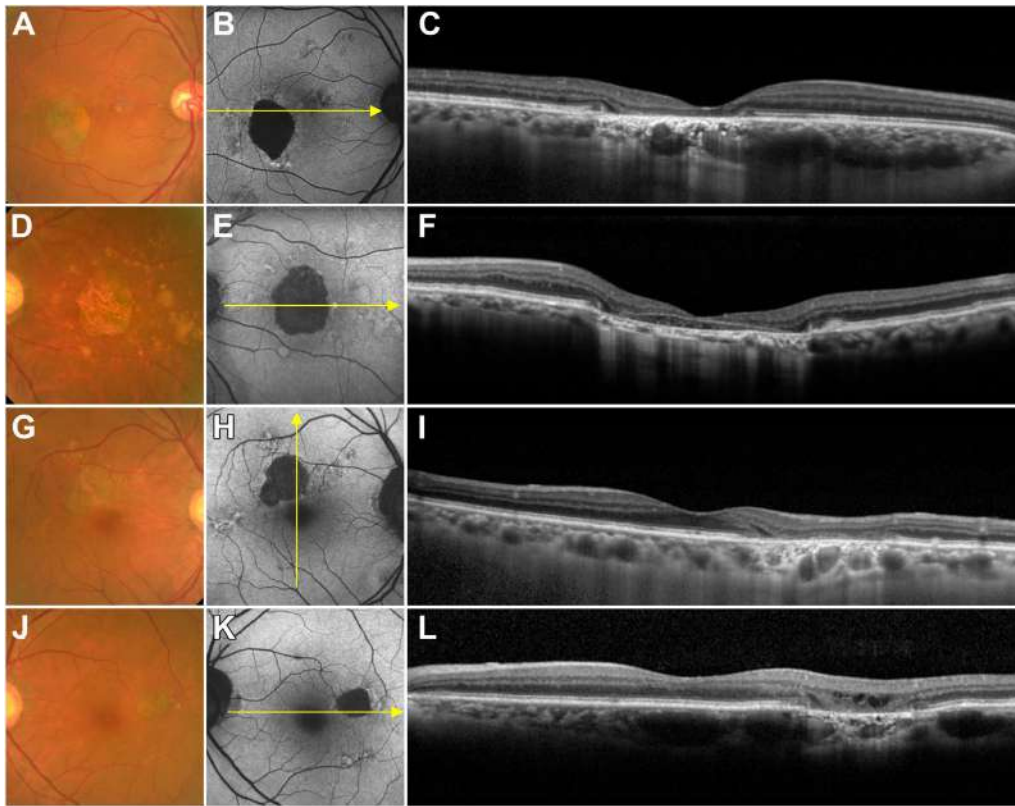


Figure 1. Multimodal imaging of pachychoroid GA in a 63-year-old man (A–C), conventional GA in a 74-year-old man (D–F) and bilateral pachychoroid GA in an 81-year-old man (G–L). A, D, G, J, Color fundus photography. B, E, H, K, Fundus autofluorescence images. C, I, Enhanced depth imaging OCT. F, L, Spectral domain OCT. Yellow arrows indicate the scan lines of OCT images, that show complete retinal pigment epithelium and outer retinal atrophy. Dilated outer choroidal vessels are seen in pachychoroid GA cases (C, I and L). Subfoveal choroidal thickness is 370 (C), 84 (F), 259 (I), and 287 μm (L), respectively. GA = geographic atrophy.

$n \times n$ table was evaluated using the Fisher exact test. Multivariable linear regression analyses were used to assess the association between the GA subtypes and the rate of GA progression (SQRT). P values of <0.05 were considered statistically significant.

Results

Of 173 study eyes, 38 (22.0%) and 135 (78.0%) were classified as pachychoroid GA and conventional GA, respectively. Table 1 shows the demographic and ocular characteristics of the patients in both groups. The pachychoroid GA group was significantly younger (70.3 vs. 78.7 years, $P < 0.001$), more male dominant (89.5 vs. 55.6%; $P < 0.001$), and had a higher prevalence of smokers (current or past; 89.7 vs. 52.5%; $P < 0.001$). Moreover, the pachychoroid GA group demonstrated better BCVA (0.15 vs. 0.40 in logMAR, 20/28 vs. 20/50 in Snellen equivalent; $P = 0.002$), thicker choroid (312.4 vs. 161.6 μm ; $P < 0.001$), and smaller GA size (0.59 [median: 0.28; range: 0.05–2.81] vs. 3.76 [median: 2.41; range: 0.05–24.88] mm^2 ; $P < 0.001$) compared with the conventional GA group. None of the eyes in the pachychoroid GA group had drusen or reticular pseudodrusen, whereas 115 (85.2%) eyes had drusen and 73 (54.1%) eyes had reticular pseudodrusen

in the conventional GA group. Unifocal GA was more prevalent in the pachychoroid GA group than in the conventional GA group (94.7 vs. 49.6%; $P < 0.001$). A total of 61 (46.2%) patients in the conventional GA group had bilateral GA, whereas only 1 (2.6%) patient in the pachychoroid GA group did ($P < 0.001$). Late age-related macular degeneration was observed in the fellow eye of 9 (23.7%) eyes in the pachychoroid GA group and in that of 106 (80.3%) eyes in the conventional GA group ($P < 0.001$).

Table 2 shows the demographic and ocular characteristics of 22 eyes with pachychoroid GA and 79 eyes with conventional GA in the follow-up group. These characteristics of each group were similar to those of the entire study population. During the follow-up period (mean: 57.0 ± 32.4 [median: 56.5] and 43.2 ± 27.2 [median: 38.0] months, respectively), the mean BCVA in logMAR changed from 0.19 to 0.26 (Snellen equivalent, from 20/31 to 20/36) in the pachychoroid GA group and from 0.39 to 0.55 (Snellen equivalent, from 20/49 to 20/71) in the conventional GA group. The mean GA area increased from 0.65 ± 0.88 (median: 0.26) to 1.91 ± 2.05 (median: 1.10) mm^2 in the pachychoroid GA group and from 3.36 ± 3.61 (median: 2.29) to 7.24 ± 7.15 (median: 5.47) mm^2 in the conventional GA group (Fig 2). The mean GA progression

Table 1. Demographic and Ocular Characteristics of Pachychoroid and Conventional GA Groups

Characteristics	Pachychoroid GA	Conventional GA	P Value
Patients, n	38	135	
Age (median, range), years	70.3 ± 7.5 (70, 56–86)	78.7 ± 8.3 (80, 53–97)	<0.001
Sex, n, males (%)	34 (89.5)	75 (55.6)	<0.001
Smoking status, n, current or former (%); n = 151	26 (89.7)	64 (52.5)	<0.001
Axial length (median), mm; n = 123	23.4 ± 0.9 (23.3)	23.5 ± 0.9 (23.5)	0.752
BCVA, logMAR (Snellen equivalent)	0.15 ± 0.27 (20/28)	0.40 ± 0.45 (20/50)	0.002
CMT (median, range), μ m	143.6 ± 63.8 (149.5, 7.0–242.0)	145.3 ± 74.5 (151, 6.0–617.0)	0.283*
SFCT (median, range), μ m	312.4 ± 116.0 (322, 140.5–622.0)	161.6 ± 74.4 (153, 36.5–414.0)	<0.001†
GA area (median, range), mm ²	0.59 ± 0.76 (0.28, 0.05–2.81)	3.76 ± 4.26 (2.41, 0.05–24.88)	<0.001
GA area (SQRT) (median, range), mm	0.66 ± 0.40 (0.52, 0.23–1.68)	1.66 ± 1.01 (1.55, 0.23–4.99)	<0.001
GA location, central/non-central	16/22	74/61	0.199
GA type, unifocal/multifocal	36/2	67/68	<0.001
Drusen, n, present (%)	0 (0)	115 (85.2)	<0.001
Reticular pseudodrusen, n, present (%)	0 (0)	73 (54.1)	<0.001
Fellow eye status, GA/neovascular	1/8/0/29	61/45/22/4	<0.001
AMD/intermediate AMD/no AMD‡			

AMD = age-related macular degeneration; BCVA = best-corrected visual acuity; CMT = central macular thickness; GA = geographic atrophy; logMAR = logarithm of the minimum angle of resolution; n = number of patients; SFCT = subfoveal choroidal thickness; SQRT = square-root transformation.

*Age-adjusted.

†Age and sex-adjusted.

‡Three patients lacked information on their fellow eyes due to phthisis.

rate (SQRT) was significantly lower in the pachychoroid GA group than in the conventional GA group (0.11 ± 0.07 [median: 0.09] vs. 0.27 ± 0.18 [median: 0.25] mm/year, $P < 0.001$). There was no significant difference in the SFCT thinning rate between the 2 groups (6.5 vs. 4.1 μ m/year; $P = 0.093$).

Figure 3 presents a scatter plot showing the association between the baseline GA area (SQRT) and GA progression rate (SQRT) in the follow-up group. The baseline GA area (SQRT) in the conventional GA group showed a relatively wide range, whereas in the pachychoroid GA group, it was small in most cases. Multivariable linear regression analysis adjusted for baseline GA area (SQRT), and age showed that GA progression rate (SQRT) was significantly associated with GA subtypes ($P = 0.034$).

Discussion

In this study, we elucidated the different clinical characteristics of 2 GA subtypes in a Japanese population. Takahashi et al previously investigated pachychoroid GA in relatively younger Asian populations and showed that it is characterized by features such as a thick choroid, choroidal vascular hyperpermeability, small lesions, absence of drusen, and slow progression.¹¹ Within our current Japanese cohort, 38 (22.0%) patients were classified into the pachychoroid GA group. Notably, these patients were significantly younger and predominantly male and had better BCVA, a thicker choroid, a higher prevalence of unifocal-type GA, smaller sized GA lesions, and a slower progression rate than those with conventional GA. The present findings are consistent with those of the previous study.¹¹ In our recent report, the

GA progression rate was significantly associated with the baseline GA area, even when using the SQRT method.⁷ In the present study, multivariable linear regression analysis adjusted for baseline GA area (SQRT), and age showed that the progression rate of pachychoroid GA was significantly lower than that of the conventional GA (regression coefficient, 4.7×10^{-2} ; 95% confidence interval, 3.7×10^{-3} – 9.0×10^{-2} ; $P = 0.034$). This is the first study to demonstrate that GA progression rates were significantly different between pachychoroid and conventional GA correcting for the baseline GA area.

The clinical characteristics of GA in Asian populations remain poorly understood. Teo et al compared the clinical characteristics of GA between Asian and non-Asian populations,¹³ showing a slower GA progression rate (SQRT) in Asian populations than in non-Asian populations (0.2 vs. 0.4 mm/year measured with near-infrared imaging; $P < 0.01$; 0.1 vs. 0.3 mm/year measured on FAF; $P < 0.01$). The higher GA progression rate in Asian populations was associated with the presence of drusen and a large baseline GA area. Although the study did not account for GA subtypes (pachychoroid and conventional GA), pachychoroid GA may have been involved in the slow progression rate observed in the Asian cohort. In Asian populations, the pachychoroid is common, partially leading to various conditions such as polypoidal choroidal vasculopathy, pachychoroid neovascularization, or pachychoroid GA.¹⁴ The high prevalence of pachychoroid GA could help explain the slow GA progression rate in Asian populations.

In our cohort, the characteristics of conventional GA were more similar to those reported in White populations. This includes age (78.7 vs. 69.7–83.0 years),^{15,16} bilateral

Table 2. Demographic and Ocular Characteristics at Baseline and the Final Visit in the Follow-Up Group

Characteristics	Pachychoroid GA		Conventional GA		P value*	
	Baseline	Final	Baseline	Final	Baseline	Final
Patients, n	22		79			
Follow-up period (median, range), month	57.0 ± 32.4 (56.5, 6–123)		43.2 ± 27.2 (38.0, 6–110)		0.078	
Age (median, range), years	71.2 ± 8.7 (70.5, 56–86)	76.1 ± 7.6 (76, 63–90)	78.1 ± 8.2 (79, 53–94)	81.7 ± 7.9 (83, 58–95)	0.002	0.002
Sex, n, males (%)	20 (90.9)		43 (54.4)		0.002	
Smoking status, n, current or former (%); n = 90	16 (84.2)		34 (47.9)		0.005	
Axial length (median), mm; n = 80	23.4 ± 1.0 (23.3)		23.5 ± 0.9 (23.6)		0.447	
BCVA, logMAR (Snellen equivalent)	0.19 ± 0.30 (20/31)	0.26 ± 0.31 (20/36)	0.39 ± 0.46 (20/49)	0.55 ± 0.53 (20/71)	0.086	0.026
CMT (median, range), μm	146.5 ± 60.2 (152.5, 17.0–224.0)	121.1 ± 74.2 (146, 9.0–227.0)	148.5 ± 84.8 (151, 6.0–617.0)	116.5 ± 71.4 (105, 6.0–285.0)	0.072 [†]	0.021 [†]
SFCT (median, range), μm	325.0 ± 125.2 (324, 140.5–622.0)	287.7 ± 109.7 (292, 110.5–571.0)	164.4 ± 78.5 (155, 36.5–414.0)	150.1 ± 77.5 (143, 15.5–414.0)	<0.001 [‡]	<0.001 [‡]
CMT thinning (median, range), μm/year	4.7 ± 8.2 (2.6, –8.0 to 21.8)		13.6 ± 27.6 (5.1, –12.5 to 162.4)		0.097	
SFCT thinning (median, range), μm/year	6.5 ± 16.1 (5.4, –50.4 to 32.0)		4.1 ± 15.3 (3.4, –62 to 58.2)		0.093	
GA area (median, range), mm ²	0.65 ± 0.88 (0.26, 0.07–2.81)	1.91 ± 2.05 (1.10, 0.15–6.75)	3.36 ± 3.61 (2.29, 0.05–16.16)	7.24 ± 7.15 (5.47, 0.16–37.10)	<0.001	<0.001
GA area [SQRT] (median, range), mm	0.68 ± 0.44 (0.50, 0.26–1.68)	1.20 ± 0.70 (1.05, 0.38–2.60)	1.56 ± 0.96 (1.51, 0.23–4.02)	2.38 ± 1.26 (2.34, 0.40–6.09)	<0.001	<0.001
GA progression rate (median, range), mm ² /year	0.23 ± 0.25 (0.12, 0.02–1.08)		1.22 ± 1.13 (0.81, 0.02–4.59)		<0.001	
GA progression rate [SQRT] (median, range), mm/year	0.11 ± 0.07 (0.09, 0.02–0.34)		0.27 ± 0.18 (0.25, 0.01–0.70)		<0.001	
GA location, central/non-central	8/14	11/11	43/36	55/24	0.154	0.127
GA type, unifocal/multifocal	21/1	21/1	42/37	38/41	<0.001	<0.001
Drusen, n, present (%)	0 (0)		67 (84.8)		<0.001	
Reticular pseudodrusen, n, present (%)	0 (0)		43 (54.4)		<0.001	
MNV development, n [§]	1		5		1.000	
Fellow eye status, GA/neovascular AMD/intermediate AMD/no AMD; n = 100	1/6/0/15	3/6/0/13	30/31/15/2	34/33/9/2	<0.001	<0.001

AMD = age-related macular degeneration; BCVA = best-corrected visual acuity; CMT = central macular thickness; GA = geographic atrophy; logMAR = logarithm of the minimum angle of resolution; MNV = macular neovascularization; n = number of patients; SFCT = subfoveal choroidal thickness; SQRT = square-root transformation.

*Pachychoroid GA vs conventional GA.

[†]Age-adjusted.

[‡]Age and sex-adjusted.

[§]The subsequent period was not included in the follow-up analysis when macular neovascularization developed during the course of the disease.

^{||}In 1 patient, information on the fellow eye was lacking due to phthisis.

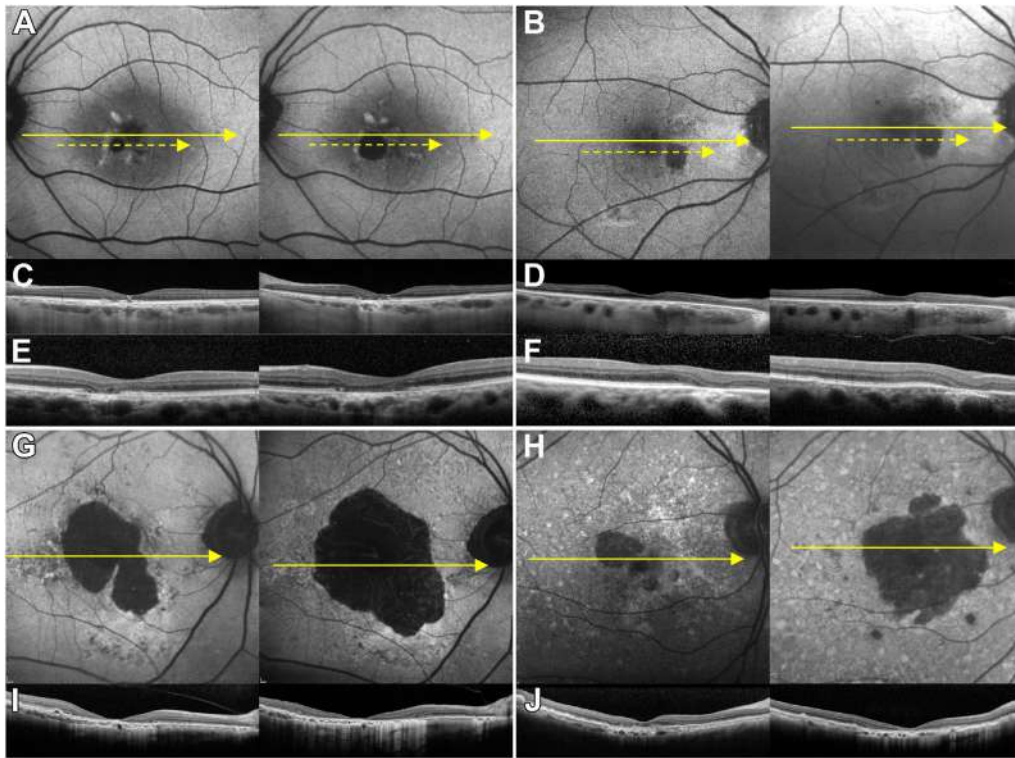


Figure 2. Progression of pachychoroid GA in a 70-year-old man with 73 months' follow-up (A, C and E), and an 86-year-old man with 42 months' follow-up (B, D and F), alongside that of conventional GA in an 83-year-old man with 92 months' follow-up (G, I) and an 87-year-old woman with 73 months' follow-up (H, J). A, B, G, H, Fundus autofluorescence images. Yellow arrows indicate the scan lines of OCT on panels C, D, I and J. Yellow dotted arrows indicate the scan lines of OCT through the GA lesion on panels E and F. Enhanced depth imaging OCT shows dilated outer choroidal vessels (C, D). Spectral-domain OCT images demonstrate complete outer retinal atrophy (E, F, I and J). In all cases, the GA area increased from baseline to the final visit. The GA progression rate (square-root transformation; SQRT) was 0.07 (A), 0.07 (B), 0.16 (G), and 0.33 mm per year (H), respectively. GA = geographic atrophy.

GA rate (46.2 vs. 23.0%–67.4%),^{17,18} multifocality rate (50.4 vs. 23.0%–77.2%),^{19,20} and reticular pseudodrusen prevalence (54.1 vs. 36%–38%)^{21,22} In addition, conventional GA of a size consistent with that defined by

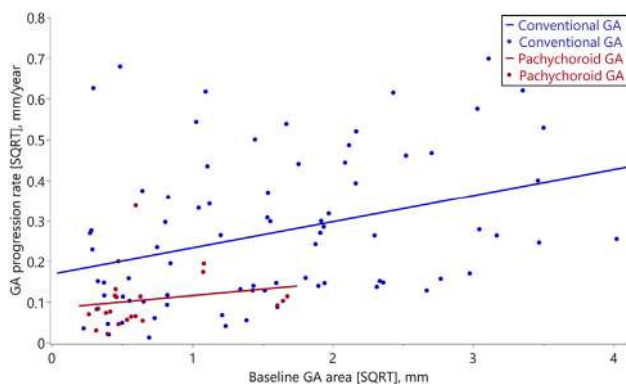


Figure 3. Scatter plot showing the association between baseline GA area (SQRT) and GA progression rate (SQRT) in the follow-up group. The red dots show the cases of pachychoroid GA; the blue dots show the cases of conventional GA. The straight lines are the regression lines of the 2 groups (pachychoroid GA group; $Y = 0.085 + 0.031 \times X$, conventional GA group; $Y = 0.169 + 0.065 \times X$). GA = geographic atrophy; sqrt = square-root transformation.

clinical trial eligibility criteria showed GA progression rate (SQRT) (0.33 mm/year) similar to that of the sham group in these trials (0.35–0.40 mm/year,^{5,6} Table 3). Our previous report showed that some characteristics of GA in a Japanese population differ from those in White populations.⁷ However, except for pachychoroid GA, drusen-related conventional GA in Asian populations presents with characteristics similar to those observed in White populations.

The pathogenesis of drusen-related GA is considered to be closely related to chronic inflammation via the complement pathway.^{23,24} Recently, complement C3 and C5 inhibitors have been approved for the treatment of GA.^{5,6} However, the pathogenesis of pachychoroid GA remains unclear. In a previous study, the patients with pachychoroid GA were found to be less likely to present with a risk allele in *ARMS2* A69S compared to those with conventional GA, whereas the frequencies of risk allele in either *CFH* I62V or *CFH* Y402H were comparable.¹¹ It is currently unknown whether complement factor inhibitors are effective against pachychoroid GA. Furthermore, given its slow progression rate, including pachychoroid GA in clinical trials may lower the margin to determine treatment efficacy. Conventional drusen-related GA in Asian populations, whose characteristics are comparable to those of

Table 3. Demographic, Ocular Characteristics and GA Progression Rates of Patients With Conventional GA > 2.5 mm² at Baseline in the Current Study and Previous Studies With White Samples

Characteristics	Current Study	Liao et al 2020 ⁵	Jaffe et al 2021 ⁶
Patients, n, (eyes)	35 (35)	81 (81)	110 (110)
Ethnicity	Japanese (100%)	White (100%)	White (97.3%)
Follow-up period, months	42.8	12	12
Age, years	76.5	78.4	78.2
Sex, %, males	57.1	39.5	28.2
Baseline GA area eligibility threshold	>2.5 mm ² and <17.5 mm ²	>2.5 mm ² and <17.5 mm ²	>2.5 mm ² and <17.5 mm ²
Baseline GA area, mm ²	6.43	8.2	7.42
Baseline GA area [SQRT], mm	2.46	2.8	2.63
GA progression rate, mm ² /year	1.96	2.12	NA
GA progression rate [SQRT], mm/year	0.33	0.35	0.40

GA = geographic atrophy; n = number of patients; SQRT = square-root transformation.

GA in White populations, could be included in the clinical trials of complement factor inhibitors or treatment targeting other pathways.

Recent studies have reported on an acquired vitelliform lesion associated with pachychoroid disease, termed pachyvittelliform maculopathy.^{25,26} Hilely et al reported that 41% of pachyvittelliform maculopathy cases developed macular atrophy and suggested that inner choroidal or choriocapillaris ischemia might cause impairment and dysfunction of the retinal pigment epithelium, leading to retinal pigment epithelium atrophy.²⁵ This proposed pathway could be a contributing factor for the development of pachychoroid GA.

In clinical practice, White patients may present with pachychoroid spectrum diseases, such as polypoidal choroidal vasculopathy or CSC. Although pachychoroid GA can also develop in White populations, the incidence of this disease is likely to differ from that in Asian populations. Consequently, clinical trials investigating treatments for GA may benefit from including GA subtypes in their eligibility criteria.

The current study has several limitations. First, this was a retrospective study, and some data were unavailable. Second, the current diagnostic criteria for pachychoroid GA continue to evolve. Choroidal thickness varies with age and axial length,²⁷ which may need to be considered at the time of diagnosis. In addition, it is often difficult to distinguish

between inherited diseases such as Stargardt disease and pachychoroid GA. In this study, patients with macular atrophy for whom inherited diseases could not be ruled out were excluded. Third, we excluded patients with a history of chronic CSC to distinguish focal atrophy due to CSC. However, determining such a history of CSC is often difficult because the condition may present subclinically. Fourth, the baseline GA area in most patients with pachychoroid GA in our cohort was small, and information on large-sized pachychoroid GA was not available. Finally, the current study did not include genetic information. Further long-term observation of a larger number of patients with pachychoroid GA, accounting for genetic information, is required to elucidate the natural course, including the GA progression rate and pathogenesis.

In conclusion, this study provides insight into the clinical characteristics of pachychoroid and conventional drusen-related GA. Asian patients with GA were male dominant and had small lesions, a relatively thick choroid, and a low GA progression rate. The high prevalence of pachychoroid GA may account for its clinical characteristics in Asian populations. Conventional drusen-related GA observed in Asian populations is similar to that observed in White populations. Researchers should consider these differences in GA subtypes when designing studies and considering interventions for GA.

Footnotes and Disclosures

Originally received: November 8, 2023.

Final revision: March 5, 2024.

Accepted: April 2, 2024.

Available online: April 10, 2024. Manuscript no. XOPS-D-23-00283.

¹ Department of Ophthalmology and Visual Sciences, Kyoto University Graduate School of Medicine, Kyoto, Japan.

² Department of Ophthalmology, Graduate School of Medicine, University of the Ryukyus, Nishihara, Okinawa, Japan.

³ Department of Ophthalmology, Graduate School of Medicine, Osaka University, Osaka, Japan.

⁴ Department of Ophthalmology, Yokohama City University Medical Center, Yokohama, Japan.

⁵ Department of Ophthalmology, Tokyo Women's Medical University, Tokyo, Japan.

⁶ Department of Ophthalmology, Kansai Medical University, Hirakata, Osaka, Japan.

⁷ Department of Ophthalmology and Micro-Technology, Yokohama City University, Yokohama, Japan.

⁸ Department of Ophthalmology, Kagoshima University, Kagoshima, Japan.

Disclosures:

All authors have completed and submitted the ICMJE disclosures form.

The authors made the following disclosures:

N. U.-A.: Financial support — Chugai Pharmaceutical; Lecturer — Santen Pharmaceutical, Novartis Pharma, Chugai Pharmaceutical, Bayer Yakuhin; Ayako Takahashi: Lecturer — Santen Pharmaceutical, Novartis Pharma, Bayer Yakuhin, MSD.

M. M.: Financial support — Novartis Pharma, Daiich-Sankyo, KANEKA CORPORATION; Lecturer — Bayer Yakuhin, Kowa Pharmaceutical, Alcon Japan, Santen Pharmaceutical, Novartis Pharma, AMO Japan, Santen Pharmaceutical, Senju Pharmaceutical, Johnson & Johnson K.K., Chugai Pharmaceutical, Japan Ophthalmic Instrument Association, Findex, TOPCON CORPORATION.

Y. M.: Lecturer — Santen Pharmaceutical; Yasunori Miyara: Financial support — Senju Pharmaceutical.

C. H.: Lecturer — Santen Pharmaceutical, Novartis Pharma, Chugai Pharmaceutical, Bayer Yakuhin.

R. M.: Lecturer — Kyowa Kirin, Chugai Pharmaceutical.

H. K.: Financial support — Novartis Pharma, Alcon Japan, Bayer Yakuhin, HOYA, Senju Pharmaceutical, Santen Pharmaceutical, AMO Japan, Otsuka Pharmaceutical, Staar Japan, Pfizer, KOWA Pharmaceutical, Nikon, Chugai Pharmaceutical, TOMEY, Canon; Consultant — Novartis Pharma, Bayer Yakuhin, Chugai Pharmaceutical, Roche, Allergan, Boehringer Ingelheim, Otsuka, Janssen Pharmaceutical; Lecturer — Novartis Pharma, Alcon Japan, Bayer Yakuhin, Senju Pharmaceutical, Santen Pharmaceutical, Chugai Pharmaceutical, Kowa Pharmaceutical, HOYA, AMO Japan, Otsuka Pharmaceutical, Pfizer, Bausch & Lomb, JFC, Canon, Nidek, Topcon, AbbVie GK, TOMEY, Sumitomo Pharma, Chugai Pharmaceutical, Roche, Sanofi, Inami.

Y. Y.: Financial support — Alcon Japan, Sanbio; Consultant — Roche, Boehringer Ingelheim; Lecturer — Chugai Pharmaceutical, Novartis Pharma, Bayer Yakuhin, Santen Pharmaceutical, Novartis India Ltd., Boehringer Ingelheim, Senju Pharmaceutical, Roche; Shares - DeepEyeVision Ltd.

T. I.: Financial support — Nidek, Topcon, Santen Pharmaceutical, Alcon Japan, Novartis Pharma, Senju Pharmaceutical, HOYA, AMO Japan, Pfizer, Otsuka Pharmaceutical; Consultant — Bayer Yakuhin, Novartis Pharma, Chugai Pharmaceutical, Boehringer Ingelheim Japan, Senju Pharmaceutical, Kyowa-kirin, Janssen Pharma; Patent — Topcon; Lecturer — Bayer Yakuhin, Novartis Pharma, Alcon Japan, Santen Pharmaceutical, Senju Pharmaceutical, Topcon, Chugai Pharmaceutical, Canon, Nidek, Otsuka Pharmaceutical, Nikon.

K. T.: Financial support — Santen Pharmaceutical, Bayer Yakuhin, Novartis Pharma, Chugai Pharmaceutical; Consultant — Senju Pharmaceutical, Kyowa-kirin; Lecturer — Santen Pharmaceutical, Bayer Yakuhin, Novartis Pharma, Senju Pharmaceutical, Chugai Pharmaceutical, Alcon Japan, Topcon, Canon, Nidek, Otsuka Pharmaceutical, Nikon.

T. S.: Financial support — Novartis Pharma, Bayer Yakuhin, Senju Pharmaceutical, Santen Pharmaceutical, Alcon Japan, Chugai Pharmaceutical, Bausch & Lomb, Kubota Pharm, Roche; Lecturer — Novartis Pharma, Bayer Yakuhin, Senju Pharmaceutical, Santen Pharmaceutical, Alcon Japan, Chugai Pharmaceutical, Bausch & Lomb, Otsuka Pharm; Grants - Health and Labor Sciences Research Grants for Research on Rare and Intractable Diseases (Grant number 20FC1029).

A. T.: Financial support — Canon, Findex, Santen Pharmaceutical, Sumitomo Pharma, AMO Japan, Senju Pharmaceutical, Wakamoto

Pharmaceutical, Alcon Japan, Otsuka Pharmaceutical, Bayer Yakuhin, Rhoto Nitten; Consultant — Senju Pharmaceutical, Boehringer Ingelheim, Bayer Yakuhin, Novartis Pharma, Sumitomo Pharma, Kyowa Kirin, Chugai Pharmaceutical; Lecturer — Bayer Yakuhin, Senju Pharmaceutical, Novartis Pharma, Santen Pharmaceutical, Alcon Japan, AMO Japan, Kowa Company, Canon, Otsuka Pharmaceutical, Wakamoto Pharmaceutical, MSD, Ellex, NIDEK CO LTD, Chugai Pharmaceutical, Johnson & Johnson K.K., Rhoto Pharmaceutical, Nikon Solutions.

This study was supported by Health and Labor Sciences Research Grants for Research on Rare and Intractable Diseases (Grant number JPMH20FC1029 and JPMH23FC1043) and the Japan Society for the Promotion of Science Grants-in-Aid for Scientific Research (JSPS KAKENHI Grant number JP 21K16895) [to N.U.-A.]. The funding organizations had no role in the design or conduct of this research. The sponsor or funding organization had no role in the design or conduct of the study.

HUMAN SUBJECTS: Human subjects data were included in this study. This study adhered to the principles of the Declaration of Helsinki and was approved by the Institutional Review Board and Ethics Committee of Kyoto University Graduate School of Medicine. The requirement for written informed consent was waived because this was a retrospective study and only anonymized data were used for analysis.

No animal subjects were included in this study.

Author Contribution:

Conception and design: Sato, Ueda-Arakawa, Takahashi, Miyake, Mori, Koizumi, Maruyama-Inoue, Yanagi, Iida, Takahashi, Sakamoto, Tsujikawa
Analysis and interpretation: Sato, Ueda-Arakawa, Takahashi, Miyara, Hara, Kitajima, Maruko, Kawai, Takahashi

Data collection: Sato, Ueda-Arakawa, Takahashi, Miyake, Mori, Koizumi, Maruyama-Inoue, Yanagi, Iida, Takahashi, Sakamoto, Tsujikawa, Miyara, Hara, Kitajima, Maruko, Kawai, Takahashi

Obtained funding: Ueda-Arakawa

Overall responsibility: Sato, Ueda-Arakawa, Takahashi, Miyake, Mori, Koizumi, Maruyama-Inoue, Yanagi, Iida, Takahashi, Sakamoto, Tsujikawa, Miyara, Hara, Kitajima, Maruko, Kawai, Takahashi

Meeting presentation: None.

Abbreviations and Acronyms:

BCVA = Best-corrected visual acuity; **CFP** = color fundus photography; **CSC** = central serous chorioretinopathy; **EDI** = enhanced depth imaging; **FAF** = fundus autofluorescence; **GA** = geographic atrophy; **logMAR** = logarithm of the minimum angle of resolution; **SD** = spectral-domain; **SFCT** = subfoveal choroidal thickness; **SQRT** = square-root transformation; **SS** = swept-source.

Keywords:

Age-related macular degeneration, Geographic atrophy, Japanese, Pachychoroid geographic atrophy, Subtype.

Correspondence:

Naoko Ueda-Arakawa, MD, PhD (Kyoto Univ), Department of Ophthalmology and Visual Sciences, Kyoto University Graduate School of Medicine, 54 Shogoin Kawahara, Sakyo, Kyoto 606-8507, Japan. E-mail: naokosp@kuhp.kyoto-u.ac.jp.

References

1. Flaxman SR, Bourne RRA, Resnikoff S, et al. Global causes of blindness and distance vision impairment 1990-2020: a systematic review and meta-analysis. *Lancet Glob Health*. 2017;5:e1221–e1234.
2. Pfau M, von der Emde L, de Sistiernes L, et al. Progression of photoreceptor degeneration in geographic atrophy secondary to age-related macular degeneration. *JAMA Ophthalmol*. 2020;138:1026–1034.

3. Rim TH, Kawasaki R, Tham YC, et al. Prevalence and pattern of geographic atrophy in asia: the Asian eye Epidemiology consortium. *Ophthalmology*. 2020;127:1371–1381.
4. Rudnicka AR, Jarrar Z, Wormald R, et al. Age and gender variations in age-related macular degeneration prevalence in populations of European ancestry: a meta-analysis. *Ophthalmology*. 2012;119:571–580.
5. Liao DS, Grossi FV, El Mehdi D, et al. Complement C3 inhibitor Pegcetacoplan for geographic atrophy secondary to age-related macular degeneration: a randomized phase 2 trial. *Ophthalmology*. 2020;127:186–195.
6. J Jaffe GJ, Westby K, Csaky KG, et al. C5 inhibitor Avacincaptad pegol for geographic atrophy due to age-related macular degeneration: a randomized pivotal phase 2/3 trial. *Ophthalmology*. 2021;128:576–586.
7. Sato Y, Ueda-Arakawa N, Takahashi A, et al. Clinical characteristics and progression of geographic atrophy in a Japanese population. *Ophthalmol Retina*. 2023;7:901–909.
8. Takahashi K, Shiraga F, Ishida S, et al. [Diagnostic criteria for atrophic age-related macular degeneration]. *Nippon Ganka Gakkai Zasshi*. 2015;119:671–677.
9. Tsujikawa A, Takahashi K, Obata R, et al. Dry age-related macular degeneration in the Japanese population. *Jpn J Ophthalmol*. 2022;66:8–13.
10. Spaide RF, Koizumi H, Pozzoni MC. Enhanced depth imaging spectral-domain optical coherence tomography. *Am J Ophthalmol*. 2008;146:496–500.
11. Takahashi A, Ooto S, Yamashiro K, et al. Pachychoroid geographic atrophy: clinical and genetic characteristics. *Ophthalmol Retina*. 2018;2:295–305.
12. Feuer WJ, Yehoshua Z, Gregori G, et al. Square root transformation of geographic atrophy area measurements to eliminate dependence of growth rates on baseline lesion measurements: a reanalysis of Age-Related Eye Disease study report no. 26. *JAMA Ophthalmol*. 2013;131:110–111.
13. Teo KYC, Fujimoto S, Sadda SR, et al. Geographic atrophy phenotypes in subjects of different ethnicity: Asia-Pacific ocular imaging society work group report 3. *Ophthalmol Retina*. 2023;7(7):593–604.
14. Cheung CMG, Lee WK, Koizumi H, et al. Pachychoroid disease. *Eye (Lond)*. 2019;33(1):14–33.
15. Lindblad AS, Lloyd PC, Clemons TE, et al. Change in area of geographic atrophy in the Age-Related Eye Disease study AREDS report number 26. *Arch Ophthalmol*. 2009;127:1168–1174.
16. Yehoshua Z, Rosenfeld PJ, Gregori G, et al. Progression of geographic atrophy in age-related macular degeneration imaged with spectral domain optical coherence tomography. *Ophthalmology*. 2011;118:679–686.
17. Holz FG, Bindewald-Wittich A, Fleckenstein M, et al. Progression of geographic atrophy and impact of fundus autofluorescence patterns in age-related macular degeneration. *Am J Ophthalmol*. 2007;143:463–472.
18. Klein R, Meuer SM, Knudtson MD, Klein BE. The epidemiology of progression of pure geographic atrophy: the Beaver Dam Eye study. *Am J Ophthalmol*. 2008;146:692–699.
19. Holekamp N, Wykoff CC, Schmitz-Valckenberg S, et al. Natural history of geographic atrophy secondary to age-related macular degeneration: results from the prospective Proxima A and B clinical trials. *Ophthalmology*. 2020;127:769–783.
20. Agrón E, Domalpally A, Cukras CA, et al. Reticular pseudodrusen status, ARMS2/HTRA1 genotype, and geographic atrophy enlargement: age-Related Eye Disease study 2 report 32. *Ophthalmology*. 2023;130:488–500.
21. Domalpally A, Agrón E, Pak JW, et al. Prevalence, risk, and genetic association of reticular pseudodrusen in age-related macular degeneration: age-Related Eye Disease study 2 report 21. *Ophthalmology*. 2019;126:1659–1666.
22. Gabrielle PH, Seydou A, Arnould L, et al. Subretinal drusenoid deposits in the elderly in a population-based study (the Montra-chet study). *Invest Ophthalmol Vis Sci*. 2019;60:4838–4848.
23. Fritsche LG, Igl W, Bailey JN, et al. A large genome-wide association study of age-related macular degeneration highlights contributions of rare and common variants. *Nat Genet*. 2016;48:134–143.
24. Yates JR, Sepp T, Matharu BK, et al. Complement C3 variant and the risk of age-related macular degeneration. *N Engl J Med*. 2007;357:553–561.
25. Hilely A, Au A, Lee WK, et al. Pachyvittelliform maculopathy: an optical coherence tomography analysis of a novel entity. *Br J Ophthalmol*. 2023;0:1–7.
26. Iovino C, Ramtohul P, Au A, et al. Vittelliform maculopathy: diverse etiologies originating from one common pathway. *Surv Ophthalmol*. 2023;68:361–379.
27. Wei WB, Xu L, Jonas JB, et al. Subfoveal choroidal thickness: the Beijing Eye study. *Ophthalmology*. 2013;120:175–180.

厚生労働科学研究費補助金（難治性疾患政策研究事業）
分担研究報告書

網膜色素変性に関する研究

研究分担者	宮崎大学・医学部・教授 池田 康博
	名古屋大学・医学系研究科・教授 西口 康二
研究協力者	長崎大学・医学系研究科・教授 大石 明生
	(株) ビジョンケア 高橋 政代
	神戸アイセンター病院・副院長 平見 恭彦
	九州大学・医学系研究科・准教授 村上 祐介

研究要旨

網膜色素変性は眼科における難病として患者数が最も多い疾患である。現在我々は患者レジストリを進めており、そのデータを研究や新規治療法に利活用する試みを行なっている。令和6年末の時点で現在の登録数は約5600名であり、さらなる登録数増加に向けて参加施設数を増やすことなどを検討している。また、「網膜色素変性の診療ガイドライン」は約10年前に作成されたもので改訂が必要な時期となっており、令和6年よりガイドライン改訂メンバーを組織してガイドラインの第2版作成を開始している。改訂版ではMinds方式に従ってクリニカルクエスションとその回答を加える予定である。さらに、患者会であるJRPSと連携を強化し、患者会総会や講演会などにおいて最近の研究成果や新しい情報などを提供する活動を続けていく予定である。

A. 研究目的

網膜色素変性は眼科における難病で患者数が最も多い疾患である。罹患数はおよそ3000-4000人に1人であり、夜盲、視野狭窄などの症状で発症して徐々に進行し、末期には重度の視機能障害に至りうる疾患である。原因となる遺伝子は数多くあり、現時点ではRPR65遺伝子異常による稀なタイプを除けば治療法がない状態である。令和6年度の目的は以下の2つである。

(1) 患者レジストリ数の増加

これまで我々は難病プラットフォームを活用して網膜色素変性の患者レジストリ

を進めてきた。これをさらに推進して登録患者数を増やす。

(2) 診療ガイドラインの改訂

網膜色素変性の診療ガイドラインは2016年に作成されているが、その内容のいくつかは古くなっている。そこで改訂が必要な部分を修正することにより、改訂版の網膜色素変性の診療ガイドライン作成を進めることを目標にする。

(3) 患者や家族への啓発活動

網膜色素変性は、患者会「公益社団法人 日本網膜色素変性症協会：JRPS」が組織されており、多くの各都道府県に支部も

存在する。患者やその家族に対する情報提供を促進する目的で患者会の全国大会や支部会に参加して最新の研究成果を説明する情報提供を促進する。

B. 研究方法

(1) 患者レジストリ数の増加

研究者から前回の登録を行なった後にさらに受診した患者のデータなどをまとめて一括登録してもらうように協力施設に依頼する。また、遺伝性網膜疾患の診療や遺伝子診断を多く実施している施設に声をかけて参加施設をさらに増やす。

(2) 診療ガイドラインの改訂

現在網膜色素変性を実際に診療している研究者 10 名程度に声をかけて参加メンバーを募り、最終的には令和 7 年の 9 月を目処に診療ガイドライン改定して、日本眼科学会のガイドライン委員会に提出することを予定している。

(3) 全国および支部の患者会に積極的に参加し、患者と家族と情報交換を行う。

(倫理面への配慮)

レジストリ研究にあたっては倫理委員会承認のもと登録を開始している。また、遺伝子診断については各施設での倫理委員会承認のもと解析を行っている。

C. 研究結果

(1) 患者レジストリ数の増加

令和 6 年度末の段階で、網膜色素変性患者レジストリの参加施設は 27 施設であり、登録患者数は約 5600 名であった。

(2) ガイドラインの改訂

現時点では、以下のような構成案でガ

イドラインの改訂を行なっている。

本文（全体を通して：常染色体優性、劣性を 常染色体顕性（優性）、 常染色体潜性（劣性）に変更する。）

I 定義、病因、疫学

（II 病型分類→杯体ジストロフィーを除外）

III 網膜色素変性の類縁疾患

IV 診断

V 鑑別診断

VI 治療

（VII 開発研究中の治療→「VII クリニカルクエスト」に変更）

クリニカルクエスト（案）

CQ1: 視機能障害の進行を抑制できる内服薬やサプリメント、点眼薬は存在するか？

CQ2: 白内障手術を施行するタイミングは？

CQ3: 黄斑浮腫の治療（薬物治療）

CQ4: 黄斑合併症の治療（手術治療）

CQ5: 遺伝子検査は推奨されるか？

CQ6: 出生前診断や着床前診断を行うことができるか？

CQ7: 疾患の進行を抑制させる因子、悪化させる因子はあるか？

CQ8: 現在開発中の治療はあるか？（人工網膜、細胞移植、オプトジェネティクス等を含む）

(3) 患者や家族への啓発活動

令和 6 年度の JRPS 患者会は 9 月 24 日に大分で行われ、研究受賞者の研究内容の紹介とともに網膜色素変性の治療に向けた日本および世界の動向について池田が説明を行った。

また、10 月 14 日には東京で JRPS 創立

30 周年記念特別座談会：「遺伝性網膜疾患診療における課題と展望」が開催され、近藤司会のもと最新の情報提供を行った。

D. 考察

(1) 患者レジストリ数の増加

レジストリ患者数に関しては、令和 6 年末の時点で、約 5600 例の症例データが登録されている。登録は各施設で継続中であるが、現時点で目標（約 7000 例）の達成は困難な状況となっている。そのため、登録施設の追加を含め改善策を検討中である。

(2) 診療ガイドラインの改訂

2016 年に作成された診療ガイドラインは、特に遺伝子検査、病態メカニズム、治療法などについて改訂が必要と考えられていた。現在は新しいガイドライン改訂メンバーとともに部分的に分担して改訂を進めている。今回のガイドラインでは Minds 方式に従ってクリニカルクエスチョンとその回答を加えることで、診療する医師にとつ

てわかりやすいガイドラインとすることを目指している。

(3) 患者や家族への啓発活動

網膜色素変性は眼科において難病として登録されている患者が最も多い疾患であり、患者会の活動も活発である。本研究グループのグループ長の池田は患者会 JRPS の学術理事を務めており、今後も患者会やホームページを通じて患者および家族と密な情報交換を行っていく予定である

E. 結論

患者レジストリ数のさらなる増加に向けて活動を行う。網膜色素変性の診療ガイドラインの改訂を進め、診療する医師により役立つガイドラインを作成する。患者会や難病 HP などを通じて、患者および家族との交流を深める。

F. 健康危険情報

なし

G. 研究発表

1. 論文発表

- 1) Murakami Y, Hisai T, Shimokawa S, Fukushima M, Fujiwara K, Hirata A, Takada A, Miyahara F, Nakashima N, Kobayakawa Y, Arima M, Mawatari G, Ishizu M, Kaida T, Miyata K, Ikeda Y, Sonoda KH. Study protocol for a prospective natural history registry investigating the relationships between inflammatory markers and disease progression in retinitis pigmentosa: the RP-PRIMARY study. Jpn J Ophthalmol. 2025 Online ahead of print.
- 2) Fukushima M, Tao Y, Shimokawa S, Zhao H, Shimokawa S, Funatsu J, Hisai T, Okita A, Fujiwara K, Hisatomi T, Takeda A, Ikeda Y, Sonoda KH, Murakami Y. Comparison of Microperimetry and Static Perimetry for Evaluating Macular Function and Progression in Retinitis Pigmentosa. Ophthalmol Sci. 2024 Jul 20;4(6):100582.

- 3) Mawatari G, Hiwatashi S, Motani T, Nagatomo S, Ando E, Kuwahata T, Ishizu M, Ikeda Y. Efficacy of a wearable night-vision aid in patients with concentric peripheral visual field loss: a randomized, crossover trial. *Jpn J Ophthalmol*. 2024 Jul;68(4):321-326.
- 4) Goto K, Koyanagi Y, Akiyama M, Murakami Y, Fukushima M, Fujiwara K, Iijima H, Yamaguchi M, Endo M, Hashimoto K, Ishizu M, Hirakata T, Mizobuchi K, Takayama M, Ota J, Sajiki AF, Kominami T, Ushida H, Fujita K, Kaneko H, Ueno S, Hayashi T, Terao C, Hotta Y, Murakami A, Kuniyoshi K, Kusaka S, Wada Y, Abe T, Nakazawa T, Ikeda Y, Momozawa Y, Sonoda KH, Nishiguchi KM. Disease-specific variant interpretation highlighted the genetic findings in 2325 Japanese patients with retinitis pigmentosa and allied diseases. *J Med Genet*. 2024 Jun 20;61(7):613-620.
- 5) Kominami T, Tan TE, Ushida H, Jain K, Goto K, Bylstra YM, Sajiki AF, Mathur RS, Ota J, Lim WK, Nishiguchi KM, Fenner BJ. Fundus autofluorescence features specific for EYS-associated retinitis pigmentosa. *PLoS One*. 2025 Feb 19;20(2):e0318857.
- 6) Kominami T, Ueno S, Ota J, Inooka T, Oda M, Mori K, Nishiguchi KM. Classification of fundus autofluorescence images based on macular function in retinitis pigmentosa using convolutional neural networks. *Jpn J Ophthalmol*. 2025 Mar;69(2):236-244.
- 7) Natsume K, Kominami T, Goto K, Koyanagi Y, Inooka T, Ota J, Kawano K, Yamada K, Okuda D, Yuki K, Nishiguchi KM, Ushida H. Phenotypic variability of RP1-related inherited retinal dystrophy associated with the c.5797 C > T (p.Arg1933*) variant in the Japanese population. *Sci Rep*. 2024 Oct 27;14(1):25669.
- 8) Hirami Y, Mandai M. The potential of induced pluripotent stem cell-derived retinal organoids in regenerative medicine. *Regen Med*. 2024 May 3;19(5):221-224.
- 9) Hiraoka M, Urakawa Y, Kawai K, Yoshida A, Hosakawa J, Takazawa M, Inaba A, Yokota S, Hirami Y, Takahashi M, Ohara O, Kurimoto Y, Maeda A. Copy number variant detection using next-generation sequencing in EYS-associated retinitis pigmentosa. *PLoS One*. 2024 Jun 24;19(6):e0305812.
- 10) Ikeda HO, Hasegawa T, Abe H, Amino Y, Nakagawa T, Tada H, Miyata M, Oishi A, Morita S, Tsujikawa A. Efficacy and Safety of Branched Chain Amino Acids on Retinitis Pigmentosa: A Randomized, Double-Blind, Placebo-Controlled Clinical Trial. *Transl Vis Sci Technol*. 2024 Aug 1;13(8):29.


2. 学会発表

- 1) 網膜色素変性で視力を尽くさぬために～治療法開発の試み～，池田康博，第 128 回日本眼科学会総会市民公開講座，2024/4/21，国内.
- 2) 眼疾患に対する遺伝子治療の現状，池田康博，JSGCT（日本遺伝子細胞治療学会）教育プログラム 2024，2024/7/15，国内.
- 3) 網膜色素変性に対する視細胞保護遺伝子治療の医師主導治験（第 1/2a 相），池田康博，第 63 回日本網膜硝子体学会総会（シンポジウム），2024/12/7，国内.

H. 知的財産権の出願・登録状況

1. 特許取得 なし
2. 実用新案登録 なし
3. その他 なし

Disease-specific variant interpretation highlighted the genetic findings in 2325 Japanese patients with retinitis pigmentosa and allied diseases

Kensuke Goto ¹, Yoshito Koyanagi,^{1,2} Masato Akiyama,^{2,3} Yusuke Murakami,² Masatoshi Fukushima,² Kohta Fujiwara,² Hanae Iijima,⁴ Mitsuyo Yamaguchi,⁴ Mikiko Endo,⁵ Kazuki Hashimoto,⁶ Masataka Ishizu,⁷ Toshiaki Hirakata,⁸ Kei Mizobuchi,⁹ Masakazu Takayama,¹⁰ Junya Ota,¹ Ai Fujita Sajiki,¹ Taro Kominami,¹ Hiroaki Ushida,¹ Kosuke Fujita,¹ Hiroki Kaneko,¹ Shinji Ueno,^{1,11} Takaaki Hayashi,⁹ Chikashi Terao,¹² Yoshihiro Hotta,¹⁰ Akira Murakami,⁸ Kazuki Kuniyoshi,¹³ Shunji Kusaka,¹³ Yuko Wada,¹⁴ Toshiaki Abe,¹⁵ Toru Nakazawa,⁶ Yasuhiro Ikeda,⁷ Yukihide Momozawa,⁴ Koh-Hei Sonoda,² Koji M Nishiguchi¹

► Additional supplemental material is published online only. To view, please visit the journal online (<https://doi.org/10.1136/jmg-2023-109750>).

For numbered affiliations see end of article.

Correspondence to

Dr Koji M Nishiguchi, Department of Ophthalmology, Nagoya University Graduate School of Medicine, Nagoya, 466-8560, Japan; kmn@med.nagoya-u.ac.jp and Professor Koh-Hei Sonoda, Department of Ophthalmology, Graduate School of Medical Sciences, Kyushu University, Fukuoka, 812-8582, Japan; k.sonoda.a74@m.kyushu-u.ac.jp

KG and YK contributed equally.

Received 10 November 2023
Accepted 2 March 2024



© Author(s) (or their employer(s)) 2024. No commercial re-use. See rights and permissions. Published by BMJ.

To cite: Goto K, Koyanagi Y, Akiyama M, *et al.* *J Med Genet* Epub ahead of print: [please include Day Month Year]. doi:10.1136/jmg-2023-109750

ABSTRACT

Background As gene-specific therapy for inherited retinal dystrophy (IRD) advances, unified variant interpretation across institutes is becoming increasingly important. This study aims to update the genetic findings of 86 retinitis pigmentosa (RP)-related genes in a large number of Japanese patients with RP by applying the standardised variant interpretation guidelines for Japanese patients with IRD (J-IRD-VI guidelines) built upon the American College of Medical Genetics and Genomics and the Association for Molecular Pathology rules, and assess the contribution of these genes in RP-allied diseases.

Methods We assessed 2325 probands with RP (n=2155, including n=1204 sequenced previously with the same sequencing panel) and allied diseases (n=170, newly analysed), including Usher syndrome, Leber congenital amaurosis and cone-rod dystrophy (CRD). Target sequencing using a panel of 86 genes was performed. The variants were interpreted according to the J-IRD-VI guidelines.

Results A total of 3564 variants were detected, of which 524 variants were interpreted as pathogenic or likely pathogenic. Among these 524 variants, 280 (53.4%) had been either undetected or interpreted as variants of unknown significance or benign variants in our earlier study of 1204 patients with RP. This led to a genetic diagnostic rate in 38.6% of patients with RP, with *EYS* accounting for 46.7% of the genetically solved patients, showing a 9% increase in diagnostic rate from our earlier study. The genetic diagnostic rate for patients with CRD was 28.2%, with RP-related genes significantly contributing over other allied diseases.

Conclusion A large-scale genetic analysis using the J-IRD-VI guidelines highlighted the population-specific genetic findings for Japanese patients with IRD; these findings serve as a foundation for the clinical application of gene-specific therapies.

INTRODUCTION

Inherited retinal dystrophy (IRD) is a disorder characterised by the degeneration of photoreceptors and the retinal pigment epithelium, leading

WHAT IS ALREADY KNOWN ON THIS TOPIC

⇒ Genetic screening studies for retinitis pigmentosa (RP) have reported variable diagnosis rates due to variant interpretation criteria.

WHAT THIS STUDY ADDS

⇒ Applying the Japanese inherited retinal dystrophy variant interpretation guidelines resulted in the detection of 107 new disease-associated variants, leading to a 9% increase in the genetic diagnosis rate for patients with RP compared with our earlier study.

HOW THIS STUDY MIGHT AFFECT RESEARCH, PRACTICE OR POLICY

⇒ This result allowed us to substantially update the genetic background of Japanese patients with RP and may provide an important foundation for gene-specific therapy for RP.

to symptoms such as night blindness and visual impairment.^{1–3} Retinitis pigmentosa (RP, OMIM 268000) is the most common form of IRD, with a prevalence of approximately 1 in 3000–4000 people; thus, an estimated 2.5 million people worldwide have RP.^{1–4} Recent advancements in gene/variant-specific therapies suggest that IRD might now be amenable to interventions.⁵ Given the progress of genomic medicine, there is a growing interest in the standardised interpretation of variants that can be reproduced by different institutes.

Genetic screening studies for RP have reported variable diagnosis rates, in the range of 37.4–66.6% in Western countries^{6–9} and 29.6–72.1% in Asia.^{10–13} The rate may be lower in Japan, ranging from 29.6% to 47.9%,^{10–14–16} depending on the report. The variation in these figures could arise from whether the American College of Medical Genetics and Genomics and the Association for

Molecular Pathology (ACMG/AMP) guidelines¹⁷ were applied for variant interpretation or how they were applied, as these guidelines require specification of multiple items that take into account the unique biological and epidemiological characteristics of each inherited disease.¹⁸ Without predefined guidelines, variant interpretation can differ substantially between institutes, which may contribute to the variability in genetic interpretation of a given variant.¹⁹ Japan has a different genetic architecture of IRD compared with Western countries and even neighbouring countries,^{14,20,21} leading the Japanese Retina and Vitreous Society to publish a modified set of guidelines, the Japanese inherited retinal dystrophy variant interpretation (J-IRD-VI) guidelines. These guidelines are built upon predefined ACMG/AMP rules based on a thorough discussion among the expert members of key genetic laboratories and allow a uniform interpretation of variants tailored specifically for Japanese patients.²²

In our previous collaborative genetic study using a next-generation sequencing (NGS) panel of 86 genes associated with RP, the rate of genetically solved cases (diagnosis rate) in 1204 patients with RP was 29.6%.¹⁰ However, the ACMG/AMP guidelines were not applied for variant interpretation and a unique set of criteria was adopted, which relied heavily on the interpretation of previous reports, without taking into consideration the quality of the evidence provided in the literature. In addition, only typical RP phenotype was included in the study, leaving out the genetic background of allied diseases, which are sometimes difficult to differentiate from RP.

The purpose of this study was to update the genetic findings using the J-IRD-VI guidelines and expand our assessment to include a larger number of patients, especially those with a phenotype that overlapped with RP. This study may serve as a foundation for future gene/variant-specific therapies for IRD in Japan.

MATERIALS AND METHODS

Study subjects

An overview of the study is shown in [figure 1](#). We collected DNA samples from 2662 patients with IRD from nine Japanese facilities in the Japan Retinitis Pigmentosa Registry Project (2002–2021), namely Nagoya University Hospital (n=790), Kyushu University Hospital (n=706), Tohoku University Hospital (n=336), Yuko Wada Eye Clinic (n=327), Kindai University Hospital (n=203), University of Miyazaki Hospital and Miyata Eye Hospital (n=112), Juntendo University Hospital (n=87), the Jikei University Hospital (n=63) and Hamamatsu University Hospital (n=38).

Patient selection

From a total of 2662 patients, we selected for analysis patients with RP and patients with allied diseases with clinical findings that overlap with RP, including Usher syndrome, Leber congenital amaurosis (LCA), cone-rod dystrophy (CRD), choroideraemia and Bietti crystalline dystrophy (BCD). Clinical diagnoses were made by well-trained ophthalmologists based on symptoms such as visual acuity loss, visual field loss, photophobia and night blindness, fundus examination, electroretinogram, fundus autofluorescence images and optical coherence tomography images. We excluded patients (n=258) with IRD with substantially different phenotypes from RP. We also excluded related patients (n=80). As a result, we enrolled 2325 probands with non-syndromic RP (n=2155, including n=1204 we had previously sequenced with the same sequencing panel¹⁰) or allied diseases (n=170), such as Usher syndrome (n=32), LCA (n=15), CRD (n=78), choroideraemia (n=11) or BCD (n=34).

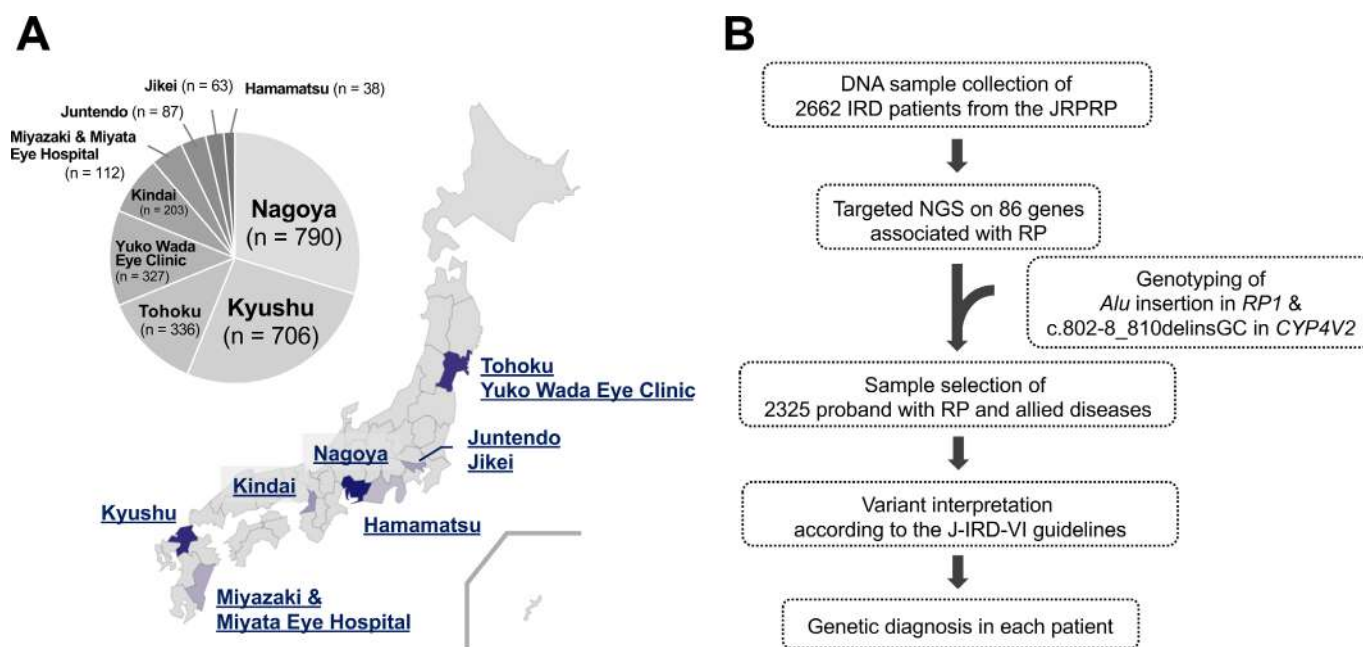


Figure 1 Japanese facilities collecting patients with IRD and workflow overview in this study. (A) The proportion of 2662 patients with IRD from nine facilities across Japan and their geographical distribution. (B) The workflow following DNA sample collection. Hamamatsu, Hamamatsu University Hospital; IRD, inherited retinal dystrophy; Jikei, the Jikei University Hospital; J-IRD-VI, Japanese inherited retinal dystrophy variant interpretation; JRPRP, Japan Retinitis Pigmentosa Registry Project; Juntendo, Juntendo University Hospital; Kindai, Kindai University Hospital; Kyushu, Kyushu University Hospital; Miyazaki, University of Miyazaki Hospital; Nagoya, Nagoya University Hospital; NGS, next-generation sequencing; RP, retinitis pigmentosa; Tohoku, Tohoku University Hospital.

Table 1 Characteristics of 2325 patients with RP and allied diseases

Diagnosis	RP	Usher syndrome	LCA	CRD	Choroideraemia	BCD
Patients, n	2155	32	15	78	11	34
Sex (male/female)	1020/1135	12/20	6/9	46/32	11/0	9/25
Age, years	54.2 (4–93)	45.5 (10–80)	25.3 (3–57)	55.4 (3–84)	48.5 (3–84)	55.8 (27–82)
Visual acuity (logMAR), n (%)						
≤0.5	1302 (60.4)	19 (59.4)	2 (13.3)	20 (25.6)	9 (81.8)	20 (58.8)
0.5<, ≤1.3	381 (17.7)	2 (6.3)	4 (26.7)	38 (48.7)	1 (9.1)	7 (20.6)
>1.3	391 (18.1)	9 (28.1)	8 (53.3)	18 (23.1)	1 (9.1)	6 (17.6)
Unknown	81 (3.8)	2 (6.3)	1 (6.7)	2 (2.6)	0 (0)	1 (2.9)
Inheritance form, n (%)						
AD	284 (13.2)	0 (0)	0 (0)	9 (11.5)	0 (0)	2 (5.9)
AR	410 (19.0)	12 (37.5)	6 (40)	8 (10.3)	0 (0)	12 (35.3)
X linked	34 (1.6)	0 (0)	0 (0)	0 (0)	6 (54.5)	0 (0)
Sporadic	1182 (54.8)	16 (50)	9 (60)	59 (75.6)	3 (27.3)	19 (55.9)
Unknown	245 (11.4)	4 (12.5)	0 (0)	2 (2.6)	2 (18.2)	1 (2.9)
Consanguinity of patients, n (%)	152 (7.1)	2 (6.3)	8 (53.3)	4 (5.1)	0 (0)	3 (8.8)

Visual acuity is derived from the right eye. The values of the decimal visual acuity were converted into the logMAR units. The inheritance forms were determined based on clinical examination and interview.
AD, autosomal dominant; AR, autosomal recessive; BCD, Bietti crystalline dystrophy; CRD, cone-rod dystrophy; LCA, Leber congenital amaurosis; logMAR, logarithm of the minimum angle of resolution; RP, retinitis pigmentosa.

Target sequencing for 86 genes

We used a previously established panel of 86 genes associated with RP and allied diseases.¹⁰ These genes include 83 genes associated with RP that were registered in the Retinal Information Network (RetNet) as of 19 September 2017, as well as 3 additional genes (*CHM*, *CEP290* and *IMPG1*) that are major causative genes for other IRDs. Our study was designed to capture the coding regions of the transcripts as well as 2 bp into each exon-adjacent intron and also include a deep intronic variant, c.2991+1655 A>G, in *CEP290*. Multiplex PCR-based target sequencing for 86 genes was performed using a HiSeq 2500 instrument (Illumina, San Diego, California, USA) as described previously.²³

Analysis of sequencing data

Analysis of sequence data was performed as previous reported.¹⁰ Sequencing reads were demultiplexed using bcl2fastq2 V.2.20 (Illumina), followed by alignment to the human reference genome (hg19) using Burrows-Wheeler Aligner (V.0.7.17). Post-alignment processing, including indel realignment, was performed with the Genome Analysis Toolkit (V.3.7). The final set of identified variants was annotated using ANNOVAR (V.3.4) and SnpEff (V.4.3). We defined the covered region as a region with bases having ≥20 sequencing reads in the target region. The coverage per base was calculated as the number of covered samples divided by the number of all samples. The cover rate per gene (%) was defined as the average coverage per base of

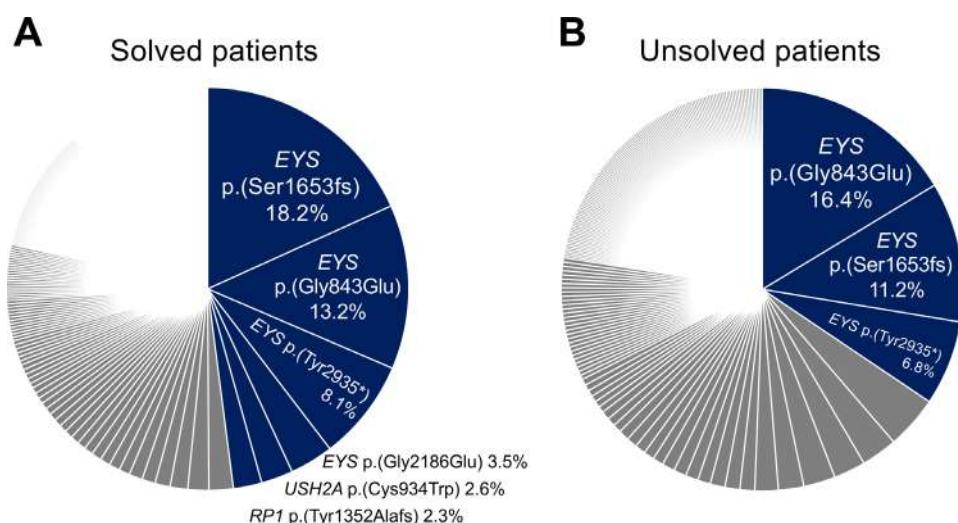


Figure 2 High-frequency pathogenic variants in solved and unsolved patients with RP. (A) The proportion of causative variants detected in solved patients with RP. A total of 1485 alleles of causative variants were detected in solved patients with RP. High-frequency variants detected with more than 30 alleles are highlighted in the blue area. (B) The proportion of pathogenic or likely pathogenic variants carried in unsolved patients with RP. A total of 587 alleles of pathogenic or likely pathogenic variants were detected in unsolved patients with RP. High-frequency variants detected with more than 30 alleles are highlighted in the blue area. RP, retinitis pigmentosa.

the target region. We successfully sequenced $\geq 98.0\%$ of the targeted regions of the 86 genes in all 2325 samples and used all samples for further analysis. The average read depth (\pm SD) was 1410 (± 359) per sample. We called variants in the regions with ≥ 20 read depth, which included 99.65% of the targeted regions (online supplemental table 1). We confirmed the presence of pathogenic variants through visual inspection using the integrative genomics viewer, making manual corrections for annotations when multiple alternative alleles or single-nucleotide variants with deletions were identified at the same site. This led to the reassignment of annotations for 10 variants across four genes (see online supplemental figure 1 and table 2).

Genotyping of the founder variants in *RP1* and *CYP4V2*

In addition to NGS panel of 86 genes, we analysed each of two variants associated with IRDs^{24–26} in a different way, with *Alu* insertion in *RP1* and c.802-8_810del17insGC in *CYP4V2*; these genes are not detectable with our NGS panel. To screen *Alu* insertion in exon 4 in *RP1* in all patients, we searched for *Alu* sequences in FASTQ files obtained by NGS using a grep search program, as previously reported.²⁷ We selected patients for whom we had either detected *Alu* sequences in at least one read or who were heterozygous for pathogenic variants in *RP1* as the subjects for genotyping. Genotyping was performed using an optimised PCR-based method for the selected patients as previously described.²⁴ Among the subjects, 23 patients whose genotyping of *Alu* insertion was previously reported by us²⁴ were referenced for those results. To screen c.802-8_810del17insGC in *CYP4V2* in all patients, we developed a grep search program for FASTQ format files. We searched for a unique 20-base sequence containing c.802-8_810del17insGC in *CYP4V2* using the grep command in Linux (online supplemental table 3), and the allele frequency (AF) is calculated as (alternative allele read count)/[(alternative allele read count)+(reference allele read count)] in all patients. AFs ranging from 0.25 to 0.75 were defined as heterozygotes, while frequencies ranging from 0.85 to 1.0 were defined as homozygotes.

Variant interpretation

Among the 86 genes in our NGS panel, 2 genes that had previously been reported as associated with RP but whose pathogenicity has been questioned by recent studies^{28–30} were excluded from our analysis, resulting in a final set of 84 genes for interpretation of pathogenicity. We interpreted the variants according to the J-IRD-VI guidelines²² published by the Japanese Retina and Vitreous Society. A detailed description of the evaluation procedures is provided below. The automated application AutoPVS1 (<http://autopvs1.genetics.bgi.com/>)³¹ (accessed on 16 August 2022) was used to evaluate the PVS1 criteria for null variants. As defined in the ACMG guideline criteria for hearing loss,³¹ we defined exons containing null variants with an AF exceeding 0.3% in the Genome Aggregation Database (gnomAD)³² as lacking functional significance. To assess the frequency of variants in general populations (BA1, BS1, PM2), we used the gnomAD total population, the gnomAD population max, the Human Genetic Variation Database and Tohoku Medical Megabank Organization (ToMMo) 8.3KJPN. BA1 was not applied based on an expert opinion for variants previously reported as being pathogenic by multiple groups but meeting the BA1 cut-off value (online supplemental table 4).^{33–38} To calculate ORs for minor alleles in the PS4 criteria, ToMMo 38KJPN for autosome and 14KJPN for chromosome X were used as ancestry-matched controls. To evaluate PM3, we counted the number of probands

with heterozygous pathogenic variants and those with homozygotes from both our subject patients and the prior literature listed in the Human Genome Mutation Database Professional (HGMD Professional, V.2022.2). The strength of PM3 was assessed by summing the counts of these two sets of probands. In the computational evidence category (PP3, BP4, BP7), we employed predictive tools: REVEL³⁹ and Splicing AI.⁴⁰ The PP5 criteria were evaluated based on ClinVar (accessed on 20 August 2022). The BP2 criteria were applied to variants founded in cases with homozygous pathogenic variants within the same gene.

Criteria for genetic diagnosis

We performed a genetic diagnosis using the variants regarded as ‘pathogenic’ or ‘likely pathogenic’ by the J-IRD-VI guidelines, as well as the two founder variants, *Alu* insertion in *RP1* and c.802-8_810del17insGC in *CYP4V2*. We applied the genetic inheritance forms defined in RetNet for each gene, following the classic Mendelian inheritance pattern and attempted to determine the causative variant and make a genetic diagnosis in each case as previously reported.¹⁰ If a gene was registered on RetNet in multiple inheritance forms, we determined the genetic inheritance form of each variant based on the prior literature. Furthermore, when a patient had pathogenic variants in multiple genes leading to a genetic diagnosis, all the genes were listed as potential causative genes, rather than selecting just one. Finally, we regarded patients whose causative genes were determined as ‘solved’ and patients whose causative genes could not be determined as ‘unsolved’.

Comparative analysis in variant interpretation with other populations

The J-IRD-VI was applied to variants reported as Caucasians specific in the Leiden Open Variation Database in the previous literature.⁴¹ We chose and interpreted 47 variants in *EYS* according to the J-IRD-VI. The results of interpretation were compared with those according to the ACMG/AMP guidelines in the literature.

RESULTS

Results of variant interpretations of 86 genes in 2325 patients

The clinical characteristics of the patients are summarised in table 1. The modes of inheritance as obtained from both the clinical history of the proband and the examination of the relatives were as follows: autosomal dominant in 284 (13.2%), autosomal recessive in 410 (19.0%), X linked in 34 (1.6%) and sporadic in 1182 (54.8%) (table 1). A comprehensive list of variant interpretation using J-IRD-VI guidelines is shown in online supplemental table 5. We identified a total of 3564 variants, including 2143 missense variants, 169 nonsense variants, 168 frameshift indels, 40 non-frameshift indels, 53 canonical splice site variants and 973 synonymous variants.

The detected variants were interpreted according to the J-IRD-VI guidelines using an in-house program. As a result, 211 variants were interpreted as pathogenic, 313 variants as likely pathogenic, 1880 variants as variants of unknown significance (VUS), 516 variants as likely benign and 644 variants as benign. Among the 524 variants interpreted as pathogenic or likely pathogenic, 209 (39.9%), 249 (47.5%) and 290 (55.3%) had not previously been reported in our earlier study of 1204 patients with typical RP, HGMD or ClinVar, yielding 107 new disease-associated variants. This included 71 variants considered VUS or benign variants in the previous study. At the same time,

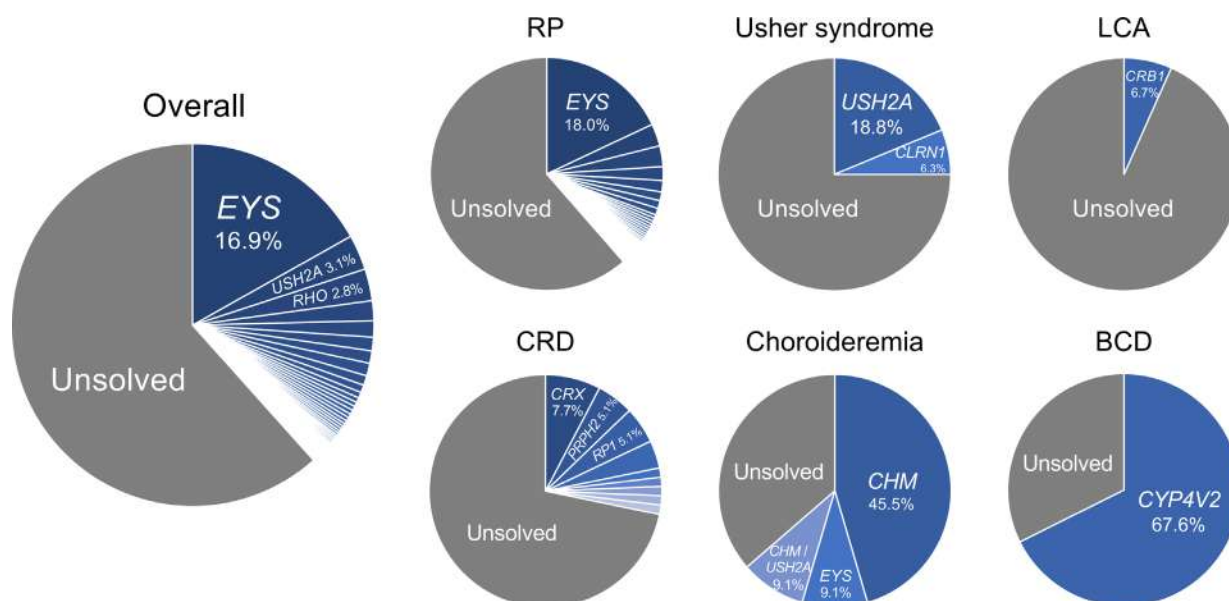


Figure 3 Percentage of solved patients and proportion of causative genes. The pie chart displays the overall and disease-specific diagnostic rates along with the proportion of disease-causing genes. The blue area represents the proportion of genetically solved patients, whereas the grey area represents that of unsolved patients. BCD, Bietti crystalline dystrophy; CRD, cone-rod dystrophy; LCA, Leber congenital amaurosis; RP, retinitis pigmentosa.

118 variants considered pathogenic or likely pathogenic were reassigned to the VUS or benign categories. Thus, only 245 out of 363 pathogenic or likely pathogenic variants (67.5%) in the previous study maintained the same interpretation in the current study.

We applied the J-IRD-VI guidelines to variants in *EYS* reported in Caucasians⁴¹ and found that 29 out of 47 variants (61.7%) maintained the same interpretation in the ACMG/AMP guidelines, while the interpretation changed in 38.3% (online supplemental figure 2). Among these, 13.8% of the pathogenic or likely pathogenic variants in the ACMG/AMP guidelines in the literature were reclassified to VUS (online supplemental table 6).

Genotyping results of *Alu* insertion in *RP1* and c.802-8_810del17insGC in *CYP4V2*

Two frequent variants in *RP1* and *CYP4V2* are known to be associated with RP and allied diseases and are missed by the standard analysis pipeline; thus, we analysed them in a different way. To look for the known common 328bp *Alu* insertion (c.4052_4053ins328, p.(Tyr1352Alafs)) in *RP1*,^{24,26} we conducted screening of FASTQ files using a grep search program²⁷ in all patients. *Alu* sequences were detected in at least one read for 24 patients. Then, we selected a total of 138 patients for whom we either detected *Alu* sequences in at least one read or who were heterozygous for pathogenic variants in *RP1* as the subjects for genotyping. These samples were further analysed with a PCR-based method. We found that 24 patients were heterozygous for the *Alu* insertion and 10 were homozygous. Among the 24 patients who were heterozygous carriers of *Alu* insertions, 18 were found to have another pathogenic variant in *RP1*. As for the splice site variant c.802-8_810del17insGC in *CYP4V2*, which is associated with BCD,²⁵ we screened all patients by searching for a 20-base sequence encompassing the variant region in FASTQ files using software. This revealed that 22 patients, including 16 with RP and 5 with BCD, were heterozygous and 16, including 13 with BCD, were homozygous for this change (online supplemental table 7). Among the 22 patients who were heterozygous,

5 with BCD and 1 with RP were found to have another pathogenic variant in *CYP4V2*.

High-frequency pathogenic variants in solved and unsolved patients with RP

Figure 2 summarises the proportion of causative variants detected in the solved patients with RP (n=831) and pathogenic or likely pathogenic variants detected in unsolved patients with RP (n=1324) (figure 2B). In particular, p.(Ser1653fs), p.(Gly843Glu) and p.(Tyr2935*) in *EYS* and *Alu* insertion (p.(Tyr1352Alafs)) in *RP1* were found in 27.2% (226 of 831), 20.1% (167 of 831), 11.9% (99 of 831) and 2.9% (24 of 831) of solved patients, accounting for 18.2%, 13.2%, 8.1% and 2.3% of the total alleles of causative variants, respectively (figure 2A). Among unsolved patients, 37.0% (490 of 1324) were found to carry pathogenic or likely pathogenic variants. Specifically, p.(Gly843Glu), p.(Ser1653fs) and p.(Tyr2935*) in *EYS* were detected in 7.3% (96 of 1324), 5.0% (66 of 1324) and 3.0% (40 of 1324) of unsolved patients, accounting for 16.4%, 11.2% and 6.8% of the total alleles of pathogenic or likely pathogenic variants carried in unsolved patients, respectively (figure 2B).

Genetic diagnosis with the detected pathogenic variants

The overall genetic diagnosis rate was 38.4% (892 of 2325) for RP and allied diseases (figure 3). The figure was 38.6% (831 of 2155) for RP, 25.0% (8 of 32) for Usher syndrome, 6.7% (1 of 15) for LCA, 28.2% (22 of 78) for CRD, 63.6% (7 of 11) for choroideraemia and 67.6% (23 of 34) for BCD. The results for causative genes and variants for a total of 2325 patients are summarised in online supplemental table 8. Of note, we detected 15 patients with pathogenic or likely pathogenic variants in two genes, including 14 patients with RP and 1 patient with choroideraemia (online supplemental figure 9). Consequently, we conducted the co-segregation analysis in the families of three patients and it allowed us to exclude irrelevant variants and to identify the truly causative genes in all three patients with two causative genes (online supplemental figure 3).

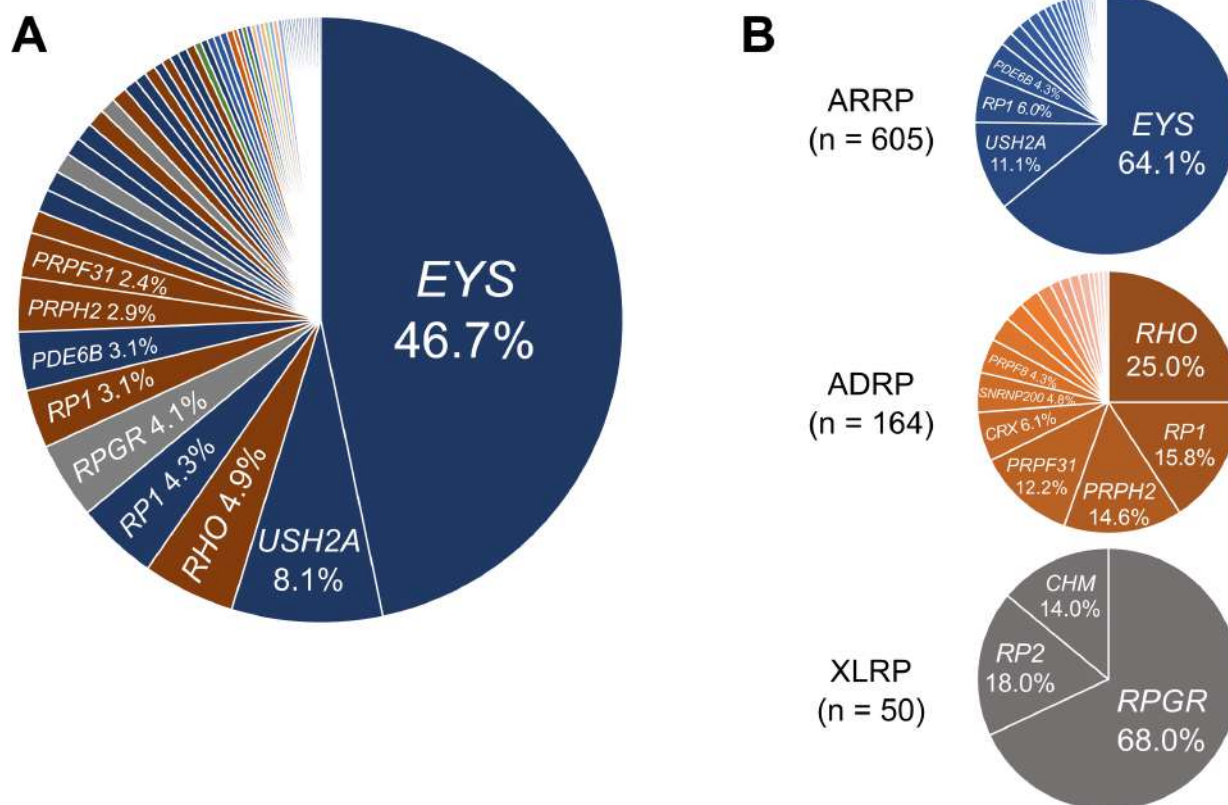


Figure 4 Proportion of causative genes in solved patients with RP. (A) The proportion of causative genes in solved patients with RP. The blue area represents the proportion of autosomal recessive genes, the brown area represents autosomal dominant genes and the grey area represents X linked genes. The green area represents multiple causative genes. (B) The proportion of causative genes based on the inheritance pattern. The pie chart excludes 12 patients in whom multiple causative genes with different inheritance patterns were detected. AD RP, autosomal dominant RP; ARR RP, autosomal recessive RP; n, number of patients; RP, retinitis pigmentosa; XL RP, X linked RP.

Among the patients with typical RP, 831 were genetically diagnosed with 320 pathogenic or likely pathogenic variants in 49 genes (figure 4A). Pathogenic variants in *EYS*, which has previously been reported to be the major gene responsible for RP in the Japanese population, explained RP in nearly half (388 of 831, 46.7%) of solved patients, followed by *USH2A* (67 of 831, 8.1%), *RHO* with dominant inheritance (41 of 831, 4.9%), *RP1* with recessive inheritance (36 of 831, 4.3%) and *RPGR* (34 of 831, 4.1%). The breakdown of solved cases by inheritance pattern based on clinical information was 47.2%, 43.9%, 33.6% and 41.2% for autosomal dominant, autosomal recessive, sporadic and X linked, respectively. When separately analysed by inheritance pattern of each gene reported in RetNet, *EYS* (388 of 605, 64.1%) and *USH2A* (67 of 605, 11.1%) accounted for 75.2% of patients diagnosed with autosomal recessive RP (figure 4B). Meanwhile, three genes (*RHO*, *RP1* and *PRPH2*) explained more than half of solved cases with autosomal dominant RP (91 of 164, 55.5%). In X linked RP, pathogenic variants in *RPGR* were found in the large majority of solved patients (n=34 of 50, 68.0%).

In Usher syndrome, a total of 8 of 32 patients (25.0%) were genetically diagnosed. In LCA, only 1 of 15 patients was genetically diagnosed, while no pathogenic variant was detected in the remaining 14 (93.3%) patients. In CRD, variants in *CRX*, *PRPH2* and *RP1* were the most commonly linked to the disease, each accounting for 7.7%, 5.1% and 5.1% of the disease, respectively. Of the 11 patients diagnosed with choroideraemia, pathogenic variants in *CHM* were detected in six patients (54.5%). Variants in the *CYP4V2* gene explained 67.6% (23 of 34) of patients with BCD, and

c.802-8_810del17insGC was detected in 5 compound heterozygotes and 14 homozygotes.

DISCUSSION

In this study, we performed target sequencing in 2155 patients with RP and an additional 170 patients with allied diseases. This is nearly double the number of patients with RP as in our previous study, although 1204 patients from the previous study were also included in the present one.¹⁰ We interpreted the detected variants according to the J-IRD-VI guidelines which are based on specified ACMG/AMP rules and tailored explicitly for IRD in the Japanese population.²² Our results showed that the genetic diagnosis rate was 38.6% in the patients with RP, which is higher than the corresponding rate of 29.6% in our previous work,¹⁰ which adopted a different variant interpretation pipeline. Our findings are supported by the diagnostic contribution of 107 newly assigned variants not reported in ClinVar, HGMD or our previous work, which comprised 20.4% of all pathogenic or likely pathogenic variants detected in this study. In addition, extra genotyping of common *Alu* insertion in *RP1* and a splice site variant in *CYP4V2*, both missed by our automated NGS analysis, contributed to the increased diagnosis rate.

Although 1204 patients examined in our previous work were also included in this study, only 67.5% of pathogenic or likely pathogenic variants had the same interpretation in the earlier work and this one. This could largely be attributed to the difference in interpretation criteria; the previous study adopted variant interpretation posted in ClinVar and HGMD. As a result, the rate of contribution of

the most prevalent disease genes changed considerably. In particular, the proportion of *EYS* jumped from 30.9% to 46.7% in the current study, which may be explained in part by the recent establishment of a very frequent variant (p.(Gly843Glu) in *EYS*) as pathogenic.³⁶ Additionally, through a stringent application of J-IRD-VI guidelines, nearly all variants in *RP1L1*, which was previously the fifth most prevalent RP-related gene in Japan and accounted for 4.8% of all solved RP cases, were excluded in this study due to the high AF in the general population as defined in the J-IRD-VI guidelines. Consequently, the current study has greatly enhanced the understanding of the genetic architecture of Japanese patients with RP.

This study also found that 37.0% of the patients with unsolved RP carried pathogenic or likely pathogenic recessive variants in one of the 86 RP-related genes. The AF of many of these variants was higher than would be expected in the general population. For example, the AF of p.(Ser1653fs) was 2.49% in patients with unsolved RP and is 0.43% in the general population. This may indicate that some of these heterozygous variants play a role in the disease in unsolved cases and that there is a yet-unidentified pathogenic recessive variant in trans that escaped the NGS panel sequence and standard analysis pipeline. Indeed, in an earlier analysis, we carried out a genome-wide association study of RP, which showed a peak in the *EYS* locus that surpassed genome-wide significance ($p=3.79 \times 10^{-10}$) and for which no corresponding exonic variant in *EYS* was linked,³⁶ indicating that there may be at least one more undiscovered high-frequency variant in this gene. Furthermore, through long read sequencing of 15 heterozygous carriers of an *EYS* pathogenic variant, we identified a large structural variant encompassing multiple exons in *EYS* in two cases (13.3%),⁴² suggesting the presence of undiscovered structural variants. Nevertheless, a more complex non-Mendelian inheritance factor may also complicate genetic diagnosis,^{43–45} although the degree of its importance in the context of overall genetic diagnosis remains largely unknown.

This study reports genetic analysis results of IRD cases with phenotypical overlap with RP in a somewhat limited number of patients. We found a significant contribution of RP-related genes in the genetic diagnosis rate of CRD (22 of 78 patients, 28.2%), although the figure was smaller than for RP (38.6%). Unlike RP, variants in *CRX* were the most frequent causes of CRD and *EYS* variants accounted for the disease in only 3.8% of cases. This was in contrast to patients with BCD or choroideraemia, both rarely diagnosed as RP, in which variants in *CYP4V2* and *CHM*, respectively, explained most patients. Meanwhile, we reached genetic diagnosis in only 1 of 15 patients with LCA. Among the four major causative genes (*CRB1*, *NMNAT1*, *RPGRIP1* and *GUCY2D*) that reportedly explain approximately 60% of Japanese patients with LCA, only *CRB1* was analysed in the current study as per the study design because other genes have not been associated with RP phenotype in the RetNet. Therefore, the low genetic diagnostic rate in patients with LCA is consistent with the past reports and indicates that genes causing RP and LCA are largely different in the Japanese population.^{15,46} Nevertheless, these findings are important in the era of genomic medicine because many emerging treatments for IRD are developed for each disease gene with less emphasis on the clinical diagnosis itself; thus, understanding the phenotypical spectrum of each disease gene is critical for the clinical application of these treatments.

There are several limitations to this study. First, the J-IRD-VI guidelines used for variant interpretation are customised for and validated in only Japanese patients with IRD. For example, mainly Japanese databases were designed to assess the rarity or enrichment of a variant in question. This means that the same analysis pipeline may not be applicable to countries outside Japan, even neighbouring Asian countries. Nevertheless, since Japan consists of islands geographically isolated from elsewhere, it is unavoidable that there

will be unique criteria for a sensitive and specific genetic diagnosis. Second, the RP-related genes analysed in the current study were selected based on those reported as causing non-syndromic RP in RetNet as of 2017. They are not updated, nor do they comprehensively cover genes reported for phenotypically related diseases such as CRD or LCA; nevertheless, important novel RP-associated genes have not been reported in the Japanese since 2017. It is likely that adopting whole-exome sequencing or whole-genome sequencing would lead to an increased diagnostic rate, particularly in non-RP cases. Lastly, the number of non-RP cases analysed was too small to reach any conclusions. Nevertheless, the data are sufficient to determine that there is a significant overlap between genes in RP and CRD and that observing this is rare in some genes but more frequent in other genes, such as *CRX*, *PRPH2* or *RP1*.

In conclusion, our study stringently applied IRD-specific ACMG/AMP rules intended to unify the genetic diagnosis of the disease within Japan in a large number of patients with RP and allied diseases. This allowed us to substantially update the genetic background of Japanese patients with RP by detecting many new disease-associated variants. The results may serve as an important foundation for developing future gene-specific or variant-specific treatments.

Author affiliations

- ¹Department of Ophthalmology, Nagoya University Graduate School of Medicine, Nagoya, Japan
- ²Department of Ophthalmology, Graduate School of Medical Sciences, Kyushu University, Fukuoka, Japan
- ³Department of Ocular Pathology and Imaging Science, Graduate School of Medical Sciences, Kyushu University, Fukuoka, Japan
- ⁴Laboratory for Genotyping Development, RIKEN Center for Integrative Medical Sciences, Kanagawa, Japan
- ⁵RIKEN Center for Integrative Medical Sciences, Kanagawa, Japan
- ⁶Department of Ophthalmology, Tohoku University Graduate School of Medicine, Sendai, Japan
- ⁷Department of Ophthalmology, University of Miyazaki Faculty of Medicine, Miyazaki, Japan
- ⁸Department of Ophthalmology, Juntendo University Graduate School of Medicine, Tokyo, Japan
- ⁹Department of Ophthalmology, The Jikei University School of Medicine, Tokyo, Japan
- ¹⁰Department of Ophthalmology, Hamamatsu University School of Medicine, Hamamatsu, Japan
- ¹¹Department of Ophthalmology, Hirosaki University Graduate School of Medicine, Hirosaki, Japan
- ¹²Laboratory for Statistical and Translational Genetics, RIKEN Center for Integrative Medical Sciences, Kanagawa, Japan
- ¹³Department of Ophthalmology, Kindai University Faculty of Medicine, Osaka-sayama, Japan
- ¹⁴Yuko Wada Eye Clinic, Sendai, Japan
- ¹⁵Division of Clinical Cell Therapy, Tohoku University Graduate School of Medicine United Centers for Advanced Research and Translational Medicine, Sendai, Japan

Acknowledgements We acknowledge the Laboratory for Genotyping Development in RIKEN and the RIKEN-IMS Genome Platform.

Contributors KH, MI, THi, KM, MT, JO, AFS, TK, HU, HK, SU, THa, YH, AM, KK, SK, YW, TA, TN, YI, K-HS and KMN collected the samples and clinical data. KG, YK, HI, MY, ME, KFujit, CT and YMo performed the experiments and analysed the data. KG, YK, MA, YMo, K-HS and KMN contributed to the manuscript preparation and editing. All authors contributed to study conception and design and data interpretation, and approved the final manuscript.

Funding The study was supported by the Japan Retinitis Pigmentosa Registry Project and grants from Japan Agency for Medical Research and Development (23ek0109632 to YI, 23ym0126071h0002 and 23ek0109660h0001 to KMN), Japan Society for the Promotion of Science (20K23005 and 22K16969 to YK, 22K20958 to AFS, 22K09831 to SU, 21K09756 to THa, 22K09825 to KK and 23H03059 to KMN), Japanese Retinitis Pigmentosa Society (JRPS) Research Grant to YK, Nagoya University Hospital Funding for Clinical Research to KMN and Takayanagi Retina Research Award to YK.

Map disclaimer The depiction of boundaries on this map does not imply the expression of any opinion whatsoever on the part of BMJ (or any member of its group) concerning the legal status of any country, territory, jurisdiction or area or of its authorities. This map is provided without any warranty of any kind, either express or implied.

Competing interests KMN reports grants from JCR Pharmaceuticals Co, Sysmex and Novartis Pharma Co; consulting fees from Sysmex and Novartis Pharma Co; and lecture fees from Sysmex, Novartis Pharma Co and Janssen Co. KMN has patents related to gene therapy for retinitis pigmentosa. In addition, KMN is an advisory board member of Sysmex and Novartis Pharma Co.

Patient consent for publication Not applicable.

Ethics approval This study involves human participants and received ethical approval from the Institutional Review Board of Nagoya University Graduate School of Medicine (2020-0598). This study was conducted in accordance with the principles of the Helsinki Declaration. All participants provided written informed consent at their respective recruiting institute.

Provenance and peer review Not commissioned; externally peer reviewed.

Data availability statement Data are available in a public, open access repository. We have uploaded variants reported in this study in ClinVar.

Supplemental material This content has been supplied by the author(s). It has not been vetted by BMJ Publishing Group Limited (BMJ) and may not have been peer-reviewed. Any opinions or recommendations discussed are solely those of the author(s) and are not endorsed by BMJ. BMJ disclaims all liability and responsibility arising from any reliance placed on the content. Where the content includes any translated material, BMJ does not warrant the accuracy and reliability of the translations (including but not limited to local regulations, clinical guidelines, terminology, drug names and drug dosages), and is not responsible for any error and/or omissions arising from translation and adaptation or otherwise.

ORCID iD

Kensuke Goto <http://orcid.org/0000-0001-5007-9384>

REFERENCES

- Hartong DT, Berson EL, Dryja TP. Retinitis pigmentosa. *Lancet* 2006;368:1795–809.
- Campochiaro PA, Mir TA. The mechanism of cone cell death in retinitis pigmentosa. *Prog Retin Eye Res* 2018;62:24–37.
- Sancho-Pelluz J, Arango-Gonzalez B, Kustermann S, et al. Photoreceptor cell death mechanisms in inherited retinal degeneration. *Mol Neurobiol* 2008;38:253–69.
- Dias MF, Joo K, Kemp JA, et al. Molecular genetics and emerging therapies for retinitis pigmentosa: basic research and clinical perspectives. *Prog Retin Eye Res* 2018;63:107–31.
- Russell S, Bennett J, Wellman JA, et al. Efficacy and safety of voretigene neparvovex (AAV2-hrpe65V2) in patients with RPE65-mediated inherited retinal dystrophy: a randomised, controlled, open-label, phase 3 trial. *Lancet* 2017;390:849–60.
- Stone EM, Andorf JL, Whitmore SS, et al. Clinically focused molecular investigation of 1000 consecutive families with inherited retinal disease. *Ophthalmology* 2017;124:1314–31.
- Colombo L, Maltese PE, Castori M, et al. Molecular epidemiology in 591 Italian probands with nonsyndromic retinitis pigmentosa and usher syndrome. *Invest Ophthalmol Vis Sci* 2021;62:13.
- Goetz KE, Reeves MJ, Gagadam S, et al. Genetic testing for inherited eye conditions in over 6,000 individuals through the eyeGENE network. *Am J Med Genet C Semin Med Genet* 2020;184:828–37.
- Weisschuh N, Obermaier CD, Battke F, et al. Genetic architecture of inherited retinal degeneration in Germany: a large cohort study from a single diagnostic center over a 9-year period. *Hum Mutat* 2020;41:1514–27.
- Koyanagi Y, Akiyama M, Nishiguchi KM, et al. Genetic characteristics of retinitis pigmentosa in 1204 Japanese patients. *J Med Genet* 2019;56:662–70.
- Gao F-J, Li J-K, Chen H, et al. Genetic and clinical findings in a large cohort of Chinese patients with suspected retinitis pigmentosa. *Ophthalmology* 2019;126:1549–56.
- Kim Y-J, Kim Y-N, Yoon Y-H, et al. Diverse genetic landscape of suspected retinitis pigmentosa in a large Korean cohort. *Genes (Basel)* 2021;12:675.
- Chen T-C, Huang D-S, Lin C-W, et al. Genetic characteristics and epidemiology of inherited retinal degeneration in Taiwan. *NPJ Genom Med* 2021;6:16.
- Numa S, Oishi A, Higasa K, et al. EYS is a major gene involved in retinitis pigmentosa in Japan: genetic landscapes revealed by stepwise genetic screening. *Sci Rep* 2020;10:20770.
- Suga A, Yoshitake K, Minematsu N, et al. Genetic characterization of 1210 Japanese pedigrees with inherited retinal diseases by whole-exome sequencing. *Hum Mutat* 2022;43:2251–64.
- Maeda A, Yoshida A, Kawai K, et al. Development of a molecular diagnostic test for retinitis pigmentosa in the Japanese population. *Jpn J Ophthalmol* 2018;62:451–7.
- Richards S, Aziz N, Bale S, et al. Standards and guidelines for the interpretation of sequence variants: a joint consensus recommendation of the American college of medical genetics and genomics and the association for molecular pathology. *Genet Med* 2015;17:405–24.
- Oza AM, DiStefano MT, Hemphill SE, et al. Expert specification of the ACMG/AMP variant interpretation guidelines for genetic hearing loss. *Hum Mutat* 2018;39:1593–613.
- Britten-Jones AC, Gocuk SA, Goh KL, et al. The diagnostic yield of next generation sequencing in inherited retinal diseases: a systematic review and meta-analysis. *Am J Ophthalmol* 2023;249:57–73.
- Hosono K, Ishigami C, Takahashi M, et al. Two novel mutations in the EYS gene are possible major causes of autosomal recessive retinitis pigmentosa in the Japanese population. *PLoS One* 2012;7:e31036.
- Iwanami M, Oshikawa M, Nishida T, et al. High prevalence of mutations in the EYS gene in Japanese patients with autosomal recessive retinitis pigmentosa. *Invest Ophthalmol Vis Sci* 2012;53:1033–40.
- Fujinami K, Nishiguchi KM, Oishi A, et al. Specification of variant interpretation guidelines for inherited retinal dystrophy in Japan [preprint]. *Jxiv* 2023.
- Momozawa Y, Akiyama M, Kamatani Y, et al. Low-frequency coding variants in CETP and CFB are associated with susceptibility of exudative age-related macular degeneration in the Japanese population. *Hum Mol Genet* 2016;25:5027–34.
- Nishiguchi KM, Fujita K, Ikeda Y, et al. A founder Alu insertion in RP1 gene in Japanese patients with retinitis pigmentosa. *Jpn J Ophthalmol* 2020;64:346–50.
- Wada Y, Itabashi T, Sato H, et al. Screening for mutations in CYP4V2 gene in Japanese patients with bietti's crystalline corneoretinal dystrophy. *Am J Ophthalmol* 2005;139:894–9.
- Nikopoulos K, Cisarova K, Quinodoz M, et al. A frequent variant in the Japanese population determines quasi-mendelian inheritance of rare retinal ciliopathy. *Nat Commun* 2019;10:2884.
- Won D, Hwang J-Y, Shim Y, et al. In silico identification of a common mobile element insertion in exon 4 of RP1. *Sci Rep* 2021;11:13381.
- de Bruijn SE, Fiorentino A, Ottaviani D, et al. Structural variants create new topological-associated domains and ectopic retinal enhancer-gene contact in dominant retinitis pigmentosa. *Am J Hum Genet* 2020;107:802–14.
- Jin Z-B, Mandai M, Homma K, et al. Allelic copy number variation in FSCN2 detected using allele-specific genotyping and multiplex real-time PCRs. *Invest Ophthalmol Vis Sci* 2008;49:3799–805.
- Zhang Q, Li S, Xiao X, et al. The 208delG mutation in FSCN2 does not associate with retinal degeneration in Chinese individuals. *Invest Ophthalmol Vis Sci* 2007;48:530–3.
- Xiang J, Peng J, Baxter S, et al. AutoPVS1: an automatic classification tool for PVS1 interpretation of null variants. *Hum Mutat* 2020;41:1488–98.
- Lek M, Karczewski KJ, Minikel EV, et al. Analysis of protein-coding genetic variation in 60,706 humans. *Nature* 2016;536:285–91.
- Zernant J, Collison FT, Lee W, et al. Genetic and clinical analysis of ABCA4-associated disease in African American patients. *Hum Mutat* 2014;35:1187–94.
- Valverde D, Riveiro-Alvarez R, Bernal S, et al. Microarray-based mutation analysis of the ABCA4 gene in Spanish patients with stargardt disease: evidence of a prevalent mutated allele. *Mol Vis* 2006;12:902–8.
- Lee W, Zernant J, Su P-Y, et al. A genotype-phenotype correlation matrix for ABCA4 disease based on long-term prognostic outcomes. *JCI Insight* 2022;7:e156154.
- Nishiguchi KM, Miya F, Mori Y, et al. A hypomorphic variant in EYS detected by genome-wide Association study contributes toward retinitis pigmentosa. *Commun Biol* 2021;4:140.
- Bowne SJ, Sullivan LS, Blanton SH, et al. Mutations in the Inosine monophosphate dehydrogenase 1 gene (IMPDH1) cause the RP10 form of autosomal dominant retinitis pigmentosa. *Hum Mol Genet* 2002;11:559–68.
- Wang X-T, Mion B, Aherne A, et al. Molecular recruitment as a basis for negative dominant inheritance? Propagation of misfolding in oligomers of IMPDH1, the mutated enzyme in the RP10 form of retinitis pigmentosa. *Biochim Biophys Acta* 2011;1812:1472–6.
- Ioannidis NM, Rothstein JH, Pejaver V, et al. REVEL: an ensemble method for predicting the pathogenicity of rare missense variants. *Am J Hum Genet* 2016;99:877–85.
- Jaganathan K, Kyriazopoulou Panagiotopoulou S, McRae JF, et al. Predicting splicing from primary sequence with deep learning. *Cell* 2019;176:535–48.
- Messchaert M, Haer-Wigman L, Khan MI, et al. EYS mutation update: in silico assessment of 271 reported and 26 novel variants in patients with retinitis pigmentosa. *Hum Mutat* 2018;39:177–86.
- Sano Y, Koyanagi Y, Wong JH, et al. Likely pathogenic structural variants in genetically unsolved patients with retinitis pigmentosa revealed by long-read sequencing. *J Med Genet* 2022;59:1133–8.
- Khanna H, Davis EE, Murga-Zamalloa CA, et al. A common allele in RRGRI1L is a modifier of retinal degeneration in ciliopathies. *Nat Genet* 2009;41:739–45.
- Kajiwara K, Berson EL, Dryja TP. Digenic retinitis pigmentosa due to mutations at the unlinked peripherin/RDS and ROM1 loci. *Science* 1994;264:1604–8.
- Katsanis N, Ansley SJ, Badano JL, et al. Triallelic inheritance in bardet-biedl syndrome, a mendelian recessive disorder. *Science* 2001;293:2256–9.
- Hosono K, Nishina S, Yokoi T, et al. Molecular diagnosis of 34 Japanese families with leber congenital amaurosis using targeted next generation sequencing. *Sci Rep* 2018;8:8279.



ORIGINAL ARTICLE

Efficacy of a wearable night-vision aid in patients with concentric peripheral visual field loss: a randomized, crossover trial

Go Mawatari¹ · Shogo Hiwatashi¹ · Tsubasa Motani¹ · Saori Nagatomo¹ · Eri Ando¹ · Toshiki Kuwahata¹ · Masataka Ishizu¹ · Yasuhiro Ikeda^{1,2}

Received: 10 October 2020 / Accepted: 1 April 2021 / Published online: 1 May 2021
© Japanese Ophthalmological Society 2021

Abstract

Purpose To investigate the efficacy of our wearable night-vision aid in patients with concentric peripheral visual field loss.

Study Design Prospective, single blind, three-group, and three-period crossover clinical study.

Methods The study included patients with concentric peripheral visual field loss, a best-corrected visual acuity (decimal visual acuity) of 0.1 or higher in the better eye, and the presence of a central visual field. HOYA MW10 HiKARI® (HOYA Corporation), our original wearable night-vision aid, was used as the test device with three types of camera lenses (standard-, middle-, and wide-angle lenses). Under both bright and dark conditions, the angle of the horizontal visual field was measured using each of the three lens types for each group. The baseline angle was measured when each participant wore the night-vision aid (powered off).

Results The study included 21 participants. Under bright condition, the perceived horizontal visual field was significantly wider than the baseline setup when using the standard-angle lens (“the standard lens”); the middle-angle lens (“the middle lens”) was significantly wider than both the baseline setup and the standard lens; and the wide-angle lens (“the wide lens”) was significantly wider than the other lenses. Under dark condition, the perceived horizontal visual field was again significantly wider when using the middle lens than the baseline setup and the standard lens, and when using the wide lens, the perceived horizontal visual field was again wider than when using the other lenses. The control in the bright condition was significantly wider ($p < 0.001$) than when used in the dark condition, while the standard-angle lens in the dark condition was significantly wider ($p = 0.05$) than when used in the bright condition. In regards to the middle and wide lenses, there was no statistically significant result emerging from either of the illumination conditions.

Conclusion Our wearable night-vision aid with a middle-angle or wide-angle lens appears to provide wider visual field images in patients with concentric peripheral visual field loss, regardless of whether the illumination conditions are bright or dark.

Keywords Wearable night-vision aid · Concentric peripheral visual field loss · Retinitis pigmentosa · Glaucoma · Low vision

Introduction

Patients with retinitis pigmentosa (RP) or advanced glaucoma experience not only night blindness, but also concentric peripheral visual field loss. Owing to concentric peripheral visual field loss, these patients have a poorer quality of life (QOL) [1].

Scanning, reverse monacle, concave lens, and prism membrane approaches are visual field enlargement methods for managing concentric peripheral visual field loss. Moreover, in recent years, there have been reports of new methods, such as multi-periscopic prism device and enhanced

Corresponding Author: Yasuhiro Ikeda

✉ Yasuhiro Ikeda
ymocl@med.miyazaki-u.ac.jp

¹ Department of Ophthalmology, Faculty of Medicine, University of Miyazaki, Miyazaki, Japan

² 5200 Kihara, Kiyotake, Miyazaki 889-1692, Japan



Fig. 1 Photograph of the test device

depth navigation through augmented reality depth mapping, for these patients [2, 3]. However, very few visual aids are currently available for daily life.

We invented a wearable night-vision aid for RP [4, 5], which is already on the market in Japan. This night-vision aid is a head mounted-type wearable device that includes an outer camera lens, a high-sensitivity camera sensor, and a high-performance see-through display. In the present study, we modified the camera lenses of our device to be replaceable. The angle of the image projected on the see-through display can be modified according to the lens angle. Thus, a wide-angle image is obtained on wearing our night-vision aid with a wide-angle lens.

We considered that a night-vision aid might be useful for patients with concentric peripheral visual field loss as it may provide them with wider visual field images and improve their QOL; No previous studies have been conducted on this topic. In this study, we aimed to investigate the efficacy of our wearable night-vision aid for its possible influence upon providing wider horizontal visual field images in patients with concentric peripheral visual field loss.

Methods

Participants

The study included patients with visual field contraction at the University of Miyazaki Hospital, Japan. The inclusion criteria were: a best-corrected visual acuity (decimal visual acuity) of 0.1 or higher in the better eye and the presence of a central visual field. The exclusion criterion was the inability to perform normal visual field examinations competently.

This study was approved by the Miyazaki University Ethics Review Board (study number: I-0047) and adhered



Fig. 2 Actual images obtained using each lens at the same position. **a** Standard-angle lens. **b** Middle-angle lens. **c** Wide-angle lens

to the Declaration of Helsinki. All study participants provided informed consent before any study-related procedures were undertaken.

Test device

The night-vision aid HOYA MW10 HiKARI® (HOYA Corporation) was used as the test device. A photograph of the device is shown in Fig. 1. Whenever a subject had a refractive error, a corrective lens was placed inside the device. The outer light-shielding lenses were removed from the device during the test. We examined the following three types of camera lenses, which can be attached to the device: standard-angle lens (maximum horizontal angle of 27°), middle-angle lens (maximum horizontal angle of 90°), and wide-angle lens (maximum horizontal angle of 142°). Figure 2 shows actual images of the device with each lens. The

settings of the device during the examination were: camera magnification, 0.9; brightness, 1.0; and color, standard.

Examination conditions

Figure 3a and b show the examination conditions. The examination chin rest was placed 1.0-m in front of the fixation point on a black wall, and a bilateral symmetrical 1.7-m scale was drawn. A 6.5×6.5-cm cross pattern was used for the fixation point. To observe the see-through display more clearly, participants used a shield film to shield the outer vision, except when the test device was powered off (Fig. 3c). Participants were tested under the following two different illumination conditions: 20,000 lx or more (bright) and 0.2 to 1.2 lx (dark). We confirmed the illuminance under each illumination condition with an illuminance meter (FT3424, Hioki E.E Corporation).

Study design and examination methods

This study had a three-group, three-period crossover clinical trial design. The participants were allocated to the three groups (1:1:1) by stratified randomization. The allocation was performed and managed by one researcher (S.H). The allocation researcher was distinct from the examiner (G.M). In Group 1, participants used the standard-angle lens, middle-angle lens, and wide-angle lens in the first, second, and third periods, respectively. In Group 2, participants used the middle-angle lens, wide-angle lens, and standard-angle lens in the first, second, and third periods, respectively. In Group 3, participants used the wide-angle lens, standard-angle lens, and middle-angle lens in the first, second, and third periods, respectively.

The test in this study was single-blinded, and participants were not informed about the type of camera lens inserted in the device they were using. The carryover effect was assumed to be nearly zero, so no washout period was provided.

We instructed participants to respond when the target appeared while fixating at the fixation point in accordance

with the kinetic visual field examination theory. The target was set to move from the most peripheral area bilaterally at 3.0-cm/s. We measured the horizontal visual field three times in two directions (right and left). First, in the bright condition, the visual field was measured while wearing the test device with the power off. Second, in the dark condition, the visual field was measured while wearing the test device with power off following 15 min of dark adaptation. These measurements were performed in all three groups. For participants who were not able to see the fixation point in the dark condition with the test device was powered off, a value of 0° was recorded. The target was a white circle (3.0-cm in diameter) attached to the tip of a stick.

Sample size and statistical analysis

No effect size could be obtained from previous studies. Therefore, in this study the effect size was estimated to be large, with the partial η^2 set to 0.14. With a power of 80% for detection and with an alpha error of 0.05, according to the above conditions, 20 cases were calculated by G*power, and 24 patients were recruited with consideration of attrition [6, 7].

Values measured in centimeters were converted to angles using the trigonometric function. Decimal visual acuity was adopted for visual acuity in all measurements, and the values were converted to the logarithm of the minimum angle of resolution (logMAR), and spheres and cylinder powers were converted to their spherical equivalents for statistical analysis.

For the horizontal visual field of the V4e isopter on the Goldmann perimeter (GP), the visual field results of both eyes were overlapped, and the visual field of the wider eye was adopted for the right and left visual fields. Then, the adopted visual field was calculated by ImageJ (v1.53k; National Institutes of Health) [8]. For the results of the GP, the data closest to the measurement data were used.

First, we investigated the carryover effect by applying an analysis of variance (ANOVA) model including the carryover effect. Next, the interaction was investigated, also using an ANOVA model including the interaction between the effect of the lens angle and the different periods. Following this, we performed Friedman's test to compare the visual field of each lens with the test device powered off. After that, we used a Wilcoxon signed-rank exact test to examine the results of each lens under bright and dark conditions. Finally, we performed a one-way ANOVA to compare the participants' backgrounds (age, visual acuity, and V4e isopter on the GP). When there were statistically significant differences found in the results, we performed multiple comparisons using the Bonferroni correction as a post hoc comparison. The significance level was set to 5%



Fig. 3 Examination conditions. **a** Layout of the examination. **b** Photograph of the actual examination condition. **c** Use of a shield film to shield the outer vision, except when the night-vision aid is powered off

Table 1 Characteristics of participants

	Group 1	Group 2	Group 3
age, years, mean \pm SD	46.57 \pm 17.48	47.00 \pm 18.39	53.9 \pm 19.04
logMAR visual acuity, mean \pm SD	0.39 \pm 0.23	0.35 \pm 0.34	0.08 \pm 0.25
V4e isopter, degrees, mean \pm SD	24.98 \pm 13.72	34.97 \pm 13.72	35.41 \pm 16.30
SD; standard deviation			

Table 2 Results of the horizontal visual field angle for each lens condition under the two illumination conditions

		illumination conditions	
		bright	dark
outer lens conditions	control, degrees, mean \pm SD	31.81 \pm 17.50	20.21 \pm 18.34
	standard-angle, degrees, mean \pm SD	21.27 \pm 6.26	21.96 \pm 6.36
	middle-angle, degrees, mean \pm SD	47.86 \pm 14.65	48.78 \pm 15.51
	wide-angle, degrees, mean \pm SD	80.84 \pm 33.05	82.93 \pm 32.63
SD; standard deviation			

(two-sided). To evaluate any reduction in visual field due to the use of the night-vision aid, we analyzed the correlation between the V4e isopter on the GP and the results obtained with each camera lens. Therefore, the boundary value as to whether the V4e isopter on the GP was above or below the diagonal line was determined by the cutoff value of the receiver operating characteristic (ROC) curve. If an approximated straight line intersected with the diagonal line in a scatter plot depicting the correlation of the visual field angle between the V4e isopter on the GP and each camera lens condition, the threshold was determined by the cutoff value of the ROC curve.

EZR statistical analysis software (ver.1.54; Saitama Medical Center, Jichi Medical University) was used in this study [9].

Results

Participant characteristics

The study included 21 patients (12 men and 9 women), and the average patient age was 49.2 ± 17.7 years. Among these patients, 15 had a history of RP, 5 had a history of secondary glaucoma with proliferative diabetic retinopathy, and 1 had bilateral optic atrophy. The average visual acuity of the better eye was 0.27 ± 0.30 (logMAR). All participants were allocated to three groups, and there were no statistically significant differences in age, visual acuity, and the V4e isopter between the groups ($p=0.71$, $p=0.10$, and $p=0.35$, respectively) (Table 1).

Carryover effect, period effect, and interaction between the lens angle and period

The results of repeated measured ANOVA under the bright condition, indicated no significant differences among the

groups nor was there any effect according to period ($p=0.70$ and $p=0.67$, respectively). Although there was a significant difference in the interaction among the groups and period ($p<0.001$), the post hoc test showed no significant difference among the periods ($p=0.99$). Under the dark condition, there were no significant differences among the groups nor among the periods ($p=0.82$ and $p=0.72$, respectively). Although there was a significant difference in the interaction among the groups and period ($p<0.001$), the post hoc test showed no significant difference among any of the periods ($p=0.99$).

Efficacy of horizontal visual field enlargement

Table 2 shows the results of the horizontal visual field angle for each lens condition under the two illumination conditions.

Under the bright condition, the perceived horizontal visual field using the standard-angle lens was significantly wider than when the test device powered off (control; $p=0.029$), while when using the middle-angle lens the perceived horizontal visual field was significantly wider than when using either the control or the standard-angle lens ($p<0.001$ and $p<0.001$, respectively). Moreover, when using the wide-angle lens, the perceived horizontal visual field was significantly wider than when using the control or the other lenses (all $p<0.001$). The visual field angle using the middle-angle lens was approximately 225% wider than when using the standard-angle lens, and the visual field angle when using the wide-angle lens was approximately 169% wider than when using the middle-angle lens. It is also significant that with the wide-angle lens, four participants recorded the maximum measurable angle.

Under the dark condition, similar trends were observed in the perceived horizontal visual field. The visual field angle using the middle-angle lens was approximately 222% wider

than when using the standard-angle lens, and the visual field angle using the wide-angle lens was approximately 170% wider than when using the middle-angle lens.

The results when comparing visual fields using each lens under the two illumination conditions were: control ($p < 0.001$), standard-angle lens ($p = 0.005$), middle-angle lens ($p = 0.166$), and wide-angle lens ($p = 0.126$). The visual field control under the bright condition was significantly wider than under the dark condition, whereas when using

the standard-angle lens in the dark condition, the visual field was significantly wider than in the bright condition.

Figure 4 shows a scatter plot depicting the correlation between each camera lens condition and the V4e isopter. As Fig. 4a-i shows, almost all plots of the control and V4e isopter were located on the diagonal line. In Fig. 4a-ii, the plots of the standard-angle lens intersected on the diagonal line, and the cutoff value and areas under the curve (AUC) were 26.534 and 0.4889, respectively. In Fig. 4a-iii and iv, most plots of the middle-angle lens and wide-angle lens were located above the diagonal line. Under the dark condition, similar trends were observed (Fig. 4b). In Fig. 4b-ii, plots of the standard-angle lens intersected on the diagonal line, and the cutoff value and AUC were 23.285 and 0.551, respectively.

Discussion

According to our results, when the test device was powered off, the horizontal visual field was wider under the bright condition than under the dark condition. This might be associated with the participants' condition, with 15 of the 21 participants having a history of RP. Meanwhile, a horizontal visual field expansion effect was observed under not only the bright condition but also under the dark condition, since the test device has the potential to assist patients with night blindness [4, 5].

A visual field defect can lead to reduced QOL. Previous studies show a correlation between the degree of peripheral visual field loss and QOL in patients with RP, and it is also determined that a more severe visual field defect is associated with a slower reading speed in patients with glaucoma, and that visual field abnormality is associated with both vision-related function and physical function [1, 10, 11]. The findings of this study suggest that a test device with a middle-angle or wide-angle lens can provide a wider visual field for users, and this wider visual field can lead to a better QOL.

When the residual visual field is 45° or less, the risk of collision is reported to be the highest [12]. Based on the current study's results, when patients with concentric peripheral visual field loss use our wearable night-vision aid with a middle-angle or wide-angle lens, they can obtain a visual field of 45° or more. Thus, using our wearable night-vision aid with a middle-angle or wide-angle lens might be useful in reducing the risk of pedestrian collisions in daily life.

When patients used the night-vision aid with a standard-angle lens, the most common response was that, "the screen is small" [13]. Therefore, our study's results suggest that if a patient has $> 23^\circ$ under bright conditions or 27° under dark conditions in the V4e isopter of the Goldmann perimeter,

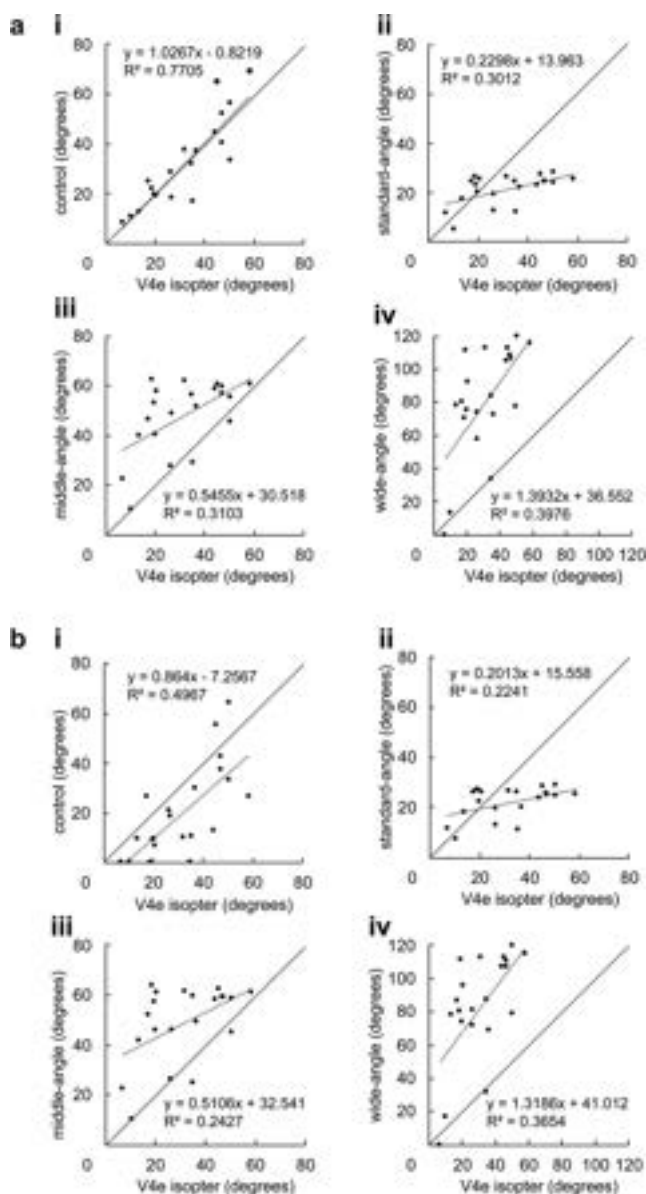


Fig. 4 Scatter plot depicting the correlation between each camera lens condition and the V4e isopter on the Goldmann perimeter. **a** Bright condition, **a-i** Control and V4e isopter, **a-ii** Standard-angle lens and V4e isopter, **a-iii** Middle-angle lens and V4e isopter, and **a-iv** Wide-angle lens and V4e isopter. **b** Dark condition. **b-i** Control and V4e isopter, **b-ii** Standard-angle lens and V4e isopter, **b-iii** Middle-angle lens and V4e isopter, and **b-iv** Wide-angle lens and V4e isopter

there is a possibility that the patient may feel that the screen is small when using a normal lens.

To our knowledge, this is the first study to reveal horizontal visual field expansion in patients with concentric peripheral visual field loss using a wearable device (our night-vision aid) with a middle-angle or wide-angle lens under both bright and dark conditions.

This study has four important limitations. First, we did not examine the vertical visual field. Because the inferior visual field is reported to be very important when walking [14], in future studies, the effect of our wearable night-vision aid on the vertical visual field should be verified. Second, we did not verify the instrument's efficacy within the scope of the patients' daily lives. For example, one previous study reports that enhanced depth navigation through augmented reality depth mapping reduces contact during walking by 50–70% in patients with low vision [3]. Therefore, in future studies, it should be verified whether our night-vision aid is effective in daily life, such as in reducing the likelihood of collisions when walking. Third, the percentage change in the visual field angle with each outer lens was not correlated with the difference in the outer lens angle when using our night-vision aid. However, the result of the wide-angle lens was included, and it recorded the maximum measurable angle. The cause was not made clear in this study. Therefore, it may be necessary to consider using scales larger than 1.7-m in the future. Finally, when using middle- and wide-angle lenses, there exists the possibility of effecting visual acuity. However, no analysis of visual acuity was performed in this study. Future studies should therefore analyze any effect on visual acuity due to changes in the lens angle.

In conclusion, our wearable night-vision aid when fitted with a middle-angle or wide-angle lens appears to provide wider visual field images for patients with concentric peripheral visual field loss, regardless of whether the illumination conditions are bright or dark. The findings suggest that our wearable night-vision aid may be effective for patients with low vision.

Acknowledgements The HOYA corporation provided material support, but had no role in the study design, conduct, analysis, and interpretation, or writing of the report.

Declarations

Conflict of interest G. Mawatari, None; S. Hiwatashi, None; T. Motani, None; S. Nagatomo, None; E. Ando, None; T. Kuwahata, None; M. Ishizu, None; Y. Ikeda, Financial support (Alcon, Senju, Santen, HOYA, Chugai, Bayer, Ellex), Personal financial interest (ViXion), Consultant (Novartis, HOYA, ViXion), Patent (ID Pharma), Royalties (Bayer, Kowa, Otsuka, Chugai, NIDEK, ViXion, Santen, Senju,

Novartis).

References

1. Yanagisawa M, Kato S, Kobayashi M, Watanabe M, Ochiai M. Relationship between vision-related quality of life and different types of existing visual fields in Japanese patients. *Int Ophthalmol*. 2012;32:523–9.
2. Peli E, Vargas-Martin F, Kurukuti NM, Jung J-H. Multi-periscopic prism device for field expansion. *Biomed Opt Express*. 2020;11:4872–89.
3. Angelopoulos AN, Ameri H, Mitra D, Humayun M. Enhanced depth Navigation through augmented reality depth mapping in patients with Low Vision. *Sci Rep*. 2019;9:11230.
4. Ikeda Y, Suzuki E, Kuramata T, Kozaki T, Koyama T, Kato Y, et al. Development and evaluation of a visual aid using see-through display for patients with retinitis pigmentosa. *Jpn J Ophthalmol*. 2015;59:43–7.
5. Ikeda Y, Nakatake S, Funatsu J, Fujiwara K, Tachbana T, Murakami Y, et al. Night-vision aid using see-through display for patients with retinitis pigmentosa. *Jpn J Ophthalmol*. 2019;63:181–5.
6. Faul F, Erdfelder E, Lang A-G, Buchner A. G*Power 3: a flexible statistical power analysis program for the social, behavioral, and biomedical sciences. *Behav Res Methods*. 2007;39:175–91.
7. Faul F, Erdfelder E, Buchner A, Lang A-G. Statistical power analyses using G*Power 3.1: tests for correlation and regression analyses. *Behav Res Methods*. 2009;41:1149–60.
8. Schneider CA, Rasband WS, Eliceiri KW. NIH Image to ImageJ: 25 years of image analysis. *Nat Methods*. 2012;9:671–5.
9. Kanda Y. Investigation of the freely available easy-to-use software 'EZR' for medical statistics. *Bone Marrow Transpl*. 2013;48:452–8.
10. Ramulu PY, Maul E, Hochberg C, Chan ES, Ferrucci L, Friedman DS. Real-World Assessment of physical activity in Glaucoma using an accelerometer. *Ophthalmology*. 2012;119:1159–66.
11. Qiu M, Wang SY, Singh K, Lin SC. Association between Visual Field Defects and Quality of Life in the United States. *Ophthalmology*. 2014;121:733–40.
12. Peli E, Apfelbaum H, Berson EL, Goldstein RB. The risk of pedestrian collisions with peripheral visual field loss. *J Vis*. 2016;16:5.
13. Kiuchi K. Subjective evaluation on the usefulness of MW10-HiKARI in patients with ocular diseases. *Rinsho Ganka*. 2021;75:232–8. (In Japanese).
14. Yuki K, Asaoka R, Ono T, Awano-Tanabe S, Murata H, Tsubota K. Evaluation of fear of falling in patients with primary Open-Angle Glaucoma and the importance of Inferior Visual Field damage. *Invest Ophthalmol Vis Sci*. 2020;61:52.

Publisher's Note Springer Nature remains neutral with regard to jurisdictional claims in published maps and institutional affiliations.

Springer Nature or its licensor (e.g. a society or other partner) holds exclusive rights to this article under a publishing agreement with the author(s) or other rightsholder(s); author self-archiving of the accepted manuscript version of this article is solely governed by the terms of such publishing agreement and applicable law.

厚生労働科学研究費補助金（難治性疾患政策研究事業）

分担研究報告書

黄斑ジストロフィに関する研究

研究分担者 国立病院機構東京医療センター・視覚研究部・部長・角田 和繁
弘前大学・医学研究科・眼科教授・上野 真治
三重大学・医学系研究科・眼科教授・近藤 峰生
研究協力者 慈恵医科大学・葛飾医療センター・眼科教授・林 孝彰

研究要旨

黄斑ジストロフィ（Macular Dystrophy：指定難病 301）は、両眼の黄斑機能が進行性に低下する遺伝性網脈絡膜疾患の総称である。以前に我々が作成したガイドラインでは、黄斑ジストロフィは具体的な 6 疾患とそれ以外に分かれている。しかし主要な 6 疾患以外の稀な黄斑ジストロフィの実態に関してはほとんど明らかにされていない。そこで今回我々は、国内で発症数や病態が十分に解明されていない「全身疾患に伴う希少な黄斑ジストロフィ」について調査を行なった。黄斑ジストロフィを比較的多く診療している日本臨床視覚電気生理学会の理事 20 施設に対しアンケート調査を依頼した。その結果、13 施設より回答が得られ、合計の患者数は以下のとおりであった。ミトコンドリア関連黄斑ジストロフィ：6 例、脊髄小脳変性症（SCA）関連黄斑ジストロフィ：2 例、家族性ドルーゼン：8 例、Myotonic dystrophy type 1 に合併する黄斑ジストロフィ：1 例、白点状眼底に合併する黄斑ジストロフィ：8 例、Alport 症候群に合併する黄斑ジストロフィ：8 例、その他、希少な全身疾患に伴う黄斑ジストロフィ：10 例。予想以上に「全身疾患に伴う希少な黄斑ジストロフィ」の患者数が少ないことが判明した。今後は、ホームページなどを通じて眼科医、患者およびその家族にこのような稀な黄斑ジストロフィの情報提供ができる体制を進めることが重要であると考えられた。

A. 研究目的

黄斑ジストロフィ（Macular Dystrophy：指定難病 301）は、両眼の黄斑機能が進行性に低下する遺伝性網脈絡膜疾患である。患者の多くは視力低下、中心視野欠損、色覚異常などを訴える。

厚労省の黄斑ジストロフィの基準では 6 疾患とそれ以外に分かれているが、主要な 6 疾患以外の稀な黄斑ジストロフィの実態

に関してはほとんど明らかにされていない。

そこで本年度は、国内で発症数や病態が十分に解明されていない「全身疾患に伴う希少な黄斑ジストロフィ」について、専門家に対して調査を行ったので報告する。

B. 研究方法

黄斑ジストロフィを比較的多く診療し

ている医師が多く所属している日本臨床視覚電気生理学会の理事 20 施設に対し、過去 5 年間のうちに以下の疾患に関して診察した患者数をアンケート形式で調査した：ミトコンドリア関連黄斑ジストロフィ、脊髄小脳変性症（SCA）関連黄斑ジストロフィ、家族性ドルーゼン、Myotonic dystrophy type 1 に合併する黄斑ジストロフィ、白点状眼底に合併する黄斑ジストロフィ、Alport 症候群に合併する黄斑ジストロフィ、その他、希少な全身疾患に伴う黄斑ジストロフィ。

（倫理面への配慮）

今回の研究に関しては患者の個人情報はいずれも匿名化し、倫理面に十分配慮して行った。

C. 研究結果

20 施設中 13 施設より回答が得られ、合計患者数は以下のとおりであった。

ミトコンドリア関連黄斑ジストロフィ：6 例、脊髄小脳変性症（SCA）関連黄斑ジストロフィ：2 例、家族性ドルーゼン：8 例、Myotonic dystrophy type 1 に合併する黄斑ジストロフィ：1 例、白点状眼底に合併する黄斑ジストロフィ：8 例、Alport 症候群に合併する黄斑ジストロフィ：8 例、その他、希少な全身疾患に伴う黄斑ジストロフィ：10 例。

結果として、予想以上に上記のような黄斑ジストロフィの頻度が低いことが判明した。

D. 考察

黄斑ジストロフィは本研究班によるガイドラインにおいて主要な 6 つの黄斑ジストロフィとその他のタイプのものに分類されている。後者のその他の黄斑ジストロフィには様々な疾患があり、中には全身疾患を伴うものもある。しかしながら、後者の稀な黄斑ジストロフィに関する情報は非常に乏しく、例えば神経内科や耳鼻科から眼の異常に関して眼科医に依頼があったとしても、我々眼科医が参考にすべき情報が見つけないという状況である。

今回の調査結果により、黄斑ジストロフィの専門家であっても、このような稀な黄斑ジストロフィに遭遇する機会は非常に稀であることが判明した。そこで、今後は我々の研究班において、海外の清書や論文、また数少ない日本の典型的患者の所見をまとめて論文化、あるいはわかりやすい解説書を作成し、ホームページなどを通じて眼科医、患者やその家族に情報提供できるような作業を進めていくことが重要であると考えられた。

E. 結論

日本におけるミトコンドリア関連黄斑ジストロフィなどの比較的稀な黄斑ジストロフィの患者数の調査を専門家内で行なった結果、予想以上に患者数が少ないことが確認された。今後は、海外の文献と日本における典型例を参考にこれらの稀な黄斑ジストロフィの情報を広く発信していくことが重要であると考えられた。

F. 健康危険情報：なし

1. 論文発表

- 1) Suga A, Mizobuchi K, Inooka T, Yoshitake K, Minematsu N, Tsunoda K, Kuniyoshi K, Kawai Y, Omae Y, Tokunaga K; NCBN Controls WGS Consortium; Hayashi T, Ueno S, Iwata T. A homozygous structural variant of RPGRIP1 is frequently associated with achromatopsia in Japanese patients with IRD. *Genet Med Open*. 2024 Mar 26;2:101843.
- 2) Inooka T, Hayashi T, Tsunoda K, Kuniyoshi K, Kondo H, Mizobuchi K, Suga A, Iwata T, Yoshitake K, Kondo M, Goto K, Ota J, Kominami T, Nishiguchi KM, Ueno S. GENETIC ETIOLOGY AND CLINICAL FEATURES OF ACHROMATOPSIA IN JAPAN. *Retina*. 2024 Oct 1;44(10):1836-1844.
- 3) Miura M, Makita S, Yasuno Y, Azuma S, Mino T, Hayashi T, Kameya S, Tsunoda K. Multimodal imaging analysis of autosomal recessive bestrophinopathy: Case series. *Medicine (Baltimore)*. 2024 Jul 19;103(29):e38853.
- 4) Ueno S, Hayashi T, Tsunoda K, Aoki T, Kondo M. Nationwide epidemiologic survey on incidence of macular dystrophy in Japan. *Jpn J Ophthalmol*. 2024 May;68(3):167-173.
- 5) Mizobuchi K, Hayashi T, Tanaka K, Kuniyoshi K, Murakami Y, Nakamura N, Torii K, Mizota A, Sakai D, Maeda A, Kominami T, Ueno S, Kusaka S, Nishiguchi KM, Ikeda Y, Kondo M, Tsunoda K, Hotta Y, Nakano T. Genetic and Clinical Features of ABCA4-Associated Retinopathy in a Japanese Nationwide Cohort. *Am J Ophthalmol*. 2024 Aug;264:36-43.
- 6) Kominami T, Ueno S, Ota J, Inooka T, Oda M, Mori K, Nishiguchi KM. Classification of fundus autofluorescence images based on macular function in retinitis pigmentosa using convolutional neural networks. *Jpn J Ophthalmol*. 2025 Mar;69(2):236-244.
- 7) Inooka T, Hayashi T, Tsunoda K, Kuniyoshi K, Kondo H, Mizobuchi K, Suga A, Iwata T, Yoshitake K, Kondo M, Goto K, Ota J, Kominami T, Nishiguchi KM, Ueno S. GENETIC ETIOLOGY AND CLINICAL FEATURES OF ACHROMATOPSIA IN JAPAN. *Retina*. 2024 Oct 1;44(10):1836-1844.
- 8) Higa N, Hayashi T, Mizobuchi K, Iwasa M, Kubota S, Kuniyoshi K, Kameya S, Kondo H, Kondo M, Nakano T. A novel RPE65 variant p.(Ala391Asp) in Leber congenital amaurosis: a case report and literature review in Japan. *Front Med (Lausanne)*. 2024 Sep 18;11:1442107.
- 9) Sato T, Kuniyoshi K, Hayashi T, Nishiwaki H, Mizobuchi K, Kusaka S. Clinical course of two siblings with potassium voltage-gated channel modifier subfamily V member 2 (KCNV2)-associated retinopathy. *Doc Ophthalmol*. 2024

Jun;148(3):173-182.

- 10) Goto K, Koyanagi Y, Akiyama M, Murakami Y, Fukushima M, Fujiwara K, Iijima H, Yamaguchi M, Endo M, Hashimoto K, Ishizu M, Hirakata T, Mizobuchi K, Takayama M, Ota J, Sajiki AF, Kominami T, Ushida H, Fujita K, Kaneko H, Ueno S, Hayashi T, Terao C, Hotta Y, Murakami A, Kuniyoshi K, Kusaka S, Wada Y, Abe T, Nakazawa T, Ikeda Y, Momozawa Y, Sonoda KH, Nishiguchi KM. Disease-specific variant interpretation highlighted the genetic findings in 2325 Japanese patients with retinitis pigmentosa and allied diseases. J Med Genet. 2024 Jun 20;61(7):613-620.

2. 学会発表

- 1) Kazushige Tsunoda; ‘Fundus albipunctatus as a progressive disease with peripheral retinal atrophy’, Electrophysiology of Vision Symposium, The 132nd Annual Meeting of Korean Ophthalmological Society in conjunction with APSOPRS, Seoul, 2024/11/29-12/12
- 2) 角田和繁, 全視野網膜電図 (ERG) の有用性と課題, シンポジウム 22 視機能障害検出法の進歩と課題, 第 78 回日本臨床眼科学会, 京都, 2024/11/14-17

H. 知的財産権の出願・登録状況

1. 特許取得 なし
2. 実用新案登録 なし
3. その他 なし



ARTICLE

A homozygous structural variant of *RPGRIP1* is frequently associated with achromatopsia in Japanese patients with IRD



Akiko Suga¹, Kei Mizobuchi², Taiga Inooka³, Kazutoshi Yoshitake⁴, Naoko Minematsu¹, Kazushige Tsunoda⁵, Kazuki Kuniyoshi⁶, Yosuke Kawai⁷, Yosuke Omae⁷, Katsushi Tokunaga⁷, NCBN Controls WGS Consortium, Takaaki Hayashi^{2,*}, Shinji Ueno^{8,*}, Takeshi Iwata^{1,*}

ARTICLE INFO

Article history:

Received 16 October 2023

Received in revised form

21 March 2024

Accepted 21 March 2024

Available online 26 March 2024

Keywords:

Achromatopsia

Genome sequencing

RPGRIP1

Structural variant

ABSTRACT

Purpose: Achromatopsia (ACHM) is an early-onset cone dysfunction caused by 5 genes with cone-specific functions (*CNGA3*, *CNGB3*, *GNAT2*, *PDE6C*, and *PDE6H*) and by *ATF6*, a transcription factor with ubiquitous expression. To improve the relatively low variant detection ratio in these genes in a cohort of exome-sequenced Japanese patients with inherited retinal diseases (IRD), we performed genome sequencing to detect structural variants and intronic variants in patients with ACHM.

Methods: Genome sequencing of 10 ACHM pedigrees was performed after exome sequencing. Structural, non-coding, and coding variants were filtered based on segregation between the affected and unaffected in each pedigree. Variant frequency and predicted damage scores were considered in identifying pathogenic variants.

Results: A homozygous deletion involving exon 18 of *RPGRIP1* was detected in 5 of 10 ACHM probands, and variant inheritance from each parent was confirmed. This deletion was relatively frequent (minor allele frequency = 0.0023) in the Japanese population but was only homozygous in patients with ACHM among the 199 Japanese IRD probands analyzed by the same genome sequencing pipeline.

Conclusion: The deletion involving exon 18 of *RPGRIP1* is a prevalent cause of ACHM in Japanese patients and contributes to the wide spectrum of *RPGRIP1*-associated IRD phenotypes, from Leber congenital amaurosis to ACHM.

© 2024 The Authors. Published by Elsevier Inc. on behalf of American College of Medical Genetics and Genomics. This is an open access article under the CC BY-NC-ND license (<http://creativecommons.org/licenses/by-nc-nd/4.0/>).

The Article Publishing Charge (APC) for this article was paid by Takeshi Iwata

Akiko Suga and Kei Mizobuchi contributed equally to this article.

The names of the NCBN Controls WGS Consortium will appear at the end of the article.

*Correspondence and requests for materials should be addressed to Takeshi Iwata, Division of Molecular and Cellular Biology, National Institute of Sensory Organs, NHO Tokyo Medical Center, 2-5-1, Higashigaoka Meguro-ku, Tokyo 152-8902 Japan. *Email address:* takeshi.iwata@kankakuki.jp OR Takaaki Hayashi, Department of Ophthalmology, The Jikei University School of Medicine, 3-25-8 Nishi-shimbashi, Minato-ku, Tokyo 105-8461, Japan. *Email address:* taka@jikei.ac.jp OR Shinji Ueno, Department of Ophthalmology, Hirosaki University Graduate School of Medicine, 5 Zaifu-cho Hirosaki-shi, Aomori 036-8562, Japan. *Email address:* uenos@hirosaki-u.ac.jp

Affiliations are at the end of the document.

doi: <https://doi.org/10.1016/j.gimo.2024.101843>

2949-7744/© 2024 The Authors. Published by Elsevier Inc. on behalf of American College of Medical Genetics and Genomics. This is an open access article under the CC BY-NC-ND license (<http://creativecommons.org/licenses/by-nc-nd/4.0/>).

Introduction

Inherited retinal diseases (IRDs) are a group of phenotypes associated with reduced visual acuity and are mostly due to a photoreceptor dysfunction, which leads to progressive retinal degeneration. Achromatopsia (ACHM) is a congenital cone dysfunction with severely reduced visual acuity but a stationary natural history from an early age. Affected patients have nystagmus, photophobia, absent or markedly reduced color vision, and reduced visual acuity from birth or early infancy. With electroretinography (ERG), ACHM is characterized by severely reduced cone responses with normal/subnormal rod responses. The fundus typically appears normal, but detailed imaging of the retinal structure with optical coherence tomography (OCT) reveals variability in the macular structure, with an ellipsoid zone that is either continuous or disrupted.¹ Long-term clinical studies indicate that visual acuity, rod responses, and retinal structure are generally stable for several years to decades.² ACHM is inherited in an autosomal recessive pattern with a prevalence of 1 in 30,000 worldwide.³ Six genes, *CNGA3* (HGNC:2150, NM_001298.2), *CNGB3* (HGNC:2153, NM_019098.5), *GNAT2* (HGNC:4394, NM_001377295.2), *PDE6C* (HGNC:8787, NM_006204.4), *PDE6H* (HGNC:8790, NM_006205.3), and *ATF6* (HGNC:791, NM_007348.4), are causal for ACHM.² *ATF6* is ubiquitously expressed and involved in the maintenance of cellular homeostasis, whereas the remaining genes encode cone-specific phototransduction proteins.⁴ Genetic studies on patients with IRD have shown relatively high solved ratios for ACHM. For example, 67% (6/9 cases) of the patients with ACHM were solved by genome sequencing in the United Kingdom,⁵ and 95.2% (56/62 cases) were solved by the panel sequencing of known IRD genes in Germany.⁶ Even with Sanger sequencing targeting the coding sequences of *CNGA3* and *CNGB3*, biallelic variants were detected in 45.5% (10/22 pedigrees) of the patients with ACHM.⁷ Consistent with the known genetic background of ACHM; *CNGB3* and *CNGA3* account for approximately 70% to 80% of the cases.² Those studies identified *CNGB3* as the most frequent causal gene and its founder variant, c.1148del p.(Thr383Ilefs*13), as the most prevalent. In contrast, in the previous exome sequencing of 1210 Japanese IRD pedigrees, we identified pathogenic variants in only 34% of the pedigrees with cone dysfunction (14/41 pedigrees, including ACHM and blue cone monochromatism).⁸ Among the patients with genetically solved cone dysfunction, *CNGA3* accounted for 22% (3/14) but *CNGB3* did not. Further, the *CNGB3* founder variant, c.1148del, was not detected in the exome-sequenced patients with IRD either in a heterozygous or in a homozygous manner. Therefore, we expected a contribution of exome-undetectable structural variants and non-coding variants in known ACHM genes and/or other genes in Japanese patients with ACHM.

RPGRIP1 (HGNC:13436, NM_020366.4) encodes a coiled-coil protein that interacts with the RPGR protein and anchors it to the photoreceptor primary cilia.⁹ A pathogenic variant of *RPGRIP1* was first identified in patients with

Leber congenital amaurosis (LCA) with severely reduced vision from early childhood, pigmented fundi, and non-recordable ERGs for both rod and cone responses.¹⁰ Over 250 variants of *RPGRIP1* are currently known, most of which are associated with LCA; associations with retinitis pigmentosa and cone-rod dystrophy (CORD) are observed at lower rates.¹¹ Although *RPGRIP1* pathogenic variants may underlie 5% of LCA cases,¹² our previous exome sequencing study did not identify *RPGRIP1* pathogenic variants in patients with any of the 28 phenotypes, including LCA (54 pedigrees) and CORD (157 pedigrees).⁸ Recent next-generation sequencing efforts have identified pathogenic non-coding variants and large structural variants partially disrupting *RPGRIP1* exon(s) in patients with IRD,¹³ which encouraged us to reexamine unresolved IRD cases with genome sequencing to detect structural variants and noncoding variants in addition to the coding region variants detected by exome sequencing.

Herein, we report the identification of a homozygous deletion involving exon 18 of *RPGRIP1* (NC_000014.9:g.21326547_21327885del NM_020366.4:c.2710+374_2895+78del; *RPGRIP1*-ex18-DEL) in 5 of 10 clinically diagnosed unrelated ACHM probands in the Japanese IRD cohort. These patients had severely reduced visual acuity from birth or early infancy, and ERG responses were normal from rods but nonrecordable from cones. Genome sequencing revealed that *RPGRIP1*-ex18-DEL was homozygous in the patients and heterozygous in their parents. It was significantly enriched in patients with ACHM compared with the Japanese control population, accounting for 11% of pedigrees with cone dysfunction syndrome in our exome-sequenced and genome-sequenced Japanese IRD cohort.

Materials and Methods

Recruitment of patients and their family members

Ten clinically diagnosed ACHM probands and their family members (2 affected and 19 unaffected) were enrolled in this study at 4 institutions in Japan (NHO Tokyo Medical Center, The Jikei University School of Medicine, Nagoya University, and Kindai University). These participants were part of a genome-sequenced IRD cohort (199 pedigrees, [Supplemental Figure 1](#)) collected by the Japan Eye Genetics Consortium.¹⁴ Recruitment and sample collection were conducted in accordance with the Declaration of Helsinki. All participants provided written informed consent at their respective recruiting institutes. The study was approved by the ethics boards of each institute.

Clinical evaluation

We performed comprehensive ophthalmic examinations, including medical review (age at onset and chief complaint),

decimal best-corrected visual acuity (BCVA), fundus photographs, fundus autofluorescence imaging using a Spectralis HRA (Heidelberg Engineering) and/or Optos 200Tx/California Ultra-Wide Field Retinal Imaging System (Optos), OCT (Spectralis, or Carl Zeiss Meditec AG), and Goldmann kinetic perimetry (Haag Streit). Full-field ERG was recorded following the protocols of the International Society for Clinical Electrophysiology of Vision (ISCEV)¹⁵ using a light-emitting diode built-in electrode (LE-4000, Tomey), a Ganzfeld dome with an EOG-ERG Ganzfeld stimulator (Electrophysiology system; LACE Elettronica), or RETeval (LKC Technologies). Detailed ERG procedures and conditions were as previously reported.¹⁶⁻¹⁹ Pedigree trees were drawn by f-tree (v4.2.1).²⁰

Genome sequencing

Blood samples were collected at each institute, and genomic DNA was extracted by Advanced GenoTechs. All patients and healthy controls were genome sequenced by the same pipeline as part of the Japan Leading Project for Rare Disease WGS.^{21,22} In detail, genome sequencing was performed using NovaSeq6000 (Illumina) at 150 bp paired-end. Sequences in FASTQ data are mapped to a GRCh38 reference sequence by an in-house data analysis pipeline²¹ equivalent to bwa (v0.7.15)²³ and GATK (v4.1.0).²⁴ The mapping and variant calls were performed using the Parabricks v3.5.0 (Nvidia). Mapped sequence files were used for variant calling by our in-house pipeline. In detail, short sequence variants (single-nucleotide variants [SNVs] and insertions/deletions shorter than 50 bp [short indels]) were called by a GATK-haplotype caller as previously reported.⁸ Variants were annotated by ANNOVAR (2019Oct24)²⁵ and Splice AI (1.3).²⁶ For the detection of structural variants, sequences were processed by GATK-SV (v0.12-beta)²⁷ using the single mode with MELT (v2.2.2).²⁸

Variant filtration and interpretation

To identify pathogenic variants in each patient with IRD, we used pedigree-based variant segregation as previously reported.⁸ SNVs and short indels in known IRD causal genes (Supplemental Table 1) were examined. Variants with a minor allele frequency (MAF) <0.005 in gnomAD and 8.3 KJPN and frequent population-specific variants in *EYS* (NM_001142800.2:c.2528G>A, MAF = 1.89×10^{-2} in 8.3 KJPN) and *RP1* (NM_006269.2:c.5797C>T, MAF = 5.40×10^{-3} in 8.3 KJPN) were considered. The MAFs of structural variants were referenced to gnomAD-SV (v.2.1), 8.3 KJPN-SV,²⁹ and NCBN Controls WGS.²¹ Variants were segregated between the affected and unaffected in each family as follows. For pedigrees with dominant inheritance of the phenotype, variants shared only among patients were selected. For pedigrees comprising the patient and his or her unaffected family members, recessive, X-linked, and sporadic inheritance patterns were considered. Variants were selected if they were homozygous or heterozygous in patient(s) but not

homozygous in unaffected family members. Compound heterozygosity was examined if each parent carried different alleles. For pedigrees comprising only probands, all genotypes were considered. The pathogenicity of short-read variants and structural variants was predicted according to the American College of Medical Genetics and Genomics guidelines using InterVar³⁰ and AnnotSV,³¹ respectively.

Short-read mapping was confirmed with integrated genome visualization software (IGV, v2.1.6).³²

Confirmation of the break point

RPGRIP1-exon18-DEL was confirmed by polymerase chain reaction (PCR) and Sanger sequencing using previously reported primers for PCR (Fw: 5'-GAGCCCGAGTGCCTTTACTG-3'; Rv: 5'-CCAGCTTCAATGGGAACCTC-3'),³³ and nested primers for sequencing (Fw: 5'-TTGCCCAGGCTAGTAGCTGGG-3'; Rv: 5'-TTCAAGTGATTCTCCTGCC TC-3'). The break-point sequence of *RPGRIP1* exon 22-24 DUP was confirmed by PCR amplification and Sanger sequencing (primers Fw: 5'-TGTGGCAGATCCTGGA GTCA-3'; Rv: 5'-GCAGGGCTGCCAAAACCTTAC-3').

To confirm the break-point sequence of *CNGA3* *Alu* insertion, PCR-amplified target region was subcloned into pMD20 by TA-cloning (Mighty TA-cloning Reagent Set for PrimeSTAR, TAKARA) and Sanger sequenced. The following primers were used for PCR amplification and sequencing (Fw: 5'-GATGCCCAATGACCTCCATCTT-3'; Rv: 5'-GGTAAGGGTCAAGGTGGACCAG-3'). The subfamily of the inserted *Alu* sequence was annotated by Dfam.³⁴

Statistical analysis

The enrichment of *RPGRIP1*-ex18-DEL in the ACHM probands was examined by a one-sided binominal test using rstatix (0.7.2) on R (4.2.3).

Results

Clinical findings

Table 1 summarizes the clinical findings from 8 patients with biallelic *RPGRIP1* structural variants. All patients were diagnosed with ACHM based on medical review, visual acuity, retinal structure, and functional findings. Detailed clinical findings from a representative patient (JU0960) are shown in Figure 1. Multimodal retinal imaging revealed a normal appearance by fundus photograph and fundus autofluorescence imaging (Figure 1A, upper 3 panels) and blurred outer retinal layers (including the ellipsoid zone) by OCT (Figure 1A, lower panels). Full-field ERG showed normal rod system function (Figure 1B, dark adapted [DA] 0.01) and combined rod and cone system functions (Figure 1B, DA 3.0 and DA 10.0), with severely impaired

Table 1 Summary of the clinical findings of patients with ACHM with *RPGRIP1* exon18 deletion

Case		Subjective Symptom					BCVA (logMAR) RE LE	Fundus Photograph	FAF	OCT	FF-ERG ^c	Visual Field Test	
Family ID ^a	Patient ID	Age ^b	Gender	Nystagmus	Photophobia	Color Vision Abnormality						Central	Peripheral
N051	N1051	21	M	+	+	+	0.40 0.52	Normal appearance	Normal appearance	Blurred EZ appearance	Rod: subnormal Rod & cone: decreased a- and b-waves Cone: non-recordable 30-Hz flicker: non-recordable	Relative central scotoma of I-4e	Constricted
	N0051	24	F	+	+	+	1.00 1.00	Normal appearance	Normal appearance	Normal appearance	Rod; normal Rod & cone: normal a- and b-waves cone: non-recordable 30-Hz flicker: non-recordable	Noncentral scotoma	Constricted
N058	N0058	39	F	+	+	+	1.52 1.70	Normal appearance	Normal	Blurred EZ	Rod; normal Rod & cone: normal a- and b-waves cone: non-recordable 30-Hz flicker: non-recordable	Relative central scotoma of III-4e in RE and II-4e in LE	Constricted
NISO 199	KA-199	35	F	+	+	+	1.10 1.10	Macular atrophy	Hypo-AF corresponding to macular atrophy area	Disrupted EZ corresponding to macular atrophy area	Rod; normal Rod & cone: normal a- and b-waves cone: non-recordable 30-Hz flicker: non-recordable	Relative central scotoma of I-4e	Constricted
NISO 472	KA-472	5	F	+	+	+	1.10 1.10	Normal appearance	Normal appearance	Blurred EZ	Rod; normal Rod & cone: normal a- and b-waves cone: non-recordable 30-Hz flicker: non-recordable	Noncentral scotoma	Preserved
J134	JU0960	5	M	+	+	+	0.82 1.00	Normal appearance	Normal appearance	Blurred EZ	Rod; normal Rod & cone: normal a- and b-waves cone: non-recordable 30-Hz flicker: non-recordable	Relative central scotoma of I-3e	Preserved
J138	JU0011	24	M	+	+	+	1.15 1.00	Normal appearance	Hypo-AF at fovea and hyper-AF around the area	Blurred EZ at fovea and disrupted EZ at parafovea	Rod; normal Rod & cone: normal a- and b-waves cone: non-recordable 30-Hz flicker: non-recordable	Relative central scotoma of I-3e	Preserved
NISO 143	KA-143	21	F	+	+	+	1.52 1.52	Normal appearance	Not Done	Blurred EZ	Rod; normal Rod & cone: slightly decreased a- and normal b-waves cone: non-recordable 30-Hz flicker: non-recordable	Not Done	

^aJ, The Jikei University School of Medicine; N, Nagoya university; NISO, NHO Tokyo Medical Center.

^bAge, age at first visit; BCVA, best-corrected visual acuity; DA, dark adapted; EZ, ellipsoid zone; FAF, fundus autofluorescence imaging; FF-ERG, full-field electroretinogram; LA, light adapted; LE, left eye; OCT, optical coherence tomography; RE, right eye.

^cRod, DA 0.01, Rod and cone (DA 3.0 or DA 10); Cone, (LA 3.0); 30-Hz flicker, (LA 3.0-flicker).

cone function (Figure 1B, light adapted [LA] 3.0 and LA 3.0 flicker). The clinical course of visual acuity in the patient revealed that the logMAR BCVA remained around 1.0 for about 15 years (Figure 1C). These findings are consistent with the ACHM phenotype.

Detection of homozygous *RPGRIP1* SV in Japanese patients with achromatopsia

These 10 ACHM pedigrees were previously analyzed by exome sequencing, but no pathogenic variants with homozygous or compound heterozygous genotypes were identified. Genome sequencing detected homozygous *RPGRIP1*-ex18-DEL, in 5 of 10 unrelated ACHM probands (Figure 2A and B, Table 2). These pedigrees were genome sequenced as complete trios (proband and their healthy parents), except for the father of N058, and variant inheritance was traced by genotype. A homozygous 1339-bp deletion in probands was confirmed by Sanger sequencing (Figure 2C) following PCR amplification of the target region (Supplemental Figure 2). This variant was previously reported as a deletion of exon 17 in a Japanese patient with LCA.¹³ Annotation of the exon number changed according to the recent identification of a new exon corresponding to the 5'UTR.¹³ Although *RPGRIP1*-ex18-DEL was predicted to cause premature termination of the *RPGRIP1* protein (NP_065099.3:p.(Asp905Serfs*6)),³³ its exact effect on transcripts and proteins has yet to be experimentally confirmed. Two other ACHM probands were heterozygous for *RPGRIP1*-ex18-DEL (Table 2, JU0011 and KA-143), and 1 of these patients had a previously reported *RPGRIP1* nonsense variant³⁵ in trans (Figure 2D and E).

Another proband had a novel partial duplication of *RPGRIP1* coding exons (NC_000014.9: g.21338066_21348664_dup NM_020366.4:c.3339+3361_3748+362dup; *RPGRIP1* ex22-24 DUP) in trans (Figure 3A and B). Genomic PCR confirmed the heterozygosity of the *RPGRIP1*-ex18-DEL in I-2 and II-1, and the *RPGRIP1* ex22-24 DUP in I-1 and II-1, respectively (Figure 3C). The break point of the duplicated region was revealed by Sanger sequencing (Figure 3D).

To examine the contribution of *RPGRIP1*-ex18-DEL to ACHM in association with other ACHM causal genes, we reviewed rare SNVs (population-maximum MAF < 0.005 in gnomAD) in *CNGA3*, *CNGB3*, *GNAT2*, *PDE6C*, *PDE6H*, and *ATF6* for all these patients. No heterozygous or homozygous pathogenic or likely pathogenic ClinVar variants were detected. NISO472 II-1 was heterozygous for *CNGA3*: p.(Asp193Asn), which was of uncertain significance.

In the other 3 ACHM pedigrees, no *RPGRIP1* pathogenic variant was detected. We identified a *CNGA3* missense variant, c.1072G>A p.(Glu358Lys), and an *Alu* insertion as a compound heterozygous genotype in NISO177 (Table 2). A 356 bp *AluY* insertion with 18 bp target site duplication was shown by Sanger sequencing following the TA-cloning of the target region amplified by PCR (Supplemental Figure 3). Both variants were of uncertain significance, and further validation

was required. No pathogenic/candidate pathogenic variants were detected in the other 2 pedigrees.

In total, genome sequencing identified homozygous *RPGRIP1*-ex18-DEL in 5 of 10 (50%) ACHM probands, and *RPGRIP1*-ex18-DEL in trans with other *RPGRIP1* nonsense/truncating variants in 2 ACHM probands (20%, 2/10) (Table 2).

Enrichment of homozygous *RPGRIP1*-exon18-DEL in achromatopsia

Compared with the general MAF of *RPGRIP1*-ex18-DEL in the Japanese population (0.0023, 1/444 in 8.3 KJPN), the MAF = 0.60 (12/20) in our 10 ACHM probands was extremely high ($P = 4.74 \times 10^{-24}$, one-sided binominal test). To determine if this variant was prevalent among Japanese patients with IRD independent of the phenotype, we reviewed the *RPGRIP1*-ex18-DEL genotype for all genome-sequenced IRD probands (Supplemental Figure 1, $n = 199$). Homozygous *RPGRIP1*-ex18-DEL was found only in the 5 previously mentioned ACHM patients (Table 2). Heterozygous *RPGRIP1*-ex18-DEL was found in 2 ACHM patients (Table 2) and 2 additional patients diagnosed with LCA. These patients with LCA were from the same family, and both had another structural variant (NC_000014.9:g.21276147_21280265del; *RPGRIP1*-ex1-DEL) in trans. Their detailed phenotypes were reported recently.³⁶

Discussion

In our genome sequencing analysis of 10 ACHM pedigrees, 5 probands were homozygous for the same pathogenic variant, *RPGRIP1*-ex18-DEL. No other probands in our genome-sequenced IRD cohort ($n = 199$) were homozygous for this variant, indicating that homozygous *RPGRIP1*-ex18-DEL primarily accounts for ACHM.

Ophthalmic examinations revealed a typical ACHM phenotype among the patients, including symptoms of nystagmus, photophobia, color vision abnormality, and stable visual acuity after initial severe reduction. In addition to the detailed phenotype of JU0960 in this report, phenotypes of N1051 and N0051 were previously reported as ACHM and incomplete ACHM, respectively, before the genetic examination.³⁷ A normal fundus photograph and normal rod function with severely impaired cone function are characteristic of ACHM, rather than LCA.² Biallelic *RPGRIP1* variants are mainly associated with an LCA phenotype.¹⁰ However, some IRD cases with *RPGRIP1* pathogenic variants have been clinically diagnosed as CORD in variable regions and populations.^{11,38} In addition, in studies of Japanese patients with LCA with *RPGRIP1* variants, cases with heterozygous *RPGRIP1*-ex18-DEL were notable for the lack of general fundus abnormality and subnormal rod ERG responses with unrecordable cone responses.^{36,39} Furthermore, in the initial report of *RPGRIP1*-ex18-DEL (mentioned as exon 17

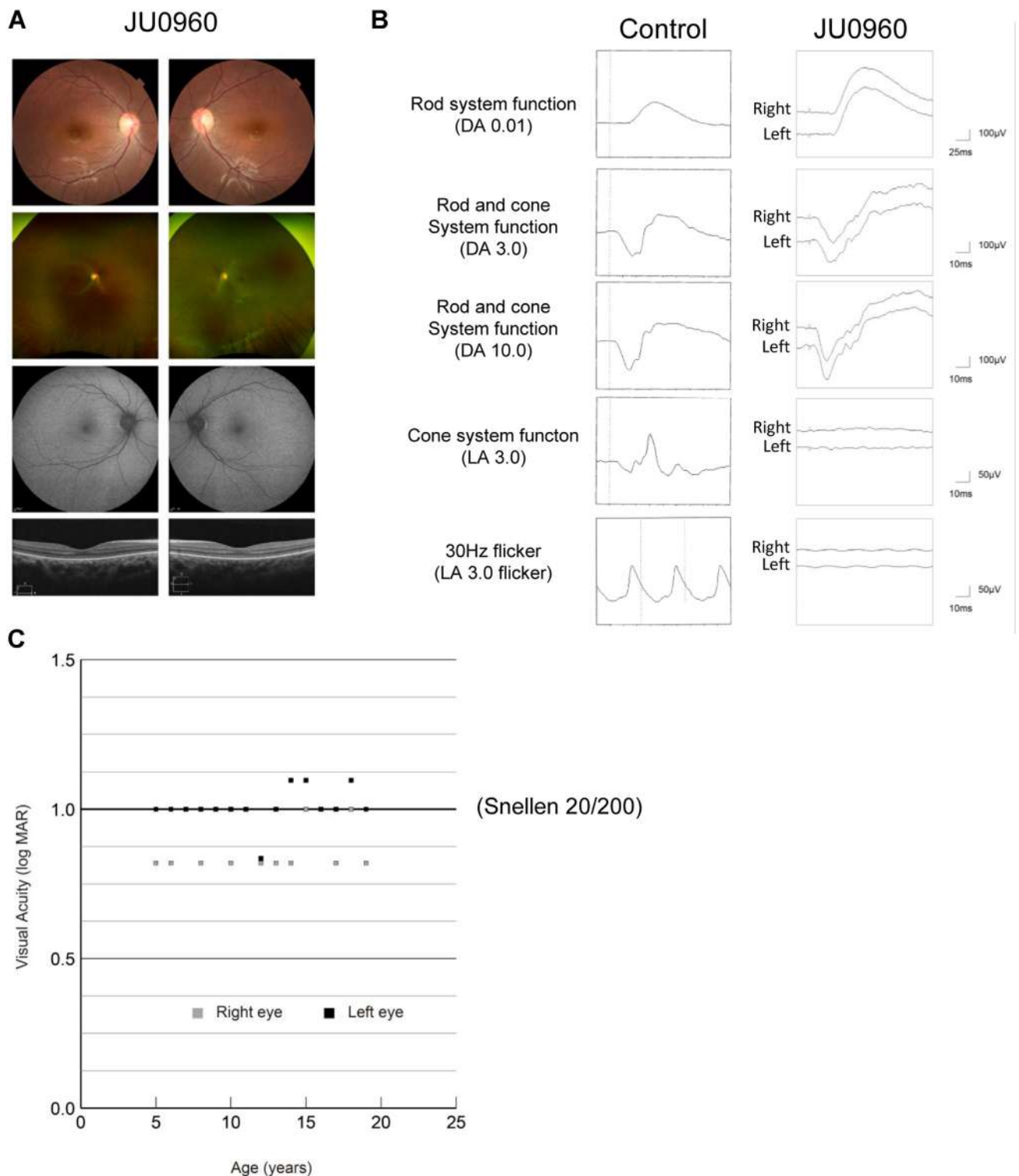


Figure 1 Clinical findings from a representative patient (JU0960). A. Multimodal retinal imaging showed a normal appearance by fundus photograph (first and second panels) and fundus autofluorescence imaging (third panel) and blurred outer retinal layer ellipsoid zone by OCT (fourth panel). B. Full-field electroretinography showed normal rod system function (DA 0.01) and combined rod and cone system functions (DA 3.0 and DA 10.0) with unrecordable cone system function (LA 3.0) and 30-Hz flicker responses (LA 3.0 flicker). C. The clinical course of visual acuity revealed that logMAR BCVA remained around 1.0 for about 15 years.

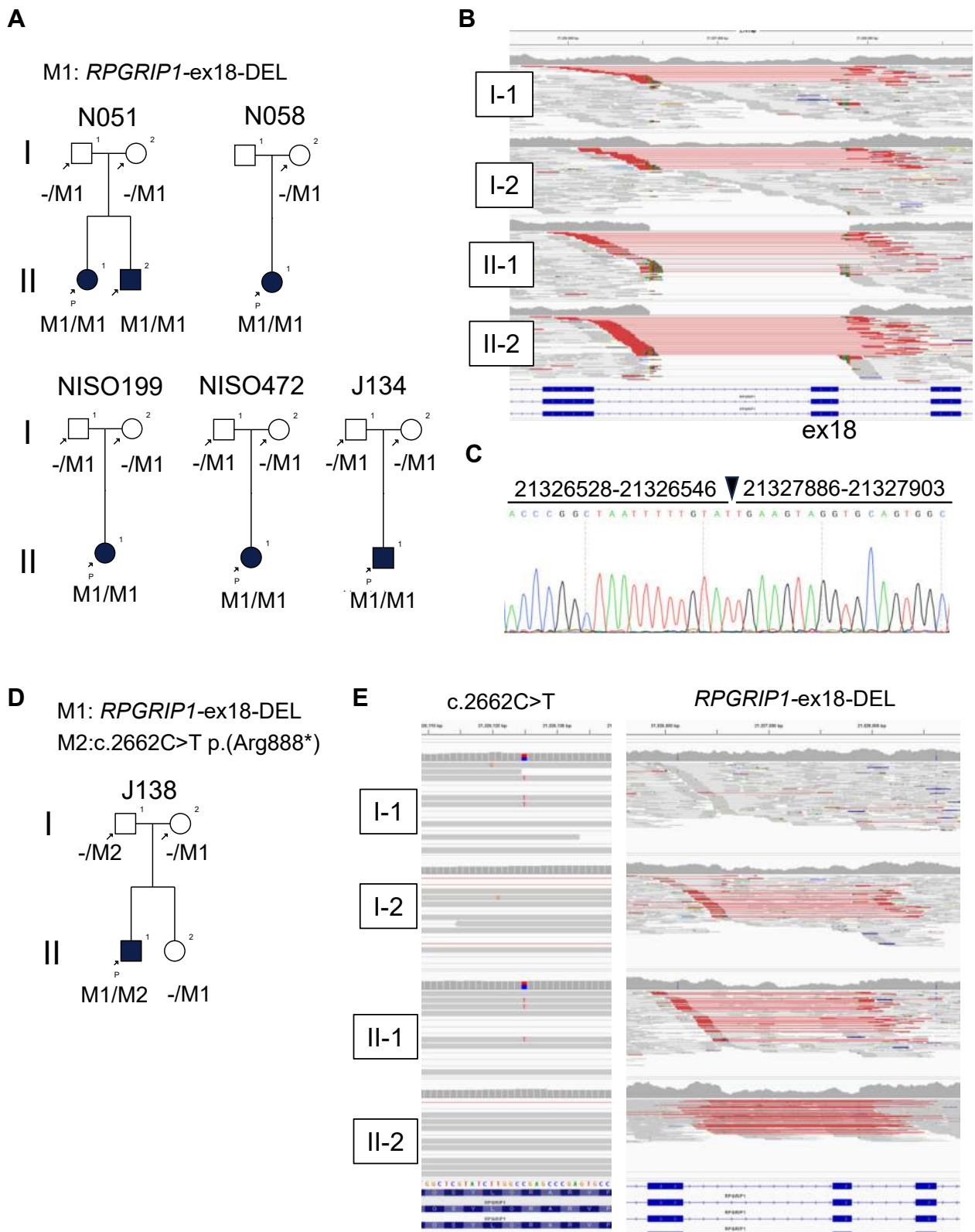


Figure 2 Identification of *RPGRIP1*-ex18-DEL in ACHM proband. A. Family trees of the patients with ACHM (black) and their healthy parents (white). B. Read alignments of N051 displayed by IGV. Red lines indicate deletions in the read sequences compared with the reference. C. Sanger sequencing identifies the exact break point (black arrowhead) using the PCR product of N051 II-1. Chromosomal position based on NC_000014.9 (hg38) is indicated. D. Family tree of J138 showing variant inheritance of *RPGRIP1*-ex18-DEL and c.2662C>T. E. Read alignments showing c.2662C>T and *RPGRIP1*-ex18-DEL. Clinically examined and genome-sequenced participants are indicated by arrows. Proband is indicated by P, males are indicated by rectangles, and females are indicated by circles.

Table 2 Overview of molecular findings of genome-sequenced patients with achromatopsia

IDs			Pathogenic Variant				Population Frequency			Prediction of Pathogenicity						
Family	Patient	Gene	Genotype	gnotation(hg38)	cnotation	pnotation	gnomAD (max)	gnomAD (EAS)	ExAC (All)	Variant Class (ACMG)	PolyPhen2	SIFT	REVEL	VEST4	ClinVar	Reference
N051	1051	RPGRIP1	Homozygous	g.21326547_21327885del	c.271_0+374_2895+78del	p.?	NA	NA	NA	0.0023	Pathogenic (Class 5)					33
	51	RPGRIP1	Homozygous	g.21326547_21327885del	c.2710+374_2895+78del	p.?	NA	NA	NA	0.0023	Pathogenic (Class 5)					33
N058	0058	RPGRIP1	Homozygous	g.21326547_21327885del	c.2710+374_2895+78del	p.?	NA	NA	NA	0.0023	Pathogenic (Class 5)					33
N150	KA-199	RPGRIP1	Homozygous	g.21326547_21327885del	c.2710+374_2895+78del	p.?	NA	NA	NA	0.0023	Pathogenic (Class 5)					33
199																
N150	KA-472	RPGRIP1	Homozygous	g.21326547_21327885del	c.2710+374_2895+78del	p.?	NA	NA	NA	0.0023	Pathogenic (Class 5)					33
472																
J134	JU0960	RPGRIP1	Homozygous	g.21326547_21327885del	c.2710+374_2895+78del	p.?	NA	NA	NA	0.0023	Pathogenic (Class 5)					33
J138	JU0011	RPGRIP1	Compound heterozygous	chr14:g.21326125C>T	c.2662C>T	p.(Arg888*)	0.00003425	0	NA	0.000155	Likely pathogenic (Class 4)	NA	Tolerant	NA	0.754	VUS
N150	KA-143	RPGRIP1	Compound heterozygous	g.21326547_21327885del	c.2710+374_2895+78del	p.?	NA	NA	NA	0.0023	Pathogenic (Class 5)					33
143				g.21326547_21327885del	c.2710+374_2895+78del	p.?	NA	NA	NA	0.0023	Pathogenic (Class 5)					33
N150	KA-177,	CNGA3	Compound heterozygous	chr14:g.21338066_21348664_dup	c.3339+3361_3748+362dup	p.?	NA	NA	NA	NA	VUS (Class 3)	Benign	Tolerant	0.517	0.524	novel
177	KA-178			g.98396296G>A	c.1126G>A	p.(Glu376Lys)	0.000008838	0	NA	0	VUS (Class 3)					novel
				g.98396034_98396035insN[356]	c.864_865insN[356]	p.?	NA	NA	NA	NA	VUS (Class 3)					novel

Variant descriptions for *RPGRIP1* are based on NC_000014.9 for gnotation and NM_020366.4 for cnotation. Variant descriptions for *CNGA3* are based on NC_000002.12 for gnotation and NM_001298.2 for cnotation.

VUS, variants with uncertain significance.

deletion) from Japanese patients with LCA, the authors noted that 1 patient had recordable scotopic ERG with unrecordable cone response at 5 years old.³³ Considering our data and previous studies on *RPGRIP1*-associated IRD phenotypes, *RPGRIP1* may be causal for a spectrum of photoreceptor-associated phenotypes, from functional defects primarily in cones (ACHM and CORD) to photoreceptor degeneration in both rods and cones (LCA and early-onset retinitis pigmentosa). Further studies on structural variants and SNVs will reveal the correlations between these genetic variants and phenotypes.

In our previous exome sequencing report, population-frequent SNVs of *EYS* (NM_001142800.2:c.2528G>A) and *RP1* (NM_006269.2:c.5797C>T) were significantly enriched in retinitis pigmentosa and macular dystrophy/CORD, respectively.⁸ In this report, using genome sequencing, we show that *RPGRIP1*-ex18-DEL was significantly enriched in ACHM in the Japanese population, with the homozygous genotype mainly accounting for the phenotype. This variant was not detected in gnomAD structural variants (v2.1); therefore, it was difficult to determine the contribution of population-frequent structural variants to ACHM. However, the relatively high variant frequency in the Japanese population (MAF = 0.0023 in 8.3 KJPN) supported this idea. A further expansion of publicly available structural variant data will enable us to compare the prevalence of SVs and SV-associated IRDs between countries and populations. Our data suggest that genome sequencing is effective in detecting a relatively small deletion, such as *RPGRIP1*-ex18-DEL (1339bp). Although the depletion of exon 18 in *RPGRIP1* was detectable by the read alignment of exome sequencing (Supplemental Figure 4a), no information about the break point was available. Furthermore, the read counts on exon 18 of *RPGRIP1* appeared variable among the heterozygotes (Supplemental Figure 4b, I-2, II-1, and II-2). In contrast, genome sequence data can show the break point in the flanking intron (Figure 2B) and indicate a possible deletion between the paired reads (Figure 2B and E, red lines), which helps to reliably detect the variant. Compared with the pathogenic variant identification ratio in cone dysfunctions in our exome sequencing study (34%, 14/41 pedigrees), genome sequencing improved the detection ratio to 50% (22/44). Homozygous *RPGRIP1*-ex18-DEL accounted for 11% (5/44) of the pedigrees diagnosed as cone dysfunctions. Because the previous study did not separate ACHM from other phenotypes of cone dysfunction (blue cone monochromatism and others), the contribution of *RPGRIP1*-ex18-DEL to ACHM in Japanese patients with IRD might be underestimated.

Because *RPGRIP1* is expressed in both rod and cone photoreceptors, the molecular pathology that primarily affects cone photoreceptors in patients has yet to be clarified. Beryozkin et al¹¹ showed significantly different distributions of LCA and CORD phenotypes corresponding to the *RPGRIP1* genotypes. Homozygous premature terminations were more associated with LCA, whereas homozygous missense variants were preferentially associated with CORD. Because premature terminations are generally

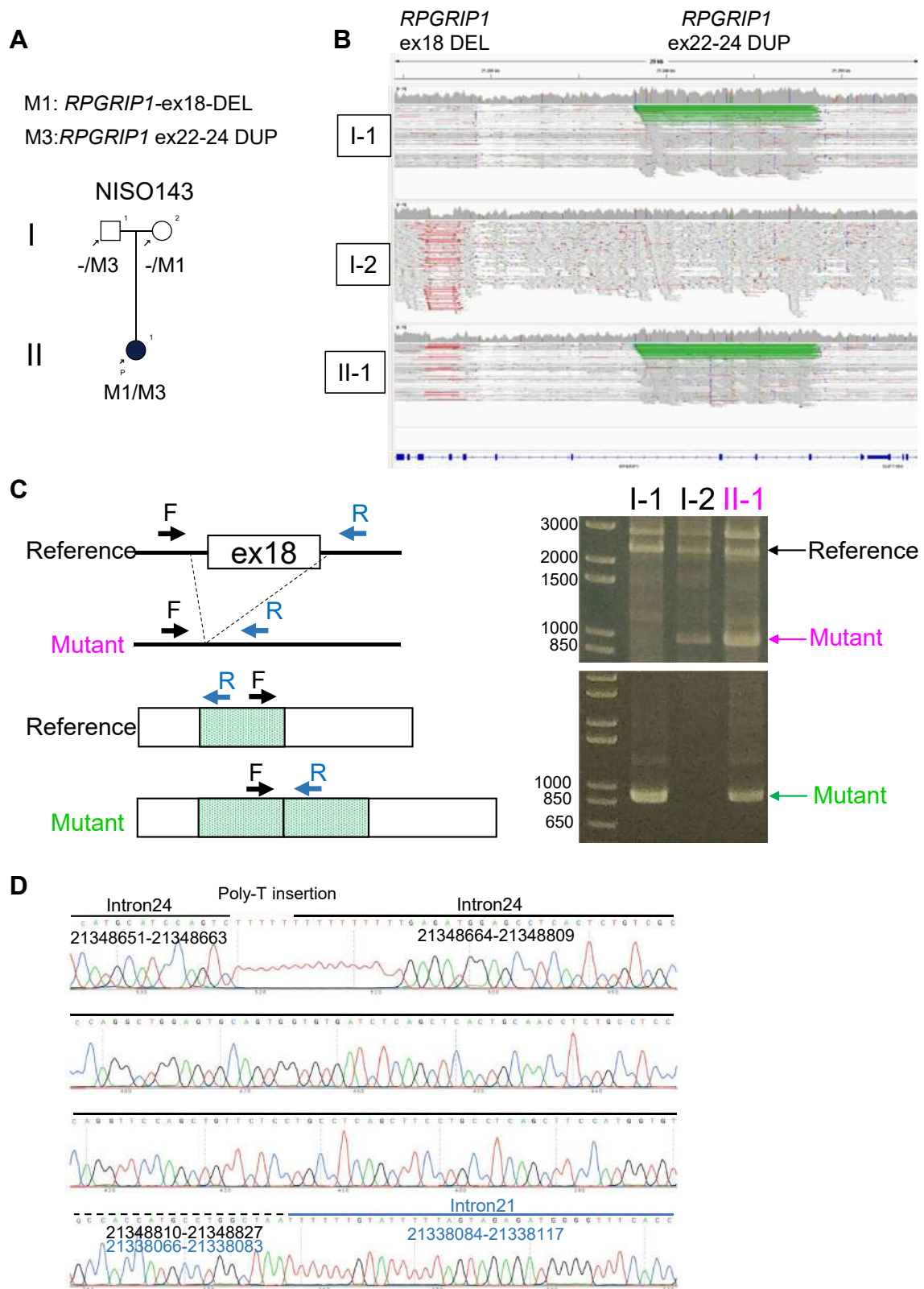


Figure 3 *RPGRIP1*-ex18-DEL and exons 22-24 duplication in NISO143. **A.** Family tree of NISO143 showing variant inheritance of *RPGRIP1*-ex18-DEL and *RPGRIP1* ex22-24 DUP. **B.** Read alignments. Red lines indicate deletions in read sequences compared with the reference, whereas green lines indicate duplications of the region. **C.** Schematic explanation and PCR band patterns to confirm *RPGRIP1*-ex18-DEL (upper panels) and *RPGRIP1* ex22-24 DUP (lower panels). **D.** Sanger sequencing identifies the break point of *RPGRIP1* ex22-24 DUP using II-1 PCR product. Dotted line indicates 18 bases aligned to both edges of the duplicated region

considered as equal to a null variant, these results suggest a correlation between phenotype severity and variant impact. Although *RPGRIP1*-ex18-DEL is predicted to cause a frameshift and premature termination resulting from the loss of 185 bases of the coding sequence, the exact impact of the deletion of exon 18 with flanking introns on both sides has yet to be tested experimentally. Considering the variable effect of deep-intron variants on RNA splicing,^{13,40} large deletions in introns 17 and 18 (1077 and 77 bp, respectively) might cause splicing errors rather than simply connecting the remaining exons. Molecular validation of *RPGRIP1*-ex18-DEL and a novel identified structural variant (*RPGRIP1* ex22-24 DUP) will provide further insights into genotype-phenotype correlations.

At present, there is no clinical treatment for ACHM, but the recessive inheritance pattern and remaining cone photoreceptor cells in patients with ACHM are appropriate for gene supplementation therapy. After the positive results of adeno-associated virus (AAV)-mediated gene supplementation experiments in ACHM animal models (eg, *Cnga3* and *Cngb3* knockout mice),^{41,42} multiple clinical studies targeting *CNGA3*- or *CNGB3*-associated ACHM are ongoing or recently completed (NCT03758404, NCT02610582, NCT02935517, NCT03001310, NCT03278873, and NCT02599922). In addition, preclinical studies of gene replacement therapy using AAV-packed mouse *Rpgrip1* cDNA and human *RPGRIP1* cDNA on *Rpgrip1* knockout mice have already been published.^{43,44} In both studies, treated eyes showed normal localization of exogenously expressed RPGRIP1 protein, rescue of the photoreceptor outer segment, and recovery of ERG responses. Although these studies rescued the LCA phenotype, these results indicate that AAV-delivered RPGRIP1 can supplement normal RPGRIP1 functions. According to the MAF in the Japanese population and current 2022 population estimates,⁴⁵ more than 600 individuals are expected to be homozygous for *RPGRIP1*-ex18-DEL in Japan ($124,947,000 \times 0.0023^2$). The exact effect of the variant remains to be elucidated, but *RPGRIP1* could be a promising clinical target for patients with ACHM in Japan.

In conclusion, we identified a frequent association of *RPGRIP1*-ex18-DEL with the ACHM phenotype in Japanese patients, further contributing to the wide spectrum of *RPGRIP1*-associated IRD phenotypes from LCA to ACHM. Detailed phenotyping and genome sequencing improved the pathogenic variant identification ratio of cone dysfunction syndromes in our cohort from 34% to 50%. Identification of homozygous *RPGRIP1*-ex18-DEL in 5 of 10 patients with ACHM suggests that this variant accounts for a non-negligible portion of Japanese patients with ACHM.

Data Availability

The raw individual genome sequence data are not publicly available because of the privacy policy. Deidentified data will

be available under the regulation of Japan leading project for rare disease WGS (<https://rare-disease-wgs.jp/en/>).

Acknowledgments

The authors thank Write Science Right (www.writescienceright.com) for checking grammatical errors of the manuscript.

Funding

Support for this work was awarded to K.T. and T.I. by the Japan Agency for Medical Research and Development (AMED) under grant number JP22ek0109493, and awarded to K.T., S.U., and T.H. by the Health Labor Sciences Research Grant (20FC1029).

Author Information

Conceptualization: A.S., T.I.; Data Curation: A.S., K.M., T.I., K.Y.; Funding Acquisition: T.I., K.Tsunoda, S.U., T.H.; Investigation: A.S., K.Y., N.M., K.M.; Methodology: A.S., K.Tsunoda, T.H., S.U., T.I.; Project Administration: T.I.; Resources: Y.K., Y.O., K.Tokunaga, NCBN Controls WGS Consortium; Supervision: T.I.; Writing-original draft: A.S., K.M.; Writing-review and editing: K.K., K.Tsunoda, K.K., T.H., S.U., T.I.

ORCIDs

Akiko Suga: <https://orcid.org/0000-0001-6609-2647>
 Kei Mizobuchi: <https://orcid.org/0000-0001-5389-6507>
 Kazutoshi Yoshitake: <https://orcid.org/0000-0002-8247-9443>
 Kazuki Kuniyoshi: <https://orcid.org/0000-0003-0242-5662>
 Yosuke Kawai: <https://orcid.org/0000-0003-0666-1224>
 Katsushi Tokunaga: <https://orcid.org/0000-0001-5501-0503>
 Takaaki Hayashi: <https://orcid.org/0000-0002-1535-0279>
 Shinji Ueno: <https://orcid.org/0000-0001-5716-3626>
 Takeshi Iwata: <https://orcid.org/0000-0003-1447-0081>

Ethics Declaration

The study was approved by the ethics board of NHO Tokyo Medical Center (R18-029), and also by the ethics boards of all participating institutions. Recruitment and sample collection were conducted in accordance with the Declaration of Helsinki. All participants provided written informed consent at their respective recruiting institutes.

Conflict of Interest

The authors declare no conflicts of interest.

Additional Information

The online version of this article (<https://doi.org/10.1016/j.gimo.2024.101843>) contains supplemental material, which is available to authorized users.

Affiliations

¹Division of Molecular and Cellular Biology, National Institute of Sensory Organs, NHO Tokyo Medical Center, Tokyo, Japan; ²Department of Ophthalmology, The Jikei University School of Medicine, Tokyo, Japan; ³Department of Ophthalmology, Nagoya University Graduate School of Medicine, Aichi, Japan; ⁴Laboratory of Aquatic Molecular Biology and Biotechnology, Aquatic Bioscience, Graduate School of Agricultural and Life Sciences, The University of Tokyo, Tokyo, Japan; ⁵Division of Vision Research, National Institute of Sensory Organs, NHO Tokyo Medical Center, Tokyo, Japan; ⁶Department of Ophthalmology, Kindai University Faculty of Medicine, Osaka, Japan; ⁷Genome Medical Science Project, National Center for Global Health and Medicine, Tokyo, Japan; ⁸Department of Ophthalmology, Hirosaki University Graduate School of Medicine, Aomori, Japan

Members of the NCBN Controls WGS Consortium

Hatsue Ishibashi-Ueda, Tsutomu Tomita, Michio Noguchi, Ayako Takahashi, Yu-ichi Goto, Sumiko Yoshida, Kotaro Hattori, Ryo Matsumura, Aritoshi Iida, Yutaka Maruoka, Hiroyuki Gatanaga, Masaya Sugiyama, Satoshi Suzuki, Kengo Miyo, Yoichi Matsubara, Akihiro Umezawa, Kenichiro Hata, Tadashi Kaname, Kouichi Ozaki, Haruhiko Tokuda, Hiroshi Watanabe, Shumpei Niida, Eisei Noiri14, Koji Kitajima, Yosuke Omae, Reiko Miyahara, Hideyuki Shimanuki, Yosuke Kawai, and Katsushi Tokunaga

References

- Hirji N, Georgiou M, Kalitzeos A, et al. Longitudinal assessment of retinal structure in achromatopsia patients with long-term follow-up. *Invest Ophthalmol Vis Sci*. 2018;59(15):5735-5744. [http://doi.org/10.1167/iovs.18-25452](https://doi.org/10.1167/iovs.18-25452)
- Hirji N, Aboshiha J, Georgiou M, Bainbridge J, Michaelides M. Achromatopsia: clinical features, molecular genetics, animal models and therapeutic options. *Ophthalmic Genet*. 2018;39(2):149-157. [http://doi.org/10.1080/13816810.2017.1418389](https://doi.org/10.1080/13816810.2017.1418389)
- Aboshiha J, Dubis AM, Carroll J, Hardcastle AJ, Michaelides M. The cone dysfunction syndromes. *Br J Ophthalmol*. 2016;100(1):115-121. [http://doi.org/10.1136/bjophthalmol-2014-306505](https://doi.org/10.1136/bjophthalmol-2014-306505)
- Kohl S, Zobor D, Chiang WC, et al. Mutations in the unfolded protein response regulator ATF6 cause the cone dysfunction disorder achromatopsia. *Nat Genet*. 2015;47(7):757-765. [http://doi.org/10.1038/ng.3319](https://doi.org/10.1038/ng.3319)
- Carss KJ, Arno G, Erwood M, et al. Comprehensive rare variant analysis via whole-genome sequencing to determine the molecular pathology of inherited retinal disease. *Am J Hum Genet*. 2017;100(1):75-90. [http://doi.org/10.1016/j.ajhg.2016.12.003](https://doi.org/10.1016/j.ajhg.2016.12.003)
- Weisschuh N, Obermaier CD, Battke F, et al. Genetic architecture of inherited retinal degeneration in Germany: a large cohort study from a single diagnostic center over a 9-year period. *Hum Mutat*. 2020;41(9):1514-1527. [http://doi.org/10.1002/humu.24064](https://doi.org/10.1002/humu.24064)
- Johnson S, Michaelides M, Aligianis IA, et al. Achromatopsia caused by novel mutations in both CNGA3 and CNGB3. *J Med Genet*. 2004;41(2):e20. [http://doi.org/10.1136/jmg.2003.011437](https://doi.org/10.1136/jmg.2003.011437)
- Suga A, Yoshitake K, Minematsu N, et al. Genetic characterization of 1210 Japanese pedigrees with inherited retinal diseases by whole-exome sequencing. *Hum Mutat*. 2022;43(12):2251-2264. [http://doi.org/10.1002/humu.24492](https://doi.org/10.1002/humu.24492)
- Zhao Y, Hong DH, Pawlyk B, et al. The retinitis pigmentosa GTPase regulator (RPGR)-interacting protein: subserving RPGR function and participating in disk morphogenesis. *Proc Natl Acad Sci U S A*. 2003;100(7):3965-3970. [http://doi.org/10.1073/pnas.0637349100](https://doi.org/10.1073/pnas.0637349100)
- Dryja TP, Adams SM, Grimsby JL, et al. Null RPGRIP1 alleles in patients with Leber congenital amaurosis. *Am J Hum Genet*. 2001;68(5):1295-1298. [http://doi.org/10.1086/320113](https://doi.org/10.1086/320113)
- Beryozkin A, Aweidah H, Carrero Valenzuela RD, et al. Retinal degeneration associated with RPGRIP1: a review of natural history, mutation spectrum, and genotype-phenotype correlation in 228 patients. *Front Cell Dev Biol*. 2021;9:746781. [http://doi.org/10.3389/fcell.2021.746781](https://doi.org/10.3389/fcell.2021.746781)
- Huang CH, Yang CM, Yang CH, Hou YC, Chen TC. Leber's congenital amaurosis: current concepts of genotype-phenotype correlations. *Genes (Basel)*. 2021;12(8):1261. [http://doi.org/10.3390/genes12081261](https://doi.org/10.3390/genes12081261)
- Jamshidi F, Place EM, Mehrotra S, et al. Contribution of noncoding pathogenic variants to RPGRIP1-mediated inherited retinal degeneration. *Genet Med*. 2019;21(3):694-704. [http://doi.org/10.1038/s41436-018-0104-7](https://doi.org/10.1038/s41436-018-0104-7)
- Iwata T. Japan to Global Eye Genetics Consortium: extending research collaboration for inherited eye diseases. *Asia Pac J Ophthalmol (Phila)*. 2022;11(4):360-368. [http://doi.org/10.1097/APO.0000000000000535](https://doi.org/10.1097/APO.0000000000000535)
- Robson AG, Frishman LJ, Grigg J, et al. ISCEV Standard for full-field clinical electroretinography (2022 update). *Doc Ophthalmol*. 2022;144(3):165-177. [http://doi.org/10.1007/s10633-022-09872-0](https://doi.org/10.1007/s10633-022-09872-0)
- Katagiri S, Hayashi T, Kondo M, et al. RPE65 mutations in two Japanese families with Leber congenital amaurosis. *Ophthalmic Genet*. 2016;37(2):161-169. [http://doi.org/10.3109/13816810.2014.991931](https://doi.org/10.3109/13816810.2014.991931)
- Mizobuchi K, Hayashi T, Ohira R, Nakano T. Electroretinographic abnormalities in Alport syndrome with a novel COL4A5 truncated variant (p.Try20GlyfsTer19). *Doc Ophthalmol*. 2023;146(3):281-291. [http://doi.org/10.1007/s10633-023-09935-w](https://doi.org/10.1007/s10633-023-09935-w)
- Hayashi T, Gekka T, Goto-Omoto S, Takeuchi T, Kubo A, Kitahara K. Novel NR2E3 mutations (R104Q, R334G) associated with a mild form of enhanced S-cone syndrome demonstrate compound heterozygosity. *Ophthalmology*. 2005;112(12):2115. [http://doi.org/10.1016/j.ophtha.2005.07.002](https://doi.org/10.1016/j.ophtha.2005.07.002)
- Kato K, Kondo M, Sugimoto M, Ikesugi K, Matsubara H. Effect of pupil size on flicker ERGs recorded with RETeval system: new mydriasis-free full-field ERG system. *Invest Ophthalmol Vis Sci*. 2015;56(6):3684-3690. [http://doi.org/10.1167/iovs.14-16349](https://doi.org/10.1167/iovs.14-16349)
- Tokutomi T, Fukushima A, Yamamoto K, Bansho Y, Hachiya T, Shimizu A. f-treeGC: a questionnaire-based family tree-creation software for genetic counseling and genome cohort studies. *BMC Med Genet*. 2017;18(1):71. [http://doi.org/10.1186/s12881-017-0433-4](https://doi.org/10.1186/s12881-017-0433-4)
- Kawai Y, Watanabe Y, Omae Y, et al. Exploring the genetic diversity of the Japanese population: insights from a large-scale whole genome sequencing analysis. *PLoS Genet*. 2023;19(12):e1010625. [http://doi.org/10.1371/journal.pgen.1010625](https://doi.org/10.1371/journal.pgen.1010625)
- RDWGS. Accessed December 7, 2023. <https://rare-disease-wgs.jp/en/>

23. Li H, Durbin R. Fast and accurate short read alignment with Burrows-Wheeler transform. *Bioinformatics*. 2009;25(14):1754-1760. <http://doi.org/10.1093/bioinformatics/btp324>
24. Franke KR, Crowgey EL. Accelerating next generation sequencing data analysis: an evaluation of optimized best practices for Genome Analysis Toolkit algorithms. *Genomics Inform*. 2020;18(1):e10. <http://doi.org/10.5808/GI.2020.18.1.e10>
25. Wang K, Li M, Hakonarson H. ANNOVAR: functional annotation of genetic variants from high-throughput sequencing data. *Nucleic Acids Res*. 2010;38(16):e164. <http://doi.org/10.1093/nar/gkq603>
26. Jaganathan K, Kyriazopoulou Panagiotopoulou S, McRae JF, et al. Predicting splicing from primary sequence with deep learning. *Cell*. 2019;176(3):535-548.e24. <http://doi.org/10.1016/j.cell.2018.12.015>
27. Collins RL, Brand H, Karczewski KJ, et al. A structural variation reference for medical and population genetics. *Nature*. 2020;581(7809):444-451. <http://doi.org/10.1038/s41586-020-2287-8>
28. Gardner EJ, Lam VK, Harris DN, et al. The Mobile Element Locator Tool (MELT): population-scale mobile element discovery and biology. *Genome Res*. 2017;27(11):1916-1929. <http://doi.org/10.1101/gr.218032.116>
29. Otsuki A, Okamura Y, Ishida N, et al. Construction of a trio-based structural variation panel utilizing activated T lymphocytes and long-read sequencing technology. *Commun Biol*. 2022;5(1):991. <http://doi.org/10.1038/s42003-022-03953-1>
30. Li Q, Wang K. InterVar: clinical interpretation of genetic variants by the 2015 ACMG-AMP guidelines. *Am J Hum Genet*. 2017;100(2):267-280. <http://doi.org/10.1016/j.ajhg.2017.01.004>
31. Geoffroy V, Herenger Y, Kress A, et al. AnnotSV: an integrated tool for structural variations annotation. *Bioinformatics*. 2018;34(20):3572-3574. <http://doi.org/10.1093/bioinformatics/bty304>
32. Robinson JT, Thorvaldsdóttir H, Winckler W, et al. Integrative genomics viewer. *Nat Biotechnol*. 2011;29(1):24-26. <http://doi.org/10.1038/nbt.1754>
33. Suzuki T, Fujimaki T, Yanagawa A, et al. A novel exon 17 deletion mutation of RPGRIP1 gene in two siblings with Leber congenital amaurosis. *Jpn J Ophthalmol*. 2014;58(6):528-535. <http://doi.org/10.1007/s10384-014-0339-z>
34. Wheeler TJ, Clements J, Eddy SR, et al. Dfam: a database of repetitive DNA based on profile hidden Markov models. *Nucleic Acids Res*. 2013;41(database issue):D70-D82. <http://doi.org/10.1093/nar/gks1265>
35. Khan AO, Abu-Safieh L, Eisenberger T, Bolz HJ, Alkuraya FS. The RPGRIP1-related retinal phenotype in children. *Br J Ophthalmol*. 2013;97(6):760-764. <http://doi.org/10.1136/bjophthalmol-2012-303050>
36. Torii K, Nishina S, Morikawa H, et al. The structural abnormalities are deeply involved in the cause of RPGRIP1-related retinal dystrophy in Japanese patients. *Int J Mol Sci*. 2023;24(18):13678. <http://doi.org/10.3390/ijms241813678>
37. Ueno S, Nakanishi A, Sayo A, et al. Differences in ocular findings in two siblings: one with complete and other with incomplete achromatopsia. *Doc Ophthalmol*. 2017;134(2):141-147. <http://doi.org/10.1007/s10633-017-9577-y>
38. Khan AO. RPGRIP1-related retinal disease presenting as isolated cone dysfunction. *Ophthalmic Genet*. 2023;44(6):595-597. <http://doi.org/10.1080/13816810.2023.2175224>
39. Miyamichi D, Nishina S, Hosono K, et al. Retinal structure in Leber's congenital amaurosis caused by RPGRIP1 mutations. *Hum Genome Var*. 2019;6:32. <http://doi.org/10.1038/s41439-019-0064-8>
40. Bauwens M, Garanto A, Sangermano R, et al. ABCA4-associated disease as a model for missing heritability in autosomal recessive disorders: novel noncoding splice, cis-regulatory, structural, and recurrent hypomorphic variants. *Genet Med*. 2019;21(8):1761-1771. <http://doi.org/10.1038/s41436-018-0420-y>
41. Michalakakis S, Mühlfriedel R, Tanimoto N, et al. Restoration of cone vision in the CNGA3^{-/-} mouse model of congenital complete lack of cone photoreceptor function. *Mol Ther*. 2010;18(12):2057-2063. <http://doi.org/10.1038/mt.2010.149>
42. Carvalho LS, Xu J, Pearson RA, et al. Long-term and age-dependent restoration of visual function in a mouse model of CNGB3-associated achromatopsia following gene therapy. *Hum Mol Genet*. 2011;20(16):3161-3175. <http://doi.org/10.1093/hmg/ddr218>
43. Pawlyk BS, Smith AJ, Buch PK, et al. Gene replacement therapy rescues photoreceptor degeneration in a murine model of Leber congenital amaurosis lacking RPGRIP. *Invest Ophthalmol Vis Sci*. 2005;46(9):3039-3045. <http://doi.org/10.1167/iovs.05-0371>
44. Pawlyk BS, Bulgakov OV, Liu X, et al. Replacement gene therapy with a human RPGRIP1 sequence slows photoreceptor degeneration in a murine model of Leber congenital amaurosis. *Hum Gene Ther*. 2010;21(8):993-1004. <http://doi.org/10.1089/hum.2009.218>
45. Current population estimates as of October 1, 2022. Statistics Bureau of Japan. Accessed October 10, 2023. <https://www.stat.go.jp/english/data/jinsui/2022np/index.html>

Genetic and Clinical Features of ABCA4-Associated Retinopathy in a Japanese Nationwide Cohort

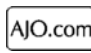


KEI MIZOBUCHI, TAKAAKI HAYASHI, KOJI TANAKA, KAZUKI KUNIYOSHI, YUSUKE MURAKAMI, NATSUKO NAKAMURA, KAORUKO TORII, ATSUSHI MIZOTA, DAIKI SAKAI, AKIKO MAEDA, TARO KOMINAMI, SHINJI UENO, SHUNJI KUSAKA, KOJI M NISHIGUCHI, YASUHIRO IKEDA, MINEO KONDO, KAZUSHIGE TSUNODA, YOSHIHIRO HOTTA, AND TADASHI NAKANO

- **PURPOSE:** To clarify the genetic and clinical features of Japanese patients with ABCA4-associated retinopathy.
- **DESIGN:** Retrospective, multicenter cohort study.
- **METHODS:** Patients with retinal degeneration and biallelic ABCA4 variants were recruited from 13 different hospitals. Whole exome sequencing analysis was used for genetic testing. Comprehensive ophthalmic examinations were performed on matched patients. The primary outcome measure was identifying multimodal retinal imaging findings associated with disease progression.
- **RESULTS:** This study included 63 patients: 19 with missense/missense, 23 with missense/truncation, and 21 with truncation/truncation genotypes. In total, 62 variants were identified, including 29 novel variants. Six patients had a mild phenotype characterized by foveal-sparing or preserved foveal structure, including 4 with missense/missense and 2 with missense/truncation genotypes. The p.Arg212His variant was the most frequent in patients with mild phenotypes (4/12 alleles). Clinical

findings showed a disease duration-dependent worsening of the phenotypic stage. Patients with the truncation/truncation genotype exhibited rapid retinal degeneration within a few years and definite fundus autofluorescence imaging patterns, including hyper autofluorescence at the macula and few or no flecks.

- **CONCLUSIONS:** Our results indicate that missense/missense or missense/truncation genotypes, including the p.Arg212His variant, are associated with a relatively mild phenotype. In contrast, the truncation/truncation genotype causes rapid and severe retinal degeneration in Japanese patients with ABCA4-associated retinopathy. These data are vital in predicting patient prognosis, guiding genetic counseling, and stratifying patients for future clinical trials. (Am J Ophthalmol 2024;264: 36–43. © 2024 The Author(s). Published by Elsevier Inc. This is an open access article under the CC BY-NC-ND license (<http://creativecommons.org/licenses/by-nc-nd/4.0/>))

 Supplemental Material available at AJO.com.
Accepted for publication March 11, 2024.

Department of Ophthalmology (K.M., T.H., T.N.), The Jikei University School of Medicine, Tokyo, Japan; Department of Ophthalmology, Katsushika Medical Center (T.H.), The Jikei University School of Medicine, Tokyo, Japan; Division of Ophthalmology, Department of Visual Sciences (K.T.), Nihon University School of Medicine, Nihon University Hospital, Tokyo, Japan; Department of Ophthalmology (K.K., S.K.), Kindai University Faculty of Medicine, Osaka-sayama, Japan; Department of Ophthalmology (Y.M.), Graduate School of Medical Sciences, Kyushu University, Fukuoka, Japan; Department of Ophthalmology (N.N.), The University of Tokyo, Tokyo, Japan; Department of Ophthalmology (K.T., Y.H.), Hamamatsu University School of Medicine, Hamamatsu, Shizuoka, Japan; Department of Ophthalmology (A.M.), Teikyo University, Tokyo, Japan; Department of Ophthalmology (D.S., A.M.), Kobe City Eye Hospital, Kobe, Japan; Department of Ophthalmology (T.K., S.U., K.M.N.), Nagoya University Graduate School of Medicine, Aichi, Japan; Department of Ophthalmology (S.U.), Hiroshima University Graduate School of Medicine, Aomori, Japan; Department of Ophthalmology (Y.I.), Faculty of Medicine, University of Miyazaki, Miyazaki, Japan; Department of Ophthalmology (M.K.), Mie University Graduate School of Medicine, Mie, Japan; Division of Vision Research (K.T.), National Institute of Sensory Organs, NHO Tokyo Medical Center, Tokyo, Japan

Inquiries to Takaaki Hayashi, Department of Ophthalmology, Katsushika Medical Center, The Jikei University School of Medicine, Tokyo, Japan; e-mail: taka@jikei.ac.jp

IN 1997, STARGARDT DISEASE (STGD1, MIM: 248200) WAS first reported to be caused by biallelic variants of the ATP-binding cassette transporter, alpha 4 subunit (ABCA4) gene.¹ These variants are associated with several retinal conditions, including bull's-eye maculopathy,² macular atrophy,³ fundus flavimaculatus,⁴ cone-rod dystrophy, and retinitis pigmentosa.^{5–7} ABCA4-associated retinopathy is a commonly inherited retinal disorder, affecting approximately 1 in 8000 to 10,000 people.^{8,9} A recent national survey in the United Kingdom reported a yearly incidence of 0.127 per 100,000 population,¹⁰ which is 5 times higher than that observed in a study from the Nationwide Epidemiological Survey of Macular Dystrophy in Japan.¹¹ Previous large cohort studies have identified genotype-phenotype correlations in patients with ABCA4-associated retinopathy, showing that disease severity correlates with variant severity and worsens over time.^{12,13}

Notably, several therapies, including oral treatments¹⁴ and gene therapies using adeno-associated viruses,¹⁵ other large vectors,^{16,17} and antisense oligonucleotides,¹⁸

have recently been explored. However, *ABCA4*-associated retinopathy is rare among the Japanese, accounting for 1.7% of inherited retinal disorder cases (20 of 1210 pedigrees).¹⁹ With imminent clinical trials, it is crucial to thoroughly investigate this retinopathy's genetic and clinical characteristics in Japanese patients to precisely evaluate treatment efficacy and timing of interventions. This study represents the first nationwide Japanese cohort focused on *ABCA4*-associated retinopathy, aiming to elucidate the genetic and clinical profiles of patients with this condition, particularly concerning disease progression and genotype.

METHODS

• **ETHICS STATEMENT:** The Institutional Review Boards of The Jikei University School of Medicine (approval number 24-231 6997), Nihon University School of Medicine (approval number 20211105), Kindai University Faculty of Medicine (approval number 22-132 and R05-071), Kyushu University (approval number 536-08), The University of Tokyo (approval number 2018191G), Hamamatsu University School of Medicine (approval number 14-040), Teikyo University (approval number 10-007-5), Kobe City Eye Hospital (approval number E19002), Nagoya University Graduate School of Medicine (approval Number: 2020-0598), University of Miyazaki (approval number G-0118), Mie University Graduate School of Medicine (approval number MIE-2429), and the National Hospital Organization Tokyo Medical Center (approval number R18-029) approved this study. The study protocol followed the Declaration of Helsinki, and all participants provided written informed consent.

• **INCLUSION CRITERIA:** We studied 3324 patients with inherited retinal disorders who underwent genetic analysis. The inclusion criteria for patients were retinal degeneration conditions, such as macular dystrophy, cone-rod dystrophy, and retinitis pigmentosa phenotypes. Eligible patients exhibited either homozygous or compound heterozygous variants in the *ABCA4* gene as confirmed by genetic analysis across the consortium of 13 participating hospitals. The phenotypes were determined using findings from multimodal retinal imaging, visual field testing, and full-field electroretinography.

• **MOLECULAR GENETIC ANALYSIS:** Genetic testing was performed using whole exome sequencing analysis based on previously described methods.²⁰⁻²³ The pathogenicity of the *ABCA4* variants was evaluated using the Human Gene Mutation Database Professional (HGMD, <http://www.hgmd.cf.ac.uk/>), ClinVar (<https://www.ncbi.nlm.nih.gov/clinvar/>), Genome Aggregation Database (gnomAD, <https://gnomad.broadinstitute.org/>), and the Japanese Multi Omics Reference Panel (jMorP; <https://jmorp.megabank.tohoku.ac.jp/>).

Patients with biallelic *ABCA4* variants were classified into 3 groups according to their genotypes (missense/missense, missense/truncation, and truncation/truncation) based on a modified method from a previous study.²⁴ Consequently, canonical and non-canonical splice site, frameshift, and stop-gain variants were defined as truncation variants.

• **CLINICAL EXAMINATIONS:** Comprehensive ophthalmic examinations, including medical review (age at onset and chief complaint), decimal best-corrected visual acuity (BCVA), fundus photograph, and short-wavelength fundus autofluorescence imaging (FAF) were performed using Spectralis HRA (Heidelberg Engineering, Heidelberg, Germany), and/or Optos 200Tx/California, ultrawidefield retinal imaging system (Optos, Dunfermline, UK), optical coherence tomography (OCT; Carl Zeiss Meditec AG, Dublin, CA, USA), and Goldmann perimetry (Haag Streit, Bern, Switzerland).

Phenotypic stage analysis

We analyzed the correlations between the phenotypic stage, disease duration, and BCVA across 3 genotypes. Based on the findings of well-established studies,^{4,13,25} the ophthalmologists K.M. and T.H. conducted independent evaluations of the phenotypic stages, utilizing fundus imaging and specific criteria outlined below:

Stage I: Macular lesions limited to the macula, exhibiting irregular pigmentary alterations, a bull's-eye maculopathy, or a distinctive "beaten-bronze" appearance.

Stage II: Macular lesions with characteristic yellowish flecks that emanate from the macula and extend beyond the vascular arcades and optic disc.

Stage III: Diffuse atrophy of the macular choriocapillaris with associated resorption of flecks within the macular area.

Stage IV: Extensive atrophy of the choriocapillaris accompanied by pigment deposition in the central posterior pole or further.

Representative images of each stage are shown in Figure 1.

Statistical analysis

Statistical analyses were performed using IBM SPSS Statistics version 27.0 (IBM Corp, Armonk, NY, USA), R and R-studio (version 3.6.3; <http://www.R-project.org/>). Bonferroni's multiple comparison test was used to determine the significant differences in the age at onset and patients with each genotype. Decimal BCVA was converted to a logarithm of the minimum angle of resolution (logMAR) units for statistical analysis. Furthermore, the BCVA of counting fingers, hand motions, and light perceptions were converted to 2.0, 2.4, and 2.7 logMAR units, respectively.²⁶ Kaplan-Meier survival curves with the log-rank test were used to compare survival experiences (logMAR BCVA) among the

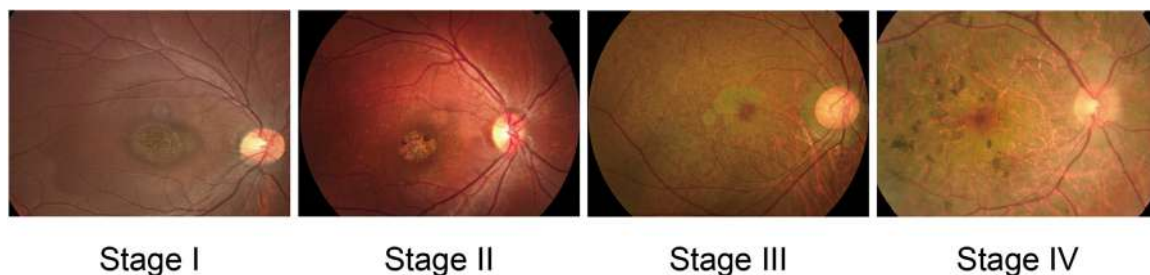


FIGURE 1. Representative imaging of each stage in patients with ABCA4-associated retinopathy.

Stage I: Macular lesions limited to the macula, exhibiting irregular pigmentary alterations, a bull's-eye maculopathy, or a distinctive "beaten-bronze" appearance. Stage II: Macular lesions with characteristic yellowish flecks that emanate from the macula and extend beyond the vascular arcades and optic disc. Stage III: Diffuse atrophy of the macular choriocapillaris with associated resorption of flecks within the macular area. Stage IV: Extensive atrophy of the choriocapillaris accompanied by pigment deposition in the central posterior pole or further.

3 genotypes. A significance threshold of $P < .05$ was established, and for cases where this was achieved among the 3 genotypes, a Bonferroni correction was applied to pinpoint which genotype pairs exhibited significant differences, using an adjusted significance level of $P < .017$.

RESULTS

• **MOLECULAR GENETIC FINDINGS:** In total, 63 patients who met the inclusion criteria were recruited, and 62 variants were identified, including 29 novel ones (Supplemental Tables 1 and 2). Of these variants, 42 were missense (67.7%), 9 were stop-gain (14.5%), 6 were frameshift (9.7%), and 5 were canonical/noncanonical splice-site variants (8.1%). The patients were categorized into 3 genotype groups: 19 (30.2%), 23 (36.5%), and 21 (33.3%) with missense/missense, missense/truncation, and truncation/truncation genotypes, respectively.

• **CLINICAL FINDINGS:** Supplemental Table 1 presents the clinical findings in the 63 patients with biallelic ABCA4 variants, including the age at onset, symptoms, disease duration (from onset to examination), BCVA (first and last examinations), and the phenotypic stage (first and last examinations).

Age at onset

Patients with truncation/truncation genotypes had a younger age at onset (7.29 ± 2.37 years; range, 3-11 years) than did those with missense/missense genotypes (26.44 ± 19.46 years; range, 6-68 years; $P = .000$) and missense/truncation (17.81 ± 11.75 years; range, 6-40 years; $P = .030$) genotypes. However, the patients with missense/missense and missense/truncation genotypes ($P = .234$) showed no differences in the age at onset (Figure 2).

Survival curves of visual acuity

Kaplan–Meier survival curves were initially plotted using a cutoff of 1.0 logMAR unit (equivalent to 0.1 a decimal visual acuity) to estimate the changes in BCVA during the disease course in all 63 patients. The survival curves indicated that BCVA required a median duration of 42 years to reach a 1.0 logMAR unit. Subsequently, comparing the BCVA progression among the 3 genotypes (missense/missense, missense/truncation, and truncation/truncation) showed that the median age for BCVA to reach a 1.0 logMAR unit was the late 60s, approximately 50 years, and approximately 30 years in patients with the missense/missense, missense/truncation, and truncation/truncation genotypes, respectively (Figure 3). The genotype comparison results were as follows: a significant difference was observed between the missense/missense and truncation/truncation genotypes ($P = .003$), as well as between the missense/truncation and truncation/truncation genotypes ($P = .003$). However, no significant difference was noted when comparing the missense/missense genotype with the missense/truncation genotype ($P = .900$) (Figure 3).

Phenotypic stage

Supplemental Figure 1 illustrates the correlations among the phenotypic stage, disease duration, and logMAR BCVA for the 3 genotypes. Among 15 patients with the missense/missense genotype, all but 5 patients (JU0266, JU2182, JU2189, JU2211, and Teikyo1024) exhibited an early stage (stage I or II) within the first 20 years of disease onset. Patients exhibited varying correlations between phenotypic stage and disease duration, and between phenotypic stage and logMAR BCVA. In 18 patients with the missense/truncation genotype, there was a tendency for the phenotypic stage to progressively worsen over time; however, some (JU0717, JU2154, and Kinki141-107) remained at an early stage (stage I or II) despite having had the disease for >20 years. This pattern was also observed in the correlation between the phenotypic stage and logMAR BCVA.

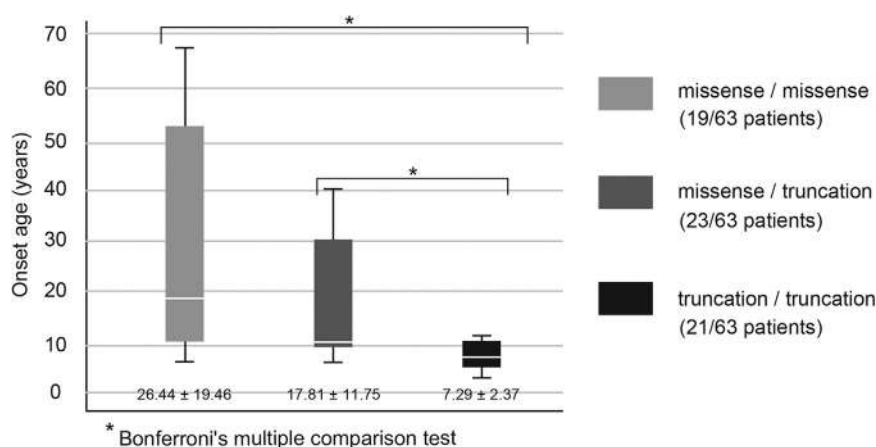


FIGURE 2. Age at onset across genotypes. Patients with the truncation/truncation genotype have a significantly younger age at onset (7.29 ± 2.37 years; range, 3-11 years) compared with those with missense/missense (23.60 ± 16.45 years; range, 6-50 years) and missense/truncation (16.90 ± 11.27 years; range, 6-40 years) genotypes, with P -values of <0.001 and 0.020 , respectively. However, the missense/missense and missense/truncation genotypes show no significant differences in age at onset ($P = .234$).

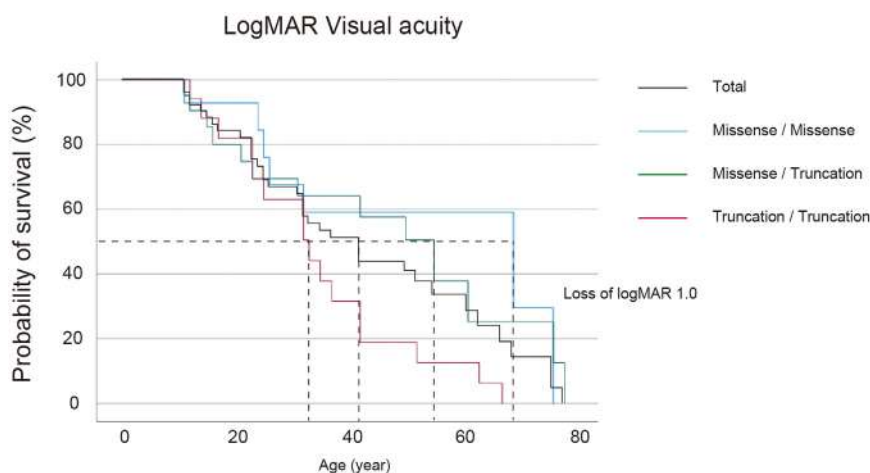


FIGURE 3. Survival curves and clinical course of visual acuity. Kaplan–Meier survival curves are plotted using a cut-off of 1.0 logMAR unit, equivalent to 0.1 a decimal visual acuity. In all 63 patients, the survival curves indicate that the median duration required for best-corrected visual acuity (BCVA) to decline to a 1.0 logMAR unit in half of the patients is 42 years. When comparing progression among the 3 genotypes, we find that the median age in patients when BCVA reaches a 1.0 logMAR unit is the late 60s, approximately 50 years, and approximately 30 years for the missense/missense, missense/truncation, and truncation/truncation genotypes, respectively. Log-rank test with Bonferroni correction is applied for the comparisons. The genotype comparison results show significant differences between missense/missense and truncation/truncation ($P = .003$) and between missense/truncation and truncation/truncation ($P = .003$) but not between missense/missense and missense/truncation ($P = .900$).

In 15 patients with the truncation/truncation genotype, a clear time-dependent progression of the phenotypic stage was observed. Furthermore, logMAR BCVA also deteriorated with the worsening of the phenotypic stage.

Multimodal retinal imaging

Supplemental Figure 2 shows the detailed multimodal retinal images of representative patients across the 3 genotypes.

Missense/missense genotype

In patients with missense/missense genotypes, fundus photography findings generally showed a gradually worsened

phenotypic stage over time. However, this trend was not observed in patients with foveal sparing or a preserved foveal structure (JU2151, JU2182, and JU2211). Flecks were observed in all early stage patients (KA304, KA241, KA115, and JU2151) but were absent in those at the end-stage (Teikyo1024, JU0266, JU2182, JU2189, and JU2211). FAF imaging revealed hypo-AF in the macular region, indicating macular degeneration or atrophy with a combination of hypo-AF and hyper-AF. This was consistent with flecks in the surrounding area in early-stage patients. In contrast, end-stage patients showed hypo-AF extending beyond the arcade vessels. The OCT

findings demonstrated foveal-sparing or preserved foveal structure in some patients, specifically those identified as JU2151 (p.Arg212His and p.His1865Tyr), JU2182 (p.Asp586Glu and p.Gly2041Asp), JU2189 (p.Arg212His and p.Arg212His), and JU2211 (p.Arg212His and p.Asn269Ser). Conversely, a different group of patients showed a disruption of the outer retinal layers at the fovea, including KA304 (p.Arg511Cys and p.Val675Ile), KA241 (p.Gly1623Ser and p.Arg1862Cys), and KA115 (p.Thr1019Met and p.Cys1488Tyr). Over the 8-year follow-up, the 68-year-old patient (JU2189) exhibited progressive damage to the outer retinal layers at the fovea.

Missense/truncation genotype

Fundus photography findings indicated that the phenotypic stage consistently worsened with increasing disease duration in patients with the missense/truncated genotype. Notably, all patients but one (KA074) had flecks throughout the disease course. The FAF findings revealed hypo-AF in the macular area, consistent with macular degeneration or atrophy, with or without additional hypo-AF and hyper-AF around the area, corresponding to flecks in all patients. OCT findings revealed foveal sparing in 2 patients (JU0657 and JU2208) and a disruption of the outer retinal layers at the fovea in other patients (N528, JU0099, JU0666, and KA074). However, 1 patient (JU0657) exhibited this disruption in the outer retinal layers at the fovea over time.

Truncation/truncation genotype

Fundus photography initially showed discoloration or a normal appearance in patients with the truncation/truncation genotype; however, all patients had rapidly increased retinal degeneration from the arcade vessels to the peripheral retina as the disease progressed. Only a few or no flecks were observed throughout the disease course. During the first examination, FAF findings revealed a normal appearance or hypo-AF in the macular region, with hyper-AF around the area (beyond the arcade vessels). Over time, all patients but one (JU1315) exhibited an expansion of hypo-AF beyond the arcades of vessels. In patient JU1315, hypo-AF was localized to the macular region, a finding that aligns with the expected macular degeneration or atrophy, accompanied by areas of both hypo-AF and hyper-AF nearby. The OCT findings revealed that during the disease course, there was a disruption in the outer retinal layers at the fovea in all patients studied.

DISCUSSION

This study characterized the genetic and clinical features in 63 Japanese patients with biallelic ABCA4 variants.

In total, 62 distinct ABCA4 variants were identified, including 41 missense (67.2%), 9 stop-gain (14.8%), 6

frameshifts (9.8%), and 5 splice site variants (8.2%). These findings are consistent with those of previous studies.^{12,13} A previously proposed genotype-phenotype correlation, with phenotypic severity dependent on variant severity, was observed in our cohort, particularly regarding age at onset (Figure 2) and visual acuity (Figure 3). Regarding the mild phenotype characterized by foveal sparing or preserved foveal structure, a large Spanish cohort of 506 patients with STGD1 reported only 8 cases of foveal sparing¹² predominantly with genotypes comprising 6 missense/missense and 2 missense/truncation genotypes. Our study observed a mild phenotype in 6 out of 63 patients, with 4 (JU2151, JU2182, JU2189, and JU2211) and 2 (JU0657 and JU2208) with the missense/missense and missense/truncation genotypes, respectively. Previous research suggests that milder phenotypes are strongly associated with the hypomorphic variants (p.Gly1961Glu and p.Arg2030Gln),²⁷⁻³⁰ and these vary across ethnic groups.²⁵ Notably, the p.Arg212His variant was the most frequently observed (4 of 12 alleles) in our patients with a mild phenotype (JU0657, JU2151, JU2182, JU2189, JU2208, and JU2211), suggesting it as a possible hypomorphic variant in Japanese patients with ABCA4-associated retinopathy. The p.Arg212His variant has also been detected in previously reported cases of STGD1³¹⁻³³; however, detailed clinical features have not been described. In contrast, a previous study has shown that the alternative variant (p.Arg212Cys) in a homozygous state is associated with a mild phenotype with retention of some ABCA4 protein function.³⁰ This supports our findings indicating that the p.Arg212His variant is also associated with a mild phenotype.

Previous large cohort studies have elucidated the clinical features and disease progression in patients with biallelic ABCA4 variants.^{12,13} Wang et al. described the disease progression in 42 patients with long-term follow-up, suggesting that the phenotypic stage progressed in a time-dependent manner.¹³ Consistent with these findings, our study observed a similar time-dependent progression of the phenotypic stage (retinal degeneration) (Supplemental Figure 1). However, no correlation was found between the phenotypic stage and disease duration in patients with a mild phenotype. This suggests that the actual disease duration may be longer than perceived because of subtle symptoms. Our research also investigated clinical variations based on genotype. A previous study found distinct clinical features in patients with rapid-onset chorioretinopathy (ROC), linked to more deleterious variants, such as truncating variant, differing from other ABCA4-associated retinopathy variants.³⁴ This study observed that deterioration of the macula began with an intense/hyper-AF and homogeneous signal on FAF, followed by a coalescing pattern of ROC within the subsequent decade.³⁴ Similarly, disease progression is characterized by an expansion of areas with decreased AF of the macula.^{35,36} Particularly in cases where the disease onset occurs in childhood, the rate of progression tends to be more rapid than that in adult-onset.³⁷ In

our cohort, hyper-AF was also observed in patients with the truncation/truncation genotype, subsequently, areas of decreased AF appeared and expanded (Supplemental Figure 2). Consequently, the previous and current studies indicate that hyper-AF at the macula is a characteristic finding in early-stage patients with the truncation/truncation genotype.

Furthermore, the early-stage disease differences in the presence of flecks based on the genotype were also investigated. The term “fundus flavimaculatus” is often used to describe the phenotype of retinal flecks without atrophy. Flecks are thought to correlate with disease severity. They originate from degenerating photoreceptor cells, impaired by the functional failure of the retinal pigment epithelium (RPE),^{38,39} and correlate with disease severity.⁴⁰ Our findings revealed that flecks were prevalent in patients with missense/missense and missense/truncation genotypes but are less common in those with truncation/truncation genotypes (Supplemental Figure 2). Longitudinal studies of flecks observed on OCT may help understand the differences in flecks observed using FAF imaging.^{38,39} Flecks initially appear as hyperreflective bands from the RPE to the outer nuclear layer (ONL), followed by the thinning of the ONL on OCT. Subsequently, as the fleck deposition dissipates, OCT reveals the disruption of the outer retinal layers, including the ellipsoid zone (EZ). These results indicate that the rapid disease progression leads to little or no fleck deposition, resulting in the sudden appearance of atrophic retinal areas. The presence of few or no flecks in the early stages of the disease may also characterize patients with the truncation/truncation genotype. The differences in fleck presentation in the early stages of the disease could predict the degree of progression and genotype.

Additionally, recent studies have investigated the progression of ABCA4-associated retinopathy with respect to retinal imaging, microperimetry, and electroretinogram (ERG) findings. Both cross-sectional and longitudinal assessments have reported changes in retinal sensitivity measured by microperimetry and alterations in the EZ observed through OCT in childhood-onset STGD1.^{41,42} Assessment using microperimetry has shown that the rate of progression in children is significantly greater than that in adults.⁴¹ Moreover, OCT studies have revealed that quantifying the area of EZ loss offers greater sensitivity than measurements of EZ loss width for evaluating progression.⁴² One study has outlined the potential of using ERG evaluation and FAF imaging results to predict disease progression,⁴³ with patients categorized into 3 ERG groups based on retinal function²⁹ and 3 FAF groups according to the extent of hypo-AF and retinal background appearance.⁴⁴ This study has found a strong correlation between ERG and FAF results. It is sug-

gested that patients assessed in early childhood who possess at least 1 truncation variant and exhibit poor initial BCVA or both, are likely to show a more extensive retinal involvement or progress to a more severe phenotype over time than what baseline FAF imaging might indicate.⁴³ This enables the possibility of informing patients by comparing FAF with the current gold standard of ERG, thereby aiding in prognostication. They may help determine the appropriate timing for therapeutic intervention and assess the effectiveness of treatment in ongoing gene therapy.

This study has some limitations, including the small cohort size and the absence of whole-genome sequencing data, which may have overlooked additional deep intronic variants.²⁵ Furthermore, the limitations encompass the lack of microperimetry assessment, grouping of ERG and ultrawidefield FAF evaluation, and assessment of EZ loss. Further research using a larger patient cohort, comprehensive genomic data, and imaging and functional evaluation of the retina is necessary to substantiate our findings.

In conclusion, our study suggests that the missense/missense or missense/truncation genotypes, including the p.Arg212His variant, are associated with a milder phenotype of ABCA4-associated retinopathy. However, the truncation/truncation genotype is associated with a more rapid and severe retinal degeneration in Japanese patients with ABCA4-associated retinopathy. These findings are crucial for predicting patient prognosis, providing genetic counseling, and stratifying patients for future clinical trials.

CREDIT AUTHORSHIP CONTRIBUTION STATEMENT

Kei Mizobuchi: Writing – original draft, Formal analysis, Conceptualization. **Takaaki Hayashi:** Writing – review & editing, Supervision, Resources, Project administration, Methodology, Investigation, Funding acquisition, Formal analysis, Data curation, Conceptualization. **Koji Tanaka:** Data curation. **Kazuki Kuniyoshi:** Data curation. **Yusuke Murakami:** Data curation. **Natsuko Nakamura:** Data curation. **Kaoruko Torii:** Data curation. **Atsushi Mizota:** Data curation. **Daiki Sakai:** Data curation. **Akiko Maeda:** Data curation. **Taro Kominami:** Data curation. **Shinji Ueno:** Data curation. **Shunji Kusaka:** Data curation. **Koji M Nishiguchi:** Writing – review & editing, Data curation. **Yasuhiro Ikeda:** Writing – review & editing, Data curation. **Mineo Kondo:** Writing – review & editing, Data curation. **Kazushige Tsunoda:** Writing – review & editing, Data curation. **Yoshihiro Hotta:** Writing – review & editing, Data curation. **Tadashi Nakano:** Writing – review & editing.

Funding/Support: This study was partly supported by JSPS KAKENHI, Grant Numbers 21K09756 and 24K12771 to TH, 21K09712 to KT, 22K09831 to SU, and 22K09825 to KK. The Health and Labor Sciences Research Grants (23FC1043) for Research on Rare and Intractable Diseases also supported this research. The funders played no role in the study design, data collection and analysis, publication decision, or manuscript preparation. Financial Disclosures: The authors have made the following disclosure. TH received research funds from Alcon, Johnson and Johnson Vision, AMO, Daiichi Sankyo, Chugai, Santen, Mitsubishi Tanabe Pharma, Senju, Bayer, Otsuka, Kyowa Kirin, Ritz Medical, Uni-hite, and Kuribara. The remaining authors declare no financial disclosures. All authors attest that they meet the current ICMJE criteria for authorship.

REFERENCES

- Allikmets R, Singh N, Sun H, et al. A photoreceptor cell-specific ATP-binding transporter gene (ABCR) is mutated in recessive Stargardt macular dystrophy. *Nat Genet.* 1997;15:236–246.
- Michaelides M, Chen LL, Brantley Jr MA, et al. ABCA4 mutations and discordant ABCA4 alleles in patients and siblings with bull's-eye maculopathy. *Br J Ophthalmol.* 2007;91:1650–1655.
- Michaelides M, Hunt DM, Moore AT. The genetics of inherited macular dystrophies. *J Med Genet.* 2003;40:641–650.
- Fishman GA. Fundus flavimaculatus. A clinical classification. *Arch Ophthalmol.* 1976;94:2061–2067.
- Maugeri A, Klevering BJ, Rohrschneider K, et al. Mutations in the ABCA4 (ABCR) gene are the major cause of autosomal recessive cone-rod dystrophy. *Am J Hum Genet.* 2000;67:960–966.
- Martínez-Mir A, Bayés M, Vilageliu L, et al. A new locus for autosomal recessive retinitis pigmentosa (RP19) maps to 1p13-1p21. *Genomics.* 1997;40:142–146.
- Cremers FP, van de Pol DJ, van Driel M, et al. Autosomal recessive retinitis pigmentosa and cone-rod dystrophy caused by splice site mutations in the Stargardt's disease gene ABCR. *Hum Mol Genet.* 1998;7:355–362.
- Pontikos N, Arno G, Jurkute N, et al. Genetic basis of inherited retinal disease in a molecularly characterized cohort of more than 3000 families from the United Kingdom. *Ophthalmology.* 2020;127:1384–1394.
- Goetz KE, Reeves MJ, Gagadam S, et al. Genetic testing for inherited eye conditions in over 6,000 individuals through the eyeGENE network. *Am J Med Genet C Semin Med Genet.* 2020;184:828–837.
- Spiteri Cornish K, Ho J, Downes S, Scott NW, Bainbridge J, Lois N. The epidemiology of Stargardt disease in the United Kingdom. *Ophthalmol Retina.* 2017;1:508–513.
- Ueno S, Hayashi T, Tsunoda K, Aoki T, Kondo M. Nationwide epidemiologic survey on incidence of macular dystrophy in Japan. *Jpn J Ophthalmol.* 2024 Online ahead of print. PMID: 38568448. doi:10.1007/s10384-024-01060-8.
- Del Pozo-Valero M, Riveiro-Alvarez R, Blanco-Kelly F, et al. Genotype-phenotype correlations in a Spanish cohort of 506 families with biallelic ABCA4 pathogenic variants. *Am J Ophthalmol.* 2020;219:195–204.
- Wang Y, Sun W, Zhou J, et al. Different phenotypes represent advancing stages of ABCA4-associated retinopathy: a longitudinal study of 212 Chinese families from a tertiary center. *Invest Ophthalmol Vis Sci.* 2022;63:28.
- Kubota R, Birch DG, Gregory JK, Koester JM. Randomised study evaluating the pharmacodynamics of emixustat hydrochloride in subjects with macular atrophy secondary to Stargardt disease. *Br J Ophthalmol.* 2022;106:403–408.
- McClements ME, Barnard AR, Singh MS, et al. An AAV dual vector strategy ameliorates the Stargardt phenotype in adult abca4(-/-) mice. *Hum Gene Ther.* 2019;30:590–600.
- Kong J, Kim SR, Binley K, et al. Correction of the disease phenotype in the mouse model of Stargardt disease by lentiviral gene therapy. *Gene Ther.* 2008;15:1311–1320.
- Binley K, Widdowson P, Loader J, et al. Transduction of photoreceptors with equine infectious anemia virus lentiviral vectors: safety and biodistribution of StarGen for Stargardt disease. *Invest Ophthalmol Vis Sci.* 2013;54:4061–4071.
- Shen X, Corey DR. Chemistry, mechanism and clinical status of antisense oligonucleotides and duplex RNAs. *Nucleic Acids Res.* 2018;46:1584–1600.
- Suga A, Yoshitake K, Minematsu N, et al. Genetic characterization of 1210 Japanese pedigrees with inherited retinal diseases by whole-exome sequencing. *Hum Mutat.* 2022;43:2251–2264.
- Katagiri S, Yoshitake K, Akahori M, et al. Whole-exome sequencing identifies a novel ALMS1 mutation (p.Q2051X) in two Japanese brothers with Alström syndrome. *Mol Vis.* 2013;19:2393–2406.
- Mizobuchi K, Hayashi T, Yoshitake K, et al. Novel homozygous CLN3 missense variant in isolated retinal dystrophy: a case report and electron microscopic findings. *Mol Genet Genomic Med.* 2020;8:e1308.
- Mizobuchi K, Hayashi T, Katagiri S, et al. Characterization of GUCA1A-associated dominant cone/cone-rod dystrophy: low prevalence among Japanese patients with inherited retinal dystrophies. *Sci Rep.* 2019;9:16851.
- Mizobuchi K, Hayashi T, Matsuura T, Nakano T. Clinical characterization of autosomal dominant retinitis pigmentosa with NRL mutation in a three-generation Japanese family. *Doc Ophthalmol.* 2022;144:227–235.
- Kong X, Fujinami K, Strauss RW, et al. Visual acuity change over 24 months and its association with foveal phenotype and genotype in individuals with Stargardt disease: ProgStar Study Report No. 10. *JAMA Ophthalmol.* 2018;136:920–928.
- Cremers FPM, Lee W, Collin RWJ, Allikmets R. Clinical spectrum, genetic complexity and therapeutic approaches for retinal disease caused by ABCA4 mutations. *Prog Retin Eye Res.* 2020;79:100861.
- Grover S, Fishman GA, Alexander KR, Anderson RJ, Derlacki DJ. Visual acuity impairment in patients with retinitis pigmentosa. *Ophthalmology.* 1996;103:1593–1600.
- Cella W, Greenstein VC, Zernant-Rajang J, et al. G1961E mutant allele in the Stargardt disease gene ABCA4 causes bull's eye maculopathy. *Exp Eye Res.* 2009;89:16–24.

28. Burke TR, Fishman GA, Zernant J, et al. Retinal phenotypes in patients homozygous for the G1961E mutation in the ABCA4 gene. *Invest Ophthalmol Vis Sci*. 2012;53:4458–4467.
29. Fujinami K, Lois N, Davidson AE, et al. A longitudinal study of Stargardt disease: clinical and electrophysiologic assessment, progression, and genotype correlations. *Am J Ophthalmol*. 2013;155:1075–1088.e1013.
30. Fakin A, Robson AG, Chiang JP, et al. The effect on retinal structure and function of 15 specific ABCA4 mutations: a detailed examination of 82 hemizygous patients. *Invest Ophthalmol Vis Sci*. 2016;57:5963–5973.
31. Webster AR, Heon E, Lotery AJ, et al. An analysis of allelic variation in the ABCA4 gene. *Invest Ophthalmol Vis Sci*. 2001;42:1179–1189.
32. Booi JC, Bakker A, Kulumbetova J, et al. Simultaneous mutation detection in 90 retinal disease genes in multiple patients using a custom-designed 300-kb retinal resequencing chip. *Ophthalmology*. 2011;118:160–167.e161-163.
33. Schulz HL, Grassmann F, Kellner U, et al. Mutation spectrum of the ABCA4 gene in 335 Stargardt disease patients from a multicenter German cohort-impact of selected deep intronic variants and common SNPs. *Invest Ophthalmol Vis Sci*. 2017;58:394–403.
34. Tanaka K, Lee W, Zernant J, et al. The rapid-onset chorioretinopathy phenotype of ABCA4 disease. *Ophthalmology*. 2018;125:89–99.
35. Strauss RW, Munoz B, Ho A, et al. Progression of Stargardt disease as determined by fundus autofluorescence in the retrospective progression of Stargardt disease study (ProgStar Report No. 9. *JAMA Ophthalmol*. 2017;135:1232–1241.
36. Strauss RW, Kong X, Ho A, et al. Progression of Stargardt disease as determined by fundus autofluorescence over a 12-month period: ProgStar Report No. 11. *JAMA Ophthalmol*. 2019;137:1134–1145.
37. Georgiou M, Kane T, Tanna P, et al. Prospective cohort study of childhood-onset Stargardt disease: fundus autofluorescence imaging, progression, comparison with adult-onset disease, and disease symmetry. *Am J Ophthalmol*. 2020;211:159–175.
38. Sparrow JR, Marsiglia M, Allikmets R, et al. Flecks in recessive Stargardt disease: short-wavelength autofluorescence, near-infrared autofluorescence, and optical coherence tomography. *Invest Ophthalmol Vis Sci*. 2015;56:5029–5039.
39. Paavo M, Lee W, Allikmets R, Tsang S, Sparrow JR. Photoreceptor cells as a source of fundus autofluorescence in recessive Stargardt disease. *J Neurosci Res*. 2019;97:98–106.
40. Cukras CA, Wong WT, Caruso R, Cunningham D, Zein W, Sieving PA. Centrifugal expansion of fundus autofluorescence patterns in Stargardt disease over time. *Arch Ophthalmol*. 2012;130:171–179.
41. Tanna P, Georgiou M, Aboshiha J, et al. Cross-sectional and longitudinal assessment of retinal sensitivity in patients with childhood-onset Stargardt disease. *Transl Vis Sci Technol*. 2018;7:10.
42. Tanna P, Georgiou M, Strauss RW, et al. Cross-sectional and longitudinal assessment of the ellipsoid zone in childhood-onset Stargardt disease. *Transl Vis Sci Technol*. 2019;8:1.
43. Daich Varela M, Laich Y, Hashem SA, Mahroo OA, Webster AR, Michaelides M. Prognostication in Stargardt disease using fundus autofluorescence: improving patient care. *Ophthalmology*. 2023;130:1182–1190.
44. Fujinami K, Lois N, Mukherjee R, et al. A longitudinal study of Stargardt disease: quantitative assessment of fundus autofluorescence, progression, and genotype correlations. *Invest Ophthalmol Vis Sci*. 2013;54:8181–8190.

厚生労働科学研究費補助金（難治性疾患政策研究事業）
分担研究報告書

近視性脈絡膜萎縮に関する研究

研究分担者 東京医科歯科大学・医歯学総合研究科・教授 大野 京子
研究協力者 千葉大学・医学研究院・教授 馬場 隆之
京都大学・医学系研究科・特定講師 三宅 正裕
横浜市立大学・医学研究科・客員教授 柳 靖雄

強度近視は、眼球の伸長や変形によって網膜剥離、黄斑円孔、脈絡膜新生血管などの合併症を引き起こし、視力低下や失明に至る可能性のある疾患である。令和6年に我々は、「近視性黄斑部新生血管の診療ガイドライン」を発出し、眼科医に向けて診断および治療の指針を示した。現在我々は、後部ぶどう腫を伴う強度近視の患者から得られたDNAサンプルを用いて、後部ぶどう腫を伴う強度近視に関連する遺伝子を探索する研究を行なっている。また日本眼科学会、日本眼科医会、日本近視学会、日本小児眼科学会などと連携し、近視の患者やその家族に対して進行予防や治療に関する正しい情報を提供する啓発活動が続けている。

A. 研究目的

強度近視は、眼球の伸長や変形によって網膜剥離、黄斑円孔、脈絡膜新生血管などの合併症を引き起こし、視力低下や失明につながる可能性のある疾患である。また日本人の10%以上が強度近視であり、その約40%程度が黄斑症を発症しており、視力低下を防ぐための啓発活動も重要である。我々は令和6年に「近視性黄斑部新生血管の診療ガイドライン」を発出して、眼科医に向けて診断および治療の指針を示した。

今年度の目的は以下の2つである。

(1) 強度近視を有する患者の中でも、特に後部ぶどう腫を伴う近視性網膜脈絡膜萎縮の患者は重度の視機能低下となりやすい。そこで、このような患者から得られた血液サンプルを用いて原因遺伝子の探索を

進める。

(2) 日本眼科学会、日本眼科医会、日本近視学会、日本小児眼科学会などと連携し、患者へ疾患啓発や予防・新規治療法などの情報提供を行う。

B. 研究方法

(1) 遺伝子解析：病的近視を有する症例の中で、後部ぶどう腫を有する強度近視患者のDNAサンプルを用いて、全エクソーム解析または全ゲノム解析を行い、病的近視における後部ぶどう腫に関連する遺伝子群を解析する。

(3) 疾患啓発活動：一般市民に対する公開講座、テレビやマスコミにおける近視の予防や合併症治療の講演などを行う。

（倫理面への配慮）

今回の研究に関しては患者の個人情報は全て匿名化し、倫理面に十分配慮して行った。

C. 研究結果

(1) 全エクソーム解析と全ゲノム解析の結果と診療録から得られた患者の臨床情報を用いて、疾患バイオリソースセンターで、病的近視における後部ぶどう腫に関連する遺伝子を現在解析中である。

(3) 市民公開講座、テレビやマスコミにおける報道などに積極的に参加し、近視の疫学、予防、および合併症の説明や、最新の治療法紹介などを行った。

D. 考察

(1) 強度近視に関する遺伝学的研究は近年大きく進展し、強度近視に関連する遺伝子変異や経路が明らかになってきている。最近の海外の2万人近い検体を用いた全エクソームシーケンス研究でも、いくつかの候補遺伝子のバリエントが同定されている。

G. 研究発表

1. 論文発表

- 1) 大野京子、三宅正裕、柳靖雄、白澤誠、近藤峰生、生野恭司. 近視性黄斑部新生血管の診療ガイドライン. 日本眼科学会雑誌. 128:719-729, 2024.
- 2) Ohno-Matsui K, Igarashi-Yokoi T, Azuma T, Sugisawa K, Xiong J, Takahashi T, Uramoto K, Kamoi K, Okamoto M, Banerjee S, Yamanari M. Polarization-Sensitive OCT Imaging of Scleral Abnormalities in Eyes With High Myopia and Dome-Shaped Macula. JAMA Ophthalmol. Apr 1;142(4):310-319, 2024.
- 3) Lin ZX, Zhang XJ, Tang FY, Zhang Y, Kam KW, Young AL, Ip P, Cheung CY, Pang CP, Tham CC, Chen LJ, Ohno-Matsui K, Yam JC. Association of Retinal Microvasculature With Myopia Progression in Children: The Hong Kong Children Eye Study. Invest Ophthalmol Vis Sci. 2025 Apr 1;66(4):64.
- 4) Moriyama M, Kamoi K, Kimura K, Tateishi U, Ohno-Matsui K. Evaluating the

これらの知見は、強度近視に関わる複雑な遺伝および神経経路の関与を示唆している。我々の遺伝子研究の特徴は、特に重度の視力低下をきたしやすい後部ぶどう腫と関連する遺伝子を探索しているという点にある。

(2) 日本を含むアジア地域では近視は主要な視力低下の原因となっている。最近では近視の進行予防が期待される様々な治療法の臨床応用が進んでおり、これらの情報を正しく眼科医や患者および家族に提供するための体制作りは重要である。

E. 結論

後部ぶどう腫を伴う強度近視に関連する原因遺伝子群の探索が進行中である。また、近視の進行予防や治療に関する正しい情報提供ができる体制作りに引き続き努めることが重要である。

F. 健康危険情報：なし

- Volume of Eyes With Pathologic Myopia Using 3D MRI. Invest Ophthalmol Vis Sci. 2025 Apr 1;66(4):13.
- 5) Lu H, Wu Y, Xiong J, Zhou N, Yamanari M, Okamoto M, Sugisawa K, Takahashi H, Chen C, Wang Y, Wang Z, Ohno-Matsui K. Whorl-Like Collagen Fiber Arrangement Around Emissary Canals in the Posterior Sclera. Invest Ophthalmol Vis Sci. 2025 Mar 3;66(3):35.
 - 6) Kamei T, Miyake M, Kido A, Wada S, Hiragi S, Hata M, Akada M, Niimi K, Ogino K, Oishi A, Nishida A, Tamura H, Tsujikawa A. Annual Trend of Myopia and High Myopia in Children in Japan: A Nationwide Claims Database Study. Ophthalmol Sci. 2025 Feb 3;5(4):100729.
 - 7) Jiang L, Huang L, Dai C, Zheng R, Miyake M, Mori Y, Nakao SY, Morino K, Ymashiro K, Miao YB, Li Q, Ren W, Ye Z, Li H, Yang Z, Shi Y. Genome-Wide Association Analysis Identifies LILRB2 Gene for Pathological Myopia. Adv Sci (Weinh). 2024 Oct;11(40):e2308968.
 - 8) Kido A, Miyake M, Watanabe N. Interventions to increase time spent outdoors for preventing incidence and progression of myopia in children. Cochrane Database Syst Rev. 2024 Jun 12;6(6):CD013549.

2. 学会発表

- 1) Ohno-Matsui K, Lu H, Yamanari M. Novel whorl-like collagen fiber arrangement around emissary canals in the posterior sclera. Macula Society. Feb. 13, Charlotte Harbor, Florida, USA, 2025.

H. 知的財産権の出願・登録状況

1. 特許取得 なし
2. 実用新案登録 なし
3. その他 なし

近視性黄斑部新生血管の診療ガイドライン

厚生労働科学研究費補助金難治性疾患政策研究事業網膜脈絡膜・視神経萎縮症に関する
調査研究班近視性黄斑部新生血管診療ガイドライン作成ワーキンググループ[†]

要 約

病的近視の黄斑部新生血管(MNV)は、病的近視患者の中心視力障害の主要な原因である。近視性 MNV は、病的近視眼に生じる MNV と定義され、病的近視の定義は、病的近視のメタ解析(META-PM)分類に従う。光干渉断層計(OCT)を主体とする画像診断が有用であるが、単純型黄斑部出血との鑑別が難しい場合にはフルオレセイン蛍光眼底造影(FA)や光干渉断層血管撮影(OCTA)の施行を考慮する。OCT 所見や FA から MNV に活動性があると判断された場合には治療が必要である。治療の第一

選択は抗血管内皮増殖因子(VEGF)薬療法であり、導入期の1回投与と必要時投与(PRN法)を原則とする。活動性の低下した MNV の周囲に生じる黄斑部萎縮は、長期的な視力低下の主因となる。

キーワード：病的近視、黄斑部新生血管(MNV)、光干渉断層計(OCT)、黄斑部萎縮、抗血管内皮増殖因子(VEGF)薬療法

I はじめに

病的近視の黄斑部新生血管(macular neovascularization: MNV)は、病的近視患者の約10%に生じ¹⁾、中心視力障害の主要な原因である。病的近視や加齢黄斑変性で見られる黄斑部の新生血管は「脈絡膜新生血管(choroidal neovascularization: CNV)」と呼ばれてきたが、黄斑部の網膜血管由来の新生血管も含まれることから、近年では国際的に「MNV」と呼ばれることが多くなった。そこで本ガイドラインでは、CNVではなくMNVという用語を使用することとした。加齢黄斑変性など他の原因によるMNVに比べて小型で活動性が低いことが多く、見逃しやすい病態である。発症年齢も新生血管型加齢黄斑変性よりも若年であり、50歳未満に限ると、MNVの6割は近視性MNVであると報告されている¹⁾。さらに、MNVの活動性が低下した後に、MNV周囲に生じる黄斑部萎縮が長期予後を左右する重要な問題である。

抗血管内皮増殖因子(vascular endothelial growth factor: VEGF)薬療法は多施設前向き無作為化比較試験において無治療よりも有意に改善効果を示した唯一の治療法で^{2)~4)}、現時点での近視性MNVに対する治療の第一選択である。詳細については後述するが、近視性MNVの活動性は新生血管型加齢黄斑変性によるMNVと比べ低いため、新生血管型加齢黄斑変性と異なる治療プロトコルを要するなど注意が必要である。

今回、厚生労働科学研究費補助金難治性疾患政策研究事業網膜脈絡膜・視神経萎縮症に関する調査研究班を中心に、近視性MNVの診断、検査方法、鑑別診断、治療方法についてのガイドラインを作成した。

II 診 断

1. 定 義

近視性 MNV は、病的近視眼に生じる MNV と定義される。病的近視の定義は、病的近視のメタ解析(META-

[†]：厚生労働科学研究費補助金難治性疾患政策研究事業網膜脈絡膜・視神経萎縮症に関する調査研究班近視性黄斑部新生血管診療ガイドライン作成ワーキンググループ

委 員：大野 京子(東京医科歯科大学大学院医歯学総合研究科眼科学分野)

三宅 正裕(京都大学大学院医学研究科眼科学)

柳 靖雄(横浜市立大学大学院医学研究科視覚再生外科学教室)

白澤 誠(鹿児島大学大学院医歯学総合研究科先進治療科学専攻感覚器病学講座眼科学分野)

近藤 峰生(三重大学大学院医学系研究科臨床医学系講座眼科学)

生野 恭司(いくの眼科)

Corresponding author：113-8510 東京都文京区湯島1-5-45 東京医科歯科大学大学院医歯学総合研究科眼科学分野 大野 京子

利益相反：三宅正裕(カテゴリーF：ノバルティス，第一三共，カテゴリーP)

analysis for Pathologic Myopia : META-PM)分類に基づき、びまん性萎縮以上の眼底変化もしくは後部ぶどう腫を有するとされる^{5)~7)}。

2. 診 断

病的近視患者が急激な視力低下、中心暗点、歪視を訴えた場合に近視性 MNV の発症を疑う。病的近視に伴う眼底変化と MNV の存在を確認することが診断に必須である。後述の鑑別診断の項であげる疾患を鑑別する必要があるが、なかでも lacquer cracks の形成に伴う単純型黄斑部出血⁸⁾⁹⁾との鑑別は、治療方針が大きく変わるため重要である。眼底所見と光干渉断層計(optical coherence tomography : OCT)だけでは単純型黄斑部出血との鑑別が難しい場合がしばしばあるため、フルオレセイン蛍光眼底造影(fluorescein angiography : FA)または光干渉断層血管撮影(OCT angiography : OCTA)によって MNV の存在を確認する必要がある。MNV の存在が確認できない症例に対する抗 VEGF 薬療法は推奨されない。

3. 症 状

自覚症状は急激な視力低下、中心暗点、歪視などである。近視性牽引黄斑症例ではもともと軽度の歪視があることが多いため歪視の増悪を自覚しにくい場合や、検査所見上も MNV が同定しづらい場合もあるが、病的近視患者の MNV において自覚症状は鋭敏な指標であるため、患者の訴えをよく聞くことが重要である。

4. 検査所見

1) 眼底撮影

近視性 MNV の検眼鏡的所見として、灰白色の網膜下隆起性病変が典型的であり、通常は中心窩あるいは傍中心窩下に存在し、新生血管型加齢黄斑変性の MNV に比べて小型である(図 1A)。時に大型のコーヌスの辺縁に生じることもある¹⁰⁾。網膜出血を伴う場合もあるが、広範囲の出血がみられることは少ない。病的近視による萎縮性変化を伴うため、検眼鏡的には MNV がはっきりしないことも多い(図 2A)。発症から時間が経過した症例では MNV の周囲に高度な網脈絡膜萎縮を来し、MNV 自体には色素沈着が起こって Fuchs 斑と呼ばれる所見を呈する。

2) OCT

検眼鏡的に MNV を同定できなくとも、自覚症状がある場合は OCT を施行する。典型的には、MNV が網膜色素上皮(retinal pigment epithelium : RPE)を越えて網膜下に進展する、いわゆる type 2 MNV の所見を呈する(図 1G, 図 3D)。活動期には MNV 周囲の網膜下出血、網膜下液、嚢胞様黄斑浮腫、フィブリン析出などの滲出性変化を伴うが、滲出性変化は強くないことも多いため、自覚症状を訴える場合は細かな変化にも注意して観察する。抗 VEGF 薬療法などで瘢痕化した MNV は RPE によって囲い込まれ、OCT 上では高反射のラインで縁取られて観察される(図 4D)。高反射のラインが明瞭であるかどうかの観察は MNV の活動性評価に非常に有用である。MNV

が再燃するとそのラインが不明瞭化するが、この変化は強くない場合も多いため、十分に囲い込まれていた時期の OCT 画像とよく比較することが重要である。

3) OCTA

OCTA は非侵襲的に血流の有無を評価することができるが、MNV の活動性の評価には向かない。OCTA では新生血管そのものを高率で検出できる一方、瘢痕期/萎縮期であっても MNV 内部に血流シグナルを示すことが知られており、MNV が活動性のある病変なのか、すでに瘢痕化・萎縮しつつある病変なのかの区別に用いることは現状では難しい^{11)~13)}。しかし、血流の有無を評価可能であることから、MNV の同定(単純型黄斑部出血との鑑別など)に有用である。

4) FA

近視性 MNV は FA 早期から明瞭な過蛍光を示し(図 1C, 図 2C, 図 3F)、活動性のある MNV では、中期から後期にかけて蛍光色素の漏出を認める(図 1D, 図 2D, 図 3G)。FA では、検眼鏡所見や OCT でははっきりしない病変も検出可能であるため、近視性 MNV の同定や活動性を評価するうえで非常に有用である。

5) インドシアニングリーン蛍光眼底造影(indocyanine green angiography : IA)

近視性 MNV は、IA では必ずしも過蛍光を示さないため、MNV の同定や活動性の評価には FA を重視する。一方で、MNV の発症母地と考えられている lacquer cracks を検出する性能は高く、補助的診断に用いることができる。Lacquer cracks は IA 後期像で線状の低蛍光として描出される(図 1F, 図 2F, 図 3I)。

6) 眼底自発蛍光(fundus autofluorescence : FAF)

近視性 MNV の発症後、MNV 周囲の網脈絡膜萎縮は年々拡大し、長期的な視力低下の主因となるため萎縮の評価は重要である。黄斑部萎縮は低蛍光として明瞭に描出されるため、その診断および拡大の評価には FAF が有用である。

5. 鑑別診断

MNV が存在しなくても、lacquer cracks は単純型黄斑部出血と呼ばれる網膜下出血を引き起こすことがある。また、炎症性疾患である点状脈絡膜内層症(punctate inner choroidopathy : PIC)や多巣性脈絡膜炎(multifocal choroiditis : MFC)に合併する MNV も鑑別を要する。黄斑部に滲出性変化や新生血管を伴う dome-shaped macula, 傾斜乳頭症候群(下方ぶどう腫)との鑑別も重要である。

1) 単純型黄斑部出血

単純型黄斑部出血は病的近視において近視性 MNV との鑑別が最も重要な病変である(図 5)。一般的には MNV よりも良好な経過を辿り、出血は自然に吸収され、視力は改善することが多い。しかし、特に網膜下出血が濃い眼では、出血が完全に解消しても視覚障害が残ることに注意が必要である¹⁴⁾¹⁵⁾。

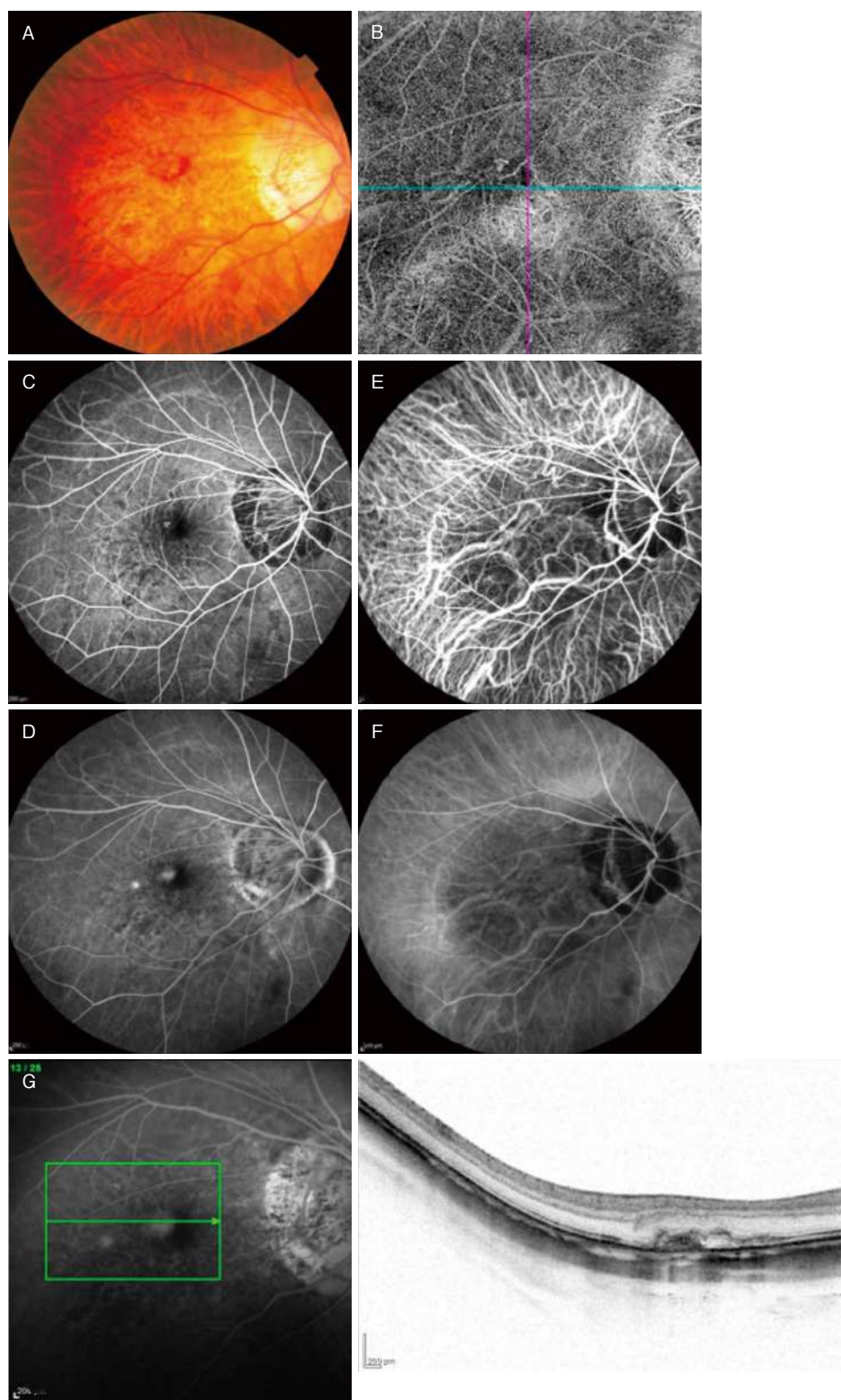


図 1 典型的な近視性黄斑部新生血管(MNV)の検査所見.

- A：眼底写真では黄斑部に出血がみられるが，近視性眼底の影響もありやや確認しづらい．加齢黄斑変性の MNV のように濃い出血になることは少ない．
- B：光干渉断層血管撮影(OCTA)において MNV が描出されている．
- C，D：フルオレセイン蛍光眼底造影(FA)の早期像において MNV が描出され(C)，後期像において漏出が拡大している(D)．
- E，F：インドシアニングリーン蛍光眼底造影(IA)では MNV 検出の感度は低く，本症例においても特記すべき所見はみられない(E：早期像，F：後期像)．
- G：光干渉断層計(OCT)では MNV と周囲の滲出病変が描出されている．近視性の MNV は小さい場合も多く，病変の疑われる部位を細かく撮影しなければ同定できないこともある．

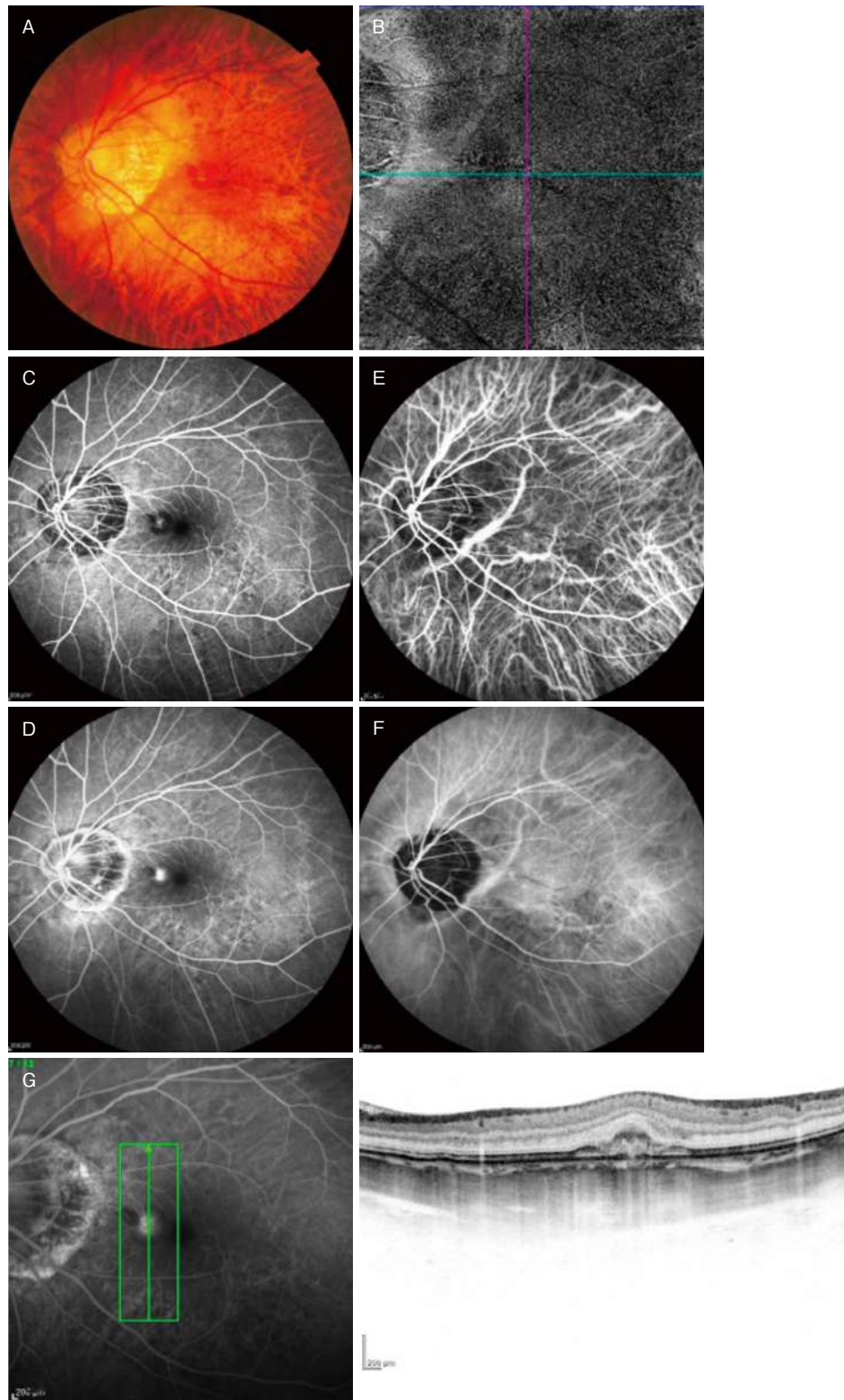


図 2 典型的な近視性 MNV の検査所見.

- A : 眼底写真では視神経乳頭と中心窩の間に出血がみられるが、近視性眼底の影響もあり確認しづらい。
 B : 他の検査結果を合わせて見ることで、この OCTA 画像においても MNV が描出されていることが分かるが、OCTA 画像のみでアーチファクトと鑑別するのは難しい。
 C, D : FA の早期像において MNV が描出され (C)、後期像において漏出が拡大している (D)。他の検査所見で MNV を同定しづらい場合でも、FA を施行することで確定診断が容易となるため、判断に迷う場合は積極的に施行すべきである。
 E, F : IA では MNV 検出の感度は低く、本症例においても MNV は描出されていない。しかし、後期像では lacquer cracks が明瞭に描出されており (F)、補助診断として有用である。E : 早期像。
 G : OCT では単純型黄斑部出血か近視性 MNV かの判別が難しい。

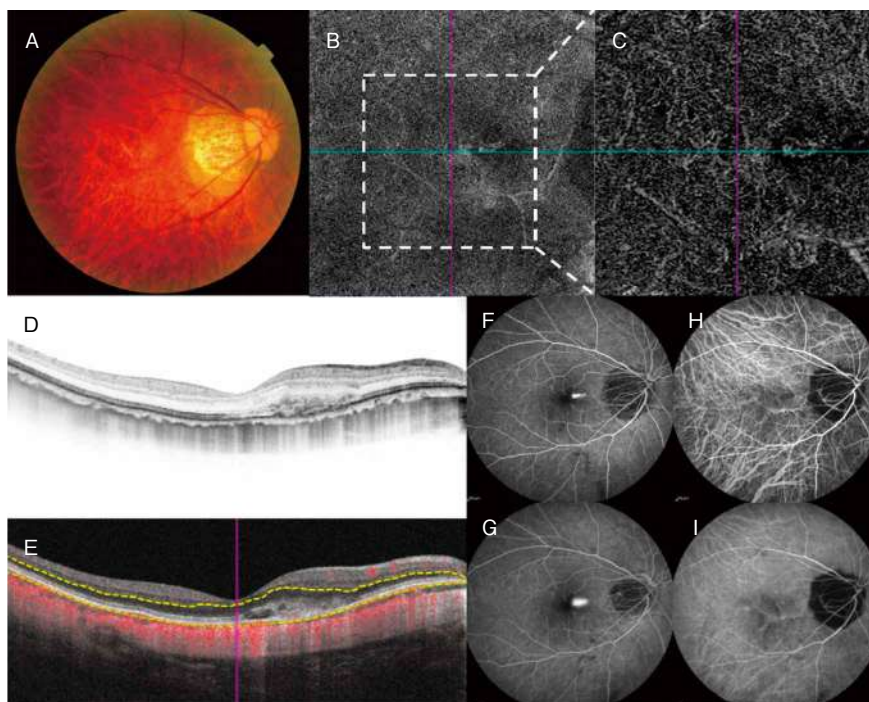


図3 近視性 MNV の治療前の所見.

- A : 眼底写真では視神経乳頭と中心窩の間に出血がみられるが、近視性眼底の影響もあり確認しづらい。
 B, C : OCTA の en face 画像 (B : 黄斑 6 mm, C : 黄斑 3 mm) において MNV 様の所見がみられるが、これらのみで MNV が存在すると診断することは難しい。
 D : OCT 画像では MNV の存在を疑う所見を認める。
 E : OCTA の B スキャン画像と照らし合わせると、OCT で MNV の存在が疑われた部位に一致して血流シグナルが存在することが分かる。この場合、FA 画像がなくとも MNV と診断可能である。ただし、projection artifact には注意が必要である。
 F, G : FA の早期像において MNV が描出され (F)、後期像において漏出が拡大している (G)。
 H, I : IA では MNV は描出されていない (H : 早期像, I : 後期像)。

近視性 MNV と単純型黄斑部出血の鑑別には FA が有用である。近視性 MNV ではブロックされた蛍光の領域内で過蛍光が示されるのと対照的に、単純型黄斑部出血では蛍光ブロックとして観察される。OCT では単純型黄斑部出血は Henle 線維層の神経線維に沿った高反射として観察されるため、鑑別診断にも有用である。OCTA は近視性 MNV と単純型黄斑部出血の鑑別に有用であるが、OCTA による判定が困難な小型の近視性 MNV の場合には、FA を施行し、慎重に鑑別するべきである。

2) 点状脈絡膜内層症 (PIC)

PIC は黄白色の眼底病変が多発する疾患である (図6)。近視眼の若年女性に好発する疾患で、後極部の脈絡膜に多発する黄色の病巣を認め、時に MNV を生じる。類似の所見を示す疾患として MFC があげられる。両者は患者背景、検査所見が類似しており、同じ病態を持つ類縁疾患であると考えられている¹⁶⁾。

PIC は、眼底検査で後極に限定された特徴的かつ小型の境界明瞭な黄白色の眼底病変が RPE および脈絡膜内層に観察されることで近視性 MNV と鑑別できる。それぞれの病巣は大きくとも 500 μ m を超えることは少ない。OCT では、炎症細胞が集簇した初期の急性炎症性病巣が

ドーム状の RPE 隆起として観察され、エリプソイドゾーン (ellipsoid zone : EZ) の途絶を伴うことが多い。経過とともにさまざまな程度に色素沈着を伴った瘢痕となる。また、PIC では発症時には炎症に伴う脈絡膜の肥厚が観察され、治療により菲薄化することが多いのに対し、近視性 MNV では治療前後でも脈絡膜厚は薄いままほとんど変化がみられないことも鑑別に有用な所見である。さらに、FA では病巣は通常、過蛍光を示し、IA の後期像では多発する過蛍光領域が観察される。FAF では検眼鏡的に明らかな病巣を含み、斑状の過蛍光を認めるため鑑別に有用である。OCTA は、PIC の急性炎症性病変と MNV を区別するのに有用である。

3) Dome-shaped macula や下方ぶどう腫のエッジなど他の原因による MNV

Dome-shaped macula や下方ぶどう腫は中等度～強度近視に伴うことが多いが、正視眼にも生じ、時に MNV を伴うことがある¹⁷⁾。MNV を伴わない場合であっても、黄斑部に滲出性変化を来すことがある。なお、dome-shaped macula は黄斑部が内方に向かって凸状に突出している状態であるが、中心窩を通る放射状スキャンのすべてで突出が観察される場合と、放射状スキャンの一部でのみ突

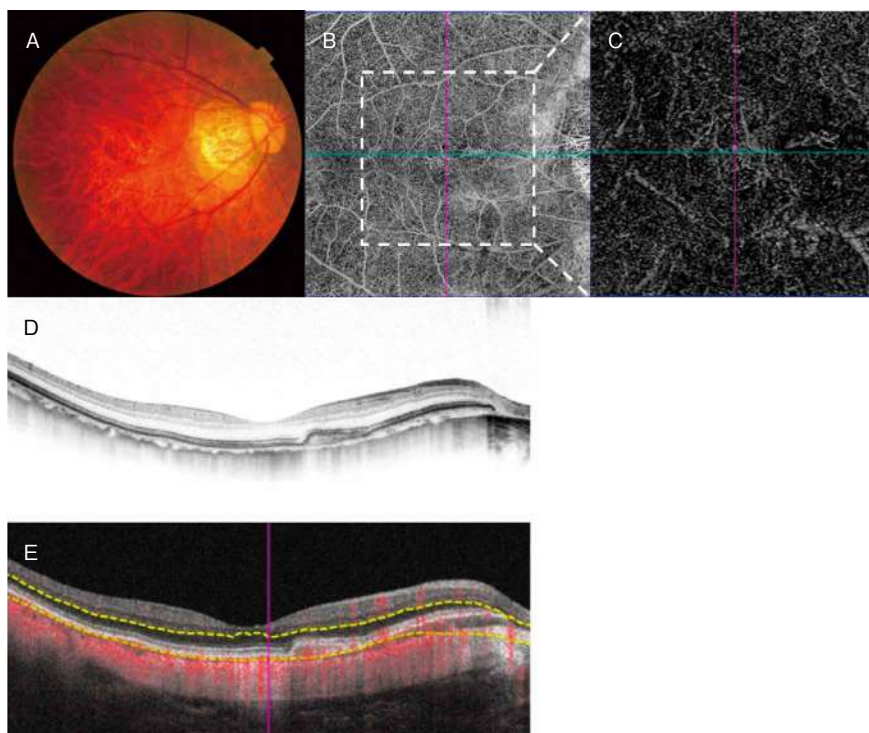


図 4 近視性 MNV の治療後の所見.

- A : もともと近視性眼底の影響もあり出血などが確認しづらかったが, 治療後の眼底写真でも同様に確認しづらい. 他の検査所見と合わせて解釈していくことが重要である.
- B, C : OCTA の en face 画像(B : 黄斑 6 mm, C : 黄斑 3 mm)において MNV 様の所見がみられる. 治療前に比して, やや血管吻合が減じ細長い糸状になったようにも見えるが, OCTA で MNV の活動性を評価することは容易ではない.
- D : OCT 画像では MNV が網膜色素上皮(RPE)で囲い込まれており, 活動性がないと判断できる. 囲い込みが不明瞭化してきた場合, MNV の再燃を考える.
- E : OCTA の B スキャン画像と照らし合わせると, RPE で囲い込まれた中に血流シグナルが存在することが分かる.

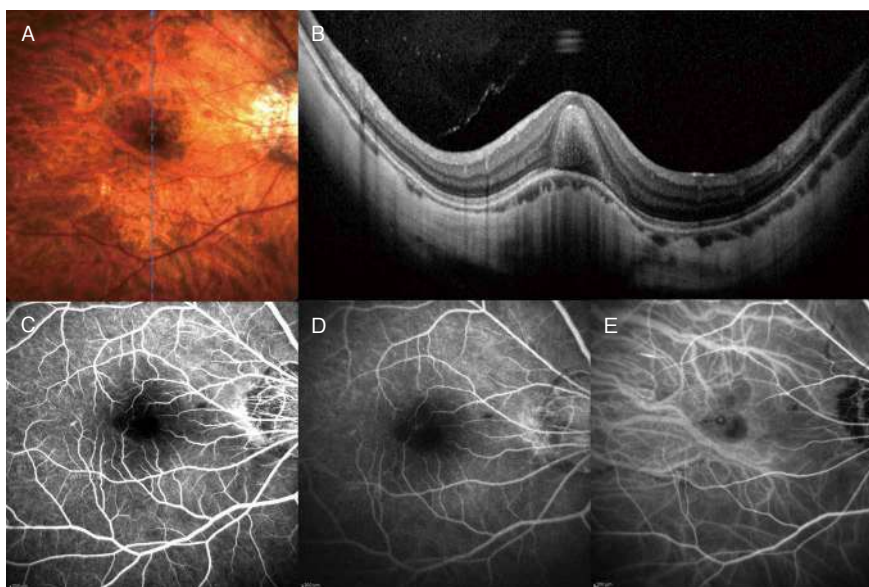


図 5 単純型黄斑部出血.

- A : 眼底写真. 豹紋状眼底の中心窩に網膜下出血を認める.
- B : OCT. 網膜下出血による高反射病巣が観察される. MNV は認めない.
- C, D : FA 早期像(C)および後期像(D). 出血による蛍光ブロックのために低蛍光が観察されるが, MNV を示唆する過蛍光は認めない.
- E : IA. 強度近視に伴う lacquer cracks を認める.

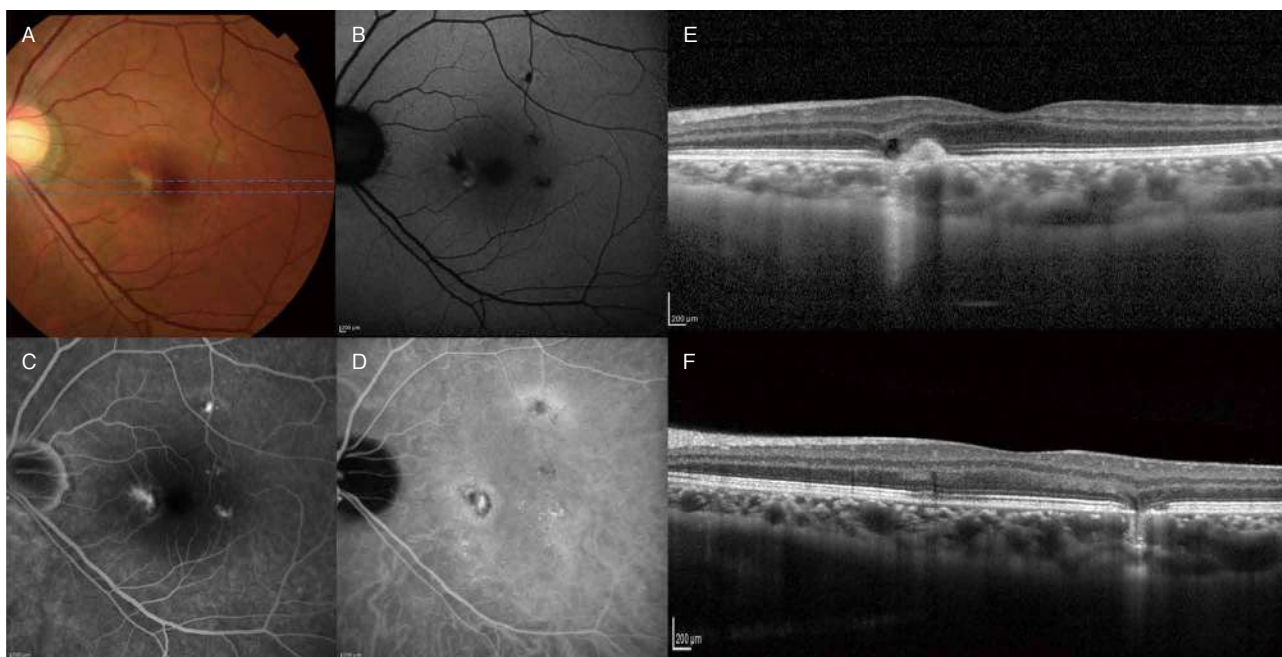


図 6 点状脈絡膜内層症(PIC)。

- A：眼底写真．中心窩鼻側に1か所の黄色病巣，耳側に3か所の淡黄色病巣を認める．
 B：眼底自発蛍光(FAF)．眼底写真で観察された4か所の病巣部位に一致して低蛍光を示し，中心窩鼻側の病巣の周囲には過蛍光を認める．
 C：FA．眼底写真で観察された病巣に一致して過蛍光を示す．
 D：IA．眼底写真で観察された病巣よりも広い範囲で多発する過蛍光病巣を認める．
 E, F：OCT．中心窩鼻側病変はドーム状のRPE隆起(E)を，その他の病巣は網膜外層から脈絡膜浅層の萎縮に伴い網膜内層が引き込まれたような像を示す(F)．

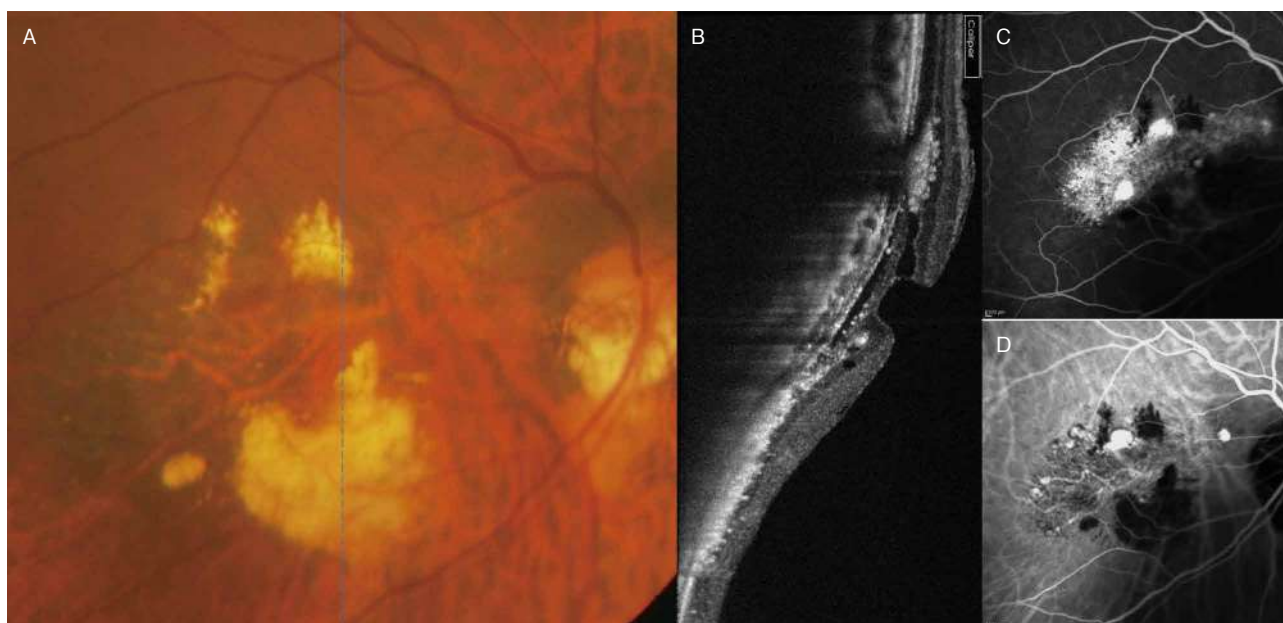


図 7 下方ぶどう腫エッジに生じるMNV.

- A：眼底写真．黄斑部に硬性白斑を伴った滲出性変化を認める．傾斜乳頭を認め，脈絡膜紋理が中心窩下方に明瞭であることから，下方ぶどう腫と診断される．
 B：OCT．垂直断で下方ぶどう腫エッジが中心窩を横切っている所見が明白である．網膜下液，網膜下高反射物質(SHRM)を多数認める．
 C：FA．MNVを示唆する過蛍光を認める．
 D：IA．RPE下のMNVを認める．本症例はMNVの末端がポリープ状に拡張しており，ポリープ状脈絡膜血管症と考えられる．

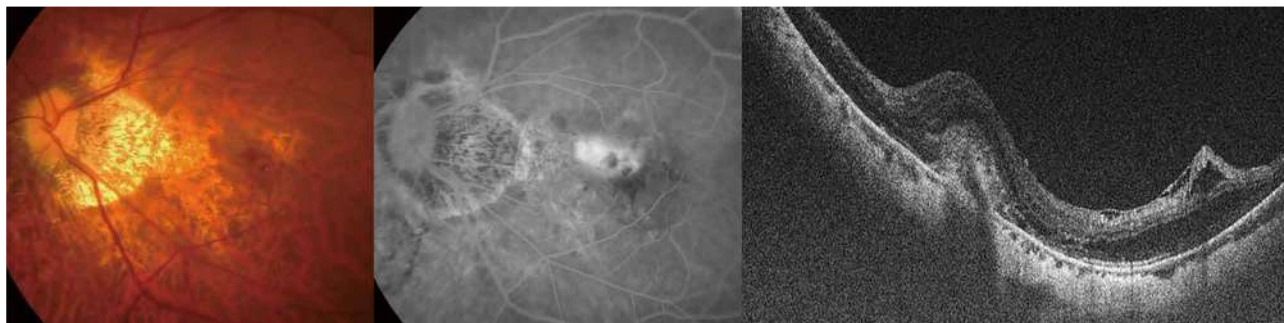


図 8 活動期の近視性 MNV.

眼底写真では黄斑部に出血を伴う MNV を認める(左). FA では色素漏出を伴う過蛍光がみられる(中央). OCT では境界がやや不明瞭な MNV がみられる(右). 右側には網膜分離症も伴っている.

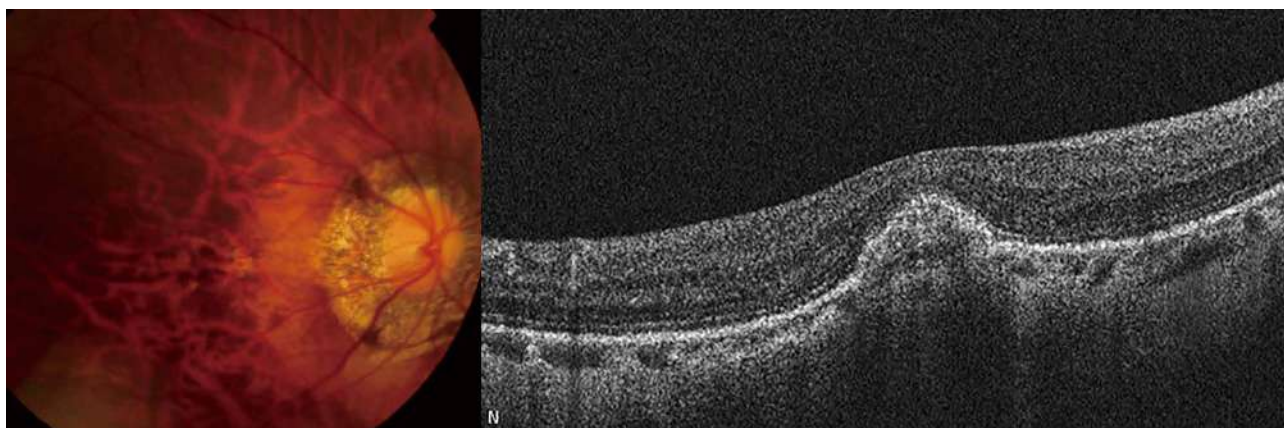


図 9 瘢痕期の近視性 MNV.

眼底写真では瘢痕期 MNV は小さく判然としない(左). OCT では RPE で囲まれた境界明瞭な MNV がみられる(右).

出が観察される場合がある. 後者については ridge-shaped macula との呼称も提唱されている¹⁸⁾. OCT では特徴的な形態を示すため, 近視性 MNV との鑑別は容易である(図 7).

6. 病期分類

1) 病期分類(活動期と瘢痕期/萎縮期¹⁹⁾)

活動期にある MNV(図 8)は, 検眼鏡的にはやや色素に富んだ灰白色の小さな網膜下隆起性病変として観察される一方, MNV が小型の症例では検眼鏡的にはっきりしない場合もある. OCT 所見では RPE より上にドーム状の高反射隆起病巣として現れる²⁰⁾. 活動期には漿液性網膜剝離や網膜浮腫などの滲出性変化を伴うことがあるが, 滲出そのものはそれほど強くないことが多い. MNV の疾患活動性を評価するうえで有用と考えられるのが FA である. また近視性 MNV では出血によるブロックがみられてもその中に過蛍光がみられることがほとんどであり, 出血で MNV が完全に覆い被されることはあまりない.

瘢痕期(図 9)では, RPE と基底膜の過形成による囲い込みで境界が比較的明瞭な隆起病巣(Fuchs 斑とも呼ばれる)がみられる.

萎縮期では, MNV の活動性が低下したのちに年余にわ

たり発症・拡大する黄斑部萎縮のために長期予後も不良である^{21)~23)}. 5 年以上で 88.9%, 10 年で 96.3% が矯正視力 0.1 以下に低下すると報告されている²⁾.

III モニタリングおよび治療

近視性 MNV の治療は, 多施設前向き無作為化比較試験で有効性が唯一証明されている抗 VEGF 薬療法が第一選択となる²⁾³⁾. 2024 年 8 月現在, 日本国内で承認されている抗 VEGF 薬はラニビズマブ(ルセンティス[®])およびそのバイオシミラー, アフリベルセプト(アイリーア[®])である.

具体的な投与法や再投与に関する治療プロトコルについては症例数の関係もあり, 無作為化比較試験などの強いエビデンスをもって確立したとはいえない. ただ世界的にはコンセンサスが形成されつつあり, Cheung らは近視性 MNV の治療ガイドラインを 2017 年に Ophthalmology 誌で発表した²⁴⁾. 要約すると, ① 近視性 MNV に対して遅滞なく抗 VEGF 薬療法を行う, ② 何らかの事情で抗 VEGF 薬療法が不可能なときは光線力学療法を行うが, 抗 VEGF 薬療法と同程度の視力予後は期待できない(本邦では保険

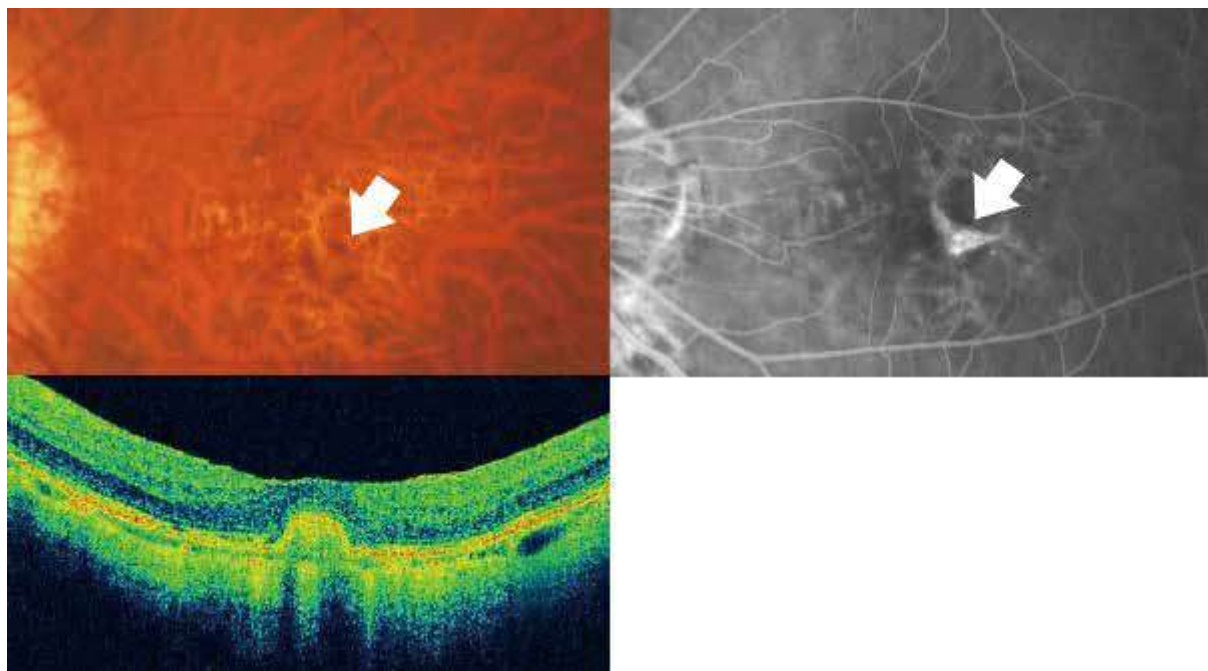


図 10 図 2 の症例に対して抗血管内皮増殖因子(VEGF)薬療法を行った 6 か月後。MNV は三日月状に瘢痕収縮し(左上, 矢印), FA でも蛍光漏出はみられない(右, 矢印)。OCT では MNV の著明な収縮と網膜下液の吸収が確認できる(左下)。

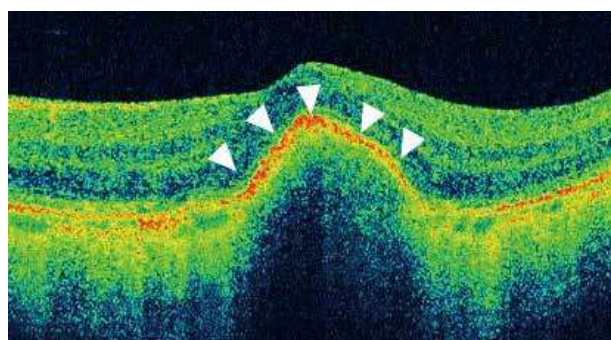


図 11 近視性 MNV に対する抗 VEGF 薬療法後にみられる典型的な RPE の囲い込み(矢頭)。

適用もないことを付け加えておく), ③ 導入期投与は 1 回のみで以後は必要時投与(*pro re nata*: PRN 法)で治療を行う, ④ OCT で網膜下液が観察されたり, 視力低下の訴えや, FA における蛍光漏出があれば再投与を考慮する, ⑤ MNV が安定すれば最大 3 か月まで投与間隔を延長する。原則は本方針に従い治療を行うことになるが, リアルワールドにおいてはより現実に即した対応が必要となる。

一般に治療に対する反応は良好で, 1 回の投与により多くの症例で網膜剝離や網膜下高反射物質(subretinal hyper-reflective material: SHRM)所見は消失する(図 10)。OCT でみられる RPE による囲い込み(encapsulation)は MNV 瘢痕化の一つの目安だが(図 11), たとえ囲い込みがみられても再発することが少なからずある。経過観察は

患者の年齢や状況に応じて, 短期的には 1~3 か月, 長期であっても数か月~1 年の間隔で OCT と眼底検査を行うのが望ましい。再発の確認は OCT を中心に行い, MNV の拡大や新規 MNV の出現が疑われれば OCTA を施行する。活動性の評価方法として, FA は有用であるが, 侵襲が高いため検査間隔や患者の全身状態などを考慮したうえで決定する。黄斑部萎縮は年々拡大し, 長期的な視力低下の主因となる。黄斑部萎縮の診断および拡大の評価には FAF が有用であるため, 必要に応じて FAF を施行することが望ましい。近視性牽引黄斑症を伴う症例では抗 VEGF 薬療法後に牽引黄斑症が悪化することもあるため慎重に適応を判断し経過をみる必要がある²⁵⁾。

治療を行っても黄斑部萎縮を来す場合も多く, 長期後は瘢痕の形成および拡大に大きく依存する²⁶⁾。若年者の場合や小型の MNV の場合は瘢痕形成が小さいことが多く予後は良好である。そのため MNV の拡大や瘢痕形成の前に発見・治療する必要がある。すなわち発症後できるだけ早期に積極的な介入が求められる。

IV おわりに

近視性 MNV の診断, 検査方法, 鑑別診断, 治療方法などについて解説した。単純型黄斑部出血や活動性のない MNV に不必要な治療を行わないよう, MNV 自体とその活動性の診断, そして長期的問題である黄斑部萎縮について理解を深めていただければ幸いである。今回のガイドラインは現時点における知見に基づいて作成された

ものであり、将来的に追加あるいは変更される可能性があることを付記しておく。

本研究は厚生労働省難治性疾患政策研究事業「網膜脈絡膜・視神経萎縮症に関する調査研究」(JPMH23FC1043)の助成を受けたものです。

文 献

- 1) Ohno-Matsui K, Yoshida T, Futagami S, Yasuzumi K, Shimada N, Kojima A, et al : Patchy atrophy and lacquer cracks predispose to the development of choroidal neovascularisation in pathological myopia. *Br J Ophthalmol* 87 : 570-573, 2003.
- 2) Ikuno Y, Ohno-Matsui K, Wong TY, Korobelnik JF, Vitti R, Li T, et al : MYRROR Investigators : Intravitreal aflibercept injection in patients with myopic choroidal neovascularization : the MYRROR Study. *Ophthalmology* 122 : 1220-1227, 2015.
- 3) Wolf S, Balciuniene VJ, Laganovska G, Menchini U, Ohno-Matsui K, Sharma T, et al : RADIANCE Study Group : RADIANCE : a randomized controlled study of ranibizumab in patients with choroidal neovascularization secondary to pathologic myopia. *Ophthalmology* 121 : 682-692, 2014.
- 4) Ohno-Matsui K, Ikuno Y, Lai TTY, Gemmy Cheung CM : Diagnosis and treatment guideline for myopic choroidal neovascularization due to pathologic myopia. *Prog Retin Eye Res* 63 : 92-106, 2018.
- 5) Ohno-Matsui K : Definition of pathologic myopia. In : Spaide RF, Ohno-Matsui K, Yannuzzi LA (Eds) : *Pathologic Myopia*. Springer Nature, Switzerland, 13-15, 2021.
- 6) Ohno-Matsui K, Kawasaki R, Jonas JB, Cheung CM, Saw SM, Verhoeven VJ, et al : META-analysis for Pathologic Myopia (META-PM) Study Group : International photographic classification and grading system for myopic maculopathy. *Am J Ophthalmol* 159 : 877-883, 2015.
- 7) Ohno-Matsui K, Wu PC, Yamashiro K, Vutipongsatorn K, Fang Y, Cheung CMG, et al : IMI Pathologic Myopia. *Invest Ophthalmol Vis Sci* 62 : 5, 2021.
- 8) Asai T, Ikuno Y, Nishida K : Macular microstructures and prognostic factors in myopic subretinal hemorrhages. *Invest Ophthalmol Vis Sci* 55 : 226-232, 2014.
- 9) Ohno-Matsui K, Ito M, Tokoro T : Subretinal bleeding without choroidal neovascularization in pathologic myopia. A sign of new lacquer crack formation. *Retina* 16 : 196-202, 1996.
- 10) Nagaoka N, Shimada N, Hayashi W, Hayashi K, Moriyama M, Yoshida T, et al : Characteristics of periconus choroidal neovascularization in pathologic myopia. *Am J Ophthalmol* 152 : 420-427, 2011.
- 11) Miyata M, Ooto S, Hata M, Yamashiro K, Tamura H, Akagi-Kurashige Y, et al : Detection of myopic choroidal neovascularization using optical coherence tomography angiography. *Am J Ophthalmol* 165 : 108-114, 2016.
- 12) Sayanagi K, Hara C, Fukushima Y, Sakimoto S, Kawasaki R, Sato S, et al : Flow pattern and perforating vessels in three different phases of myopic choroidal neovascularization seen by swept-source optical coherence tomography angiography. *Graefes Arch Clin Exp Ophthalmol* 259 : 2615-2624, 2021.
- 13) Ishida T, Watanabe T, Yokoi T, Shinohara K, Ohno-Matsui K : Possible connection of short posterior ciliary arteries to choroidal neovascularisations in eyes with pathologic myopia. *Br J Ophthalmol* 103 : 457-462, 2019.
- 14) Moriyama M, Ohno-Matsui K, Shimada N, Hayashi K, Kojima A, Yoshida T, et al : Correlation between visual prognosis and fundus autofluorescence and optical coherence tomographic findings in highly myopic eyes with submacular hemorrhage and without choroidal neovascularization. *Retina* 31 : 74-80, 2011.
- 15) Goto S, Sayanagi K, Ikuno Y, Jo Y, Gomi F, Nishida K : Comparison of visual prognoses between natural course of simple hemorrhage and choroidal neovascularization treated with intravitreal bevacizumab in highly myopic eyes : a 1-year follow-up. *Retina* 35 : 429-434, 2015.
- 16) Spaide RF, Goldberg N, Freund KB : Redefining multifocal choroiditis and panuveitis and punctate inner choroidopathy through multimodal imaging. *Retina* 33 : 1315-1324, 2013.
- 17) Cohen SY, Vignal-Clermont C, Trinh L, Ohno-Matsui K : Tilted disc syndrome (TDS) : new hypotheses for posterior segment complications and their implications in other retinal diseases. *Prog Retin Eye Res* 88 : 101020, 2022.
- 18) Xu X, Fang Y, Jonas JB, Du R, Shinohara K, Tanaka N, et al : Ridge-shaped macula in young myopic patients and its differentiation from typical dome-shaped macula in elderly myopic patients. *Retina* 40 : 225-232, 2020.
- 19) 所 敬, 丸尾敏夫, 金井 淳, 林 一彦 : 病的近視診断の手引き. 厚生省特定疾患網膜脈絡膜萎縮症調査研究班報告書, 1-14, 1987.
- 20) Baba T, Ohno-Matsui K, Yoshida T, Yasuzumi K, Futagami S, Tokoro T, et al : Optical coherence tomography of choroidal neovascularization in high myopia. *Acta Ophthalmol Scand* 80 : 82-87, 2002.
- 21) Yoshida T, Ohno-Matsui K, Yasuzumi K, Kojima A, Shimada N, Futagami S, et al : Myopic choroidal neovascularization : a 10-year follow-up. *Ophthalmology* 110 : 1297-1305, 2003.
- 22) Yoshida T, Ohno-Matsui K, Ohtake Y, Takashima T, Futagami S, Baba T, et al : Long-term visual prognosis of choroidal neovascularization in high myopia : a comparison between age groups. *Oph-*

- thalmology 109 : 712-719, 2002.
- 23) **Ahn SJ, Woo SJ, Kim KE, Park KH** : Association between choroidal morphology and anti-vascular endothelial growth factor treatment outcome in myopic choroidal neovascularization. *Invest Ophthalmol Vis Sci* 54 : 2115-2122, 2013.
- 24) **Cheung CMG, Arnold JJ, Holz FG, Park KH, Lai TYY, Larsen M**, et al : Myopic choroidal neovascularization : review, guidance, and consensus statement on management. *Ophthalmology* 124 : 1690-1711, 2017.
- 25) **Shimada N, Ohno-Matsui K, Hayashi K, Yoshida T, Tokoro T, Mochizuki M** : Macular detachment after successful intravitreal bevacizumab for myopic choroidal neovascularization. *Jpn J Ophthalmol* 55 : 378-382, 2011.
- 26) **Onishi Y, Yokoi T, Kasahara K, Yoshida T, Nagaoka N, Shinohara K**, et al : Five-year outcomes of intravitreal ranibizumab for choroidal neovascularization in patients with pathologic myopia. *Retina* 39 : 1289-1298, 2019.
-

Whorl-Like Collagen Fiber Arrangement Around Emissary Canals in the Posterior Sclera

Hongshuang Lu,¹ Yijin Wu,¹ Jianping Xiong,¹ Nan Zhou,¹ Masahiro Yamanari,² Michiaki Okamoto,² Keigo Sugisawa,¹ Hiroyuki Takahashi,¹ Changyu Chen,¹ Yining Wang,¹ Ziye Wang,¹ and Kyoko Ohno-Matsui¹

¹Department of Ophthalmology and Visual Science, Institute of Science Tokyo, Tokyo, Japan

²Tomey Corporation, Nagoya, Aichi-ken, Japan

Correspondence: Kyoko Ohno-Matsui, Department of Ophthalmology and Visual Science, Institute of Science Tokyo, 1-5-45 Yushima, Bunkyo-ku, Tokyo 1138510, Japan; k.ohno.oph@tmd.ac.jp.

Received: January 17, 2025

Accepted: February 21, 2025

Published: March 18, 2025

Citation: Lu H, Wu Y, Xiong J, et al. Whorl-like collagen fiber arrangement around emissary canals in the posterior sclera. *Invest Ophthalmol Vis Sci*. 2025;66(3):35. <https://doi.org/10.1167/iovs.66.3.35>

PURPOSE. To investigate the collagen fiber arrangement around emissary canals in the posterior sclera.

METHODS. One hundred sixty-five eyes of 93 patients who underwent polarization-sensitive optical coherence tomography (PS-OCT) examinations in 2019 in the Institute of Science Tokyo were studied. Multimodal imaging, including streamline images derived from PS-OCT data, B-scan images, and indocyanine green angiography (ICGA) images, was used to investigate the collagen fiber arrangement around emissary canals and scleral pits in vivo. Additionally, the collagen fiber arrangement around the emissary canals in porcine sclera was examined using scanning electron microscopy and light microscopy.

RESULTS. Streamline images showed whorl-like collagen fiber arrangements on all eyes, and 25 eyes were selected for the analysis. All whorls corresponded to emissary canals on B-scan images. The whorls were confirmed to correspond to the posterior ciliary artery entries in three eyes and posterior vortex vein exits in three eyes with available ICGA images. Streamline cutaway images showed that the whorls surrounded the emissary canals throughout the entire course. In 16 eyes with 20 scleral pits, whorls were seen surrounding all the pits. Microscopic study using porcine sclera confirmed the whorl-like structures around the emissary canals ex vivo and demonstrated tangentially arranged collagen fiber bundles forming the circle.

CONCLUSIONS. The collagen fibers are arranged as whorl-like structures around the vessel emissary canals in the posterior sclera, which is a knowledge gap for basic scleral histology. Additionally, this study demonstrated a strong correlation between PS-OCT findings and microscopic histology, underscoring PS-OCT's utility in detecting scleral collagen fiber arrangements.

Keywords: polarization-sensitive optical coherence tomography, scleral collagen fiber, emissary canals

The sclera, forming the outer coat of the eye, is a fibrous connective tissue composed of dense bundles of collagen, a few elastic fibers, fibroblasts, and a moderate amount of amorphous ground substance, such as proteoglycans and glycoproteins.^{1–3} The scleral collagen fibers are considered to be crucial in determining the biomechanical behavior of the eye, playing a critical role in maintaining the shape of the eye and protecting the eye from mechanical insults.

There are areas of discontinuity of the posterior sclera. The largest foramen is the optic nerve head (ONH) canal, which allows the passage of the optic nerve and central retinal artery and vein. In addition, there are 15 to 20 emissary canals where perforating scleral vessels (PSVs) penetrate the sclera, including posterior ciliary arteries (PCAs)⁴ and posterior vortex veins (VVs).^{5,6} These areas with discontinuous sclera are considered structurally vulnerable against mechanical insults especially in highly myopic eyes involv-

ing an increase of axial length and significant thinning of the sclera. Previous studies, both in vivo^{7–9} and ex vivo,^{10,11} have documented a circumferential collagen fiber arrangement around the ONH canal,^{7–11} which are believed to provide biomechanical support to the lamina cribrosa, and to the nerves and vessels that pass through it.¹² For the emissary canals, however, the scleral collagen fiber arrangements have not been thoroughly investigated.

Polarization-sensitive optical coherence tomography (PS-OCT) is a functionally extended OCT device. Unlike conventional OCT devices, which are limited to assessing the thickness and the curvature of the sclera, PS-OCT can obtain additional information on the tissue that alters the polarization state of the light. One of the optical properties that can be measured by PS-OCT is birefringence, an optical property exhibited by tissues like smooth muscles and collagen fibers, where the medium has varying refractive indices based on the state of polarized light.¹³ The optic axis of



a birefringent medium is the direction where light waves propagate at a consistent velocity, regardless of polarization. Birefringent media generally have multiple optic axes, with the “slow axis” (higher refractive index) aligning with the long axis of biological fibers. Thus PS-OCT can determine collagen fiber orientation by measuring these axes. This technique is widely used to study ocular structures, including the cornea, retinal nerve fiber layer, and sclera.^{8,14–17} In the posterior segment, the attenuation of signal penetration by the thick choroid often prevents the full thickness of normal sclera from being visualized in vivo, and highly myopic eyes, with substantially thinner choroid and sclera, are ideal for analyzing scleral structure in vivo using PS-OCT.

During our preliminary study of the posterior sclera with PS-OCT in highly myopic patients, we observed whorl-like collagen fiber arrangements that we suspected to be associated with the emissary canals of the PSVs. The primary aim of this study was to verify this hypothesis and to explore the potential structural and functional roles that these arrangements may play within the scleral matrix. To achieve this objective, we first compared multimodal in vivo imaging for highly myopic eyes and then verified the histological configuration under microscopy using porcine eyes ex vivo.

METHODS

Subject Enrollment

The study protocol was in strict adherence to the tenets of the Declaration of Helsinki and received approval from the Ethics Committee of Institute of Science Tokyo. We retrospectively analyzed the medical records of 165 eyes of 93 patients who underwent PS-OCT examinations in May and June 2019 at the Advanced Center of High Myopia at the Institute of Science Tokyo. To select cases that would allow optimal analysis of posterior scleral configuration under conditions closely resembling normal physiology, we implemented stringent exclusion criteria, including images with poor quality, such as images affected by media opacities including dense cataracts or vitreous opacity and images compromised by excessive motion or blinking artifacts; eyes with conditions that affect the performance of the segmentation algorithm and signal detection, including but not limited to extensive retinoschisis, myopic neovascularization, tractional detachment of retina, and large intrachoroidal cavi-

tion; eyes with highly irregular scleral shape or highly steep curvature; and significant scleral signal attenuation caused by thick overlying choroid.

During data screening, whorl-like collagen fiber arrangements were observed on all eyes. Because of the stringent exclusion criteria, 25 eyes from 16 patients met the inclusion criteria and were selected for further analysis. All patients were Japanese. The demographic information is shown in the Table.

PS-OCT Examination and Image Processing

In this study, we employed a prototype PS-OCT system (Tomey Co., Nagoya, Japan) using a swept laser at a 1050 nm center wavelength with 100 kHz A-scan rate. The details of this system have been described previously,¹⁸ where the depth-resolved polarization properties are measured without compromising the effective A-scan rate, enabling wide-field imaging of the fundus as well as conventional swept-source OCT. The raw PS-OCT data contained polarization properties of the target in a mathematical form called Jones matrix, which has complex-valued 2×2 matrix at each spatial pixel. The measured data were processed to obtain the optic axis by algorithms developed earlier.⁸ The contrast mechanism of birefringent collagen fiber is as follows briefly: when the propagating direction of the light is oblique or perpendicular to the optic axis, which is the case of the fundus imaging, the medium exhibits two different refractive indices that result in alteration of the state of polarization along the axial depth. The orientations of the optic axes projected on the plane perpendicular to the propagating direction of the light are determined mathematically by PS-OCT.⁸ Strictly speaking, the above description is for the case of perfectly aligned fibers. In practice, however, the scleral collagen fibers have interwoven structure, which is mostly beyond the resolution of OCT.¹⁹ As a result, we observe net birefringence created by the interwoven fibers, where birefringence of the individual fibers is partially cancelled out. The optic axis of the net birefringence is attributed as preferential orientation, which have been studied using wide-angle X-ray scattering, small-angle light scattering, second harmonic generation microscopy, and polarized light microscopy.^{10,11,20} Compared to these techniques, a unique feature of PS-OCT is the depth-resolved measurement in vivo.

78

TABLE. Demographic Information of Subjects

Parameter	Subjects for Normal Emissary Canal Analysis (25 Eyes of 16 Patients)	Subjects for Scleral Pits Analysis (16 Eyes of 14 Patients)
Age (years)	57.50 ± 14.16	65.47 ± 8.36
Gender (Number of patients)		
Male	5	5
Female	11	9
Axial length (mm)	29.72 ± 1.26	31.17 ± 1.62
Refractive error (spherical equivalent, diopters)*	−12.83 ± 4.59	−13.42 ± 4.65
Best corrected visual acuity (logMAR unit)	0.13 ± 0.34	0.66 ± 0.62
META-PM classification (Number of eyes)†		
Tessellated fundus	1	0
Diffuse choroidal atrophy	14	0
Patchy choroidal atrophy	5	4
Macular atrophy	5	12

* Eyes with intraocular lenses were excluded from this calculation.
† Grading system of pathologic myopia developed by the Meta-analysis for Pathologic Myopia (META-PM) Study Group.

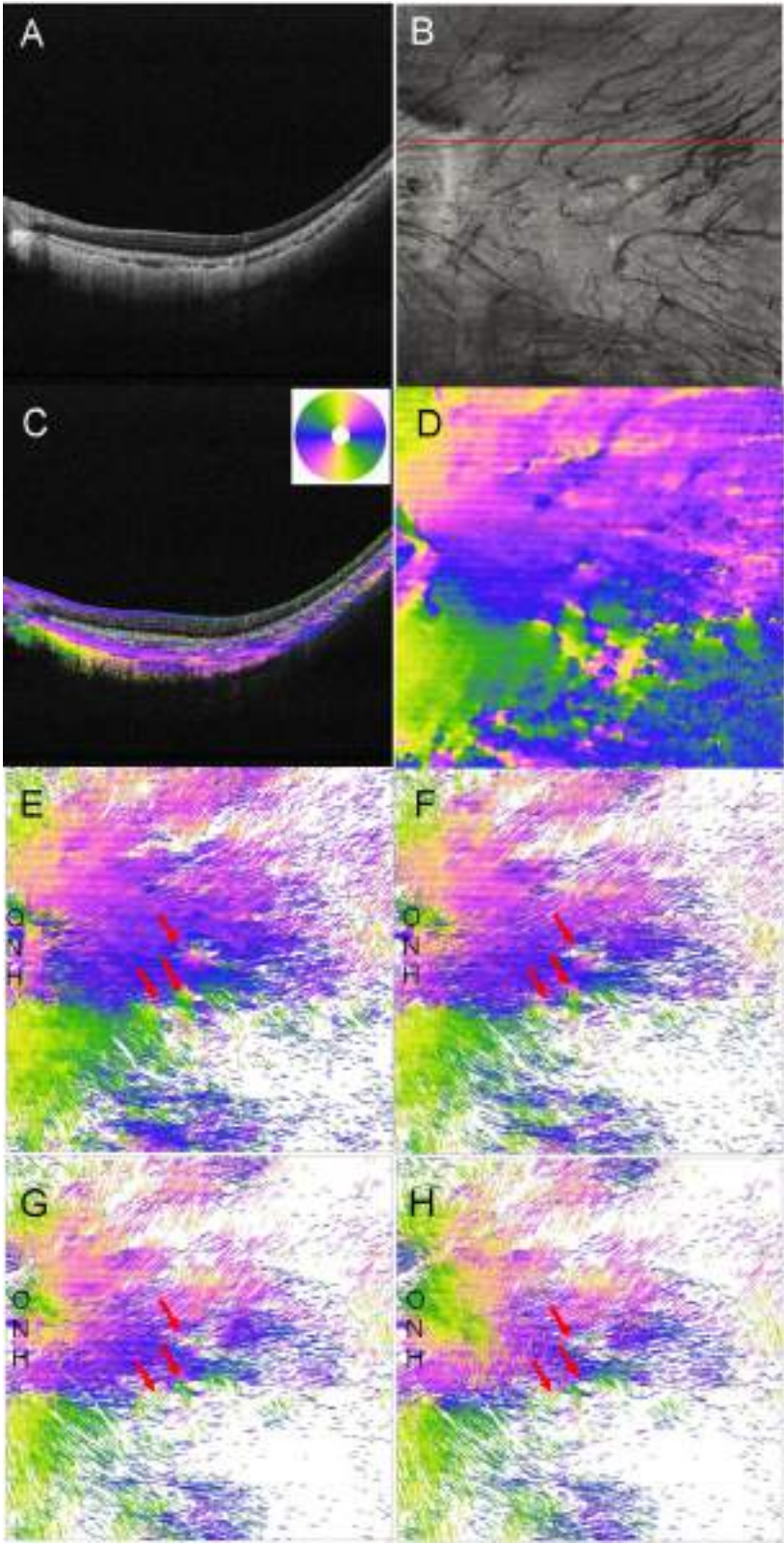


FIGURE 1. (A, B) The B-scan OCT intensity image and en face OCT intensity image at the CSI extracted from polarization-sensitive OCT (PS-OCT) data, respectively. (C) The optic axis image with a cyclic colormap to indicate the orientation of local birefringence, where the pixels above thresholds of the signal intensity and local retardation are shown and other pixels are replaced with the gray-scaled intensity. (D) The en face optic axis image of the sclera under the CSI with an axial averaging for 15 pixels (67 μm). (E) En face streamline image where upper layers of the volumetric data is cropped at the CSI level. (F) En face streamline image cropped at the level of 5 pixels (22.35 μm) lower than the CSI. (G) En face streamline image cropped at the level of 10 pixels (44.7 μm) lower than the CSI. (H) Outside view (i.e., viewing from the outer surface of the sclera). The red arrows indicate the whorl-like structures of fiber arrangements, which became increasingly obvious at deeper levels.

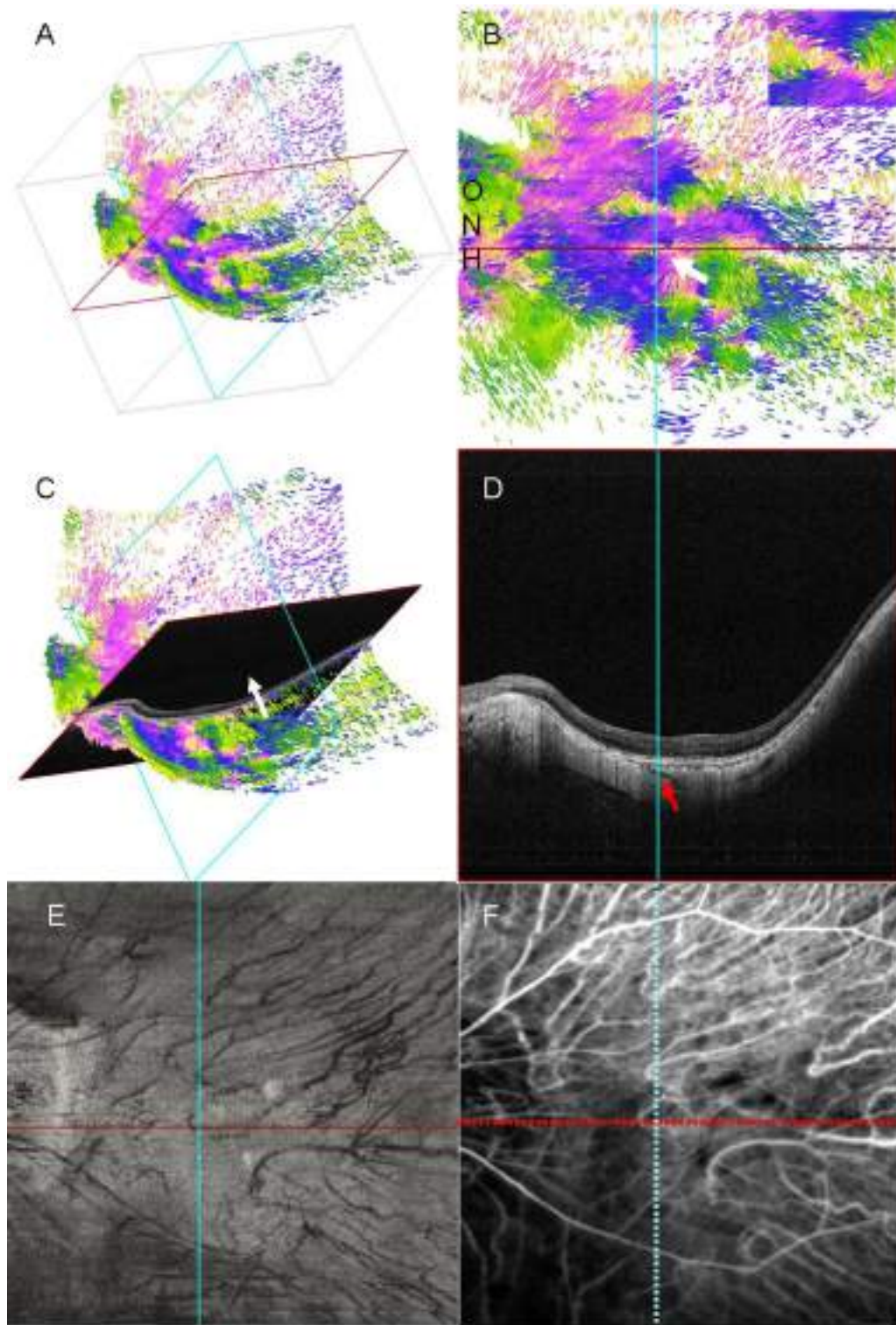


FIGURE 2. Identification of emissary canals on OCT intensity B-scan images and ICGA images. **(A)** Image showing the three-dimensional (3D) structure of the streamline rendering of the scleral fibers viewed from an oblique camera angle. **(B)** En face view with red and light blue reference lines crossing at the center of the whorl-like fiber arrangement (*white arrow*); A magnified image showing the whorl-like structure at the crossing of the red and blue reference lines is shown on the right upper corner. ONH indicates the optic nerve head. **(C)** Same 3D structure as image **A**, displaying the specific horizontal B-scan corresponding to the *red reference line* in images **A** and **B**. **(D)** OCT intensity B-scan image viewed from the camera angle indicated by the *white arrow* in image **C**. On this image, color rendering of the scleral fibers are hidden, leaving only the B-scan image and the *light blue reference line*, and an vessel emissary canal (*red arrow*) can be seen at the site indicated by the *light blue line*. **(E)** En face OCT intensity image at the CSI showing the location of the center of the whorl-like structure. **(F)** Cropped image of the ICGA arterial phase with horizontal (*red*) and vertical (*light blue*) dashed lines to indicate the same entry site of the PCA by referring to retinal vessels and choroidal vessels as the landmarks.

The retinal scans covered an area of $9 \times 9 \text{ mm}^2$, centered on the macula, and were acquired using a raster scanning protocol with 1024×256 A-scans in the horizontal and vertical directions. The system provided an axial resolution of $7.3 \mu\text{m}$ and a depth measurement range of 4.49 mm within the tissue. [Figures 1A and 1B](#) show the OCT intensity B-scan image and en face OCT intensity image extracted from PS-OCT data, respectively. [Figure 1C](#) shows the optic axis image with a cyclic colormap indicating the orientation of net birefringence. [Figure 1D](#) shows the en face optic axis image of the sclera under the choroid-sclera interface (CSI) with an axial averaging for 15 pixels ($67 \mu\text{m}$), where the axial digital resolution of $4.47 \mu\text{m}/\text{pix}$ is smaller than the optical resolution.

Because the optic axis is a vectorial contrast that shows the orientation of the net birefringence created by the fibrous tissues, plotting or rendering methods dedicated to the vectorial data are preferred. Streamline rendering is one of such methods, and it has been used to visualize scleral collagen fibers in previous studies using polarized light microscopy *ex vivo*¹⁰ and PS-OCT *in vivo*.⁸ In the current study, we used ParaView 5.12.0 (Kitware Inc., New York, NY, USA) for volumetric streamline rendering of the optic axis, and the method was the same as the previous study.⁸ [Figure 1E](#) shows the streamline image of the optic axis under the CSI.

Throughout the entire thickness of the sclera, the collagen fiber arrangements are not uniform as seen in [Figure 1C](#) and reported in previous studies.^{10,21} In addition to visualizing the en face streamline image at the level of CSI, we also created cutaway images at different depths from CSI ([Figs. 1F–H](#)).

Correspondence of Emissary Canals With Whorl-Like Structures

[Figure 2](#) showed the procedure to investigate the structural relationship between multimodal images at the site of whorl-like collagen fiber arrangements. The volumetric streamline rendering of the optic axis was created by ParaView ([Fig. 2A](#)). A horizontal (red) and vertical (blue) reference lines were introduced to pinpoint the center of the whorl-like structures ([Fig. 2B](#)). By displaying the horizontal OCT B-scan corresponding to the red reference line ([Fig. 2C](#)), the structure of the sclera at the site of the whorl center can be observed on B-scan images, indicated by the blue reference line ([Fig. 2D](#)). Characteristic hyporeflexive areas indicative of PSVs were observed, as reported by the previous study.²² The same site can also be pinpointed on the intensity image ([Fig. 2E](#)), and the retinal vessel and choroidal vessels were used as landmarks to manually crop the indocyanine green angiography (ICGA) images, and reference lines were manually added on the ICGA images to further verify if the whorl-like structures corresponded to PCA emissaries or posterior VV exits ([Fig. 2F](#)).

Collagen Fiber Arrangements Around Scleral Pits at the Site Of PSV Emissaries

As vulnerable points of the sclera, previous studies have identified focal scleral ectasia or scleral pits at the sites of emissary canals within areas of extensive choroidal patchy atrophy.^{23,24} To study the collagen fiber arrangements around these particularly fragile sites, we included cases

with choroidal patchy atrophy and scleral pits at the sites of PSV emissary canals. Because scleral pits usually occur in cases with severe conditions, the above exclusion criteria did not apply to these cases, and we included all available cases as long as the area of interest was unaffected. In this study, scleral pits were detected in 16 eyes of 14 patients. The demographic information is also shown in the [Table](#).

Basic Clinical Data Collection

The age and gender of patients were collected. All subjects underwent comprehensive ophthalmic examinations. Data included best-corrected visual acuity, refractive error (spherical equivalent), axial length (IOL Master 700; Carl Zeiss Meditec Co., Jena, Germany), and myopic maculopathy according to META-PM classification²⁵ based on fundus photos were recorded and analyzed. ICGA images were obtained with Heidelberg Spectralis HRA system (Heidelberg Engineering, Heidelberg, Germany). The largest width of the scleral opening on B-scan images at the CSI level was measured using an in-house developed analyzing software (Owl Eye, version 1.6.5; Tomey Co., Nagoya, Japan).

Ex Vivo Verification of the Whorl-Like Structures Using Porcine Eyes

Porcine eyes were obtained from a local slaughterhouse within two hours postmortem. The eyeballs were dissected into scleral eyecups, and a $4 \times 4 \text{ mm}^2$ area of the posterior scleral containing the PSVs was excised under a surgical microscope. For hematoxylin and eosin (H&E) staining, the tissue was treated by the following protocol: The tissue was first fixed with 4% paraformaldehyde and stored under 4°C overnight, dehydrated by 30% sucrose, and cryosectioned into $10 \mu\text{m}$ slices. For scanning electron microscopy (SEM) observation, the scleral tissue was fixed in 2.5% glutaraldehyde in 0.1 M phosphate buffer and stored overnight at 4°C . Because the lamina fusca is relatively loosely connected to the scleral stroma, it can get easily displaced and even detached during the dehydration process. Therefore the lamina fusca together with some superficial scleral layers were removed with a blade, and collagen fiber arrangements within the scleral stroma were observed. The tissue was then post-fixed with 1% osmium tetroxide (OsO_4) in 0.1 M phosphate buffer for two hours. After fixation, the tissue was gradually dehydrated in a graded ethanol series, starting from 50% to 90%, with each concentration applied for 10 minutes. This was followed by three consecutive 10-minute treatments in 100% ethanol. The tissues were then dried using a critical point drying apparatus (HCP-2; Hitachi Ltd., Tokyo, Japan) with liquid CO_2 . Finally, the specimen was sputter-coated with platinum before scanning electron microscope (JSM7900F; JEOL, Tokyo, Japan) observation. Cryo-sectioned slides from one eye were also treated with the SEM preparation protocol and observed under SEM.

RESULTS

Comparison of Multimodal Imaging (Streamline Images, B-Scan Intensity Images, and ICGA Images)

The average number of whorl-like structures was 8.9 ± 2.4 per eye on streamline images, ranging from six to 16 ([Fig. 3](#)).

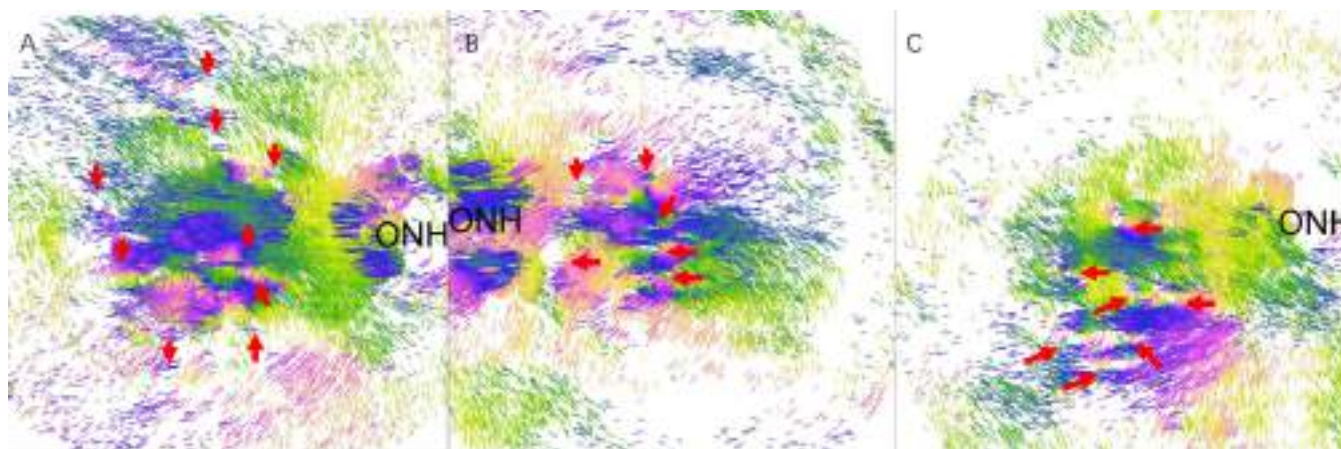


FIGURE 3. Whorl-like structures (*arrows*) visualized on streamline images of three typical cases viewed from the inside the eye. The streamline images were cropped at 20 pixels (89.4 μm) (A), 20 pixels (89.4 μm) (B), and 10 pixels (44.7 μm) (C) from choroid-sclera interface.

These structures were universally verified by B-scan intensity images to correspond to the emissary canals of PSVs (Fig. 4). Additionally, three eyes had arterial phase ICGA images, and all whorl-like structures were confirmed to encircle the PCAs (Fig. 4); in another three eyes with posterior VVs on venous phase ICGA images, exits of all posterior VVs were also observed to be surrounded by whorl-like structures (Fig. 5). The mean largest width measured on B-scan images at the level of CSI was $274.63 \pm 189.55 \mu\text{m}$ (range 70.31 μm to 843.75 μm) for PSV emissary canals.

Whorl-Like Structures Surrounding the Entire Course of the Emissary Canals

Because the scleral emissary canals may follow various courses, including perpendicular, spiral, or oblique,¹ we observed the whorl-like structures at different depths in the sclera along the entire course of the emissary canals (Fig. 6 and Supplementary Video S1). Furthermore, in four eyes, two whorl-like structures observed on the inner side of the streamline image merged into a single larger whorl-like structure on the outer side. This merger was corroborated by B-scan images, which confirmed the convergence of two emissary canals at a deeper level of the sclera (Supplementary Fig. S1).

Whorl-Like Structures Surrounding Scleral Pits at PSV Emissaries

Scleral pits are full-thickness focal scleral excavation around the PSV emissaries in pathologically myopic eyes with extensive choroidal atrophy.^{23,24} In the 16 eyes, a total of 20 pits were identified. Whorl-like structures encircled each pit, regardless of their sizes (Fig. 7). The average maximum width of the scleral pits at CSI was $471.68 \pm 219.06 \mu\text{m}$, ranging from 149.41 μm to 896.48 μm .

Microscopic Examination of Posterior Emissary Canals of Porcine Eyes

SEM and H&E staining images (Figs. 8A–E) vividly illustrated collagen bundles encircling the emissary canals. Under higher magnification, these bundles appear tangen-

tially arranged, forming a distinctive ring around the canals (Fig. 8F). Notably, one or more vessels may share a single emissary canal, and when a single vessel traverses the canal, it often adheres to one side rather than positioning centrally (Fig. 8C). In addition to the vessels, longitudinally aligned collagen fibers are observed along the vessels' path within the emissary canal (Figs. 8C, 8D).

DISCUSSION

In this study, we used PS-OCT to analyze the posterior scleral collagen fiber arrangements in highly myopic eyes, highlighting whorl-like collagen fiber configurations around the emissary canals of PSVs, mainly comprising PCAs and posterior VVs. Furthermore, our study revealed that while scleral collagen fiber arrangements were depth-dependent and exhibited significant differences between the inner and outer layers,^{10,21} the whorl-like structures around the emissary canals persisted throughout the entire thickness of the sclera and consistently aligned with the courses of the emissary canals. Even in cases with scleral pits at the emissary canals in eyes with extensive myopic choroidal atrophy, whorl-like structures remained undestroyed. Based on these findings, we hypothesize that the whorl-like structures maintain structural consistency and adaptability under both normal and pathological conditions. However, further investigations, particularly histological studies using microscopy, are necessary to verify this hypothesis across various disease states. Moreover, we examined posterior porcine sclera using H&E staining and SEM and verified the whorl-like structure around the emissary canals ex vivo. Detailed observations using SEM revealed that the whorl-like structures were tangential configuration of collagen bundles encircling the canals. The correspondence between in vivo and ex vivo results demonstrated the reliability of PS-OCT as a valuable tool to provide accurate information on the scleral structure.

Our research distinguishes itself from prior studies using PS-OCT^{7,26} by using streamline images, which provide a clearer and more intuitive depiction of the preferential orientation formed by the interwoven collagen fibers in the posterior sclera. Additionally, whereas previous studies predominantly focused on the peripapillary region, our study encompassed a broader $9 \times 9 \text{ mm}^2$ area

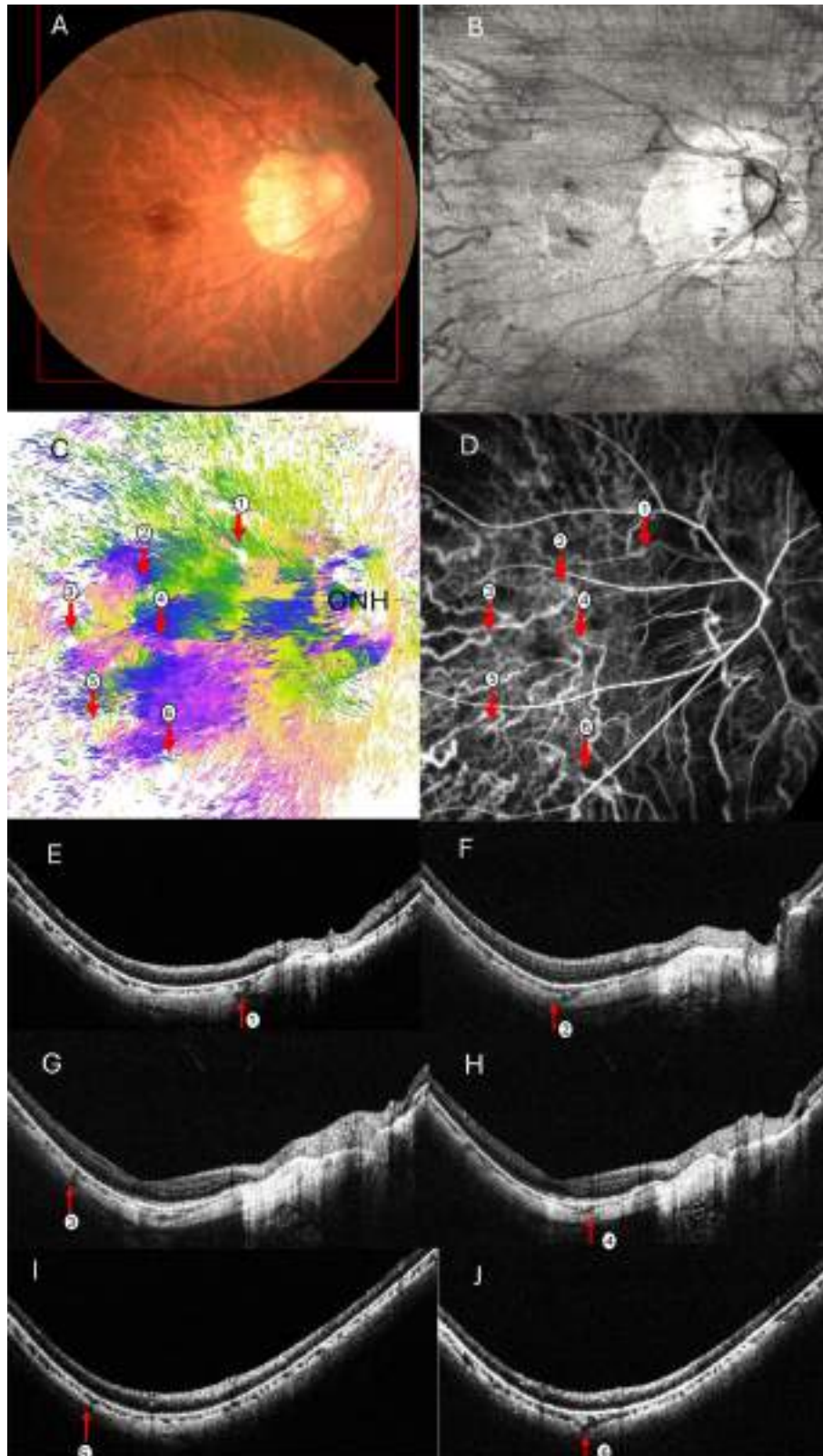


FIGURE 4. Correspondence of whorl-like structures and emissary canals of PCAs verified by both B-scan OCT intensity images and ICGA scans. **(A)** Right fundus of a 54-year-old highly myopic woman with an axial length of 30.63 mm shows diffuse choroidal atrophy around the optic nerve. The red rectangle indicates the capture area of image **B**. **(B)** The en face OCT intensity image of the sclera under CSI. **(C)** The en face streamline cutaway (20 pixels (89.4 μ m) below CSI image. Red arrows indicate the whorl-like structures. The arrows and numbers match with those on image **D**. **(D)** Arterial phase ICGA image cropped to the same area as in **B** using the retinal vessels as landmarks. Arrows indicate the point where PCAs entered the eye. The whorl-like structures on image **C** all corresponded to PCA emissaries on the ICGA image. **(E–J)** Horizontal B-scan images showing the intrascleral course of PCA (red arrows) corresponding to the numbers from 1–6 on images **C** and **D**.

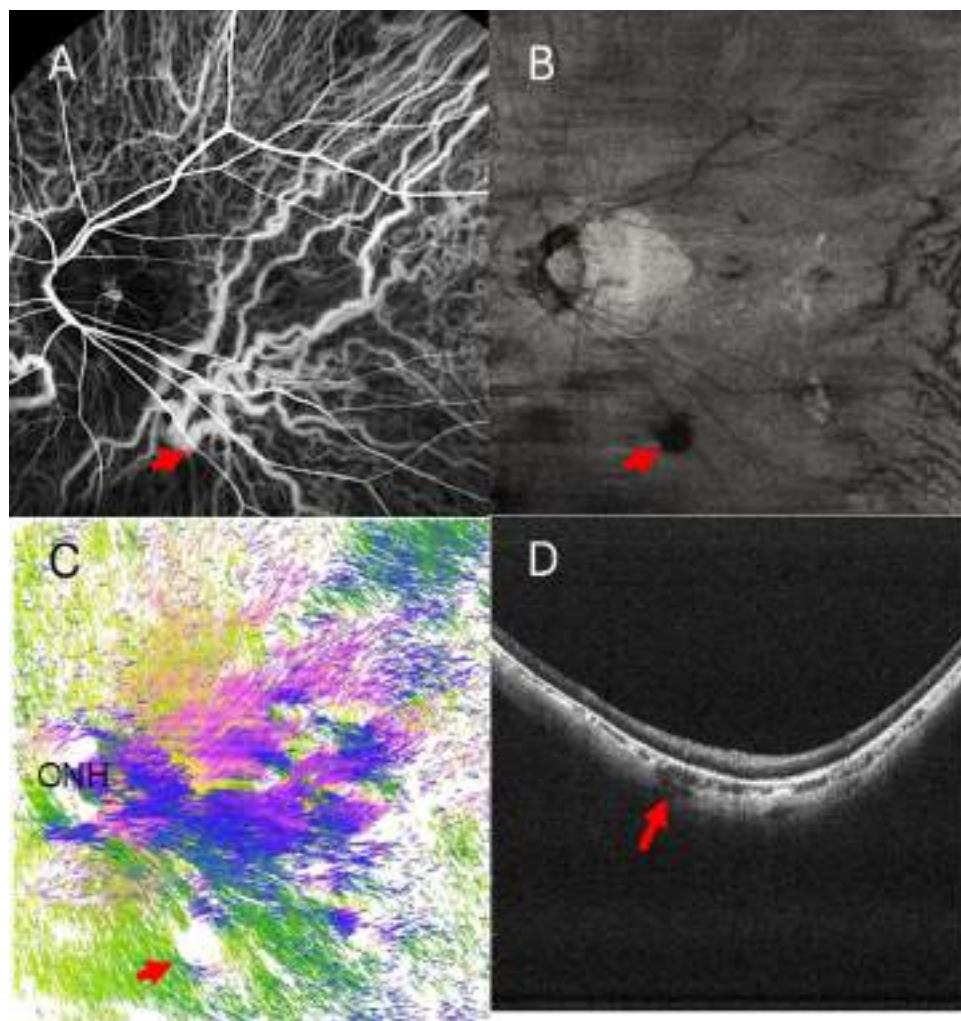


FIGURE 5. A whorl-like structure surrounding the exit of the posterior VV. **(A)** Venous phase ICGA image from a 54-year-old woman with an axial length of 30.02 mm shows a posterior VV with dilated and tortuous branches. The original ICGA image was cropped to show the area detected by PS-OCT. The *red arrow* indicates the exit of a large posterior VV. **(B)** The en face OCT intensity image at the CSI. The *red arrow* indicates a large hyporeflective area corresponding to the exit of this posterior VV. **(C)** The streamline image viewed from inside the eye shows a large whorl-like structure (*arrow*) corresponding to the site of posterior VV exit. Many other small whorl-like structures were also seen. **(D)** Horizontal B-scan OCT intensity image showing the largest width of the posterior VV. Posterior VV starts from the choroid and courses intrasclerally (between *dotted lines*). The *red arrow* indicates the site where this posterior VV exits the eye.

centered on the fovea and shed light on the macroscopic observation of fiber arrangement in the wider area of sclera.

The emissary canals of PSVs may be structurally vulnerable because they are full-thickness scleral discontinuities, and this vulnerability becomes more pronounced as the posterior sclera stretches and thins in eyes with pathologic myopia. This process can lead to a marked expansion of the canals into scleral pits.^{23,24,27} However, previous studies had not thoroughly explored the collagen fiber arrangements around vessel emissary canals within the sclera. In the book *The Sclera*,¹ it is mentioned that “The fibrils at the emissary canals run parallel to the direction of the canal”; however, this assertion lacks supporting citations or illustrative figures and does not provide a clear picture of how the fibrils are arranged around the emissary canals. Our findings contribute to a more detailed understanding of this anatomical configuration, presenting a clearer and more accurate depiction of the collagen fiber orientations

in relation to the emissary canals. The whorl-like structures formed by fibers encircling the canals may contribute to maintaining a uniform stress distribution circumferentially, thereby minimizing the risk of stress concentration at any single point. This structural arrangement likely serves a protective role, preserving the space required for vessel passage and preventing potential rupture or significant deformation in these regions under conditions of marked scleral stretching. Scleral remodeling during the progression of myopia is characterized by the loss of collagen tissue, a decrease in collagen fibril diameter, and a shift from an interwoven to a lamellar arrangement of collagen fiber bundles.^{28–32} These changes collectively contribute to the overall thinning of the scleral thickness. In the present study, we demonstrated that the whorl-like collagen fiber arrangements appear to remain largely unaffected during this remodeling process. Future ex vivo studies are needed to further investigate the associated microstructural changes.

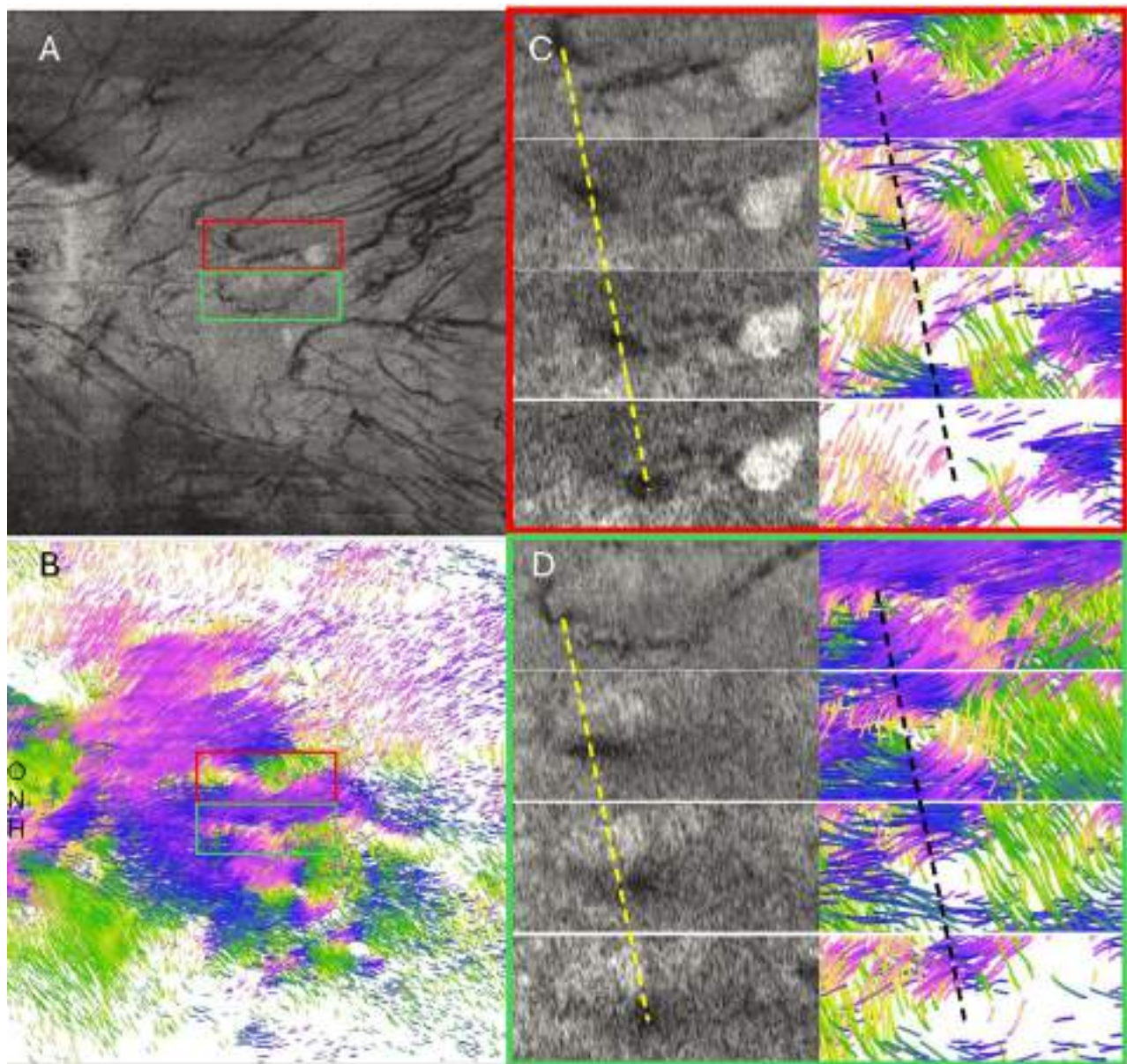


FIGURE 6. The whorl-like structures observed to encircle the entire course of the emissary canals with the oblique perforation. (A, B) En face OCT intensity image at CSI and streamline images of the sclera. The red and green rectangles indicate the areas shown in images C and D, respectively. (C, D) The cropped images from the areas of A and B indicated by the red rectangle (C) and green rectangle (D), respectively. The left column in each image shows the en face OCT intensity images extracted at the depths shifted from the CSI for 0 pixel, 10 pixels (44.7 μm), 20 pixels (89.4 μm), and 30 pixels (134.1 μm), respectively. The right column in each image shows the streamline images at the same depths of the respective intensity images in the left column. The yellow dotted lines connect the center of the hyporeflexive areas, which are indicative of the course of emissary canals, at the depths shifted from CSI for 0 and 30 pixels. It can be observed that both emissary canals are oblique within the sclera, because they perforate the sclera temporally and inferiorly from CSI to deeper levels. The black dotted lines connect the center of the whorl-like structures at the depths shifted from CSI for 0 and 30 pixels, showing corresponding lateral shift along the depths in the sclera, as well as the OCT intensity images.

Additionally, tangentially arranged collagen bundles were observed around the emissary canals under microscopy. Similar tangentially arranged fibers have also been reported to surround the ONH canal in a study by Voorhees and colleagues,³³ they pointed out that the tangentially arranged fiber might explain the expansion of the ONH canal under elevated intraocular pressure. Moreover, they performed computational modeling and demonstrated that tangentially arranged fibers showed significantly superior profile of circumferential and radial strains compared to traditional

circumferential fiber arrangement and radial fiber arrangement models.³³ Therefore the tangentially arranged fibers, which provide flexibility of expansion and near-zero strain profile,³³ might be a more deep-seated factor for the mechanical strength of such whorl-like configuration, especially in cases of scleral pits. The persistence of whorl-like structures around scleral pits, hypothesized to arise from the expansion of tangentially arranged fibers, further supports the role of collagen fiber sliding as a biomechanical mechanism contributing to ocular expansion in myopic eyes.³⁴

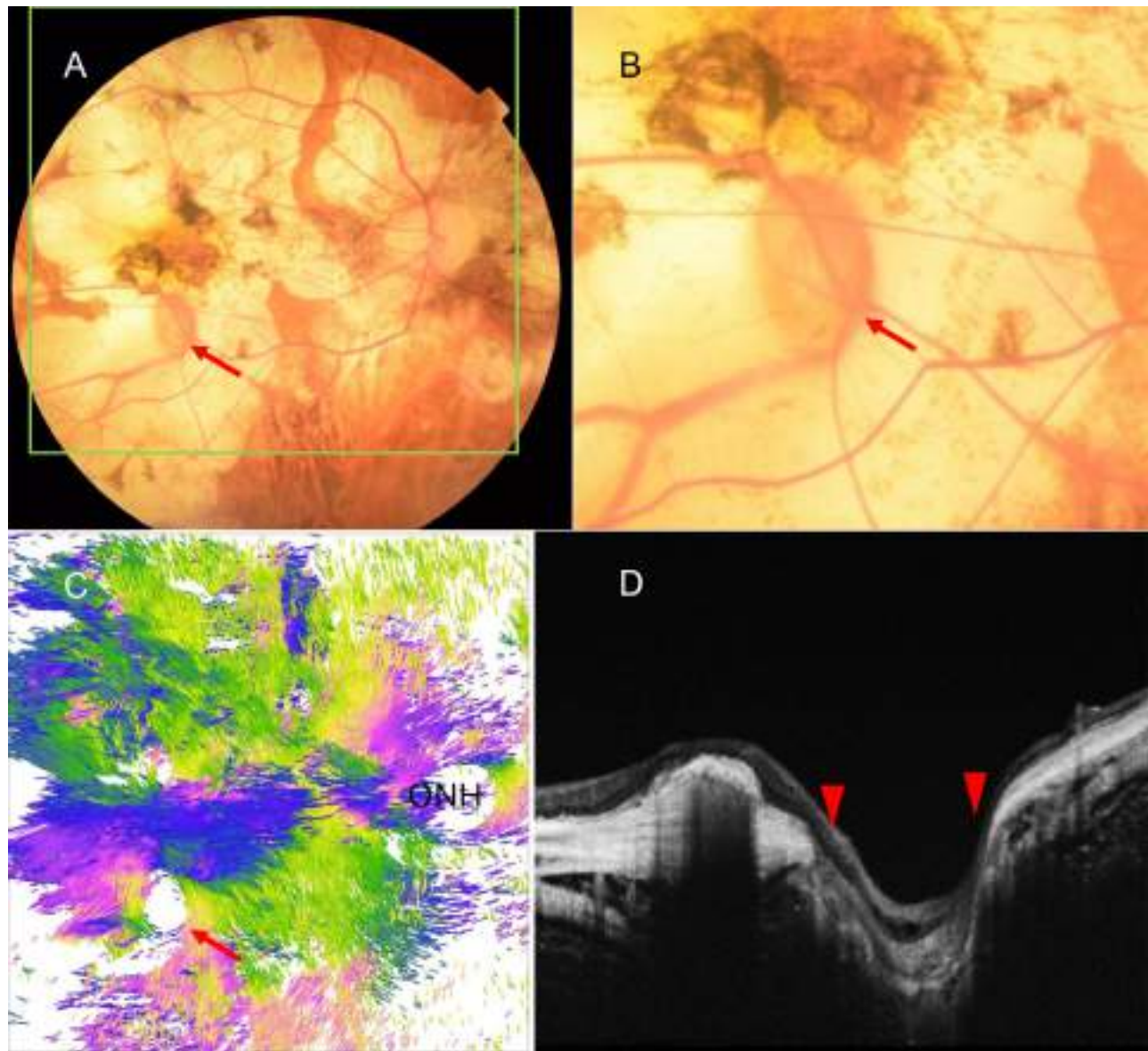


FIGURE 7. A case with whorl-like structure surrounding a large scleral pit. **(A)** Left fundus of a 59-year-old woman with an axial length of 32.64 mm shows extensive atrophy. The *red arrow* indicates the scleral pit with slightly orange color. **(B)** A magnified image of the scleral pit. Branches of the perforating scleral vessel emerges at the edge of the pit. **(C)** Streamline image of the sclera. The *red arrow* indicates a large whorl-like structure corresponding to the pit area. **(D)** A vertical scan of swept-source OCT (SS-OCT) at the pit area shows that the sclera is disrupted at the point indicated by *arrowheads*. The width of the pit is 896.48 μm .

Scleral pits are larger full-thickness scleral excavation occurring at the site of emissary canals in advanced pathologically myopic eyes with extensive choroid atrophy, which are believed to be caused by a mechanical expansion of the emissary canals as a result of axial elongation, scleral thinning and loss of overlying choroid.^{23,24,27} It has been reported to occur in 17.6% to 59% of pathologically myopic eyes.^{19,20} In our study, the largest widths measured ranged from 150 to 900 μm , while a previous small case series³⁵ reported scleral pit sizes ranging from 0.5 to 1 disc diameter (approximately 1500 μm). Both findings indicate a relatively large scleral hole on a very thin sclera. Therefore it is conceivable that these areas would be extremely vulnerable, and the whorl-like structures around scleral pits demonstrated by PS-OCT in our study may provide important

insights on how the eyes maintain integrity in such cases, and no spontaneous eye rupture occurred in such cases in our Advanced High Myopia Center.

Additionally, when scleral pits are present, the vessels are consistently located at the edge of the pits rather than at their center in color fundus photographs (Fig. 7).^{23,24,27} Under SEM examination of porcine eyes, vessels were observed to be firmly attached to one side of the emissary canal eccentrically, with many accompanying connective tissues (Fig. 8C). This anatomical structure may explain the abovementioned clinical findings.

This study has several limitations that must be acknowledged. First, it focuses exclusively on highly myopic eyes, which could exhibit different patterns of collagen fiber arrangements from those in normal human eyes. However,

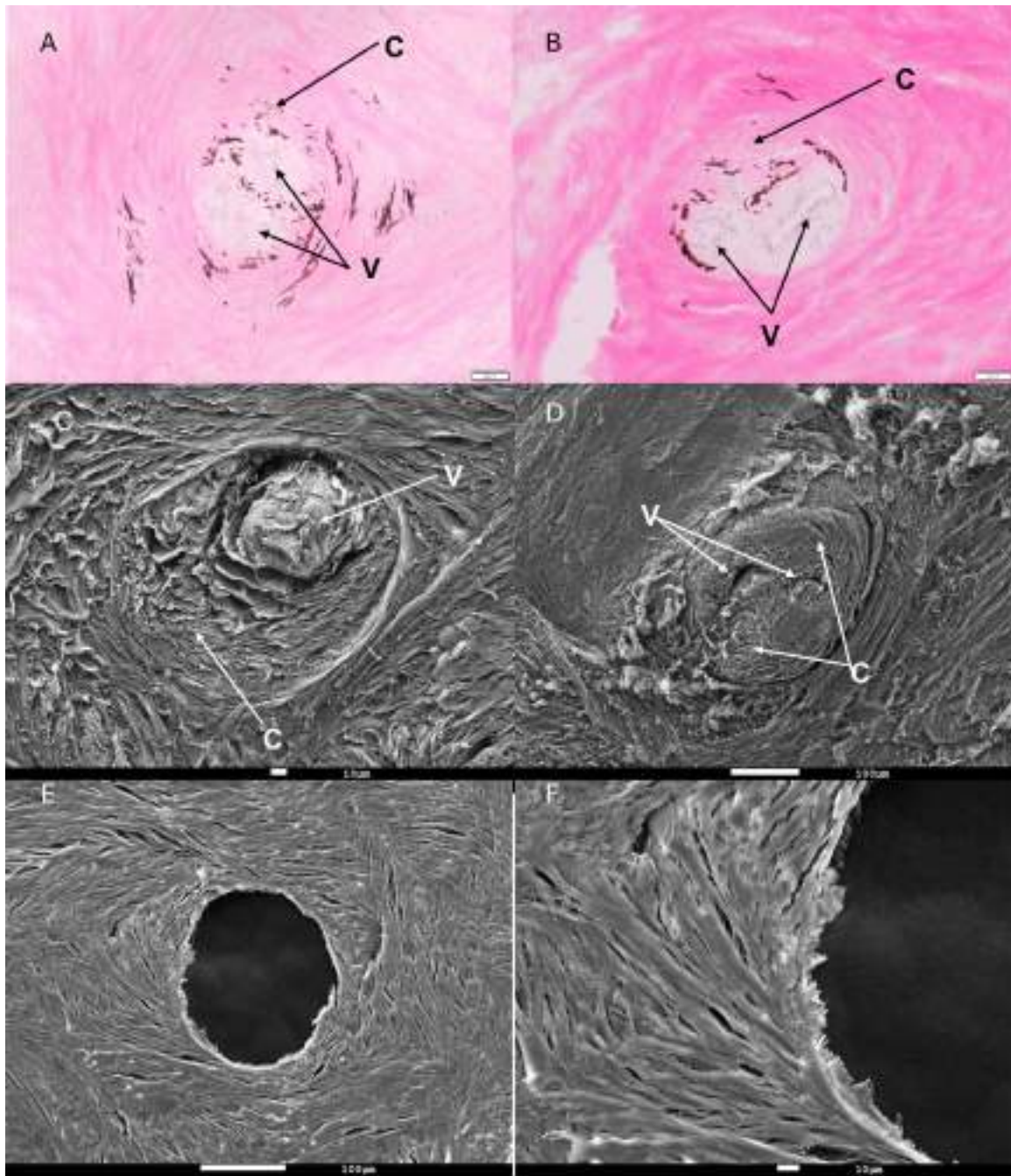


FIGURE 8. The arrangement of collagen fibers around the emissary canals in the posterior sclera of a porcine eye was examined using microscopy techniques. **(A, B)** Light microscopic images of H&E-stained 10 μm -thick scleral sections reveal a circumferential organization of collagen fibers encircling the emissary canals. Multiple vessels (V) are visible within a single canal, accompanied by surrounding collagen fibers (C). Magnification $\times 200$. Scale bars: 50 μm . **(C, D)** SEM images display one (C) or two (D) vessels (V) within the emissary canals, accompanied by collagen fibers (C). Collagen fibers around the emissary canals are arranged circumferentially. (C) A vessel is positioned eccentrically, attaching to one side of the canal. Magnification $\times 370$ for C (Scale bar: 10 μm) and $\times 160$ for D (Scale bar: 100 μm). **(E)** SEM image of a 10 μm thick slice displaying an emissary canal without vessels inside. Magnification $\times 200$. Scale bar: 100 μm . **(F)** Close-up of the lower left part of the emissary canal from image E, showing collagen fibers arranged tangentially around the canal. Magnification $\times 500$. Scale bar: 10 μm .

by microscopic observation of porcine sclera, which shares many structural similarities with human sclera and is widely used as a model for studying ocular biomechanics,³⁶ we confirmed that this configuration is a normal structure. Second, the detailed structures of the sclera,²⁰ including the hierarchical organization of collagen (from tropocollagen

molecules to microfibrils and fibrils), the crimp structures of the fibers, and the variation in fiber and bundle diameters across different scleral depths, exceed the resolution of PS-OCT, and the streamline images represent only the preferential collagen fiber orientations based on the net birefringence detected by the device. Future ex vivo studies are

needed to further investigate the associated microstructural changes around emissary canals in myopic eyes.

In conclusion, our study demonstrated the presence of whorl-like structures constructed by tangentially arranged collagen fibers around PSV emissary canals in the posterior sclera using PS-OCT in vivo and microscopy ex vivo, thereby addressing a previously unexplored aspect of scleral histology. The whorl-like structures around large scleral pits highlighted the critical role of this configuration in the structural integrity and physiological function of the eye in extremely pathological conditions. These findings not only fill a significant knowledge gap but also opens avenues for further research into the biomechanical properties of the sclera and their implications for ocular health. Further longitudinal studies using PS-OCT for highly myopic eyes might be able to detect early changes of the sclera at structurally vulnerable sites that predispose the patients to significant morphological changes like deep staphyloma before developing vision-threatening complications.

Acknowledgments

Supported by partial research funding from Tomey Corporation. Grant from the Japanese Society for Promotion of Science (number; 19H03808) to K.O.M, and grant from JST SPRING, Grant Number JPMJSP2120 to H. L.

Disclosure: **H. Lu**, None; **Y. Wu**, None; **J. Xiong**, None; **N. Zhou**, None; **M. Yamanari**, Tomey Corporation (E), JP 6463051 B2 (P), US 9593936 B2 (P), EP 2995245 B1 (P), JP 6542178 B2 (P), JP 7332131 B2 (P) issued to Tomey Corporation; **M. Okamoto**, Tomey Corporation (E); **K. Sugisawa**, None; **H. Takahashi**, None; **C. Chen**, None; **Y. Wang**, None; **Z. Wang**, None; **K. Ohno-Matsui**, Tomey Corporation (R), Santen (C), CooperVision (C)

References

- Stanford M. The sclera. M. S. De La Maza, J. Tauber, C. S. Foster 2013, ISBN: 978-1-4419-6501-1 Springer [book review]. *Graefes Arch Clin Exp Ophthalmol*. 2014;252:2027.
- Watson PG, Young RD. Scleral structure, organisation and disease. A review. *Exp Eye Res*. 2004;78:609–623.
- Meek KM. The cornea and sclera. In: Fratzl P, ed. *Collagen: Structure and Mechanics*. Boston: Springer US; 2008:359–396.
- Hayreh SS. Posterior ciliary artery circulation in health and disease: the Weisenfeld lecture. *Invest Ophthalmol Vis Sci*. 2004;45:749–757; 748.
- Moriyama M, Cao K, Ogata S, Ohno-Matsui K. Detection of posterior vortex veins in eyes with pathologic myopia by ultra-widefield indocyanine green angiography. *Br J Ophthalmol*. 2017;101:1179–1184.
- He G, Zhang X, Zhuang X, et al. A novel exploration of the choroidal vortex vein system: incidence and characteristics of posterior vortex veins in healthy eyes. *Invest Ophthalmol Vis Sci*. 2024;65(2):21.
- Willemse J, Gräfe MGO, Verbraak FD, de Boer JF. In vivo 3D determination of peripapillary scleral and retinal layer architecture using polarization-sensitive optical coherence tomography. *Transl Vis Sci Technol*. 2020;9(11):21.
- Ohno-Matsui K, Igarashi-Yokoi T, Azuma T, et al. Polarization-sensitive OCT imaging of scleral abnormalities in eyes with high myopia and dome-shaped macula. *JAMA Ophthalmol*. 2024;142:310–319.
- Komai Y, Ushiki T. The three-dimensional organization of collagen fibrils in the human cornea and sclera. *Invest Ophthalmol Vis Sci*. 1991;32:2244–2258.
- Jan N-J, Lathrop K, Sigal IA. Collagen architecture of the posterior pole: high-resolution wide field of view visualization and analysis using polarized light microscopy. *Invest Ophthalmol Vis Sci*. 2017;58:735–744.
- Gogola A, Jan NJ, Lathrop KL, Sigal IA. Radial and circumferential collagen fibers are a feature of the peripapillary sclera of human, monkey, pig, cow, goat, and sheep. *Invest Ophthalmol Vis Sci*. 2018;59:4763–4774.
- Zhang L, Albon J, Jones H, et al. Collagen microstructural factors influencing optic nerve head biomechanics. *Invest Ophthalmol Vis Sci*. 2015;56:2031–2042.
- Hecht E. *Optics*. New York: Pearson Education, Inc.; 2017.
- Patil R, Shetty R, Patel Y, et al. Phase retardation and corneal sublayer thickness repeatability using ultrahigh-resolution polarization-sensitive OCT. *J Cataract Refract Surg*. 2023;49:76–83.
- Patil R, Shetty R, Narasimhan R, et al. Mapping of corneal birefringence in thin and asymmetric keratoconus corneas with ultrahigh-resolution polarization-sensitive OCT. *J Cataract Refract Surg*. 2022;48:929–936.
- Steiner S, Schwarzhans F, Desissaire S, et al. Birefringent properties of the peripapillary retinal nerve fiber layer in healthy and glaucoma subjects analyzed by polarization-sensitive OCT. *Invest Ophthalmol Vis Sci*. 2022;63(12):8.
- Gräfe MGO, van de Kreeke JA, Willemse J, et al. Subretinal fibrosis detection using polarization sensitive optical coherence tomography. *Transl Vis Sci Technol*. 2020;9(4):13.
- Yamanari M, Mase M, Obata R, et al. Melanin concentration and depolarization metrics measurement by polarization-sensitive optical coherence tomography. *Sci Rep*. 2020;10(1):19513.
- Li Q, Karnowski K, Untracht G, et al. Vectorial birefringence imaging by optical coherence microscopy for assessing fibrillar microstructures in the cornea and limbus. *Biomed Opt Express*. 2020;11:1122–1138.
- Boote C, Sigal IA, Grytz R, Hua Y, Nguyen TD, Girard MJA. Scleral structure and biomechanics. *Prog Retin Eye Res*. 2020;74:100773.
- Pijanka JK, Spang MT, Sorensen T, et al. Depth-Dependent Changes in Collagen Organization in the Human Peripapillary Sclera. *PLoS ONE*. 2015;10(2):e0118648.
- Ohno-Matsui K, Akiba M, Ishibashi T, Moriyama M. Observations of vascular structures within and posterior to sclera in eyes with pathologic myopia by swept-source optical coherence tomography. *Invest Ophthalmol Vis Sci*. 2012;53:7290–7298.
- Xie S, Fang Y, Du R, et al. Abruptly emerging vessels in eyes with myopic patchy chorioretinal atrophy. *Retina*. 2019;40:1.
- Pedinielli A, Souied EH, Perrenoud F, Leveziel N, Caillaux V, Querques G. In Vivo visualization of perforating vessels and focal scleral ectasia in pathological myopia. *Invest Ophthalmol Vis Sci*. 2013;54:7637–7643.
- Ohno-Matsui K, Kawasaki R, Jonas JB, et al. International photographic classification and grading system for myopic maculopathy. *Am J Ophthalmol*. 2015;159:877–883.e877.
- Liu X, Jiang L, Ke M, et al. Posterior scleral birefringence measured by triple-input polarization-sensitive imaging as a biomarker of myopia progression. *Nat Biomed Eng*. 2023;7:986–1000.
- Ohno-Matsui K, Akiba M, Moriyama M. Macular pits and scleral dehiscence in highly myopic eyes with macular chorioretinal atrophy. *Retin Cases Brief Rep*. 2013;7:334–337.
- Liu KR, Chen MS, Ko LS. Electron microscopic studies of the scleral collagen fiber in excessively high myopia. *Taiwan Yi Xue Hui Za Zhi*. 1986;85:1032–1038.
- Curtin BJ, Iwamoto T, Renaldo DP. Normal and staphylomatous sclera of high myopia: an electron microscopic study. *Arch Ophthalmol*. 1979;97:912–915.

30. McBrien NA, Cornell LM, Gentle A. Structural and ultrastructural changes to the sclera in a mammalian model of high myopia. *Invest Ophthalmol Vis Sci*. 2001;42:2179–2187.
31. Funata M, Tokoro T. Scleral change in experimentally myopic monkeys. *Graefes Arch Clin Exp Ophthalmol*. 1990;228:174–179.
32. McBrien NA, Gentle A. Role of the sclera in the development and pathological complications of myopia. *Prog Retin Eye Res*. 2003;22:307–338.
33. Voorhees AP, Jan N-J, Hua Y, Yang B, Sigal IA. Peripapillary sclera architecture revisited: a tangential fiber model and its biomechanical implications. *Acta Biomaterialia*. 2018;79:113–122.
34. Rada JA, Shelton S, Norton TT. The sclera and myopia. *Exp Eye Res*. 2006;82:185–200.
35. Zhang W, Zhang Y, Xu J, Dan H, Li X, Song Z. A physical sign of pathological myopia: myopic scleral pit. *BMC Ophthalmol*. 2023;23:114.
36. Herring I, Duncan R, Pickett J, Bass C. The porcine eye as a surrogate model for the human eye: anatomical and

mechanical relationships. Available at <https://www-nrd.nhtsa.dot.gov/bio/Proceedings>. Accessed October 24, 2024.

SUPPLEMENTARY MATERIAL

SUPPLEMENTARY VIDEO. Video showing *en face* optical coherence tomography (OCT) intensity and streamline images of the sclera extracted at the shifted depths from the choroid-sclera interface (CSI) for 0 to 31 pixels (138.6 μm). From CSI to deeper levels, the positions of the emissary canals indicated by hypo-reflective area on the intensity images shift laterally, and the respective whorl-like structures on the corresponding streamline images shift accordingly at each depth.

家族性滲出性硝子体網膜症に関する研究

研究分担者

産業医科大学・医学部・教授 近藤 寛之

研究協力者

近畿大学・医学部・教授 日下 俊次

国立成育医療センター・診療部長 仁科 幸子

家族性滲出性硝子体網膜症（FEVR）は、網膜末梢の血管異常により網膜虚血、滲出性網膜剥離、牽引性網膜剥離などを呈する遺伝性の網膜疾患である。これまで本研究班では FEVR の診療ガイドラインを作成するとともに、原因遺伝子や臨床所見についての調査を進めてきた。本年度は、FEVR の常染色体顕性（AD）遺伝子の病原性変異を有することが確認された軽症の FEVR 患者の超広角フルオレセイン血管造影（UWFA）の特性を研究した。その結果、V 字型血管ノッチ、ブラシ状血管端、無血管網膜（csAR）の組み合わせは、Norrin/ β -Catenin 遺伝子の病原性変異体を有する AD-FEVR 患者のバイオマーカーとして有用であることが示唆された。

A. 研究目的

明らかにすることである。

家族性滲出性硝子体網膜症（FEVR）

は、網膜末梢の血管の異常により網膜虚血、滲出性網膜剥離、牽引性網膜剥離などを呈する遺伝性の網膜疾患である。FEVR は遺伝的に不均一な疾患であり、患者によって異なる浸透率を示す。また FEVR の眼所見は左右非対称である傾向があり、同じ家系の罹患者間でも大きく異なるという特徴を示す。

本研究班では、これまで FEVR の診療ガイドラインを作成するとともに、本症の原因遺伝子と患者の臨床所見との関連について調査および研究を進めてきた。

今年度の研究目的は、FEVR の常染色体顕性（AD）遺伝子の病原性変異を有することが確認された軽症の FEVR 患者の超広角フルオレセイン血管造影（UWFA）の特性を

B. 研究方法

Norrin/ β -catenin 遺伝子の病原性変異体を有する 27 家族の軽症 FEVR 患者 37 人を対象とした。対照は、病原性変異体を持たないか、常染色潜性遺伝子のヘテロ接合体変異を持つことが確認された 32 人の家族（保因者）とした。

患者の UWFA 画像 64 枚を対照者の UWFA 画像 60 枚と比較した。耳側網膜網膜と耳側網膜の周辺部無血管網膜の相対的な長さ、および 6 つの末梢血管変化（csAR、V 字型血管ノッチ、ブラシ状血管端、血管染色、ループ血管または吻合部、毛細血管毛細血管拡張症）の有無を患者と対照群で比較した。臨床的に有意な無血管網膜（csAR）の相対的長さのカットオフ比は、ROC 曲線を

用いて決定した。

(倫理面への配慮)

今回の研究に関しては患者の個人情報はいずれも匿名化し、倫理面に十分配慮して行った。

C. 研究結果

AD-FEVR 患者では、V 字型血管ノッチ (69%対 2% ; $P<0.001$)、ブラシ状血管端 (78%対 3% ; $P<0.001$)、csAR (83%対 22% ; $P<0.001$)、血管染色 (70%対 35% ; $P<0.001$) の網膜変化の頻度が対照群より高かった。ループ血管および/または末梢血管の吻合は、患者では対照群より有意に少ない頻度で認められた (39% vs 73% ; $P<0.001$)。毛細血管拡張症については、2 群間に有意差は認められなかった。V 字型血管ノッチ、ブラシ状血管端、csAR の組み合わせは、感度 82.8%、特異度 98.3%で、ROC 曲線の最高値は 0.9 であつ

G. 研究発表

1. 論文発表

- 1) Okamoto M, Matsushita I, Nagata T, Fujino Y, Kondo H. Angiographic Characteristics in Mild Familial Exudative Vitreoretinopathy with Genetically Confirmed Autosomal Dominant Inheritance. Ophthalmol Retina. 2025 Feb;9(2):187-193.
- 2) Oga T, Mano F, Kuniyoshi K, Iwahashi C, Kondo H, Kusaka S. Fluorescein Angiography May Predict Surgical Outcomes of Tractional Retinal Detachment in Familial Exudative Vitreoretinopathy. Ophthalmol Retina. 2025.
- 3) Kawaguchi N, Mano F, Kondo H, Kuniyoshi K, Kusaka S. Two Cases of Rubinstein-Taybi Syndrome With Retinal Detachment. Cureus. 2025 Mar 4;17(3):e80048.
- 4) Kondo H, Tsukahara-Kawamura T, Matsushita I, Nagata T, Hayashi T, Nishina S, Higasa K, Uchio E, Kondo M, Sakamoto T, Kusaka S. Familial Exudative Vitreoretinopathy With and Without Pathogenic Variants of Norrin/ β -Catenin

た。

D. 考察

V 字型血管ノッチ、ブラシ状血管端、csAR の組み合わせは、Norrin/ β -Catenin 遺伝子の病原性変異体を有する AD-FEVR 患者のバイオマーカーとして使用できることが示唆された。これらの知見は、FEVR 家系におけるより正確な分離分析を可能にし、より良い遺伝カウンセリングを提供することに役立つ可能性があると考えられた。

E. 結論

FEVR が疑われる患者において UWFA を行い、末梢血管変化を評価することで、より正確な診断や遺伝カウンセリングができることがわかった。

F. 健康危険情報 : なし

Signaling Genes. Ophthalmol Sci. 2024 Mar 15;4(5):100514.

- 5) Dong S, Zou T, Zhen F, Wang T, Zhou Y, Wu J, Nagata T, Matsushita I, Gong B, Kondo H, Li Q, Zhang H. Association of variants in GJA8 with familial acorea-microphthalmia-cataract syndrome. Eur J Hum Genet. 2024 Apr;32(4):413-420.
- 6) Tachibana K, Iwahashi C, Kuniyoshi K, Kusaka S. Long-term visual function and refractive changes after vitrectomy for stage 4 retinopathy of prematurity. Graefes Arch Clin Exp Ophthalmol. 2025 Online ahead of print.

2. 学会発表

- 1) 畦間美里ほか：家族性滲出性硝子体網膜症の顕性遺伝子異常保有者の超広角蛍光眼底所見による予測．第128回日本眼科学会総会，2024.4.18，東京国際フォーラム．
- 2) 奥一真ほか：4連発現プラスミドを用いた家族性滲出性硝子体網膜症原因遺伝子の機能解析．第128回日本眼科学会総会，2024.4.18，東京国際フォーラム．

H. 知的財産権の出願・登録状況

1. 特許取得 なし
2. 実用新案登録 なし
3. その他 なし



Fluorescein Angiography May Predict Surgical Outcomes of Tractional Retinal Detachment in Familial Exudative Vitreoretinopathy

Tomoyuki Oga, MD,¹ Fukutaro Mano, MD,¹ Kazuki Kuniyoshi, MD, PhD,¹ Chiharu Iwahashi, MD, PhD,¹ Hiroyuki Kondo, MD, PhD,² Shunji Kusaka, MD, PhD¹

Purpose: To investigate factors associated with the surgical outcomes of tractional retinal detachment (TRD) in eyes with familial exudative vitreoretinopathy (FEVR).

Design: Retrospective chart review.

Subjects: Patients who underwent surgeries for TRD associated with FEVR between April 2011 and April 2022 and had a follow-up of ≥ 18 months were included in the analysis.

Methods: Vitrectomy was performed on 47 eyes, with scleral buckling in 4 eyes and simultaneous lensectomy in 26 eyes.

Main Outcome Measures: Data, including sex, age at the first surgery, disease stage, extent of fibrovascular proliferation (FVP, within 3 hours or >3 hours), preoperative fluorescein angiography (FA) grading (grade 1: mild leakage caused by FVP, grade 2: severe leakage), surgical outcomes, and complications, were collected.

Results: The age at the initial surgery ranged from 1 month to 15 years (median: 6 months). Thirty-two eyes were from male patients, and 15 eyes were from female ones. Only 1 eye in 25 patients was affected. In 11 patients, bilateral eyes were involved. In total, 8 eyes presented with stage 3 FEVR, 31 with stage 4, and 8 with stage 5. The preoperative FA was performed on 38 of 47 eyes. There were 26 eyes with FA grade 1 and 12 eyes with FA grade 2. The retina was reattached in 33 (70.2%) eyes at the final examination. Based on the univariate logistic regression analysis, a higher retinal reattachment (RA) rate was significantly associated with a lower FEVR stage ($P = 0.0001$), FA grade ($P = 0.0008$), and preoperative extent of FVP ($P = 0.02$). In the multivariate logistic regression analysis, only FA grade was significantly associated with RA ($P = 0.04$, odds ratio: 9.0, 95% confidence interval: 1.2–7.0 \times 10).

Conclusion: Eyes with TRD associated with FEVR in patients with mild FA leakage had a higher RA rate. Hence, the use of FA in evaluating disease activity can be useful in predicting surgical outcomes.

Financial Disclosure(s): Proprietary or commercial disclosure may be found in the Footnotes and Disclosures at the end of this article. *Ophthalmology Retina* 2025;■:1–8 © 2025 by the American Academy of Ophthalmology. This is an open access article under the CC BY-NC-ND license (<http://creativecommons.org/licenses/by-nc-nd/4.0/>).

Familial exudative vitreoretinopathy (FEVR) was first described by Criswick and Schepens.¹ Familial exudative vitreoretinopathy is a genetically heterogeneous disorder characterized by abnormal vasculogenesis and retinal angiogenesis. Its clinical features are similar to those of retinopathy of prematurity but usually without a history of prematurity.¹ Familial exudative vitreoretinopathy has various patterns of inheritance (autosomal dominant, autosomal recessive, or X-linked recessive).² To date, various genes are known to be responsible for FEVR, namely, *FZD4* (frizzled-4), *NDP* (Norrie disease pseudoglioma), *LRP5* (low-density lipoprotein receptor-like protein 5), *TSPAN12* (tetraspanin 12), and *KIF11* (kinesin family member 11).³ Symptom onset generally occurs in the first decade of life. However, its severity significantly varies even between eyes in the same patient or between siblings from the same family.³

The mild forms of FEVR are often asymptomatic, and they are only associated with peripheral vascular abnormalities such as a peripheral avascular retina, vitreoretinal adhesions, venous–venous anastomoses, and super-numerous vascular branching.^{4–6}

The more severe manifestations of the disease occur in the later stages. These include neovascularization, subretinal and intraretinal hemorrhage, exudates, and extraretinal fibrovascular proliferation (FVP), which can lead to macular dragging, retinal fold, and, eventually, tractional retinal detachment (TRD) due to vitreoretinal traction.^{4,6}

Pendergast and Trese⁶ proposed an FEVR staging classification similar to that of retinopathy of prematurity. In particular, it categorizes FEVR into 5 stages based on the experiences of 26 patients with FEVR who underwent surgery. Results showed that the earlier stages of FEVR without retinal detachment (stage 2B or less) had excellent

outcomes after laser ablation or observation alone. Laser ablation alone can sometimes regress peripheral retinal detachment. However, surgical intervention (scleral buckling or vitrectomy) is required for eyes with progressive retinal detachment (stage 3A or higher).⁶

Kashani et al⁷ proposed the revised staging classification that incorporates wide-field fluorescein angiography (FA) findings into the FEVR classification for diagnostic utility in subclinical patients.

Some studies have reported the surgical outcomes of TRD in patients with FEVR.^{8–14} However, thus far, no studies have analyzed surgical outcomes based on disease activity using the degree of fluorescent leakage caused by FVP on angiography. Thus, the current study aimed to investigate the association between anatomical success and preoperative FA findings in patients with FEVR who were surgically treated.

Methods

Study Populations and Data Collections

This retrospective case study was approved by the ethics committee of Kindai University Hospital (approval number: #28-264). It was performed in accordance with the tenets of the Declaration of Helsinki. The legal guardians of all patients provided informed consent.

A chart review was conducted on 47 eyes in 36 consecutive patients with TRD associated with FEVR who had undergone surgeries between April 2011 and April 2022 and had a follow-up

of ≥ 18 months. The clinical diagnostic criteria for FEVR were as follows: peripheral retinal avascularity, nonperfusion, vascular straightening, vitreoretinal traction, retinal exudation, or retinal neovascularization in ≥ 1 eye and full-term birth. A positive family history was a supportive criterion but not mandatory.^{6,7}

Patients suspected of other conditions such as rhegmatogenous retinal detachment, retinopathy of prematurity, persistent fetal vasculature, Coats' disease, and ocular toxocariasis were excluded from the analysis. The following data were collected from the charts: sex, age at the first surgery, FEVR stages based on the classification of Kashani et al⁷ extent of FVP (limited within 3 hours or >3 hours), preoperative FA grades (based on the FA leakage), surgical procedures (vitrectomy, lensectomy, scleral buckling, and tamponades), surgical outcomes, and complications. The main outcome measure was anatomical success, defined as retinal reattachment (RA) including partial reattachment of the posterior pole at the final examination.

FA Images and Grade Classification

In this study, FA was performed using RetCam 3 (Clarity Medical Systems) during examinations under anesthesia with commercially available IV fluorescein sodium at a standard dose (pediatric dose: 0.2 ml/kg).

Fluorescein angiography leakage caused by FVP was assessed and categorized into 2 at 1 minute after dye injection. The grading systems proposed by the authors comprised grade 1, which indicated mild or moderate fluorescein leakage, and grade 2, which represented severe fluorescein leakage. In Figure 1, the preoperative FA images were evaluated by 3 masked-retina specialists (F.M., C.I., and K.K.). If the grades differed among the specialists, the senior specialist (K.K.) decided the final grade.

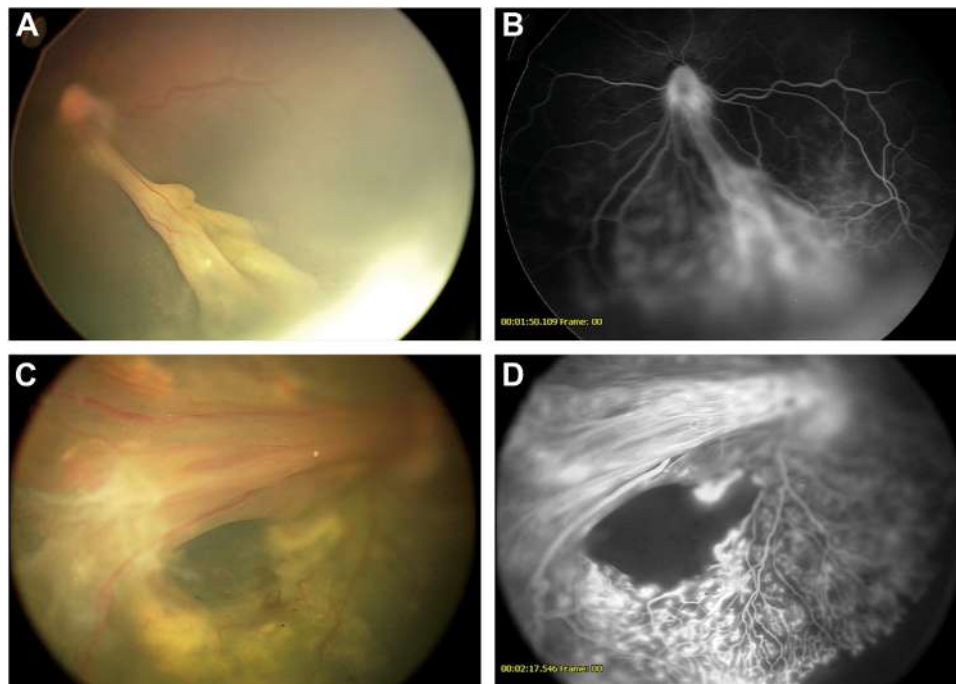


Figure 1. Representative fundus and FA images of stage 4 FEVR. **A**, Fundus images of tractional retinal detachment in the temporal retina and **(B)** corresponding FA image. Mild fluorescein leakage was observed in the early phase (FA grade 1). **C**, Fundus images of tractional retinal detachment in the temporal retina and **(D)** corresponding FA image. Severe fluorescein leakage was observed in the early phase (FA grade 2). FA = fluorescein angiography; FEVR = familial exudative vitreoretinopathy.

Table 1. Basic Characteristics of Patients with FEVR Who Underwent PPV

		Number of Eyes (%)	FA Grade 1	FA Grade 2	N/A
Sex	Male	32 (68.1)	16	9	7
	Female	15 (31.9)	10	3	2
Median age (range), yrs	0.6 (0.1–15)		0.9 (0.1–12)	0.7 (0.1–5)	0.3 (0.3–15)
FEVR stage	Stage 3	8 (17.0)	7	1	0
	Stage 4	31 (66.0)	19	8	4
	Stage 5	8 (17.0)	0	3	5
Preoperative LPC	Stage 3	2 (4.3)	0	2	0
	Stage 4	4 (6.4)	2	1	1
	Stage 5	0 (0.0)	0	0	0
FVP range	One quadrant	32 (68.1)	22	7	3
	Two or more quadrants	15 (31.9)	4	5	6

FA = fluorescein angiography; FVP = fibrovascular proliferation; LPC = laser photocoagulation; N/A = not applicable; PPV = pars plana vitrectomy; Pre-op BCVA = preoperative best-corrected visual acuity.

Gene Analyses of FEVR

Using blood samples collected from the patients, whole-exome or Sanger sequencing of the *FZD4*, *LRP5*, *TSPAN12*, *KIF11*, and *NDP* genes was performed. The details of the genetic analysis were described elsewhere.^{15,16}

Statistical Analyses

Statistical analysis was conducted using JMP ver. 17.0 (SAS Institute Inc), and data were presented as mean \pm standard deviations or median with ranges. Differences in sex, age, FEVR stage, extent of FVP, and type of genes based on FA grade were analyzed using the chi-square test. Univariate and multivariate logistic regression analyses were performed to identify the predictive factors associated with RA. *P* values of <0.05 were used to define statistical significance.

Results

Characteristics of the Patients with FEVR

Table 1 shows the baseline characteristics of the patients. The current study included 47 eyes in 36 patients who underwent vitrectomy for TRD associated with FEVR. The median age of the patients was 0.6 (range, 0.1–15) years. The median observation period was 55.1 (range, 18–144) months. There were 24 male and 12 female participants. In total, 25 patients had undergone surgeries on 1 eye only, and 11 patients had bilateral surgery. In unilateral cases, the conditions of the fellow eye significantly differed (Table 2). Preoperatively, laser ablation was performed on 6 eyes. Otherwise, the others were treatment-naïve.

Preoperative Assessment of FEVR Staging, Extent of Fibrovascular Tissue, and FA Grading

The stage of each eye during the initial surgery was classified according to the FEVR classification reported by Kashani et al.⁷ In particular, 8 eyes presented with stage 3 FEVR, 31 with stage 4, and 8 with stage 5. The preoperative extent of FVP was divided into 2: within 3 hours or >3 hours. The preoperative extents of FVP were within 3 hours in 32 eyes and >3 hours in 15 eyes (6 eyes [3–6 hours]; 1 eye [6–9 hours]; and 8 eyes [9–12 hours]).

Preoperative FA was performed on 38 of 47 eyes. There were 26 eyes with FA grade 1 (stage 3: 7 eyes; stage 4: 19 eyes; and stage 5: 0 eye) and 12 eyes with FA grade 2 (stage 3: 1 eye; stage 4: 8 eyes; and stage 5: 3 eyes). In 9 patients, bullous retinal detachment or retrolental fibroplasia obscured fundus imaging. Hence, these patients did not undergo FA.

Surgical Procedures and Their Complications

A single surgeon (S.K.) performed surgeries. Using a 23G, 25G, or 27G system, an infusion cannula was placed pars plicata where FVP did not exist or placed into the anterior chamber if extensive circumferential traction existed. After vitrectomy, FVP was carefully removed using a vitreous cutter or horizontal or vertical scissors so as not to create an iatrogenic retinal tear. Tamponade materials such as air, expansile gas, or silicone oil were appropriately selected. Scleral buckling was performed at the second surgery for the re-detached cases. A simultaneous lensectomy was performed when peripheral FVP did not allow for the resections without lens preservation or lens damage occurred during the procedures.

Table 3 shows details about the surgical procedures and their complications. Vitrectomy was performed on 47 eyes, and simultaneous lensectomy was performed on 26 eyes. The overall RA rate was 70.2% (33 of 47 eyes). For those eyes treated with a single surgery, 22 of 25 (88.0%) had RA. For those eyes treated with 2 surgeries, 9 of 17 (52.9%) had RA. For those eyes treated with 3 surgeries, 2 of 4 (50.0%) had RA. For those eyes treated with 4 surgeries, 0 of 1 (0%) had RA.

The intraoperative complications included lens damage in 6 eyes and iatrogenic retinal break in 4 eyes. Four cases experienced

Table 2. Conditions of the Treated and Fellow Eyes

	Fellow Eyes					RF
	Stage 1	Stage 2	Stage 3	Stage 4	Stage 5	
Treated eyes						
Stage 3	0	5	0	0	1	0
Stage 4	4	7	0	0	2	2
Stage 5	1	0	0	0	0	0

RF = retinal fold.

Table 3. Surgical Details and Complications

	Number of Eyes	Stage 3	Stage 4	Stage 5
Number of surgeries		1.6 ± 0.7	1.5 ± 0.7	2.1 ± 0.7
Surgical procedures				
PPV and gauge system (23G; 13, 25G; 27, 27G; 7)	47	8	31	8
Lensectomy	26	2	16	8
Encircling*	4	0	4	0
Tamponade at the initial surgery				
Air	1	0	1	0
Gas	2	0	2	0
Complications				
Lens damage	6	1	5	0
Iatrogenic retinal break	4	0	3	1
Post-op OHT	4	1	3	0
Post-op VH	7	3	2	2

OHT = ocular hypertension; Post-op = postoperative; PPV = pars plana vitrectomy; VH = vitreous hemorrhage.

*Encircling scleral buckling was performed at the second surgery for retinal re-detachment. #240 was used for 3 cases and #506 was used for 1 case.

iatrogenic retinal tears, and 2 of 4 were able to reattach with multiple surgeries (2 and 4, respectively). The postoperative complications included ocular hypertension in 4 eyes and vitreous hemorrhage in 7 eyes.

Surgical Outcomes of FEVR Based on the Preoperative Factors

Table 4 shows the surgical outcomes based on various preoperative factors. The RA rate according to the staging classification was as follows: 100% in stage 3 (8 of 8 eyes; 3A: 3 of 3 eyes; and 3B: 5 of 5 eyes), 77.4% in stage 4 (24 of 31 eyes; 4A: 5 of 6 eyes; and 4B:

19 of 25 eyes), and 12.5% in stage 5 (1 of 8 eyes). Hence, the results significantly differed (stage 3 vs. stage 4; $P = 1.0$; odds ratio [OR], 8.6×10^6 ; 95% confidence interval [CI]: not provided; stage 4 vs. stage 5; $P = 0.006$; OR, 2.4×10 ; 95% CI, $2.5-2.3 \times 10^2$). A representative pre- and postoperative fundus image in each FEVR stage classification was summarized in Figure 2.

Patients with FA grade 1 had a significantly higher RA rate based on the FA than those with FA grade (92.3%, 24 of 26 eyes vs. 41.7%; 5 of 12 eyes; $P = 0.0008$; OR, 1.7×10 ; 95% CI, $2.7-1.1 \times 10^2$). In cases of stage 4 FEVR, patients with FA grade 1 (89.5%, 17 of 19 eyes) had a significantly higher RA rate than

Table 4. Results of the Logistic Regression Analyses of Retinal Reattachment

	Number of Eyes (%)	Number of Patients with Retinal Attachment (%)	Number of Patients Without Retinal Attachment (%)	Chi-square test P value
Sex				
Male/female	32 (68.1)/15 (31.9)	23 (71.9)/10 (66.7)	9 (28.1)/5 (33.3)	0.7
Age				
Median (range), yrs	0.6 (0.1–15)	0.9 (0.1–15)	0.5 (0.3–5)	0.3
Stage				
Stage 3	8 (17.0)	8 (100.0)	0 (0.0)	0.0001
Stage 4	31 (66.0)	24 (77.4)	7 (22.6)	
Stage 5	8 (17.0)	1 (12.5)	7 (87.5)	
FA grade				
Grade 1	26 (68.4)	24 (92.3)	2 (7.7)	0.0008
Grade 2	12 (31.4)	5 (41.7)	7 (58.3)	
Range of FP				
1 quadrant	32 (68.1)	26 (81.2)	6 (18.8)	0.02
2 and more quadrants	15 (31.9)	7 (46.7)	8 (53.3)	
Gene variant				
FZD4	5	4 (80.0)	1 (20.0)	0.7
LRP5	4	4 (100.0)	0 (0.0)	0.09
NDP	3	1 (33.3)	2 (66.7)	0.1
KIF11	3	3 (100.0)	0 (0.0)	0.2
Negative for all the abovementioned genes	14	9 (64.3)	5 (35.7)	0.3
N/A	18	11 (61.1)	7 (38.9)	

FA = fluorescein angiography; FP = fibrovascular proliferation; FZD4 = Frizzled 4; KIF11 = kinesin family member 11; LRP5 = low-density lipoprotein receptor-related protein 5; NDP = Norrie disease protein.

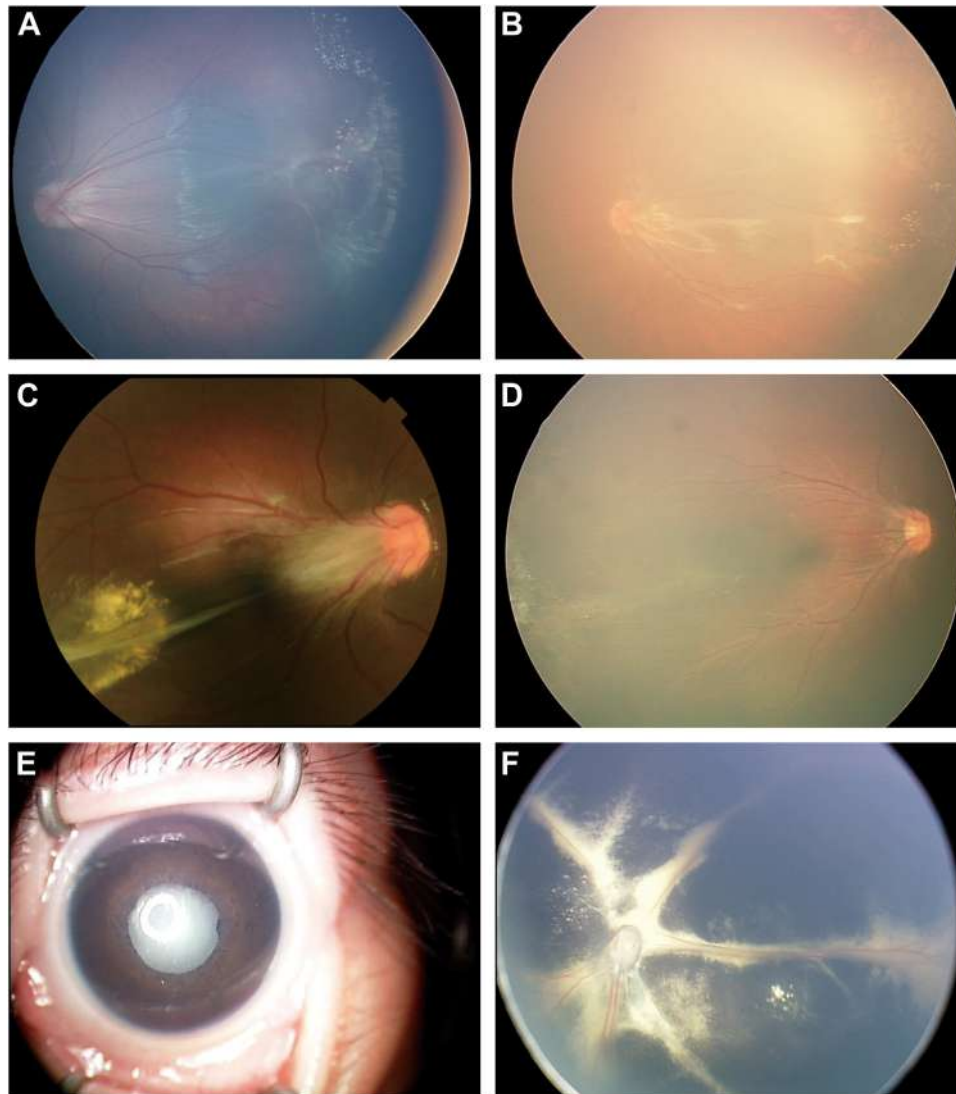


Figure 2. Representative pre- and postoperative fundus images in each FEVR stage classification. **A**, Macula-sparing retinal detachment (stage 3) was (**B**) reattached after vitrectomy. **C**, Macula-involving retinal detachment (stage 4) was (**D**) reattached after vitrectomy. **E**, Total retinal detachment with anterior chamber shallowing was (**F**) reattached after vitrectomy. FEVR = familial exudative vitreoretinopathy.

Table 5. Comparison of Preoperative and Postoperative Visual Acuity

	Preoperative logMAR BCVA	Postoperative logMAR BCVA (At the Final Examination)
FEVR Stage		
Stage 3	0.9 ± 0.4	1.0 ± 0.6
Stage 4	1.1 ± 0.5	1.3 ± 0.6
Stage 5	1.8	2.0 ± 0
FA Grade		
Grade 1	1.1 ± 0.4	1.1 ± 0.6
Grade 2	1.8	1.8 ± 0.2

BCVA = best-corrected visual acuity; FA = fluorescein angiography; FEVR = familial exudative vitreoretinopathy; logMAR = logarithm of the minimum angle of resolution.

those with FA grade 2 (50.0%, 4 of 8 eyes; $P = 0.03$; OR, 8.5; 95% CI; 1.1–6.4 × 10).

Based on the extent of FVP, the RA rates significantly differed within 3 hours and >3 hours (81.2% [26 of 32 eyes] vs. 46.7% [7 of 15 eyes]; $P = 0.02$; OR, 5.0; 95% CI, 1.3–1.9 × 10). The patients who achieved RA did not significantly differ in terms of age ($P = 0.32$) and sex ($P = 0.92$). Preoperative and postoperative visual acuity were summarized in Table 5. Among 5 cases that had measured postoperative visual acuity in the stage 5 FEVR, all were no light perception, even including the case with retinal reattachment.

Factors Associated with the Final RA

Based on the univariate logistic regression analysis, a higher RA rate was significantly associated with a lower FEVR stage, FA grade, and preoperative extent of FVP (Table 4). Meanwhile, in the multivariate logistic regression analysis using the abovementioned

Table 6. Genetic Findings and the Associations between FEVR Stages and FA Findings

		Gene Mutation																	
		FZD4			LRP5			NDP			KIF11			Negative for all the Genes			Not Tested		
FEVR Stage	3	4	5	3	4	5	3	4	5	3	4	5	3	4	5	3	4	5	
	0	5	0	2	2	0	0	3	0	1	2	0	4	5	5	1	14	3	
FA Grade	1	2	N/A	1	2	N/A	1	2	N/A	1	2	N/A	1	2	N/A	1	2	N/A	
	3	2	0	4	0	0	1	1	1	3	0	0	7	4	3	8	5	5	

FA = fluorescein angiography; FEVR = familial exudative vitreoretinopathy; FZD4 = frizzled 4; KIF11 = kinesin family member 11; LRP5 = low-density lipoprotein receptor-like protein 5; N/A = not applicable; NDP = Norrie disease pseudo glioma.

parameters, only FA grade was significantly associated with RA ($P = 0.04$; OR, 9.0; 95% CI, 1.2–7.0 \times 10).

Gene Analyses of FEVR and Surgical Outcomes

Genetic tests were performed on 29 of 47 eyes. In terms of variants, 5 eyes tested positive for the *FZD4* gene, 4 eyes for the *LRP5* gene, 3 eyes for the *NDP* gene, and 3 eyes for the *KIF11* gene. None of the eyes tested positive for *TSPAN12* mutations. In total, 13 eyes tested negative for *FZD4*, *LRP5*, *TSPAN12*, and *NDP* mutations. The genetic results were referable to those of our earlier report, which showed that families #1, #13, #16, #22, #25, #26, #27, and #32 tested positive for the *FZD4*, *LRP5*, and *NDP* genes¹⁵ and families #17 and #24 for the *KIF11* gene.¹⁶

The RA rates according to each gene mutation were 80% (4 of 5 eyes), 100% (4 of 4 eyes), and 33% (1 of 3 eyes) in patients with *FZD4*, *LRP5*, and *NDP* mutations, respectively. Further, the RA rate of patients who tested negative for all mutations was 69.2% (9 of 13 eyes). The patients did not significantly differ in terms of gene mutations and RA rates ($P = 0.75$, chi-square test). Table 6 shows the genetic findings and the associations between FEVR stages and FA findings.

Discussion

The current study investigated the surgical outcomes and factors of FEVR in a relatively large cohort of patients with TRD. The main findings were as follows: a lower

FEVR stage, the FA grade, and the extent of FVP were associated with a better anatomical success rate. In patients with stage 4 FEVR, eyes with FA grade 1 (89.5%, 17 of 19) had a significantly higher RA rate than those with FA grade 2 (50%, 4 of 8; $P = 0.03$). The RA rates were 100% and 77.4% in stage 3 and 4 FEVR, respectively. Thus, the FA grade was a useful biomarker for predicting anatomical success, particularly for stage 4 FEVR. Moreover, according to the multiple logistic regression analyses, FA grade was the only parameter that could predict postoperative RA.

Kashani et al⁷ showed that fluorescein leakage without clinical exudation (i.e., angiographic leakage) is a precursor to the exudative phase of the disease in which significant serous retinal detachment develops.

In highly asymmetric FEVR cases, defining the peripheral nonperfusion and leakage in the fellow eyes by FA is useful so that a prophylactic laser can be applied to prevent them from progressing to the same status as the worse eye. Thus, the authors showed the usefulness of wide-field angiography in managing early and asymptomatic FEVR and proposed incorporating wide-field angiographic findings into the FEVR staging system. On the contrary, the current study investigated the association between FA findings and surgical outcomes according to the RA rates. Results showed that milder degrees of FA leakage from the FVP (i.e., lower disease severity) were associated with better surgical outcomes.

Table 7. Comparisons of the Previously Published Surgical Outcomes of Vitrectomy for FEVR Based on the Type of RD and Disease Stage

Year	Author	Number of Eyes Treated	Age at Surgery	Type of RD (Number)/Disease Stage	Reattachment Rate (%)
1991	Van Nouhuys et al ¹⁷	14	5–56 yrs	Unknown/unknown	50.0
1995	Glazer et al ¹⁸	6	1.5–9 yrs	TRD/stage 4	100.0
1997	Shubert et al ¹⁹	8	1 month–17 yrs	RRD (2) and TRD (4) and VH (1)/unknown	75.0
1998	Pendergast et al ⁶	32	1 month–17 yrs	Unknown/stages 2–5	87.5
1999	Ikeda et al ⁸	28	3 months–17 yrs	RRD (25) and TRD (3)/unknown	85.7
2003	Shukla et al ⁹	14	8–46 yrs	RRD (10) and TRD (3) and ERD (1)/unknown	85.7
2014	Yamane et al ¹⁰	31	1 month–18 yrs	TRD/unknown	87.1
2016	Fei et al ¹¹	12	3 months–30 yrs	TRD/stages 3–5	41.7
2018	Sen et al ¹²	44	5 months–51 yrs	RRD (35)/TRD (9)/stages 3–5	84.1
2020	El-Khoury et al ¹³	43	3 months–16 yrs	Unknown/stages 3–5	70.0
2021	Lyu et al ¹⁴	8	N/A	TRD/stages 3–5	78.5
2024	Current study	47	1 month–15 yrs	TRD/stages 3–5	70.2

ERD = exudative retinal detachment; FEVR = familial exudative vitreoretinopathy; IVR = intravitreal ranibizumab; RD = retinal detachment; RRD = rhegmatogenous retinal detachment; TRD = tractional retinal detachment; VH = vitreous hemorrhage.

Lyu et al¹⁴ reported the treatment outcomes of intravitreal ranibizumab in eyes with a highly vascular-active stage 3 to 5 FEVR.¹⁴ Their study emphasized the efficacy of primary intravitreal ranibizumab treatment in regressing advanced FEVR and resolving retinal exudates in more than half of the eyes (16 of 28 [57%]). Notably, disease progression after intravitreal ranibizumab was associated with preexisting FVP over 1 quadrant and persistent vascular activity after the initial injection ($P < 0.05$).

In relation to this issue, El-Khoury et al¹³ evaluated the outcomes and risk factors of vitreoretinal surgery in 43 eyes with FEVR.

Their study revealed that in stage 4 eyes without exudation ($n = 5$), the failure rate was 20%. Meanwhile, in the eyes with exudation ($n = 14$), it increased to 36% ($P = 0.63$). Similarly, the failure rate was 40% in stage 5 eyes without exudation ($n = 5$). Further, in stage 5 eyes with exudation ($n = 8$), the failure rate was higher at 62% ($P = 0.40$). Based on these findings, severe cases with exudation had poorer anatomical success rates after vitrectomy. Thus, it can be useful in assessing prognosis based on the degree of FA leakage because the FA grading system in our study reflects the severity of vascular activity in FEVR.

Regarding the surgical outcomes of TRD in eyes with FEVR, the final success rate in the current study was comparable with that in a previous study conducted before 2010 (70% vs. 41.7%–87.1%) (Table 7).^{6,9–14,17–19}

Based on the FEVR stage classification originally proposed by Pendergast and Trese,⁶ the RA rates in the current study were 100%, 80.7%, and 12.5% in stage 3, 4, and 5 eyes, respectively. Because the postoperative visual prognosis of stage 5 FEVR was very poor, even RA was obtained, surgical intervention should be carefully considered for those cases. Based on our 12 years of experience, severe stage 5 FEVR might be considered inoperative. The study showed that stage 4 patients with active FA leakage should also be considered high-risk patients. Although anti-VEGF drugs were not used in our case series, further studies would be needed to clarify the effect of anti-VEGF on surgical outcomes.

The pathogenic effects of the common variants of the FEVR genes on disease severity and surgical outcomes are still under debate. Our earlier study revealed that advanced disease stages (3–5) in the more severe eye were found more frequently in probands with the Norrin/ β -catenin signaling pathway variants comprising the FZD4, LRP5, TSPAN12, and NDP genes than in those without the variants (83.3% vs. 58.4%, $P < 0.0001$).¹⁵ Meanwhile, there were no significant differences between the gene mutations and RA rates in our case series, probably because of the small number of patients. However, NDP-positive patients were more likely to have a lower chance of RA at 33%. Norrie disease pseudoglioma variants may have different features from the typical Norrin/ β -catenin gene variants. These include sporadic, symmetrical, and systemic characteristics consistent with Norrie disease.¹⁵ A genotype–phenotype correlation could not be determined because of the limited number of cases. Thus, further studies with a larger cohort should be performed.

Limitations

The current study had several limitations. It was retrospective in nature. The strength of the current study was that it included a relatively large number of patients and a long follow-up period with FEVR patients.

The degree of FA leakage could not be quantitatively evaluated, which rendered the subjective manner of the method. Fluorescein angiography was mainly performed on patients with stage 3 and 4 FEVR and rarely on patients with stage 5 FEVR. This might have influenced the statistical analyses.

Vitrectomy can be effective in achieving RA and stabilizing eyes with TRD associated with FEVR, particularly at earlier stages with lower vascular activity. Further, the FA grading system proposed by the authors can be useful in predicting the surgical outcomes of FEVR with TRD.

Footnotes and Disclosures

Originally received: October 23, 2024.

Final revision: January 29, 2025.

Accepted: February 19, 2025.

Available online: ■■■■. Manuscript no.: ORET-D-24-01064R1.

¹ Department of Ophthalmology, Faculty of Medicine, Kindai University, Osaka, Japan.

² Department of Ophthalmology, University of Occupational and Environmental Health, Kitakyushu, Japan.

Disclosure(s):

All authors have completed and submitted the ICMJE disclosures form.

The authors have no proprietary or commercial interest in any materials discussed in this article.

Meeting Presentation: A portion of the study was presented in the 60th annual meeting of the Japanese Retina and Vitreous Society, December 3–5, 2021, Chiyoda, Tokyo, Japan and it received an outstanding presentation award.

Financial support: Health and Labour Sciences Research Grants of Research on intractable disease, (JPMH23FC0201 to H.K., S.K.) from the Ministry of Health, Labour and Welfare, Japan. A grant-in-aid 20K09800 from the Ministry of Education, Culture, Sport, Science and Technology, Japan (S.K.).

HUMAN SUBJECTS: Human subjects were included in this study. This retrospective case study was approved by the ethics committee of Kindai University Hospital, Osakasayama, Japan (approval number: #28-264). It was performed in accordance with the tenets of the Declaration of Helsinki. The legal guardians of all patients provided informed consent.

No animal subjects were used in this study.

Author Contributions:

Conception and design: Oga, Mano, Kuniyoshi, Iwahashi, Kondo, Kusaka

Data collection: Oga, Mano, Kuniyoshi, Iwahashi, Kondo, Kusaka

Analysis and interpretation: Oga, Mano, Kuniyoshi, Iwahashi, Kondo, Kusaka

Obtained funding: Kondo, Kusaka

Overall responsibility: Oga, Mano, Kuniyoshi, Iwahashi, Kondo, Kusaka

Abbreviations and Acronyms:

CI = confidence interval; **FA** = fluorescein angiography; **FEVR** = familial exudative vitreoretinopathy; **FVP** = fibrovascular proliferation; **IVR** = intravitreal ranibizumab; **RA** = retinal reattachment; **TRD** = tractional retinal detachment.

Keywords:

Familial exudative vitreoretinopathy, Fluorescein angiography, Pediatric retina, Pediatric vitrectomy, Tractional retinal detachment.

Correspondence:

Shunji Kusaka, MD, PhD, Department of Ophthalmology, Faculty of Medicine, Kindai University, 377-2 Ohnohigashi, Osakasayama, Osaka 589-8511, Japan. E-mail: skusaka@gmail.com.

References

1. Criswick VG, Schepens CL. Familial exudative vitreoretinopathy. *Am J Ophthalmol*. 1969;68:578–594.
2. Gilmour DF. Familial exudative vitreoretinopathy and related retinopathies. *Eye*. 2015;29:1–14.
3. Kondo H. Complex genetics of familial exudative vitreoretinopathy and related pediatric retinal detachments. *Taiwan J Ophthalmol*. 2015;5:56–62.
4. Miyakubo H, Hashimoto K, Miyakubo S. Retinal vascular pattern in familial exudative vitreoretinopathy. *Ophthalmology*. 1984;91:1524–1530.
5. Ranchod TM, Ho LY, Drenser KA, et al. Clinical presentation of familial exudative vitreoretinopathy. *Ophthalmology*. 2011;118:2070–2075.
6. Pendergast SD, Trese MT. Familial exudative vitreoretinopathy. Results of surgical management. *Ophthalmology*. 1998;105:1015–1023.
7. Kashani AH, Brown KT, Chang E, et al. Diversity of retinal vascular anomalies in patients with familial exudative vitreoretinopathy. *Ophthalmology*. 2014;121:2220–2227.
8. Ikeda T, Fujikado T, Tano Y, et al. Vitrectomy for rhegmatogenous or tractional retinal detachment with familial exudative vitreoretinopathy. *Ophthalmology*. 1999;106:1081–1085.
9. Shukla D, Singh J, Sudheer G, et al. Familial exudative vitreoretinopathy (FEVR). Clinical profile and management. *Indian J Ophthalmol*. 2003;51:323–328.
10. Yamane T, Yokoi T, Nakayama Y, et al. Surgical outcomes of progressive tractional retinal detachment associated with familial exudative vitreoretinopathy. *Am J Ophthalmol*. 2014;158:1049–1055.
11. Fei P, Yang W, Zhang Q, et al. Surgical management of advanced familial exudative vitreoretinopathy with complications. *Retina*. 2016;36:1480–1485.
12. Sen P, Singh N, Rishi E, et al. Outcomes of surgery in eyes with familial exudative vitreoretinopathy-associated retinal detachment. *Can J Ophthalmol*. 2020;55:253–262.
13. El-Khoury S, Clement A, Chehaibou I, et al. Outcome and risk factors of vitreoretinal surgery in pediatric patients with familial exudative vitreoretinopathy. *Graefes Arch Clin Exp Ophthalmol*. 2020;258:1617–1623.
14. Lyu J, Zhang Q, Xu Y, et al. Intravitreal ranibizumab treatment for advanced familial exudative vitreoretinopathy with high vascular activity. *Retina*. 2021;41:1976–1985.
15. Kondo H, Tsukahara Kawamura T, et al. Familial exudative vitreoretinopathy with and without pathogenic variants of norrin/ β -catenin signaling genes. *Ophthalmol Sci*. 2024;4:100514.
16. Kondo H, Matsushita I, Nagata T, et al. Retinal features of family members with familial exudative vitreoretinopathy caused by mutations in KIF11 gene. *Transl Vis Sci Technol*. 2021;10:18.
17. CE. Van Nouhuys. Signs, complications, and platelet aggregation in familial exudative vitreoretinopathy. *Am J Ophthalmol*. 1991;111:34–41.
18. LC. Glazer, A. Maguire, MS. Blumenkranz, et al. Improved surgical treatment of familial exudative vitreoretinopathy in children. *Am J Ophthalmol*. 1995;120:471–479.
19. Shubert A, Tasman W. Familial exudative vitreoretinopathy: surgical intervention and visual acuity outcomes. *Graefes Arch Clin Exp Ophthalmol*. 1997;235:490–493.

Angiographic Characteristics in Mild Familial Exudative Vitreoretinopathy with Genetically Confirmed Autosomal Dominant Inheritance

Misato Okamoto, MD,^{1,2} Itsuka Matsushita, MD, PhD,¹ Tatsuo Nagata, MD, PhD,¹ Yoshihisa Fujino, MD, PhD,³ Hiroyuki Kondo, MD, PhD¹

Purpose: To determine the ultra-widefield fluorescein angiographic (UWFA) characteristics of patients with mild familial exudative vitreoretinopathy (FEVR) who had been confirmed to have pathogenic variants of the autosomal dominant (AD) genes of FEVR.

Design: Single center, observational case series.

Subjects and Controls: Thirty-seven patients with mild FEVR from 27 families who had pathogenic variants of the Norrin/ β -catenin genes were studied. The controls consisted of 32 family members who had been confirmed not to carry the pathogenic variants or had heterozygous variants of the autosomal recessive inheritance gene.

Methods: Sixty-four UWFA images from the patients were compared with 60 UWFA images from the controls. The relative length of the temporal retina to the peripheral avascular retina was determined. The cut-off ratio of the relative lengths for a clinically significant avascular retina (csAR) associated with AD-FEVR was determined using the receiver operating characteristic (ROC) curves.

Main Outcome Measures: The presence or absence of 6 peripheral vascular changes (csAR, V-shaped vascular notch, brushy vascular ends, vascular stain, loop vessels or anastomosis, and capillary telangiectasia) were compared between the patients and the controls.

Results: The csAR was set at $> 12\%$ of the length from the ora serrata to the optic disc. The patients with AD-FEVR had more frequent retinal changes than the controls for the V-shaped vascular notch (69% vs. 2%; $P < 0.001$), brushy vascular ends (78% vs. 3%; $P < 0.001$), csAR (83% vs. 22%; $P < 0.001$), and vascular stain (70% vs. 35%, $P < 0.001$). Loop vessels and/or anastomosis of peripheral vessels were found significantly less frequently in the patients than in the controls (39% vs. 73%; $P < 0.001$). No significant difference was found for capillary telangiectasia between the 2 groups. The combination of the V-shaped vascular notches, brushy vascular ends, and csAR had a sensitivity of 82.8% and specificity of 98.3%, with the highest ROC curve of 0.9.

Conclusions: The combination of V-shaped vascular notch, brushy vascular ends, and csAR can be used as a biomarker for patients with AD-FEVR who have pathogenic variants of the Norrin/ β -catenin genes. These findings will allow more accurate segregation analysis in FEVR families and allow better genetic counseling.

Financial Disclosure(s): Proprietary or commercial disclosure may be found in the Footnotes and Disclosures at the end of this article. *Ophthalmology Retina* 2025;9:187-193 © 2024 by the American Academy of Ophthalmology



Supplemental material available at www.opthalmologyretina.org.

Familial exudative vitreoretinopathy (FEVR) is an inherited retinal disorder that is associated with retinal detachments that are due to the abnormal development of the retinal vasculature.¹ The majority of the FEVR families have an autosomal dominant (AD) inheritance, whereas others have autosomal recessive (AR) and X-linked inheritance.² The expression of FEVR is highly variable, and there are some asymptomatic patients whose vascular abnormalities are mild and confined to the peripheral retina. The large variations in the clinical severity, which most likely lead to a large number of undiagnosed mild FEVR individuals are

probably due to the variable expressivity of the causative genetic abnormalities in the genes causing AD-FEVR.

The genes causing FEVR are diverse. The most common genes are the genes of the Norrin/ β -catenin signaling pathway, viz., *FZD4*, *LRP5*, *TSPAN12*, and *NDP*.² Their proteins interact with each other to form a complex on the surface of the retinal vascular endothelial cells resulting in retinal angiogenesis.³ Mutations of these genes account for 30% to 50% of all patients with FEVR.⁴ There are other genes reported to be associated with FEVR; however, their exact associations have not been definitively

determined, and their unique systemic features are distinct from the common nonsyndromic FEVR.⁴

The signs of mild FEVR tend to be undetected by ophthalmoscopic examinations, but fluorescein angiography is an effective method of detecting the mild retinal changes in patients with mild FEVR.⁵ However, because of the highly variable expression of the peripheral vascular abnormalities, it is difficult to distinguish the retinal vascular changes of mild FEVR from the normal vasculature. This then results in compromising the genetic counseling, although genetic counseling is not usually performed for patients with asymptomatic mild FEVR. Nevertheless, establishing the pathogenetic features associated with genetic anomalies will help perform more accurate genetic counseling in families with mild FEVR.

To the best of our knowledge, there has not been a study that determined the retinal signs that differentiated patients with mild FEVR from that of normal individuals based on the presence or absence of the pathogenic variants. Thus, the purpose of this study was to determine whether the ultra-widefield fluorescein angiographic (UWFA) images have characteristics that can differentiate the eyes of patients with mild AD-FEVR who had been confirmed to have pathogenic variants of the *FZD4*, *LRP5*, and *TSPAN12* genes from eyes of patients not having the pathogenic variants.

Methods

This was a retrospective observational study conducted in accordance with the tenets of the Declaration of Helsinki. The procedures were approved by the Ethics Committee of the University of Occupational and Environmental Health, Japan. A signed informed consent was obtained from all participants to perform the examinations.

Familial exudative vitreoretinopathy patients and their family members who had undergone genetic testing for pathogenic variants in the *FZD4*, *LRP5*, and *TSPAN12* genes from 2015 to 2023 at the University of Occupational and Environmental Health Hospital were studied. The details of the genetic examinations are described in detail elsewhere.⁴

The patients with mild AD-FEVR were selected (i.e., those who had at least 1 eye with stage 1 or 2 FEVR (no retinal detachment) according to the classification by Pendergast and Trese).⁶ Only eyes without a retinal detachment were analyzed. Eyes with a history of reattachment of a rhegmatogenous retinal detachments that were initially diagnosed with stage 1 or 2 FEVR were excluded.

All patients had been confirmed to carry a heterozygous variant of 1 of the Norrin/ β -catenin AD genes, (i.e., the *FZD4*, *LRP5*, or *TSPAN12* genes). The control individuals were selected from unaffected family members. Because the angiographic abnormalities of unaffected heterozygous carriers of AR-FEVR have not been evident by imaging based on our search of PubMed (<http://ncbi.nlm.nih.gov/pubmed>, terms as [autosomal recessive] AND [familial exudative vitreoretinopathy], accessed on July 31, 2024), these carriers were included in the control group. On the other hand, women who carried heterozygous *NDP* variants were excluded because affected women have been reported.⁴

The medical charts of the patients were reviewed, and the ages, refractive errors (spherical equivalent), and UWFA images were collected. The UWFA images were recorded by the Optos 200Tx imaging device (Optos PLC) with a viewer program of the V²

Vantage Pro 2.8.0.4. An image showing both the optic disc and the temporal ora serrata was used for each eye.

The UWFA images were converted to a joint photographic expert group format. The intensity of the image was increased by 1.5 \times using the Photoshop software (Adobe Inc) to make the capillary telangiectasia and vessels more visible. The images were exported to the Microsoft PowerPoint software (Microsoft Corporation).

Based on the results of our earlier study and that in the literature, the presence or absence of the 6 types of FEVR-associated peripheral vascular changes was determined.^{7–10} The 6 types were avascular retina, V-shaped vascular notch, vascular brushy end, vascular stain, loop vessels and/or anastomosis of peripheral vessels, and capillary telangiectasia (Fig. 1).

The peripheral vascular changes were considered to be present when the minimum signs of the peripheral vascular changes except for the avascular retina were present. To evaluate the extent of the avascular retina, the length of the temporal retina from the ora serrata to the center of the optic disc (a in Fig. 2), and the longest (b) and shortest (c) vascular lengths were measured using the caliper function of the Microsoft PowerPoint software (Fig. 2). A representative length of the avascular retina (d in Fig. 2) was determined to extend from the ora serrata to the middle of the longest and shortest vascular area.

$$d = a - (b + c) / 2$$

The ratio of the length of the avascular to that of the extent of the temporal retina (A) was determined as:

$$A (\%) = (d / a) \times 100$$

To determine the ratio of the length of the avascular to that of the length of the temporal retina, the receiver operating characteristic (ROC) curve was used, and a cut-off point was set as the highest correctly classified rate. An avascular retina greater than the point was set as a clinically significant avascular retina (csAR).

Statistical Analyses

Student *t* tests, Mann–Whitney *U* tests, chi-square tests, or Fisher exact tests were used for the univariate analyses. The ability of the combination of the FEVR-associated vascular changes to differentiate patients with AD-FEVR from the controls was determined by logistic regression. The statistical significance was set at *P* < 0.05. All analyses were conducted using Stata version 18 (StataCorp).

Results

Thirty-seven patients with AD-FEVR of 27 families were studied (Table 1, Fig. 3). Twenty-two of them had heterozygous pathogenic variants: 10 *FZD4*, 7 *LRP5*, and 5 *TSPAN12*. The family IDs are the same as used in our earlier report⁴: families 3, 4, 7, 13, 16, 18 to 20, 22, 30, 31, and 37 to 39 for *FZD4*; 41, 44 to 46, 48, 49 and 59 for *LRP5*; and 78, 81, 85, 86, 89 and 90 for *TSPAN12*. The control individuals were 25 family members not having the pathogenic variants, and 7 heterozygous carriers of 4 AR-FEVR families. The AR-FEVR family members had 5 heterozygous variants in the *LRP5* gene and were referred to as families 65, 67, and 75 to 77 in our earlier publication.⁴

The mean age of the patients was 27.1 \pm 12.9 years and that of the controls was 34.2 \pm 13.4 years. The mean age of the patients was significantly lower than that of the controls (*P* = 0.030, Student *t* test). The ratio of male patients was 53% in the mild FEVR group and 47% in the control group (*P* = 0.830, chi-square test). The median refractive error (spherical equivalent) of the patients was -4.2 (interquartile range [IQR], -7.5 to -1.5) diopters (D) and that of the controls was -0.8 (IQR, -3.0 to 0) D. The patients

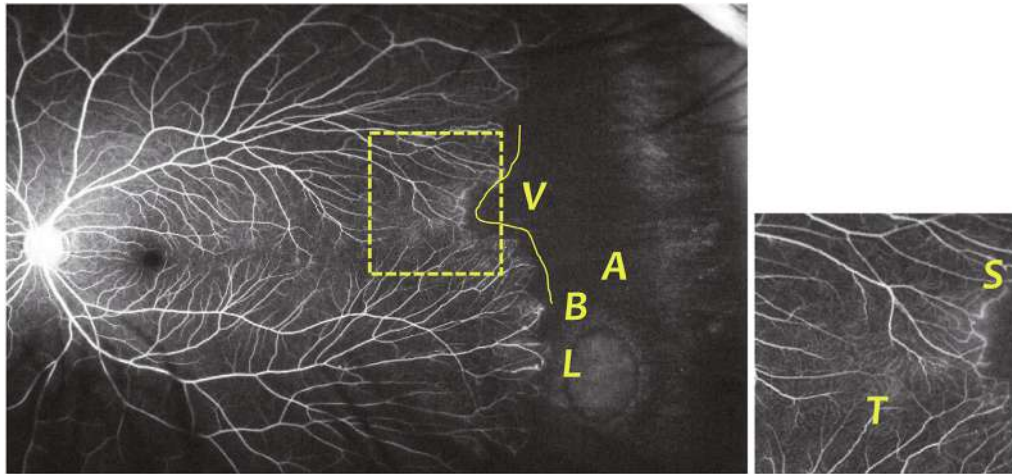


Figure 1. Six types of FEVR-associated peripheral vascular changes detected in ultra-widefield fluorescein angiographic images. **A**, avascular retina. **V**, V-shaped vascular notch. **B**, vascular brushy end. **S**, vascular stain. **L**, loop vessels or anastomosis of peripheral vessels. **T**, capillary telangiectasia. Yellow dashed boxes indicate the region shown in higher magnification in the insets with enhanced contrast.

were significantly more myopic than the controls ($P < 0.001$, Mann–Whitney U test).

A total of 124 UWFA images from 64 patients and 60 controls were studied. Ten images from 10 eyes were not used because the eyes had retinal detachments or the UWFA images of the temporal periphery were unavailable.

The cut-off ratio for the length of the avascular retina to the temporal retina (**A**) was set at 12% with the maximum correctly classified rate (85%) by the ROC curve. The sensitivity and specificity were 83% and 88% for this cut-off ratio for the length, respectively. The csAR was found significantly more frequently in the eyes of the patients (83%) than in the controls (22%; $P < 0.001$, chi-square test).

The V-shaped vascular notch was found significantly more frequently in the patients (69%) than controls (2%, $P < 0.001$,

Fisher exact test). Brushy vascular ends were also found significantly more frequently in the patients (78%) than in the controls (3%, $P < 0.001$, Fisher exact test). Vascular staining was found significantly more frequently in the patients (70%) than in the controls (35%, $P < 0.001$, chi-square test). The loop vessels and/or anastomosis were found significantly less frequently in the patients (39%) than controls (73%, $P < 0.001$, chi-square test). Capillary telangiectasias were found in 61% of the patients and 63% in the controls ($P = 0.78$, chi-square test).

A combination of the csAR, V-shaped vascular notches, and brushy vascular ends had greater sensitivity and specificity than the other combinations (Table 2). The highest ROC of 0.908 was found with the combination of these 3 anomalies with a sensitivity and specificity of 82.8% and 98.3%, respectively.

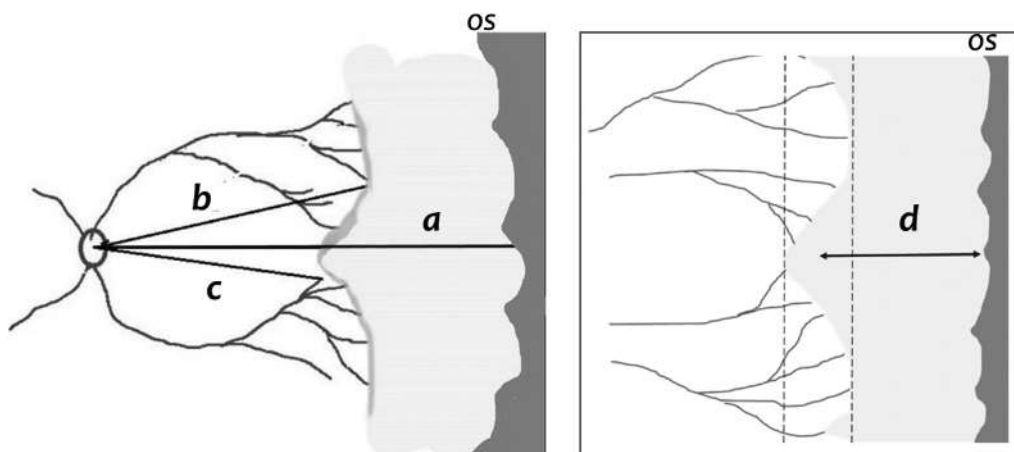


Figure 2. Determining the length of the avascular retina. The length of the temporal retina from the center of the optic disc to the ora serrata is shown as “a,” the longest (“b”) and shortest vascular length (“c”), were measured. The length of the avascular retina, “d” was determined as the middle length of b and c: $d = a - (b + c) / 2$. os = ora serrata.

Table 1. Clinical Characteristics and Ultra-widefield Angiographic Features of Patients with Autosomal Dominant Familial Exudative Vitreoretinopathy

Group	AD-FEVR	Control	P
Number of individuals (eyes)	37 (64)	32 (60)	
Age (yrs), mean (SD)	27.1 (12.9)	34.2 (13.4)	0.030
Sex (male), n (%)	19 (53%)	17 (47%)	0.830
Refractive error* (diopters), median (interquartile range)	-4.2 (-7.5 to -1.5)	-0.8 (-3.0 to 0)	< 0.001
Clinically significant avascular retina	53 (83%)	13 (22%)	< 0.001
V-shaped vascular notch	44 (69%)	1 (2%)	< 0.001
Vascular brushy end	50 (78%)	2 (3%)	< 0.001
Vascular stain	45 (70%)	21 (35%)	< 0.001
Loop vessels or anastomosis	25 (39%)	44 (73%)	< 0.001
Capillary telangiectasia	39 (61%)	38 (63%)	0.780

AD-FEVR = autosomal dominant familial exudative vitreoretinopathy; SD = standard deviation.

*Spherical equivalent.

Twenty-seven patients with AD-FEVR and 28 controls in whom both eyes were available were examined to determine whether the angiographic features were discordant between the 2

eyes. In the patients with AD-FEVR, the discordant rate of the csAR, V-shaped vascular notch, brushy vascular end, loop vessels and/or anastomosis, and capillary telangiectasia was 11%, 15%,

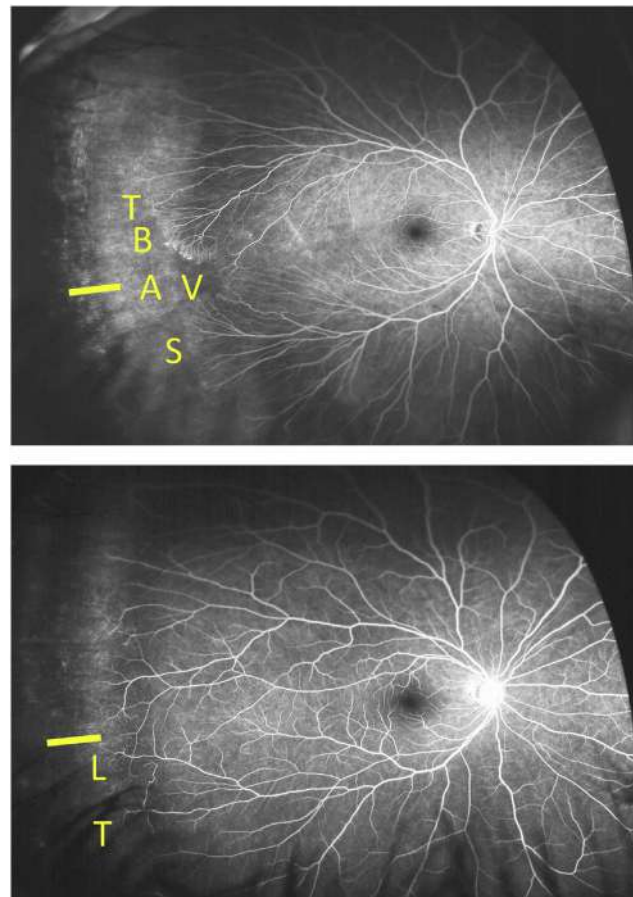


Figure 3. Representative ultra-widefield fluorescein angiographic images from a patient with autosomal dominant (AD) familial exudative vitreoretinopathy (FEVR) and a heterozygous carrier of autosomal recessive (AR) FEVR. Upper: right eye of an AD-FEVR patient carrying a heterozygous pathogenic variant in the *FZD4* gene (father of family #4 in reference 4). Lower: right eye of an AR-FEVR carrier (control) carrying a heterozygous pathogenic variant in the *LRP5* gene (father of family 76 in reference 4). Positive angiographic changes of the FEVR-associated peripheral vascular changes are shown by (A), avascular retina; (V), V-shaped vascular notch; (B), vascular brushy end; (S), vascular stain; (L), loop vessels or anastomosis of peripheral vessels; and (T), capillary telangiectasia. Yellow bars indicate the cut-off lengths of the clinically significant avascular retina (12% of the length from the ora serrata to the optic disc).

Table 2. Values of Sensitivity and Specificity for Combined Categories of Angiographic Features

Category	Sensitivity	Specificity	Correctly Classified	AUC
A + V + B	82.8%	98.3%	90.3%	0.908
A + V	87.5%	78.3%	83.1%	0.891
A + B	73.4%	98.3%	85.5%	0.899
V + B	82.8%	96.7%	89.5%	0.901

A = clinically significant avascular retina; AUC = area under the curve; B = vascular brushy end; V = V-shaped vascular notch.

11%, 26%, 33%, and 19%, respectively (Table 3). The rate of the patients presenting with angiographic features in both eyes versus in 1 eye was higher for the csAR, V-shaped vascular notch, and brushy vascular end, with values of 6.7 (20/3), 4.0 (16/4), and 6.3 (19/3), respectively. On the other hand, the rate for vascular stain, loop vessels or anastomosis and capillary telangiectasia was lower at 2.1 (15/7), 0.7 (6/9), and 2.6 (13/5), respectively.

Discussion

The results indicated that the incidence of retinal angiographic anomalies in eyes with genetically confirmed mild AD-FEVR was significantly higher than that in the control eyes. Because the retinal characteristics of mild FEVR are difficult to detect and can be confused with those present in unaffected individuals, we studied only genetically confirmed unaffected family members as controls.

We found that the V-shaped vascular notches and brushy vascular ends were highly specific features of AD-FEVR eyes. The csARs were also a significant characteristic with a threshold at 12% of the distance from the ora serrata to the optic disc. Thus, the combination of V-shaped vascular notches, brushy vascular ends, and csAR can be a biomarker for patients with AD-FEVR who had pathogenic variants of the *Norrin*/ β -catenin genes.

The V-shaped vascular notch has been characteristic for mild FEVR since first noted in 1982.^{6,9,11} A recent study of ultra-widefield scanning laser ophthalmoscopic images detected V-shaped notches in 93% of eyes of patients with mild FEVR.¹² Miyakubo et al⁹ reported that the V-shaped

notches were found in 81% of the eyes with mild FEVR. This high incidence was confirmed in our cohort at 70%, and the slightly lower incidence in our findings suggested that there may be more undiagnosed patients in the AD-FEVR families.

Pendergast and Trese⁶ diagnosed the mildest stage 1 AD-FEVR by the presence of an avascular zone. However, a peripheral avascular zone is also found in normal eyes, especially in myopic eyes,¹³ and it has been questioned whether the extent of the avascular retina can be used for the diagnosis of AD-FEVR.¹⁴ An avascular retina that extends 1.5 to 2 disc diameters from the ora serrata has been suggested to be pathological.^{9,15–17} We determined that csAR at >12% of the length from the ora serrata to the optic disc can also be used to differentiate eyes with FEVR from the control eyes. The most peripheral retina is substantially enlarged in the exported images.¹⁸ Therefore, transforming plain images into stereographic projection images was useful in allowing anatomically correct measurements and more versatile csAR definition.¹⁹ A newer version of the viewing software (the V² Vantage Pro version 2.9.2 or later) in the Optos device can produce the stereographic projected images; however, these types of images were unavailable in this study.

It remains undetermined whether heterozygous carriers of AR-FEVR have more normal retinal appearances than patients with AD-FEVR. Thus, a diagnosis of AR-FEVR is rarely made until genetic tests are performed.²⁰ Our PubMed search indicated that the retinal features of heterozygous family members with AR-FEVR were not significantly different from those of normal individuals. However, Chen et al²¹ reported that the inheritance patterns of some FEVR families were indeed indistinguishable based on the genotype and the retinal changes. Further studies are needed for determining the genotype–phenotype relationship of patients with FEVR, including peripheral retinal alterations in eyes with AR-FEVR.

We found that the sign of the loops or anastomosis was also observed in the control eyes. This sign is often referred to as right angle vessels or peripheral vascular anastomosis, and it was found in 33% to 70% of normal or non-FEVR-associated eyes.^{15,22,23} This suggests that this sign alone is

Table 3. Presence or Absence of Ultra-widefield Angiographic Features between the 2 eyes of Patients with Autosomal Dominant Familial Exudative Vitreoretinopathy

	AD-FEVR (n = 27)			Control (n = 28)		
	Present in Both Eyes	Present in 1 Eye	Absent in Both Eyes	Present in Both Eyes	Present in 1 Eye	Absent in Both eyes
Clinically significant avascular retina	20 (74%)	3 (11%)	4 (11%)	1 (4%)	8 (29%)	19 (68%)
V-shaped vascular notch	16 (59%)	4 (15%)	7 (26%)	0 (0%)	1 (4%)	27 (96%)
Vascular brushy end	19 (70%)	3 (11%)	5 (19%)	0 (0%)	2 (7%)	26 (93%)
Vascular stain	15 (56%)	7 (26%)	5 (19%)	7 (25%)	6 (21%)	15 (54%)
Loop vessels or anastomosis	6 (22%)	9 (33%)	12 (44%)	18 (64%)	3 (11%)	5 (29%)
Capillary telangiectasia	13 (48%)	5 (19%)	9 (33%)	16 (57%)	4 (14%)	8 (29%)

AD-FEVR = autosomal dominant familial exudative vitreoretinopathy.

not specific to FEVR, although Miyakubo et al⁹ reported that the retinal avascular and anastomoses were weak signs of FEVR.

Zhang et al¹⁴ reported that vascular leakages were found in 40% of the patients with AD-FEVR. The vascular stain in AD-FEVR eyes was found in the area of the brush-shaped or non-brush-shaped vascular ends, in the middle of the main retinal vessels, and in nonspecific retinal tissues (Fig. S4, available at www.ophtalmologyretina.org). Among the areas, the area of the brush border was highly associated with vascular staining. In the patients with AD-FEVR, the vascular staining was found in the area of the brush-shaped vascular ends in all but 1 eye (98%) and also found elsewhere in 20 eyes (44%). The identification may be influenced by the time the photographs were taken. The areas of the vascular staining were mainly found at the main retinal vessels and non-brush-shaped vascular ends in the control eyes. We found that when the intensity of the Optos UWFA images was increased, the vascular leakages and capillary telangiectasia were also detected in unaffected individuals. This indicated that caution is needed when a segregation analysis is based on the angiographic signs in eyes with FEVR.

Although FEVR is known to have highly discordant severities between the 2 eyes, our study showed that the key angiographic features (i.e., the csAR, V-shaped vascular notch, and brushy vascular end, were highly concordant between the 2 eyes). These signs were consistent features for the patients with AD-FEVR with pathogenic variants in the genes of the Norrin/ β -catenin signaling. The other signs were more variable between the 2 eyes.

The patients with AD-FEVR were more myopia than the controls. Since the first report of FEVR, the majority of the patients with FEVR were reported to have moderate myopic changes.¹ However, to our knowledge, there is no study that focused on how severe the myopia was in the patients. Based on our data, the cut-off ratio for the degree of myopia can be set at less than -3.0 D with the maximum correctly classified rate (70%) by the ROC curve (the sensitivity and specificity were 72% and 63%, respectively).

However, adding the myopic threshold to the combination of the csAR, V-shaped vascular notches, and brushy vascular ends did not result in greater statistical sensitivity and specificity than the combinations of the 3 (0.925 vs. 0.908; $P = 0.212$; chi-square test). Therefore, the diagnostic usefulness of myopia is limited.

Limitations

There are several limitations in this study. First, this was a retrospective study on a relatively small number of patients. Second, we analyzed the data in a binary manner (i.e., the presence or absence of the retinal anomalies). Third, not all angiographic findings were evaluated. A straightening and branching of the retinal vessels are characteristic signs of FEVR.^{7–9} However, determining the features in a binomial manner is subjective, and the analysis was not performed. Fourth, because the genetics of FEVR is complicated, only patients with the genes of the Norrin/ β -catenin signaling were evaluated. Our earlier study showed that patients with mutations in the *KIF11* gene are also FEVR causing with distinct signs. However, the gene had low penetrance,¹⁰ and the angiographic appearance tended to be inconclusive.¹⁰ Our results cannot be applied for such genes, but it would be helpful to classify FEVR genes based on the underlying mechanisms and phenotypic properties.

In conclusion, V-shaped vascular notches, brushy vascular ends, and relative long csAR were specific features in mild AD-FEVR associated with variants in the Norrin/ β -catenin signaling gene. The combination of these features can be a biomarker for individuals with mild FEVR. The findings of this study should provide information of the clinical features of FEVR, which should make genetic counseling more accurate.

Acknowledgments

The authors thank Duco Hamasaki, Professor Emeritus, Bascom Palmer Eye Institute, University of Miami, Miami, Florida, for his critical comments and valuable assistance.

Footnotes and Disclosures

Originally received: June 14, 2024.

Final revision: August 7, 2024.

Accepted: August 20, 2024.

Available online: August 27, 2024. Manuscript no. ORET-D-24-00557R1.

¹ Department of Ophthalmology, University of Occupational and Environmental Health, Kitakyushu, Japan.

² Department of Ophthalmology, Kyushu University Hospital, Fukuoka, Japan.

³ Department of Environmental Epidemiology, University of Occupational and Environmental Health, Kitakyushu, Japan.

The authors did not use any AI and AI-assisted technologies in the writing process.

Disclosures:

All authors have completed and submitted the ICMJE disclosures form.

The author(s) have made the following disclosure(s):

H.K.: Grants — Alcon Japan, Kowa, HOYA, Santen Inc; Payment or honoraria — RE Medical, Otsuka Pharmaceutical, Kowa, Santen Pharmaceutical, Sandoz, Senju Pharmaceutical, Chugai Pharmaceutical, Alcon Japan, Novartis, Bayer Yakuhin

The other authors have no proprietary or commercial interest in any materials discussed in this article.

Supported by the Japan Society for the Promotion of Science Grant-in-Aid for Scientific Research (grant no. 23K09053 [H.K.]), Tokyo, Japan; Health and Labour Sciences Research Grants of Research on intractable disease (grant no. JPMH23FC0201 [H.K.]) from the Ministry of Health, Labour and Welfare, Tokyo, Japan.

HUMAN SUBJECTS: Human subjects were included in this study. This was a retrospective observational study conducted in accordance with the tenets of the Declaration of Helsinki. The procedures were approved by the Ethics Committee of the University of Occupational and Environmental Health, Japan. A signed informed consent was obtained from all participants to perform the examinations.

No animal subjects were included in this study.

Author Contributions:

Conception and design: Fujino, Kondo

Data collection: Okamoto, Matsushita, Nagata

Analysis and interpretation: Fujino, Kondo

Obtained funding: Kondo

Overall responsibility: Kondo

Abbreviations and Acronyms:

AD = autosomal dominant; **AR** = autosomal recessive; **csAR** = clinically significant avascular retina; **D** = diopters; **FEVR** = familial exudative

vitreoretinopathy; **IQR** = interquartile range; **ROC** = receiver operating characteristic; **UWFA** = ultra-widefield fluorescein angiography.

Keywords:

Familial exudative vitreoretinopathy, FEVR, Norrin/ β -catenin genes, Ultra-widefield fluorescein angiography.

Correspondence:

Hiroyuki Kondo, 1-1, Iseigaoka, Yahatanishiku, Kitakyushu 807-8555, Japan. E-mail: kondohi@med.uoeh-u.ac.jp.

References

1. Criswick VG, Schepens CL. Familial exudative vitreoretinopathy. *Am J Ophthalmol*. 1969;68:578–594.
2. Gilmour DF. Familial exudative vitreoretinopathy and related retinopathies. *Eye (Lond)*. 2015;29:1–14.
3. Wang Y, Rattner A, Zhou Y, et al. Norrin/Frizzled4 signaling in retinal vascular development and blood brain barrier plasticity. *Cell*. 2012;151:1332–1344.
4. Kondo H, Tsukahara-Kawamura T, Matsushita I, et al. Familial exudative vitreoretinopathy with and without pathogenic variants of Norrin/ β -catenin signaling genes. *Ophthalmol Sci*. 2024;4:100514.
5. Ober RR, Bird AC, Hamilton AM, Sehmi K. Autosomal dominant exudative vitreoretinopathy. *Br J Ophthalmol*. 1980;64:112–120.
6. Pendergast SD, Trese MT. Familial exudative vitreoretinopathy. Results of surgical management. *Ophthalmology*. 1998;105:1015–1023.
7. Kashani AH, Learned D, Nudleman E, et al. High prevalence of peripheral retinal vascular anomalies in family members of patients with familial exudative vitreoretinopathy. *Ophthalmology*. 2014;121:262–268.
8. Ranchod TM, Ho LY, Drenser KA, et al. Clinical presentation of familial exudative vitreoretinopathy. *Ophthalmology*. 2011;118:2070–2075.
9. Miyakubo H, Hashimoto K, Miyakubo S. Retinal vascular pattern in familial exudative vitreoretinopathy. *Ophthalmology*. 1984;91:1524–1530.
10. Kondo H, Matsushita I, Nagata T, et al. Retinal features of family members with familial exudative vitreoretinopathy caused by mutations in KIF11 gene. *Transl Vis Sci Technol*. 2021;10:18. <https://doi.org/10.1167/tvst.10.7.18>.
11. van Nouhuys CE. Signs, complications, and platelet aggregation in familial exudative vitreoretinopathy. *Am J Ophthalmol*. 1991;111:34–41.
12. Lyu J, Zhang Q, Wang SY, et al. Ultra-wide-field scanning laser ophthalmoscopy assists in the clinical detection and evaluation of asymptomatic early-stage familial exudative vitreoretinopathy. *Graefes Arch Clin Exp Ophthalmol*. 2017;255:39–47.
13. Kaneko Y, Moriyama M, Hirahara S, et al. Areas of non-perfusion in peripheral retina of eyes with pathologic myopia detected by ultra-widefield fluorescein angiography. *Invest Ophthalmol Vis Sci*. 2014;55:1432–1439.
14. Zhang T, Wang Z, Sun L, et al. Ultra-wide-field scanning laser ophthalmoscopy and optical coherence tomography in FEVR: findings and its diagnostic ability. *Br J Ophthalmol*. 2021;105:995–1001.
15. Shah AR, Abbey AM, Yonekawa Y, et al. Widefield fluorescein angiography in patients without peripheral disease: a study of normal peripheral findings. *Retina*. 2016;36:1087–1092.
16. Blair MP, Shapiro MJ, Hartnett ME. Fluorescein angiography to estimate normal peripheral retinal nonperfusion in children. *J AAPOS*. 2012;16:234–237.
17. Hayashi W, Shimada N, Hayashi K, et al. Retinal vessels and high myopia. *Ophthalmology*. 2011;118:791–791.e2.
18. Oishi A, Hidaka J, Yoshimura N. Quantification of the image obtained with a wide-field scanning ophthalmoscope. *Invest Ophthalmol Vis Sci*. 2014;55:2424–2431.
19. Singer M, Sagong M, van Hemert J, et al. Ultra-widefield imaging of the peripheral retinal vasculature in normal subjects. *Ophthalmology*. 2016;123:1053–1059.
20. Jiao X, Ventruto V, Trese MT, et al. Autosomal recessive familial exudative vitreoretinopathy is associated with mutations in LRP5. *Am J Hum Genet*. 2004;75:878–884.
21. Chen C, Zhang X, Peng X, et al. Lrp5 biallelic mutations cause a higher incidence of severe phenotype compared with Lrp5 monoallelic mutation. *Retina*. 2022;42:1958–1964.
22. Wang X, Xu A, Yi Z, et al. Observation of the far peripheral retina of normal eyes by ultra-wide field fluorescein angiography. *Eur J Ophthalmol*. 2021;31:1177–1184.
23. Seo EJ, Kim JG. Analysis of the normal peripheral retinal vascular pattern and its correlation with microvascular abnormalities using ultra-widefield fluorescein angiography. *Retina*. 2019;39:530–536.

厚生労働科学研究費補助金（難治性疾患政策研究事業）
分担研究報告書

特発性傍中心窩毛細血管拡張症に関する研究

研究分担者	東京女子医科大学・医学部・教授 飯田 知弘 琉球大学・医学研究科・教授 古泉 英貴 京都大学・医学研究科・教授 辻川 明孝
研究協力者	千葉大学・医学研究院・教授 馬場 隆之 横浜市立大学・医学部・客員教授 柳 靖雄

特発性傍中心窩毛細血管拡張症（MacTel）は比較的稀な網膜の血管異常であり、黄斑部網膜の毛細血管が拡張する疾患の総称である。MacTel は臨床所見により 3 つのタイプに分類されるが、このうち 2 型を研究対象とする。今回我々は、眼科医にとって診断が難しい MacTel 2 型と鑑別を有する疾患について専門家で話し合いを行なった。その結果、特に陳旧性網膜静脈分枝閉塞症、放射線網膜症、滲出型加齢黄斑変性（特に RAP）、タモキシフェン網膜症などとの鑑別が重要であると考えられた。鑑別の際の注意点も話し合われた。

A. 研究目的

黄斑部毛細血管拡張症（macular telangi-ectasia: MacTel）は、特発性に黄斑部網膜の毛細血管拡張を呈する疾患群の総称である。MacTel はその臨床所見により 3 つのタイプに分類されるが、このうち 2 型を今回の研究対象とする。

MacTel 2 型の病態は不明であるが、Müller 細胞および中心窩周辺の神経の変性が原因で発症すると考えられている。患者は歪視や中心暗点などを訴え、進行すると黄斑円孔や黄斑部新生血管などを伴うこともある。

本研究班は、2022 年に本症の診療ガイドラインを日本眼科学会雑誌に発表した。今年度の目的は、眼科医にとって診断が難しい MacTel 2 型と鑑別を有する疾患と鑑別の

ポイントについて専門家で協議することである。

B. 研究方法

2022 年に発表した診療ガイドラインに基づいて MacTel 2 型を診断する上で、鑑別を有する疾患に関して MacTel 2 型の専門家で協議した。令和 6 年 7 月 15 日と 12 月 25 日の 2 日で、MacTel 研究班の 5 名により MacTel 2 型と鑑別を有する疾患群を列挙し、鑑別診断のポイントについて話し合った。

（倫理面への配慮）

今回の研究に関しては患者の個人情報はいずれも匿名化し、倫理面に十分配慮して行った。

C. 研究結果

話し合いの結果、以下の 4 疾患が特に MacTel 2 型と鑑別診断に注意を要すると考えられた。

1) 陳旧性網膜静脈分枝閉塞症

病変領域が網膜動静脈交叉部を頂点とした扇状であるので、

病変が耳側縫線を越えないという特徴を理解していれば鑑別は容易である。

2) 放射線網膜症

軟性白斑や網膜新生血管を伴い、病変が広範に及ぶことで鑑別できる。過去の放射線照射歴の聴取が最も重要である。

3) 新生血管型（滲出型）加齢黄斑変性

特に網膜血管腫状増殖 (RAP) との鑑別が重要である。MacTel 2 型は RAP に比べて発症年齢が若いこと、軟性ドルーゼン、reticular pseudodrusen や漿液性網膜色素上皮剥離がみられない点が重要であると考えられた。

4) タモキシフェン網膜症

乳癌の治療・再発予防に用いられるタモキシフェンクエン酸塩の内服歴の聴取をすることで鑑別は可能である。

D. 考察

MacTel 2 型は一般の眼科医にとっては比較的珍しい疾患であり、特徴的な所見に気づかない限り診断が難しい。そこで、今回列挙した 4 疾患との鑑別は特に重要であり、今後も眼科医への啓発が重要であると考えられた。

また MacTel 2 型の難病申請に関しては、片眼性が多く、また視力低下の程度も軽いために難病には適さないことも明らかとなってきた。そのため、本研究班の MacTel 2 型グループは来年度までで一旦終了とし、残った研究結果の解析と論文投稿を行うことが話し合われた。

E. 結論

MacTel 2 型の診断は難しく、正確な診断のためには、陳旧性網膜静脈分枝閉塞症、放射線網膜症、新生血管型（滲出型）加齢黄斑変性（特に RAP）、タモキシフェン網膜症などの鑑別が重要であると考えられた。

F. 健康危険情報：なし

G. 研究発表

1. 論文発表（令和 6 年度以前のものも含む）

- 1) 飯田知弘、辻川明孝、柳靖雄、古泉英貴、丸子一朗、大音壮太郎、坂本泰二：厚生労働科学研究費補助金難治性疾患政策研究事業網膜脈絡膜・視神経萎縮症に関する調査研究班。黄斑部毛細血管拡張症 2 型診療ガイドライン（第 1 版）。日眼会誌 126：463-471, 2022
- 2) Staurenghi G, Souied EH, Iida T, Chow DR, Wolf A, Gallego-Pinazo R, Viola F, Kaiser PK. Imaging-Guided Classification of Neovascularization in Neovascular Age-Related Macular Degeneration: Progress to Date. J Vitreoretin Dis. 2024 Oct 5:24741264241276929.

- 3) Cheung CMG, Dansingani KK, Koizumi H, Lai TYY, Sivaprasad S, Boon CJF, Van Dijk EHC, Chhablani J, Lee WK, Freund KB. Pachychoroid disease: review and update. Eye (Lond). 2025 Apr;39(5):819–834.
- 4) Cheung CMG, Chen Y, Holz F, Tsujikawa A, Sadda S. Geographic atrophy in Asia. Graefes Arch Clin Exp Ophthalmol. 2025 Online ahead of print.
- 5) Akiba R, Tu HY, Hashiguchi T, Takahashi Y, Toyooka K, Tsukamoto Y, Baba T, Takahashi M, Mandai M. Host-Graft Synapses Form Functional Microstructures and Shape the Host Light Responses After Stem Cell-Derived Retinal Sheet Transplantation. Invest Ophthalmol Vis Sci. 2024 Oct 1;65(12):8.
- 6) Yanagi Y, Takahashi K, Iida T, Gomi F, Onishi H, Morii J, Sakamoto T. Cost-effectiveness Analysis of Ranibizumab Biosimilar for Neovascular Age-Related Macular Degeneration and its Subtypes from the Societal and Patient Perspectives in Japan. Ophthalmol Ther. 2024 Oct;13(10):2629–2644.

2. 学会発表 なし

H. 知的財産権の出願・登録状況

1. 特許取得 なし
2. 実用新案登録 なし
3. その他 なし

厚生労働科学研究費補助金（難治性疾患政策研究事業）
分担研究報告書

杆体一色覚に関する研究

研究分担者 弘前大学・医学研究科・教授 上野 真治
国立病院機構東京医療センター・視覚研究部・部長 角田 和繁
研究協力者 国立成育医療センター・診療部長 仁科 幸子
慈恵医科大学・葛飾医療センター・教授 林 孝彰

研究要旨

杆体一色覚（Achromatopsia: ACHM）は、常染色体潜性遺伝を示す稀な先天性疾患であり、杆体機能はほぼ正常であるが錐体視機能が重度に障害される。ACHM は小児期より重度の視機能障害を伴うことが多く、治療がない希少疾患であるため指定難病の候補と考えられる。今回我々は指定難病に申請するために診断基準を作成し、また患者数を調査するために全国の 156 施設にアンケート形式で調査票を送付した。診断基準としては、以下の 4 つを満たすものを ACHM とした。①眼底所見は正常か、もしくは黄斑変性がみられる。黄斑の変性は進行することもある。②両眼性に低視力、羞明、重度の色覚異常きたし、その症状は生来ほとんど変化がない。特に幼少期から低視力で視力の悪化がないことが、錐体ジストロフィとの鑑別に重要である。③全視野 ERG で杆体系の応答がほぼ正常で、錐体系の応答（錐体応答とフリッカ応答）が消失している。ERG の記録は皮膚電極 ERG でも可能である。④孤発もしくは常染色体潜性遺伝形式をしめす。

A. 研究目的

杆体一色覚（Achromatopsia: ACHM）は、常染色体潜性（劣性）遺伝を示す稀な先天性疾患であり、杆体機能はほぼ正常であるにもかかわらず、錐体視細胞の機能が重度に障害される。令和 6 年度に我々は、日本における ACHM 患者 52 名における遺伝学および臨床的特徴を報告した。

今回我々は、指定難病の申請を行うための基礎資料と診断基準を作成し、患者数を調査するために全国の 156 施設にアンケート形式で調査票を送付したので、その内容について報告する。

B. 研究方法

我々が令和 6 年度に行なった 52 名の臨床所見（Inooka et al. Retina. 2024）を基に、日本で ACHM 患者を多く診療している研究者で議論することによって ACHM の診断基準を作成した。

また、また日本における ACHM の患者数を調査するために、全国の 156 施設にアンケート形式で調査票を送付した。

（倫理面への配慮）

今回の研究に関しては患者の個人情報は全て匿名化し、倫理面に十分配慮して行っ

た。

C. 研究結果

本症の診断基準として、症状と眼科検査所見を重視した。本症例の確定診断には、全視野 ERG の結果が重要であると考えられ、これを必修とした。

診断の要件を以下のように定めた。

①眼底所見は正常か、もしくは黄斑変性がみられる。黄斑の変性は進行することもある。②両眼性に低視力、羞明、重度の色覚異常きたし、その症状は生来ほとんど変化がない。特に幼少期から低視力で視力の悪化がないことが、錐体ジストロフィとの鑑別に重要である。③全視野 ERG で杆体系の応答がほぼ正常で、錐体系の応答（錐体応答とフリッカ応答）が消失している。ERG の記録は皮膚電極 ERG でも可能である。④孤発もしくは常染色体潜性遺伝形式をしめす。①－④の特徴を満たすものを、杆体一色覚と診断する。

また鑑別診断として、眼底正常な錐体ジストロフィ、青錐体一色覚、レーベル先天盲、黄斑ジストロフィ、眼白皮症などの黄斑の異常をきたす他の遺伝性網膜疾患を挙げ、

それらの疾患との鑑別診断について解説した。

D. 考察

これまで本邦において ACHM の診断基準は存在しなかったが、今回日本における臨床データを参考にした専門家の合議により初めて ACHM の診断基準を作成することができた。これまで一般の眼科臨床医では ACHM の診断は難しかったが、この診断基準が普及することにより、日本における ACHM の認知や啓発が進むと考えられた。

また、日本における患者数調査に関しては、全国の 156 施設にアンケート形式で調査票を送付して現在その結果が返送されてきている。今年度にその結果をまとめ、日本における初めての ACHM 患者の推定患者数を報告する予定である。

E. 結論

今回我々が行なった ACHM の診断基準と患者数調査は、将来この疾患を難病申請する際に貴重な資料となると考えられた。

F. 健康危険情報：なし

G. 研究発表

1. 論文発表

- 1) Inooka T, Hayashi T, Tsunoda K, Kuniyoshi K, Kondo H, Mizobuchi K, Suga A, Iwata T, Yoshitake K, Kondo M, Goto K, Ota J, Kominami T, Nishiguchi KM, Ueno S. GENETIC ETIOLOGY AND CLINICAL FEATURES OF ACHROMATOPSIA IN JAPAN. Retina. 2024 Oct 1;44(10):1836-1844.
- 2) Suga A, Mizobuchi K, Inooka T, Yoshitake K, Minematsu N, Tsunoda K, Kuniyoshi K, Kawai Y, Omae Y, Tokunaga K; NCBN Controls WGS Consortium; Hayashi T, Ueno S, Iwata T. A homozygous structural variant of RPGRIP1 is frequently associated with achromatopsia in Japanese patients with IRD. Genet Med Open. 2024 Mar

26;2:101843.

- 3) Ota J, Inooka T, Tomita R, Kominami T, Koyanagi Y, Ito Y, Terasaki H, Nishiguchi KM, Ueno S. EVALUATION OF RETINAL ARTERIOLES IN RETINITIS PIGMENTOSA: Arterial Lumen Diameter Reduced With Retinal Degeneration and Wall Thickness Related to Systemic Condition. Retina. 2025 Mar 1;45(3):532-540.
- 4) Ueno S, Hayashi T, Tsunoda K, Aoki T, Kondo M. Nationwide epidemiologic survey on incidence of macular dystrophy in Japan. Jpn J Ophthalmol. 2024 May;68(3):167-173.
- 5) Mizobuchi K, Hayashi T, Tanaka K, Kuniyoshi K, Murakami Y, Nakamura N, Torii K, Mizota A, Sakai D, Maeda A, Kominami T, Ueno S, Kusaka S, Nishiguchi KM, Ikeda Y, Kondo M, Tsunoda K, Hotta Y, Nakano T. Genetic and Clinical Features of ABCA4-Associated Retinopathy in a Japanese Nationwide Cohort. Am J Ophthalmol. 2024 Aug;264:36-43.
- 6) Morikawa H, Yoshida T, Kashizuka E, Hayashi S, Yokoi T, Tomita K, Azuma N, Nishina S. CHOROIDAL NEOVASCULARIZATION IN A CHILD WITH DOWN SYNDROME. Retin Cases Brief Rep. 2025 Mar 1;19(2):273-277.

2. 学会発表

- 1) Ueno S, Inooka T, Tsunoda K, Kuniyoshi K, Kondo H, Mizobuchi K, Suga A, Iwata T, Yoshitake K, Kondo M, Kominami T, Nishiguchi KM, Hayashi T. Fujiretina. March. 28-30, Tokyo, Japan, 2025.

H. 知的財産権の出願・登録状況

1. 特許取得 なし
2. 実用新案登録 なし
3. その他 なし

杆体一色覚(全色盲)の全国調査

別紙の診断基準を参考にいただき、貴院を受診する杆体一色覚患者について、以下の設問に従ってご教示ください。

貴施設名: _____

ご回答医師名: _____

(設問)

貴施設で、杆体一色覚と診断された患者数について教えてください。電子カルテなどの検索システムをお持ちでない施設でしたら、記憶にある範囲でのおおよその数を記入していただいても結構です。2020年1月から2024年12月の5年間の間に、杆体一色覚と診断された患者を診察されましたでしょうか？

☐ 患者該当なし。

↳ これ以降の回答は必要ありません。事務局にご返信ください。

☐ 患者該当者あり。

患者数について教えてください。電子カルテなどの検索システムをお持ちでない施設でしたら、記憶にある範囲でのおおよその数を記入していただいても結構です。

(A) 新規患者数（2020年1月～2024年12月の間に新規患者として診察した患者数）

名

(B) 継続患者（2019年12月より以前に診断され、その後継続して診察していた患者数）

名

(c) 上記の患者のうち研究などで行った遺伝子解析にて、*CNGA3*、*CNGB3*、*GNAT2*、*PDE6C*、*PDE6H*、*ATF6*もしくは*RPGRIP1*の両アレルに原因となる変異が確認された症例があれば症例数を記載してください。

(A)のうち	(B)のうち
名	名

誠に恐縮ではございますが、2025 年 3 月 31 日(土)までにご返送頂けますようお願い申し上げます。

杆体一色覚(全色盲)の概要と診断基準

1)概要

杆体一色覚は、両眼の錐体機能が生まれながらに欠損している遺伝性・非進行性の網膜疾患である。患者は低視力、羞明、昼盲を訴え、振子眼振を伴うことが多い。症状は生まれつきであり、年齢による進行はほとんどない。

2)原因

常染色体潜性遺伝の形式を示し、現在のところ原因遺伝子は *CNGA3*、*CNGB3*、*GNAT2*、*PDE6C*、*PDE6H*、*ATF6* が知られている。ただ、近年日本人の患者では新規の遺伝子変異として *RPGRIP1* のエクソン 18 の欠失に伴う症例が報告されている。

3)症状

患者は両眼性に低視力、羞明、昼盲を訴え、振子眼振を伴うことが多い。症状は生まれつきであり、年齢による進行はほとんどない。矯正視力は 0.1 程度で色覚は大幅な異常を示し、パネル D15 で Scotopic 軸をもつとされる。ただ、中には中心窩の錐体の機能が残って、比較的良好な視力や色覚を示す症例があることも知られている。

4) 所見

眼底所見は、正常な症例が多いが黄斑に変性がみられる症例もある。OCT は黄斑の変性に伴って黄斑部の外顆粒層の菲薄化を示す場合もあれば、眼底正常で黄斑の菲薄化を示さない症例もある。*GNAT2* の変異によるもの以外の症例では、網膜外層にある Ellipsoid Zone が不鮮明である。ただ眼振によりきれいに OCT が撮影できない場合も多いため、この異常はわかりにくいときもある。

本症例の確定診断には、ERG が必須である。本症であれば、杆体系の ERG (杆体応答; DA0.01、混合応答; DA3.0 もしくは DA10.0) がほぼ正常で、錐体系の ERG (錐体応答; LA3.0、フリッカ応答) が消失している。

杆体一色覚および鑑別すべき疾患の確定診断には遺伝子検査が有用であるが、現在の日本の保険診療では遺伝子検査はできないので、通常は症状・検査所見から診断を行う。

5)治療法

現時点では治療法が確立されていない。遺伝子治療について研究が推進されている。

6) 予後

幼少時より低視力であるがほとんど進行しない。

7) 診断の要件

- ①眼底所見は正常か、もしくは黄斑変性がみられる。黄斑の変性は進行することもある。
 - ②両眼性に低視力、羞明、重度の色覚異常きたし、その症状は生来ほとんど変化がない。
特に幼少期から低視力で視力の悪化がないことが、錐体ジストロフィとの鑑別に重要である。
 - ③全視野ERGで杆体系の応答がほぼ正常で、錐体系の応答（錐体応答とフリッカ応答）が消失している。ERG の記録は皮膚電極 ERG でも可能である。
 - ④孤発もしくは常染色体潜性遺伝形式をしめす。
- ①－④の特徴を満たすものを、杆体一色覚と診断する。

8) 鑑別疾患

1. 眼底正常な錐体ジストロフィ

眼底正常な錐体ジストロフィは、杆体系の応答がほぼ正常で錐体応答が消失していれば、OCT 所見や眼底所見からだけでは、杆体一色覚と鑑別が困難である。錐体ジストロフィとの鑑別に重要なのは臨床所見の経過である。錐体ジストロフィは進行性であり幼少期より視力や色覚異常が進行していれば、錐体ジストロフィが疑われる。一方、視力や色覚異常が生来変わらなければ杆体一色覚が疑われる。ただ、臨床所見から鑑別するのが難しい場合も多く、今回の調査では判断に迷う症例は杆体一色覚と診断してもかまわない。

2. 青錐体一色覚

青錐体一色覚は、X 染色体連鎖性の潜性遺伝を示す疾患で、赤錐体と緑錐体の機能が消失しているが、青錐体の機能だけが残存するきわめて稀な疾患である。杆体一色覚同様、杆体系の ERG はほぼ正常で、錐体応答は消失している。ただ、視力は0.5程度と比較的保たれる症例が多く、色覚は全色盲とは異なり、残存する青錐体によりある程度残っている。強度近視を伴うことが多い。伴性潜性遺伝のため患者は男性であり、家族歴があることが多い。青錐体 ERG で、青錐体応答が検出されることが杆体一色覚との鑑別になるが、青錐体 ERG の記録には、特殊な装置が必要で記録できる施設は限られている。青錐体一色覚と杆体一色覚は鑑別が非常に難しく、上記の杆体一色覚の診断要件では鑑別できない場合、今回の調査では杆体一色覚に含まれてもかまわない。

3. レーベル先天盲

レーベル先天盲の中には幼少期には眼底所見に大きな異常が見られず、羞明、眼振、低視力などの症状により、症状や所見からは杆体一色覚と区別が難しい症例がある。ただ、レーベル先天盲では暗順応下の全視野ERGの振幅低下を示すため、全視野ERGが鑑別に重要である。

4 黄斑ジストロフィ、眼白皮症などの黄斑の異常をきたす遺伝性網膜疾患

黄斑ジストロフィでは黄斑の変性、眼白皮症では黄斑低形成により、視力障害や羞明を訴える。眼白皮症や黄斑ジストロフィでは全視野ERGは応答で正常

GENETIC ETIOLOGY AND CLINICAL FEATURES OF ACHROMATOPSIA IN JAPAN

TAIGA INOOKA, MD, PhD,* TAKA AKI HAYASHI, MD, PhD,† KAZUSHIGE TSUNODA, MD, PhD,‡ KAZUKI KUNIYOSHI, MD, PhD,§ HIROYUKI KONDO, MD, PhD,¶ KEI MIZOBUCHI, MD, PhD,† AKIKO SUGA, PhD,** TAKESHI IWATA, PhD,** KAZUTOSHI YOSHITAKE, PhD,**†† MINEO KONDO, MD, PhD,‡‡ KENSUKE GOTO, MD, PhD,* JUNYA OTA, MD,* TARO KOMINAMI, MD, PhD,* KOJI M. NISHIGUCHI, MD, PhD,* SHINJI UENO, MD, PhD*§§

Purpose: To ascertain the characteristics of achromatopsia (ACHM) in Japan by analyzing the genetic and phenotypic features of patients with ACHM.

Methods: The medical records of 52 patients from 47 Japanese families who were clinically diagnosed with ACHM were reviewed in this retrospective observational study.

Results: Thirty-six causative variants of ACHM were identified in 26 families via whole-exome sequencing: *PDE6C* (12 families), *CNGA3* (10 families), *CNGB3* (two families), and *GNAT2* (two families). However, none of the 6 causative variants that are known to cause ACHM, or the 275 other genes listed in RetNet, were observed in 19 families. A significant trend toward older age and worsening of ellipsoid zone disruption on optical coherence tomography images was observed ($P < 0.01$). Progressive ellipsoid zone disruptions were observed in 13 eyes of seven patients during the follow-up visits. These patients harbored one or more variants in *PDE6C*.

Conclusion: The ACHM phenotype observed in this study was similar to those observed in previous reports; however, the causative gene variants differed from those in Europe. The low identification ratio of causative genes in whole-exome sequencing suggests the presence of unique hotspots in Japanese patients with ACHM that were not detectable via ordinal whole-exome sequencing.

RETINA 44:1836–1844, 2024

Achromatopsia (ACHM), a rare congenital condition inherited in an autosomal-recessive manner, impairs visual function mediated by cone photoreceptors despite almost normal rod function. Approximately 1 in 30,000 to 100,000 individuals is affected by ACHM,¹ and most patients with ACHM have poor visual acuity, photophobia, color blindness, and nystagmus.² Relatively mild phenotypes (i.e., relatively better visual acuity and color vision than that of ACHM) are observed in some patients; this is called incomplete ACHM or oligocone trichromacy.^{3,4} The following causative genes have been linked with ACHM^{2,5,6}: *CNGA3* (ACHM2, OMIM600053), *CNGB3* (ACHM3, OMIM605080), *GNAT2* (ACHM4, OMIM139340), *PDE6C* (ACHM5, OMIM600827), *PDE6H* (ACHM6, OMIM610024), and *ATF6* (ACHM7, OMIM616517).

Several studies have investigated the genetic and clinical profiles of ACHM globally.^{4,7–14} For instance, it was suggested that the causative genes differ between Europe and Asia.¹⁰ Moreover, the causative

genes may differ according to ethnicity in Asia.¹¹ Furthermore, some differences in clinical findings, including optical coherence tomography (OCT) findings and refractive errors, based on the causative gene, have been reported in patients with ACHM.^{15,16}

To the best of our knowledge, no studies have investigated the relationship between the genetic etiology and clinical profile in a large ACHM cohort in Japan. This was the first nationwide Japanese multicenter study of patients with ACHM; it aimed to evaluate the characteristics of ACHM by analyzing the genetic and phenotypical features of 52 patients with ACHM.

Materials and Methods

Participants

Fifty-two patients from 47 families (patients Nagoya0051 and Nagoya1051, Nagoya0330 and

Nagoya1330, JU149 and JU150, KA-105 and KA-110, and KA-177 and KA-178 are siblings) diagnosed with ACHM at the Nagoya University Hospital, Jikei University School of Medicine, NHO Tokyo Medical Center, Kindai University Faculty of Medicine, and the University of Occupational and Environmental Health were enrolled. The study was approved by the Ethical Review Committee of the Nagoya University of Medicine (2021-0253 22,603), Jikei University School of Medicine (24-231 6997), NHO Tokyo Medical Center (R18-029), Kindai University Faculty of Medicine (22-132), and University of Occupational and Environmental Health (UOEHCRB20-148). The study procedures were performed in accordance with the tenets of the Declaration of Helsinki developed by the World Medical Association, and all included patients provided informed consent for the study. Patients with insufficient clinical data, different causative genes (*POC1B* or *RPGRIP1*), and change in diagnosis to cone dystrophy with a normal fundus, or those unwilling to provide informed consent, were excluded.

The medical records of patients who were clinically diagnosed with ACHM were retrospectively reviewed. Patients were diagnosed based on the following clinical presentations: no detectable electroretinogram (ERG) under photopic conditions and normal or subnormal ERG under scotopic conditions with clinical symptoms (poor visual acuity from childhood, color vision defects, and nystagmus).¹⁷ Physicians specializing in inherited retinal diseases (T.H., K.T.,

K.K., H.K., K.M., and S.U.) made the diagnosis at each institute.

Clinical Examination

All the patients underwent ophthalmic examination, including the measurement of best-corrected visual acuity (BCVA); refractive errors; color vision testing performed using the Ishihara color vision test, panel D15 test, or anomaloscope; biomicroscopy with a slit-lamp microscope; fundus examinations; OCT; fundus autofluorescence (FAF); and ERG.

Visual acuity at the age of 6 years was considered the visual acuity for patients aged <6 years at the time of the initial visit. All patients had no history of cataracts or vitreoretinal surgery. The prescribed refractive correction was noted if autorefractive measurements were not available; the spherical equivalent refractive error (SER = spherical refractive error + 1/2 cylinder) was calculated and analyzed. Myopia was defined as SER ≤ −0.5 diopters, hyperopia was defined as SER ≥ +0.5 diopters, and emmetropia was defined as an SER between <+0.50 and >−0.50 diopters.

Patients underwent spectral domain OCT (SD-OCT) at their respective institutions. Foveal structures on SD-OCT images were graded into categories according to Sundaram et al.^{8,18}

Genetic Analyses

DNA samples were extracted from peripheral venous blood leukocytes using a QIAamp DNA Blood Mini Kit (Qiagen, Hilden, Germany) or Advanced GenoTechs (Tsukuba, Japan). Genetic diagnosis was performed as described previously.^{19,20} Variants were observed in the following causative genes: *CNGA3*, *CNGB3*, *GNAT2*, *PDE6C*, *PDE6H*, and *ATF6*. Some variants had been reported previously; the pathogenicity of novel variants was evaluated according to the guidelines recommended by the American College of Medical Genetics (ACMG).²¹ Variants in these six genes were not observed in some cases. Variants in the other 275 causative genes reported in the RetNet database (RetNet: <https://sph.uth.edu/retnet/>, a website that provides tables of genes and loci causing inherited retinal diseases) were considered in such cases. Cases with no variants in the 281 causative genes reported in RetNet were classified as “unknown.”

Statistical Analyses

Numerus digitorum was analyzed as 1.85 logarithm of the minimal angle of resolution (logMAR), as

From the *Department of Ophthalmology, Nagoya University Graduate School of Medicine, Nagoya, Japan; †Department of Ophthalmology, The Jikei University School of Medicine, Tokyo, Japan; ‡Division of Vision Research, National Institute of Sensory Organs, NHO Tokyo Medical Center, Tokyo, Japan; §Department of Ophthalmology, Kindai University Faculty of Medicine, Osaka-sayama, Japan; ¶Department of Ophthalmology, University of Occupational and Environmental Health, Kitakyushu, Japan; **Division of Molecular and Cellular Biology, National Institute of Sensory Organs, NHO Tokyo Medical Center, Tokyo, Japan; ††Laboratory of Aquatic Molecular Biology and Biotechnology, Aquatic Bioscience, Graduate School of Agricultural and Life Sciences, The University of Tokyo, Tokyo, Japan; ‡‡Department of Ophthalmology, Mie University School of Medicine, Tsu, Japan; and §§Department of Ophthalmology, Hirosaki University Graduate School of Medicine, Hirosaki, Japan.

Supported in part by a Health and Labour Sciences Research Grant (Grant number 23FC1043 to M.K.), the Japan Society for the Promotion of Science Grant-in-Aid for Scientific Research KA-KENHI 21K09756 and 24K12771 to T.H., and 22K09825 to K.K., and the Takayanagi Retina Research Award to T.I.

None of the authors has any conflicting interests to disclose.

Supplemental digital content is available for this article. Direct URL citations appear in the printed text and are provided in the HTML and PDF versions of this article on the journal's Web site (www.retinajournal.com).

Reprint requests: Shinji Ueno, MD, PhD, Department of Ophthalmology, Hirosaki University Graduate School of Medicine, 5 Zaifu-cho, Hirosaki, Aomori 036-8562, Japan; e-mail: uenos@hirosaki-u.ac.jp

described previously.²² Changes in BCVA over the follow-up period were determined. A generalized estimating equation (GEE) was fitted to the longitudinal data of 46 patients who were followed up more than once, using baseline values as an offset and follow-up length, expressed in years, as an independent variable. The Jonckheere–Terpstra test was performed to evaluate nonparametric data. Fisher exact test was performed to compare categorical variables. One-way analysis of variance was performed to compare parametric continuous variables, whereas the Kruskal–Wallis test was used to compare nonparametric continuous variables. *P*-values < 0.05 were considered statistically significant. Statistical analyses were performed using lme4 version 1.1 to 30 based on R version 4.4.2 (<https://www.r-project.org/>).

Results

Patient Selection

Table 1 presents the demographic characteristics of the 52 enrolled patients. The mean age at the initial visit \pm SD (range) was 23.2 ± 16.9 (2–67) years; 46 patients were followed up for a mean of 11.6 ± 7.3 (1–34) years. **Supplemental Digital Content 1** (see **Content**, <http://links.lww.com/IAE/C264>) presents individual patient results.

Visual Acuity and Refractive Error

The mean BCVA at the initial and final visits was almost identical in the right and left eyes (Table 1). The GEE fitted to the visual acuity data revealed no significant reduction in BCVA during a follow-up period of 11.6 ± 7.3 years (*P* = 0.15). A clinically obvious interocular discordance of BCVA > 0.3 logMAR (15 Early Treatment Diabetic Retinopathy Study letters) was observed in 2 patients (4%; Nagoya791 and JU2050).

Nagoya0051, a patient with incomplete ACHM, and Nagoya1051, a patient with complete ACHM, were siblings, as reported previously.²³

The median SER for the right eyes was -1.875 diopters and for the left eyes was -1.625 diopters. In all, 62 of 104 eyes (60%) were myopic (SER ≤ -0.50 diopters), 35 (34%) were hyperopic (SER $\geq +0.5$ diopters), and 7 (7%) were emmetropic (SER between > -0.50 and $< +0.50$ diopters).

No significant correlation was observed between BCVA (logMAR) and OCT grades among the patients (*P* = 0.65 in the right eye, *P* = 0.79 in the left eye; see **Figure S1, Supplemental Digital Content 2**, <http://links.lww.com/IAE/C265>).

Genotype

Causative variants of ACHM in 26 of the 47 families were identified using whole-exome

Table 1. Patient Demographic Profile

Parameters	Data at Initial Visit (n = 52)	
Male/female	22/30	
Age at initial visit, years	23.2 ± 16.9 (2–67)	
BCVA at initial visit (logMAR)	Right eye	Left eye
	0.92 ± 0.36 (0.0 to 1.85) (Snellen 20/160)	0.96 ± 0.35 (0.046 to 1.85) (Snellen 20/200)
Mean refractive error (D)	-2.3 ± 5.4 (–16.0 to +6.5)	-2.0 ± 5.1 (–14.0 to +6.5)
Intereye deference of BCVA (logMAR)	0.086 ± 0.10 (0 to 0.43) (ETDRS letters 4.3 ± 5.0 [0 to 22])	
Follow-up Data (n = 46)		
Male/female	20/26	
Age at last visit, years	33.3 ± 15.3 (7 to 71)	
Follow-up period, years	11.6 ± 7.3 (1 to 34)	
BCVA at final visit (logMAR)	Right eye	Left eye
	0.92 ± 0.36 (0.10 to 1.85) (Snellen 20/160)	0.95 ± 0.38 (0.0 to 1.85) (Snellen 20/200)
Mean refractive error (D)	-3.2 ± 4.7 (–14.5 to +4.0)	-3.1 ± 4.6 (–15.0 to +4.5)
Intereye deference of BCVA (logMAR)	0.081 ± 0.082 (0 to 0.30) (ETDRS letters 4.1 ± 4.1 [0 to 15])	
Slope of the BCVA (logMAR/year)	0.0071 ± 0.024 (–0.032 to 0.11) (ETDRS letters -0.36 ± 1.2 [–5.5 to 1.6])	0.00029 ± 0.031 (–0.12 to 0.11) (ETDRS letters -0.015 ± 1.6 [–5.5 to 6.0])

Data are mean \pm SD (range).

ETDRS, early treatment diabetic retinopathy study.

sequencing (WES). Variants were observed most commonly in 4 causative genes of ACHM: *PDE6C* (14 patients from 12 families), *CNGA3* (10 patients from 10 families), *CNGB3* (2 patients from 2 families), and *GNAT2* (2 patients from 2 families). However, ACHM caused by variants in the other described genes (*PDE6H* or *ATF6*) was not observed. Thirteen patients from 13 families had a compound heterozygous phenotype, whereas 15

patients from 13 families had a homozygous phenotype. A monoallelic variant of *CNGA3* was observed in two patients from one family (KA-177 and KA-178), whereas a monoallelic variant of *PDE6C* was observed in one patient (Nagoya-56). Among the 36 variants identified herein, 23 had been published previously^{5,6,10,12,16,24–28} and 13 were novel (Table 2, see **Figures S2-3, Supplemental Digital Content 2**, <http://links.lww.com/IAE/C265>).

Table 2. Variants Identified in 31 Patients

Patient No.	Gene	Zygoty	Variants	gnomAD (MAF)	Previous Literature
Nagoya14	<i>CNGA3</i>	C. Het.	c.847C>T: p.Arg283Trp; c.1642G>A: p.Gly548Arg	0.0000294; 0.0000147	*†References ^{6,10,11,13} ; *†References ^{10,11,24}
Nagoya467	<i>CNGA3</i>	C. Het.	c.67C>T: p.Arg23Ter; c.1495C>T: p.Arg499Ter	0.0001309; 0.0001927	Reference ²⁴ ; *Reference ¹⁰
JU0156	<i>CNGA3</i>	C. Het.	c.488C>T: p.Pro163Leu; c.1262delA: p.Lys421Serfs	None; None	Reference ⁶ ; Reference ²⁷
JU0185	<i>CNGA3</i>	C. Het.	c.1307G>A: p.Arg436Trp; c.1898T>C: p.Leu633Pro	0.001247; None	*Reference ¹⁰ ; Reference ²⁸
JU1102	<i>CNGA3</i>	C. Het.	c.1039C>T: p.Arg347Cys; c.1210T>C: p.Ser404Pro	0.0006214; None	*Reference ¹⁰ ; Novel
JU1290	<i>CNGA3</i>	Hom	c.1319G>A: p.Trp440Ter	0.00002415	*References ^{10,28}
JU1394	<i>CNGA3</i>	C. Het.	c.668G>A: p.Arg223Gln; c.997_998delGA: p.Asp333Leufs	0.0001735; None	*Reference ¹⁰ ; Reference ¹¹
JU2249	<i>CNGA3</i>	C. Het.	c.67C>T: p.Arg23Ter; c.778G>A: p.Asp260Asn	0.0001309; 0.00004410	Reference ²⁴ ; *Reference ¹⁰
KA-177	<i>CNGA3?</i>	Het.	c.1126G>A: p.Glu376Lys	0.00004411	Reference ²⁵
KA-178	<i>CNGA3?</i>	Het.	c.1126G>A: p.Glu376Lys	0.00004411	Reference ²⁵
Kinki 96-1236	<i>CNGA3</i>	C. Het.	c.997_998delGA: p.Asp333Leufs; c.1270A>G: p.Met424Val	None; None	Reference ¹¹ ; Reference ¹¹
Kinki 386-452	<i>CNGA3</i>	C. Het.	c.1642G>A: p.Gly548Arg; c.1631G>A: p.Gly544Asp	0.0000147; None	*†References ^{10,11} ; Novel
JU0011	<i>CNGB3</i>	Hom	c.1372delT: p.Cys458fs	None	Novel
JU0058	<i>CNGB3</i>	Hom	c.1372delT: p.Cys458fs	None	Novel
Nagoya53	<i>GNAT2</i>	Hom	c.730_743del14: p.His244Serfs	None	†References ^{11,16}
JU1219	<i>GNAT2</i>	Hom	c.730_743del14: p.His244Serfs	None	†References ^{11,16}
Nagoya56	<i>PDE6C?</i>	Het.	c.1375C>T: p.Gln459Ter	None	Novel
Nagoya67	<i>PDE6C</i>	Hom	c.1561T>A: p.Leu521Met	None	Novel
Nagoya155	<i>PDE6C</i>	C. Het.	c.724-1G>C; c.1711G>C: p.Gly571Arg	None; None	Novel; Reference ²⁶
JU0055	<i>PDE6C</i>	Hom	c.2201_2202del: p.Gln734fs	None	Novel
JU0149	<i>PDE6C</i>	Hom	c.1771G>A: p.Glu591Lys	0.00002414	*†References ^{10,11}
JU0150	<i>PDE6C</i>	Hom	c.1771G>A: p.Glu591Lys	0.00002414	*†References ^{10,11}
JU0332	<i>PDE6C</i>	Hom	c.1693C>T: p.Arg565Trp	0.00001471	Novel
JU0352	<i>PDE6C</i>	Hom	c.216dupG: p.Glu72fs	None	Novel
JU0727	<i>PDE6C</i>	Hom	c.2159C>T: p.Thr720Met	0.00009667	*Reference ¹⁰
JU1013	<i>PDE6C</i>	Hom	c.1271_1272del: p.Thr424fs	None	Novel
JU2050	<i>PDE6C</i>	C. Het.	c.874G>A: p.Asp292Asn; c.471T>G: p.Asp157Glu	None; 0.03774	Reference ²⁶ ; Reference ²⁶
JU2226	<i>PDE6C</i>	C. Het.	c.304C>T: p.Arg102Trp; c.1164G>T: p.Leu388Phe	None; None	Reference ⁵ ; Novel
KA-105	<i>PDE6C</i>	Hom	c.1703T>G: p.Phe568Cys	None	Novel
KA-110	<i>PDE6C</i>	Hom	c.1703T>G: p.Phe568Cys	None	Novel
Kinki 31-12	<i>PDE6C</i>	C. Het.	c.713G>A: p.Arg238Gln; c.880_881insGGCC: p.Trp294fs	0.000006577; None	Reference ²⁶ ; Novel

*Previous Literature column means that the variants had been reported in a previous study conducted in China.¹⁰

†Previous Literature column means that the variants had been reported in a previous study conducted in Korea.¹¹

C. Het., compound heterozygous; Het., heterozygous; Hom., homozygous; MAF, minor allele frequency.

Eleven variants observed in 10 families (*CNGA3*; nine variants, *PDE6C*; 2 variants) had been reported in a previous study conducted in China,¹⁰ and 5 variants observed in 5 families (*CNGA3*; 3 variants, *GNAT2*; one variant, *PDE6C*; one variant) had been reported in a previous study conducted in Korea¹¹ (Table 2). The 13 novel variants were classified according to the ACMG guidelines as pathogenic, likely pathogenic, or of uncertain significance (see **Table S1, Supplemental Digital Content 3**, <http://links.lww.com/IAE/C265>). However, in our WES analysis of 21 patients from 19 families, no causative variants were identified in the 281 genes listed in RetNet, including the 6 genes known to cause ACHM.

Genotype and Phenotype

Differences in clinical symptoms were examined according to each causative gene group to identify correlations between genotypes and phenotypes. Table 3 presents the main clinical symptoms caused by the causative genes. **Supplemental Digital Content 4** (see **Table S2**, <http://links.lww.com/IAE/C265>) summarizes the remaining symptoms. Statistical analyses were performed for the three groups that included a sufficient number of patients: *CNGA3*, *PDE6C*, and unknown causative genes. No significant correlation was observed among the groups in SER, classification of refractive error (myopic/emmetropic/hyperopic), BCVA (logMAR), or OCT grade.

Table 3. Main Genotype–Phenotype Correlation Analysis Performed for the Initial Visit

	<i>CNGA3</i> (n = 10)	<i>CNG3B</i> (n = 2)	<i>GNAT2</i> (n = 2)	<i>PDE6C</i> (n = 14)	Unknown (n = 24)	<i>P</i> (Between <i>CNGA3</i> , <i>PDE6C</i> , and Unknown)
Male/female	4/6	1/1	2/0	6/8	9/15	0.95*
Age at the initial visit, years	28.2 ± 24.1	27.5 ± 9.2	28.0 ± 15.6	20.1 ± 14.7	22.2 ± 15.7	0.88†
SER (D)						
Right	−0.43 ± 5.1	−1.8 ± 7.4	−3.6 ± 1.9	−2.9 ± 6.6	−2.7 ± 5.0	0.81‡
Left	0.21 ± 4.2	−0.63 ± 7.6	−4.8 ± 1.4	−2.8 ± 6.8	−2.4 ± 4.3	0.56‡
BCVA (logMAR)						
Right	1.0 ± 0.32 (Snellen 20/200)	1.0 ± 0 (Snellen 20/200)	1.0 ± 0 (Snellen 20/200)	0.77 ± 0.50 (Snellen 20/125)	0.94 ± 0.30 (Snellen 20/160)	0.59†
Left	1.1 ± 0.30 (Snellen 20/250)	0.91 ± 0.12 (Snellen 20/160)	1.0 ± 0.069 (Snellen 20/200)	0.84 ± 0.43 (Snellen 20/125)	0.98 ± 0.32 (Snellen 20/200)	0.39†
OCT grade						
1	3	0	2	4	8	0.51*
2	3	1	0	2	7	
3	0	1	0	3	0	
4	2	0	0	2	3	
5	2	0	0	3	4	
Fundus color						
Within normal level	7	1	2	8	12	0.63*
RPE change	0	1	0	2	6	
Retina/RPE atrophy	3	0	0	3	4	
n/a	0	0	0	1	2	

The grade of OCT findings is shown as indicated at the earliest visit.

*Fisher exact test.

†Kruskal–Wallis test.

‡One-way ANOVA.

n/a, not available; ANOVA, analysis of variance.

Fundus Images and Fundus Autofluorescence

Fundus appearance was normal in 30 patients, whereas retinal pigment epithelium (RPE) macular dystrophy was observed in 19 patients. No apparent differences were observed between the left and right eyes of each patient. No statistically significant relationship was observed between macular atrophy and the causative genes *CNG3A* and *PDE6C* and the unknown genes (Table 3; $P = 0.63$).

Fundus autofluorescence imaging data were available for 40 patients (77%). Twelve patients (30%) had normal autofluorescence findings and OCT Grade 1 or 2. Autofluorescence revealed subtle hyper-autofluorescence spots in the central macula in 4 patients (10%), and 3 of these 4 patients had OCT Grade 1. The central region was devoid of autofluorescence and surrounded by a hyper-autofluorescent ring in 12 patients (30%), and 9 of these 12 patients had OCT Grade 5. Foveal or parafoveal hyper-

autofluorescence findings were observed in 12 patients (30%), and these patients had OCT Grades of 1 to 4. Figure 1 shows the representative cases.

Optical Coherence Tomography Findings

Table 3 presents the grade distribution of the earliest OCT findings for the visit (104 eyes of 52 patients). Continuous ellipsoid zones (EZs) (foveal structure of Grade 1) were observed in 34 eyes of 17 patients (37%); EZ disruption (Grade 2) was observed in 26 eyes of 13 patients (21%); EZ was absent (Grade 3) in 8 eyes of 4 patients (8%); hyporeflective zone (Grade 4) was observed in 14 eyes of 7 patients (13%); and outer retinal atrophy, including RPE loss (Grade 5), was observed in 18 eyes of 9 patients (17%).

Analysis of the correlation between the earliest obtained OCT and age revealed a significant trend toward older age and higher-grade OCT findings ($P = 0.0073$ in the right eye; see **Figure S4**,

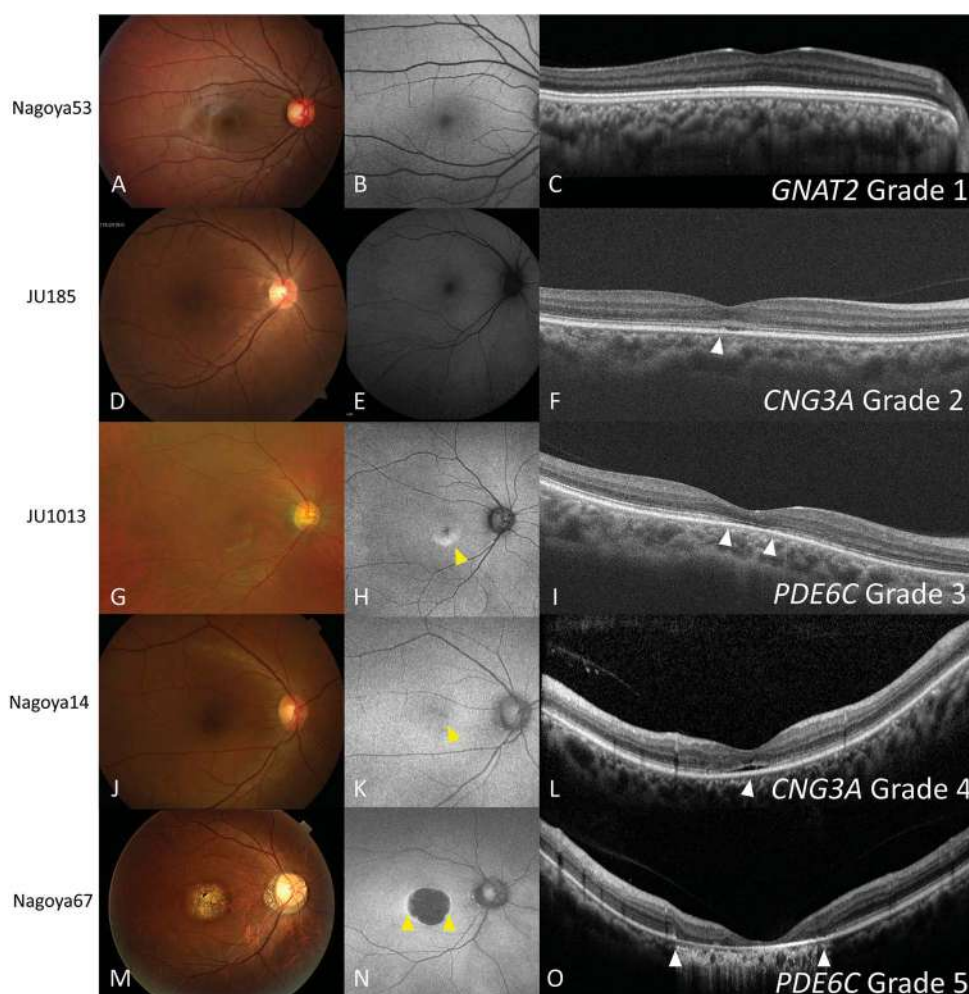


Fig. 1. The fundus, fundus autofluorescence, and OCT images of three representative patients with ACHM. Patient Nagoya53 (homozygous for the c.730_743del14 variant in *GNAT2*) has no obvious abnormalities in color fundus photographs (A), FAF (B), and OCT (C). Patient JU185 (compound heterozygous for the c.1307G>A and c.1898T>C variants in *CNGA3*) has a normal fundus (D) and FAF (E) with Grade 2 OCT characterized by a disruption of the EZ (F, white arrowhead). Patient JU1013 (homozygous for the c.1271_1272del variant in *PDE6C*) has a normal fundus (G), but FAF shows parafoveal hyperfluorescence (H, yellow arrowhead) with Grade 3 OCT characterized by a blurred EZ (I, white arrowheads). Patient Nagoya14 (compound heterozygous for the c.847C>T and c.1642G>A variants in *CNGA3*) has a normal fundus (J), but FAF shows reduced autofluorescence in the central macula (K, yellow arrowhead), with Grade 4 OCT, characterized by a hyporeflective zone, present (L, white arrowhead). Patient Nagoya67 (homozygous for the c.1561T>A variant in *PDE6C*) has RPE atrophy (M), a central region devoid of autofluorescence surrounded by a hyper-autofluorescent ring (N, yellow arrowhead) and Grade 5

OCT with outer retinal atrophy and RPE loss (O, white arrowheads).

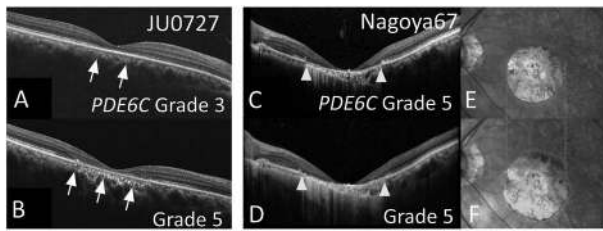


Fig. 2. Representative cases of worsening of OCT findings. The OCT classification of the right eye in patient JU0727 changed from Grade 3 (A, arrows indicating the absence of EZ) to Grade 5 (B, arrows indicating atrophy of the EZ) over 12 years. In patient Nagoya67, the edge of the EZ disruption (C, arrowheads) widened in 6 years (D, arrowheads), and the infrared images (E and F, dotted line) also show the extent of widened atrophy. Both patients had causative variants in *PDE6C*.

Supplemental Digital Content 5, <http://links.lww.com/IAE/C265>). No statistically significant relationship was observed between the earliest obtained OCT findings and SER ($P = 0.89$ in the right eye and $P = 0.93$ in the left eye).

Thirty-six patients had two or more OCT recordings available for more than 4 years of follow-up. Among these OCT recordings, the OCT grade changed in nine eyes of five patients during the follow-up period (Nagoya155, JU0149, JU0352, JU0727, and JU1013). These patients harbored variants in *PDE6C*. Figure 2, A and B show a representative case. Progressive EZ disruptions in grade 5 OCT were also observed in two eyes of one patient with variants in *PDE6C* (Nagoya67) and two eyes of one patient with a monoallelic variant in *PDE6C* (Nagoya56). Figure 2, C–F show a representative case.

Discussion

This is the largest cohort study of patients with ACHM that focused on the genotype and phenotype, especially OCT images, with an average follow-up duration of >10 years. A high prevalence of *PDE6C* variants and low prevalence of *CNGB3* variants were observed in Japan compared with the pattern of prevalence observed in Western countries. Although no changes were observed in the visual acuity of patients with ACHM, progressive macular degeneration was observed in some patients with variants in *PDE6C*.

Genetics

Compared with variants in *CNGA3* or *CNGB3* in the studies conducted in Western countries that accounted for >80% of cases of ACHM,^{9,29} variants in *PDE6C* were most commonly observed in Japan, accounting for approximately 50% of the cases with an identified causative gene (26% of all cases). The frequency of variants

in *CNGA3* was found to be highest in China, accounting for approximately 80% of cases of ACHM.¹⁰ Conversely, the frequency of the variants in *PDE6C* was considerably lower than that in Japan. A study conducted in Korea reported that variants in *CNGA3* or *PDE6C* were the most common cause of ACHM.¹¹ The similarity of the data collected in this study with those of the study in Korea may be attributed to the similar racial backgrounds of individuals from Japan and Korea.

Previous reports have indicated that causative variants are detected in at least 70% of patients with clinically diagnosed ACHM via exome analysis^{2,4,9}; however, the proportion of genetically proven cases in the present study was only 55%. This finding suggests that there may be other causative variants that cannot be identified using ordinal WES. This may have several possible explanations. First, WES cannot detect variants caused by excessively large deletions or insertions, or intronic variants, although these variants were present in the six previously reported genes causing ACHM. This was likely the case for the patients in the two families who had variants in only one allele (patients KA-177 and KA-178 [heterozygous for the c.1126G>A variant in *CNGA3*] and Nagoya56 [heterozygous for the c.1375C>T variant in *PDE6C*]). The other variant may be present in the allele of each gene in a manner that cannot be identified using ordinal WES. The identification rate may decrease if these unidentified variants become hotspots of ACHM in Japan. Second, variants may have been present in genes other than the six previously reported genes. As no causative variant listed in the genes of RetNet was detected via WES, it is possible that variants may exist in genes reported in RetNet but not in the regions detected via WES, or variants might be present in genes that are not reported in RetNet. Whole-genome sequencing analyses should be performed in the near future to identify the variants caused by introns, or large deletions or insertions, in cases with unknown causes of ACHM.

Phenotype

The structures of the EZ were relatively preserved in OCT images (Grade 1 or 2) in patients with relatively good visual acuity; however, no statistically significant correlation was observed between BCVA and OCT grades. This finding may be attributed to some patients with OCT Grade 1 or 2 having poor visual acuity. The visual function was not preserved in patients with ACHM caused by variants in *GNAT2*; however, the EZ structure was preserved. These results indicate that eyes with variants in *GNAT2* had relatively normal cone structures that lacked function.^{8,16}

Patients with ACHM have been considered to be predominately hyperopic³⁰; however, a recent study has demonstrated that patients with ACHM have a wider distribution of refractive error, ranging from myopia to hyperopia.¹⁰ A previous report focusing on the differences in refractive error according to causative genes¹⁵ revealed that patients with variants in *GNAT2*, *PDE6C*, and *PDE6H* exhibited a high prevalence of myopia (75%–80%) and that severe myopia (SER \leq -6.00 diopters) was more common in eyes with these variants than in eyes with variants in *CNGA3* or *CNGB3*. In this study, myopia and hyperopia were equally distributed in eyes with *CNGA3* or *PDE6C* variants; however, severe myopia was more prevalent in patients with the *PDE6C* variant (36%, 5 of 14 patients) than in those with the *CNGA3* variant (8%, 1 of 11 patients). The previous study included only 4 patients with variants in *PDE6C*¹⁵; conversely, the present study included 14 patients with variants in *PDE6C* and reported a trend toward myopia (especially severe myopia). Further accumulation of cases will aid in drawing strong conclusions regarding genotype–phenotype correlations.

The OCT grade was significantly advanced in older patients. However, notably, there were two cases of macular atrophy on OCT (Grade 5), even at 7 years of age (Nagoya320 and JU0150). This finding indicates that the progression of macular atrophy is not observed only in adults. In addition, worsening of OCT grade and progression of macular atrophy were observed in six patients with variants in *PDE6C* in the present study. Furthermore, macular atrophy was observed at the time of the initial examination in 3 of the 15 patients with variants in *PDE6C*. These findings may support the findings of previous reports demonstrating that eyes with variants in *PDE6C* tend to develop macular atrophy and its progression.^{5,14}

Sundaram et al proposed classifying the foveal structure on OCT images in eyes with ACHM into five grades.^{8,18} However, one report noted that their association with age remains questionable and showed a retrograde change in OCT grade (Grade 4 \rightarrow 3).¹³ The findings herein showed that the correlation between age and OCT grades was more pronounced when the order of Grades 3 and 4 was reversed (i.e., the order of the OCT Grade was 1, 2, 4, 3, and 5; see **Figure S5, Supplemental Digital Content 6**, <http://links.lww.com/IAE/C265>). Thus, the OCT classification proposed by Sundaram et al does not necessarily represent the order of progression, although it should be noted that Sundaram et al did not suggest that patients with ACHM show a natural progression of OCT grades based on age.

This study has certain limitations. First, it was a retrospective, multicenter study. Therefore, the conditions under which clinical examinations were performed were not identical. Second, although visual function, including visual acuity and visual field, is important, sufficient visual field data could not be collected.

In conclusion, variants in the causative genes of ACHM in Japan are similar to those in Asian countries, especially Korea, but different from those in Western countries. The high ratio of cases with genetically unknown causes in WES suggests the presence of unique hotspots in patients with ACHM in Japan that could not be detected via WES. The aggregation of data from different ethnic groups will enable the implementation of gene therapy in the near future.

Key words: achromatopsia, *CNGA3*, *CNGB3*, Japanese population, *PDE6C*.

References

1. Francois J. Heredity in ophthalmology. *Bull Soc Belge Ophthalmol* 1958;118:1–300.
2. Hirji N, Aboshiha J, Georgiou M, et al. Achromatopsia: clinical features, molecular genetics, animal models and therapeutic options. *Ophthalmic Genet* 2018;39:149–157.
3. Michaelides M, Holder GE, Bradshaw K, et al. Oligocone trichromacy: a rare and unusual cone dysfunction syndrome. *Br J Ophthalmol* 2004;88:497–500.
4. Thiadens AA, Slingerland NW, Roosing S, et al. Genetic etiology and clinical consequences of complete and incomplete achromatopsia. *Ophthalmology* 2009;116:1984–1989.e1.
5. Georgiou M, Robson AG, Singh N, et al. Deep phenotyping of *PDE6C*-associated achromatopsia. *Invest Ophthalmol Vis Sci* 2019;60:5112–5123.
6. Kohl S, Marx T, Giddings I, et al. Total colourblindness is caused by mutations in the gene encoding the alpha-subunit of the cone photoreceptor cGMP-gated cation channel. *Nat Genet* 1998;19:257–259.
7. Nishiguchi KM, Sandberg MA, Gorji N, et al. Cone cGMP-gated channel mutations and clinical findings in patients with achromatopsia, macular degeneration, and other hereditary cone diseases. *Hum Mutat* 2005;25:248–258.
8. Sundaram V, Wilde C, Aboshiha J, et al. Retinal structure and function in achromatopsia: implications for gene therapy. *Ophthalmology* 2014;121:234–245.
9. Kohl S, Varsanyi B, Antunes GA, et al. *CNGB3* mutations account for 50% of all cases with autosomal recessive achromatopsia. *Eur J Hum Genet* 2005;13:302–308.
10. Sun W, Li S, Xiao X, et al. Genotypes and phenotypes of genes associated with achromatopsia: a reference for clinical genetic testing. *Mol Vis* 2020;26:588–602.
11. Choi YJ, Joo K, Lim HT, et al. Clinical and genetic features of Korean patients with achromatopsia. *Genes (Basel)* 2023;14:519.
12. Kuniyoshi K, Muraki-Oda S, Ueyama H, et al. Novel mutations in the gene for α -subunit of retinal cone cyclic nucleotide-gated channels in a Japanese patient with congenital achromatopsia. *Jpn J Ophthalmol* 2016;60:187–197.

13. Tekavčič Pompe M, Vrabčič N, Volk M, et al. Disease progression in *CNGA3* and *CNGB3* retinopathy; characteristics of Slovenian cohort and proposed OCT staging based on pooled data from 126 patients from 7 studies. *Curr Issues Mol Biol* 2021;43:941–957.
14. Thiadens AA, Somervuo V, van den Born LI, et al. Progressive loss of cones in achromatopsia: an imaging study using spectral-domain optical coherence tomography. *Invest Ophthalmol Vis Sci* 2010;51:5952–5957.
15. Andersen MKG, Bertelsen M, Grønskov K, et al. Genetic and clinical characterization of Danish achromatopsia patients. *Genes (Basel)* 2023;14:690.
16. Ueno S, Nakanishi A, Kominami T, et al. In vivo imaging of a cone mosaic in a patient with achromatopsia associated with a *GNAT2* variant. *Jpn J Ophthalmol* 2017;61:92–98.
17. Adam MP, Mirzaa GM, Pagon RA, et al. GeneReviews [Internet]. Seattle, WA: University of Washington; 1993–2024.
18. Aboshiha J, Dubis AM, Cowing J, et al. A prospective longitudinal study of retinal structure and function in achromatopsia. *Invest Ophthalmol Vis Sci* 2014;55:5733–5743.
19. Katagiri S, Yoshitake K, Akahori M, et al. Whole-exome sequencing identifies a novel *ALMS1* mutation (p.Q2051X) in two Japanese brothers with Alström syndrome. *Mol Vis* 2013;19:2393–2406.
20. Ota J, Inooka T, Okado S, et al. Pathogenic variants of *MFRP* and *PRSS56* genes are major causes of nanophthalmos in Japanese patients. *Ophthalmic Genet* 2023;44:423–429.
21. Richards S, Aziz N, Bale S, et al. Standards and guidelines for the interpretation of sequence variants: a joint consensus recommendation of the American College of Medical Genetics and Genomics and the association for molecular pathology. *Genet Med* 2015;17:405–424.
22. Schulze-Bonsel K, Feltgen N, Burau H, et al. Visual acuities “hand motion” and “counting fingers” can be quantified with the freiburg visual acuity test. *Invest Ophthalmol Vis Sci* 2006;47:1236–1240.
23. Ueno S, Nakanishi A, Sayo A, et al. Differences in ocular findings in two siblings: one with complete and other with incomplete achromatopsia. *Doc Ophthalmol* 2017;134:141–147.
24. Johnson S, Michaelides M, Aligianis IA, et al. Achromatopsia caused by novel mutations in both *CNGA3* and *CNGB3*. *J Med Genet* 2004;41:e20.
25. Koeppen K, Reuter P, Ladewig T, et al. Dissecting the pathogenic mechanisms of mutations in the pore region of the human cone photoreceptor cyclic nucleotide-gated channel. *Hum Mutat* 2010;31:830–839.
26. Landrum MJ, Lee JM, Benson M, et al. ClinVar: public archive of interpretations of clinically relevant variants. *Nucleic Acids Res* 2016;44:D862–D868.
27. Rim JH, Lee ST, Gee HY, et al. Accuracy of next-generation sequencing for molecular diagnosis in patients with infantile nystagmus syndrome. *JAMA Ophthalmol* 2017;135:1376–1385.
28. Li S, Huang L, Xiao X, et al. Identification of *CNGA3* mutations in 46 families: common cause of achromatopsia and cone-rod dystrophies in Chinese patients. *JAMA Ophthalmol* 2014;132:1076–1083.
29. Kohl S, Baumann B, Rosenberg T, et al. Mutations in the cone photoreceptor G-protein alpha-subunit gene *GNAT2* in patients with achromatopsia. *Am J Hum Genet* 2002;71:422–425.
30. Aboshiha J, Dubis AM, Carroll J, et al. The cone dysfunction syndromes. *Br J Ophthalmol* 2016;100:115–121.

厚生労働科学研究費補助金（難治性疾患政策研究事業）
分担研究報告書

全国視覚障害認定の実態疫学調査に関する研究

研究分担者 岡山大学・医歯薬学総合研究科・教授 森實 祐基
鹿児島大学・医歯学総合研究科・教授 坂本 泰二
研究協力者 大阪大学・医学系研究科・教授 川崎 良

今回我々は、今後の全国視覚障害認定の実態疫学調査に関する具体的な調査内容について、どのような追加情報や解析が必要であるかを話し合った。その結果、国民に提供する必要な因子として、引き続き(1)身体障害の等級、(2)年齢、(3)性別、(4)在籍地（都道府県）、(5)原因となる眼疾患は必要であると考えられた。原因となる眼疾患として、これまで「緑内障」、「網膜色素変性」、「糖尿病網膜症」、「黄斑変性」という疾患名が使用されてきたが、特に「黄斑変性」という病名の場合に、これが加齢黄斑変性なのか、近視による黄斑症なのか、黄斑ジストロフィのような遺伝性疾患であるのかが不明であり、今後このような具体的な病名を加えることにより、国民にも有用な正しい情報提供ができると考えられた。

A. 研究目的

これまで本研究班では、全国における視覚障害認定の実態とその推移を継続的に調査してきた。最近では2019年の調査結果をまとめ、その結果視覚障害認定者数が大きく増加し、原因疾患として緑内障の占める割合が28.6%から40.7%まで大きく増加したことを英文誌に報告した(Matoba et al. JJ0. 2023)。

今回我々は、今後の全国視覚障害認定の実態疫学調査に関する具体的な調査内容について、どのような追加情報や解析が必要であるかを話し合ったので報告する。

B. 研究方法

2024年の7月15日および2025年12月25日の2回、班会議のメンバーでZOOM会議を開催して話し合った。

（倫理面への配慮）

今回の話し合いに関しては倫理委員会の承認は必要ではないが、個人情報には十分配慮して話し合いを進めた。

C. D. 研究結果および考察

話し合いの結果、国民に視覚障害者の情報を正しく提供するための必要な因子として、引き続き(1)身体障害の等級、(2)年齢、(3)性別、(4)在籍地（都道府県）、(5)原因となる眼疾患は必要であると考えられた。

原因となる眼疾患として、これまで「緑内障」、「網膜色素変性」、「糖尿病網膜症」、「黄斑変性」という疾患名が主に使用されてきたが、特に「黄斑変性」という病名の場合に、これが加齢黄斑変性なのか、近視による黄斑症なのか、黄斑ジストロフィのよう

な遺伝性疾患であるのかが不明であり、視覚障害者の正確な実態の把握が困難であるという意見があった。今後の調査にあたって、単に「黄斑変性」だけでなく、具体的な病名を使用することで、より具体的な視覚障害の原因疾患情報が得られ、国民への正しい情報提供に役立つと考えられた。

E. 結論

全国における視覚障害認定の実態とその推移に関する実態調査は、これまで同じ疾患名と調査方式で行われることにより、長

年の障害者の推移を知ることができる貴重な情報源となっている。この内容や方法を大幅に変更することは好ましくないが、「黄斑変性」の患者に対して、具体的に「加齢黄斑変性」、「近視による黄斑症」、「黄斑ジストロフィ」、「その他の黄斑変性」を追加で選択していただくことで、眼科および国民にとって貴重な情報が得られると考えられた。

F. 健康危険情報：なし

G. 研究発表

1. 論文発表（2024年以前のものも含む）

- 1) Matoba R, Morimoto N, Kawasaki R, Fujiwara M, Kanenaga K, Yamashita H, Sakamoto T, Morizane Y. A nationwide survey of newly certified visually impaired individuals in Japan for the fiscal year 2019: impact of the revision of criteria for visual impairment certification. Jpn J Ophthalmol. 2023 May;67(3):346-352.

2. 学会発表 なし

H. 知的財産権の出願・登録状況

1. 特許取得 なし
2. 実用新案登録 なし
3. その他 なし

厚生労働科学研究費補助金（難治性疾患政策研究事業）

分担研究報告書

難治性視神経症に関する研究

研究分担者

神戸大学・医学研究科・教授 中村 誠

研究協力者

北里大学・医療衛生学部・教授 石川 均

お茶の水・井上眼科クリニック・副院長 山上 明子

レーベル遺伝性視神経症（指定難病302、LHON）の症例データベースを作成し、患者の詳細な臨床情報を調査した。日本神経眼科学会評議員所属施設および関連施設においてLHONと診断された症例を対象とした。オンラインでデータベースシステムを構築し、患者性別、発症年齢、データ登録時の罹患期間、遺伝子変異箇所、診断カテゴリー、診断施設、家族歴、使用薬剤、併存疾患、最低視力、最終受診時の視力についてデータを収集した。その結果、326例の症例が登録された。データベースシステム構築によりLHONの患者の疫学的な実態がより詳細に把握できるようになった。今後さらに多数の症例の登録が望まれる。

A. 研究目的

レーベル遺伝性視神経症（指定難病 302、LHON）は、ミトコンドリア遺伝子変異により比較的急激な中心暗点で発症し、発症から数か月のうちに両眼の高度な視神経萎縮にと視力低下をきたす疾患である。

本研究班ではLHONの認定基準を作成し、厚労省研究班から支援を得て、日本神経眼科学会とともに患者レジストリ構築を進めてきた。我々は2014年および2019年に日本のレーベル遺伝性視神経症（LHON）の新規発症患者について調査を行い、総患者数を約2500人と推計している。

今回の研究の目的は、我々が集積しているLHON患者のレジストリデータを基に、現時点における日本人LHON患者の詳細な疫学データ、特に患者の属性と視覚的転帰を報告することである。

B. 研究方法

本研究は、2022年7月より日本神経眼科学会評議員会に加盟する89施設を対象とした全国規模の後方視的登録の形式で行われた。各施設に、登録用紙（https://secure2.jtbcom.co.jp/retinal_lhon/）を用いて、通院歴のあるLHON患者全員を登録するよう依頼した。

オンラインでデータベースシステムを構築し、各施設の研究協力者は患者の発症年齢、性別、罹患期間、遺伝子バリエーション（3460、11778、14484、その他）、診断カテゴリー（Definite/Probable/Possibleなど）、診断された施設、家族歴、治療歴、疾患歴、視力データなどの患者情報を入力した。

（倫理面への配慮）

今回の研究に関しては患者の個人情報全てを匿名化し、倫理面に十分配慮して行った。

mt11778G>A バリエントが抽出された。

C. 研究結果

登録された 326 例のうち、不適切なデータ入力などにより 16 例が除外され、さらに発症から 1 年以上経過が観察されていないなどの理由でさらに 37 例が除外され、最終的に 273 例の LHON 患者のデータを解析した。

性別は、男性 238 例 (87.2%)、女性 35 例 (12.8%) であった。発症年齢は平均で 33 歳 (男性の平均が 32 歳、女性の平均が 36 歳) であり、平均観察期間は約 6 年であった。診断のカテゴリーでは、Definite が 49.8%、Probable が 29.3%、Possible が 1.1%、その他が 19.8%であった。

遺伝子バリエントに関しては、11778 G>A が 87.9%、14484 T>C が 7.7%、3460 G>A が 0.3%、その他あるいは不明が 8.0%であった。

行われた治療に関しては、Idebenone 内服が 38 例、Ubidecarenone 内服が 95 例、CoenzymeQ10 内服が 19 例、ATP 内服が 11 例、ビタミン B 内服が 132 例、ビタミン C 内服が 88 例、Unoprostone 点眼が 52 例、他が 68 例、治療なしが 67 例であった (重複あり)。

重回帰分析の結果では、視力予後の悪化を規定する因子として、高齢および

D. 考察

今回我々は、レジストリに登録された患者情報を基に、多数の日本人における LHON の特徴を研究した。疫学的な特性に関しては従来の報告と同様に、若年男性の発症が多く、遺伝子バリエントは 11778 が半数近くを占めており、若年発症であることと m.11778G>A 以外のミトコンドリア変異であることが良好な視力予後と関連していた。

治療内容と視力予後に関しては、今回明確な関連はみられなかったが、これに関しては今回の研究が後ろ向き調査であり、各種治療の容量や内容、また内服期間などが症例により異なっており、現時点で明確な結論を導き出すことが困難であると考えられた。

E. 結論

データベースシステム構築により LHON の患者の疫学的な実態がより詳細に把握できるようになった。今後さらに多数の症例の登録が望まれる。

F. 健康危険情報 : なし

G. 研究発表

1. 論文発表 (2024 年以前のものも含む)

- 1) Takano F, Ueda K, Godefrooij DA, Yamagami A, Ishikawa H, Chuman H, Ishikawa H, Ikeda Y, Sakamoto T, Nakamura M. Incidence of Leber hereditary optic neuropathy in 2019 in Japan: a second nationwide questionnaire survey. Orphanet J Rare Dis. Aug 20;17(1):319, 2022.
- 2) Takano F, Ueda K, Chihara N, Arai M, Sakamoto M, Kurimoto T, Yamada-Nakanishi Y, Nakamura M. Leber Hereditary Optic Neuropathy "Plus" with the m.14487 T>C

Mutation as the Causality of Hemidystonia: A Case Report. Case Rep Ophthalmol. 2024 Nov 13;15(1):852-858.

- 3) Takano F, Ueda K, Kurimoto T, Arai M, Nagai T, Yamada-Nakanishi Y, Nakamura M. An exploratory study to evaluate efficacy and safety of frequent Transcutaneous Electrical Stimulation for Leber Hereditary Optic Neuropathy. Sci Rep. 2025 Feb 9;15(1):4829.
- 4) Takahashi Y, Kezuka T, Shikishima K, Yamagami A, Chuman H, Nakamura M, Ueki S, Kimura A, Hashimoto M, Tatsui S, Mashimo K, Ishikawa H. Usage status of biologics for the chronic treatment of optic neuritis in neuromyelitis optica spectrum disorders in Japan. Jpn J Ophthalmol. 2025 Jan;69(1):81-92.

2. 学会発表

- 1) 上田香織、山上明子、石川裕人、中馬秀樹、石川均、池田康博、近藤峰生、中村誠. レーベル遺伝性視神経症に関する患者データベースに基づく疫学調査. 日本眼科学会総会. 2025年4月18日. 東京.

H. 知的財産権の出願・登録状況

1. 特許取得 なし
2. 実用新案登録 なし
3. その他 なし

レーベル遺伝性視神経症に関する 患者データベースに基づく疫学調査

Epidemiology and natural history of Leber hereditary optic neuropathy in Japan

Kaori Ueda¹ Akiko Yamagami² Hiroto Ishikawa³ Hideki Chuman⁴
Hitoshi Ishikawa⁵ Yasuhiro Ikeda⁴ Mineo Kondo⁶ Makoto Nakamura¹

1 Division of Ophthalmology, Department of Surgery, Kobe University Graduate School of Medicine, Kobe, Japan

2 Inouye Eye Hospital, Tokyo, Japan

3 Department of Ophthalmology, Hyogo Medical University, Nishinomiya, Hyogo, Japan

4 Department of Ophthalmology, Mirai Eye and Skin Clinic, Osaka, Japan

5 Department of Ophthalmology, University of Miyazaki, Miyazaki, Japan

6 Department of Orthoptics and Visual Science, Kitasato University School of Allied Health Sciences, Kanagawa, Japan.

7 Department of Ophthalmology, Mie University Graduate School of Medicine, Mie, Japan

Japanese Ophthalmological Society COI disclosure

Kaori Ueda, Akiko Yamagami
Hiroto Ishikawa, Hideki Chuman
Hitoshi Ishikawa, Yasuhiro Ikeda
Mineo Kondo, Makoto Nakamura

All authors have no conflicts of interest to disclosure.

Introduction

- Nationwide epidemiological surveys about LHON in Japan were conducted in 2014 and 2019 in Japan.

(Ueda K, et al. J Epidemiol. 2017)

(Takano F, et al. Orphanet J Rare Dis. 2022)

- The total number of newly diagnosed cases was calculated as **69** (62 were males and 7 were females), and the total number of patients was estimated to be **2491** (2333 males and 158 females).

(Takano F, et al. Orphanet J Rare Dis. 2022)

Purpose

- This study aimed to provide detailed epidemiological data of Japanese patients with LHON, specifically patient demographics and visual outcomes.

Methods

- This study is a nationwide retrospective registry starting from July 2022 that included 89 facilities affiliated with the council members of the Japanese Neuro-Ophthalmology Society.
- Each facility was asked to register all patients with LHON with a history of hospital visits using a registration form (https://secure2.jtbcom.co.jp/retinal_lhon/).

登録

必須 は必須項目となっております。必ずご記入ください。

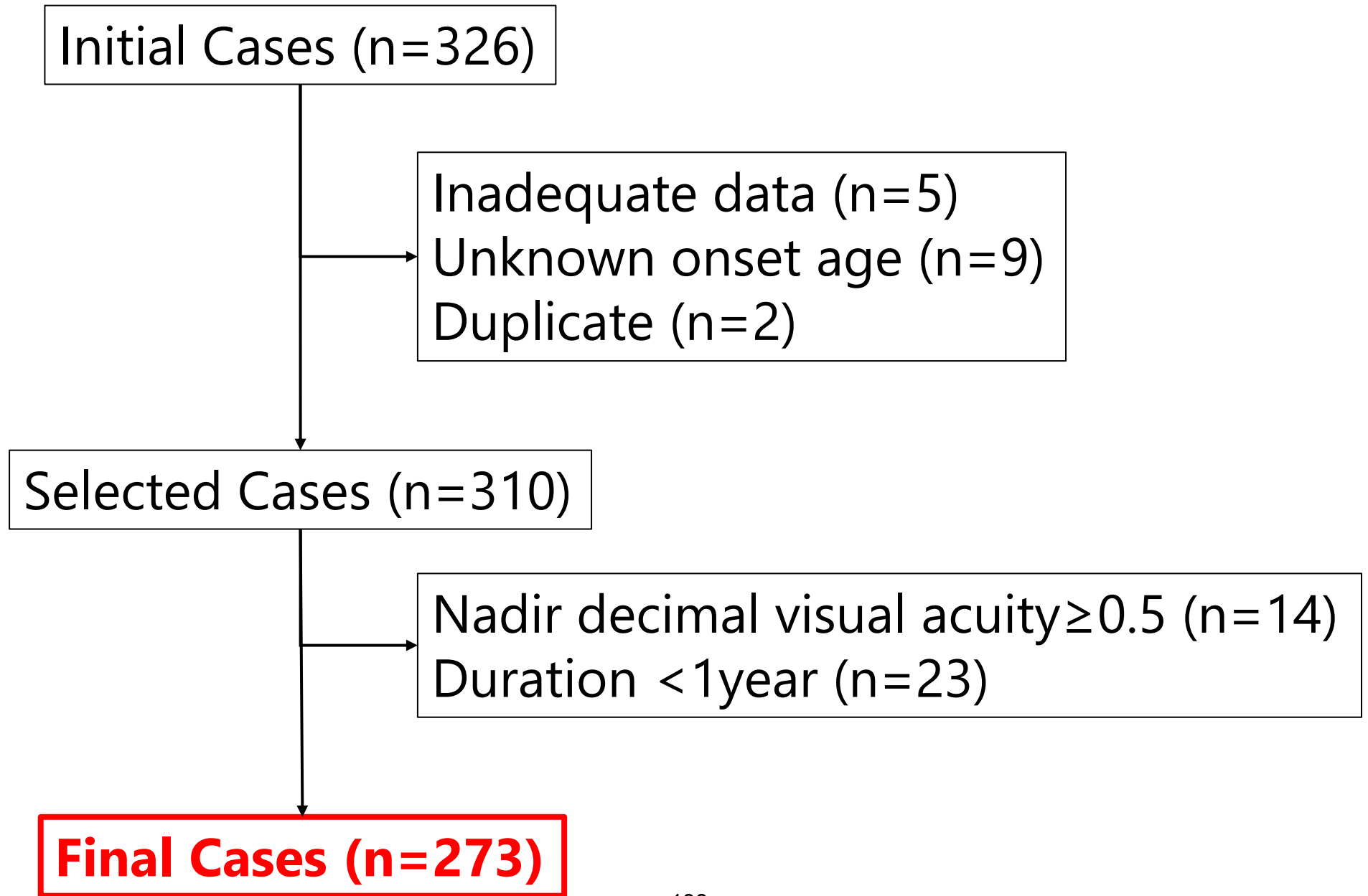
患者情報

症例コード	001-
登録施設 必須	<input type="text" value="神戸大学(コウペダイガク)"/>
登録者名 必須	<input type="text" value="選択してください"/>
症例番号	*** (* 印には自動振り分けされた数字が入ります。)
性別 必須	<input type="radio"/> 男性 <input type="radio"/> 女性
発症年齢 必須	<input type="text" value="--"/> 歳
現在年齢 必須	<input type="text" value="--"/> 歳
罹患期間 必須	<input type="text" value="--"/> 年
遺伝子変異箇所 必須 (複数選択可)	<input type="checkbox"/> 3460 <input type="checkbox"/> 11778 <input type="checkbox"/> 14484 <input type="checkbox"/> その他⇒コメント入力

Patient Information

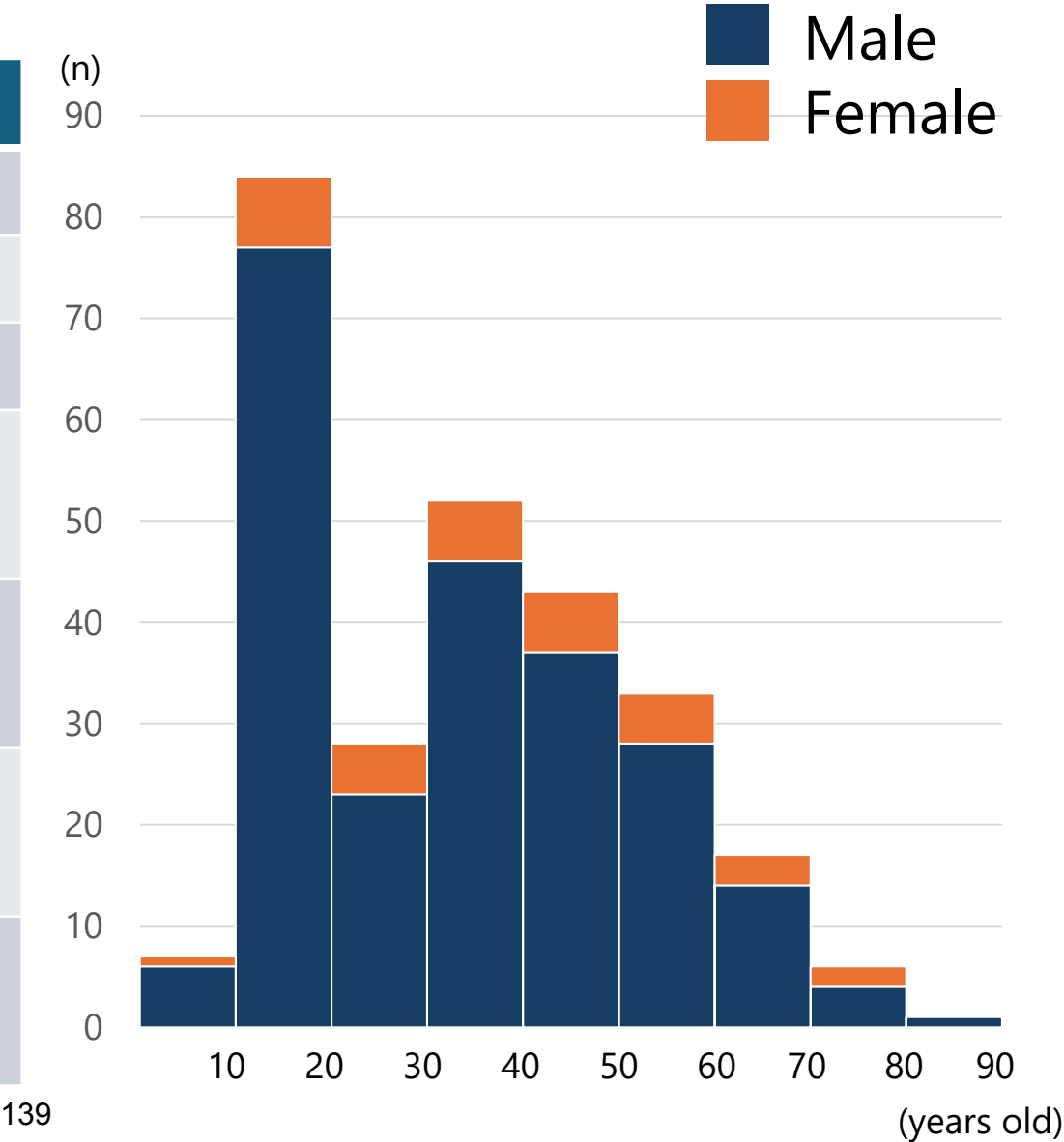
- 1) Sex
 - 2) Age at onset
 - 3) Duration of disease
 - 4) Location of mitochondrial gene variants
 - 5) **Diagnostic category**: Definite / Probable/ Possible / **Longstanding**
 - 6) Facility that diagnosed LHON
 - 7) Family history
 - 8) Medications
 - 9) Comorbid disorders
 - 10) Comorbid mitochondrial diseases
 - 11) Nadir decimal visual acuity
 - 12) Latest decimal visual acuity
- Converted to logMAR
Counting fingers 2.0/ Hand motion 2.3/ Light perception 4.0

(Carelli V, et al. *Ophthalmol Ther* 2023)



Result : Summary of the registered cases

Category		n
Number of patients	Total	273
	Male	238
	Female	35
Initial age (years old) mean (IQR)	Total	33.0 (17.0–48.0)
	Male	32.0 (16.5–47.0)
	Female	36.0 (22.0–55.0)
Duration (years) mean (IQR)		6 (2.50–11.0)



Category

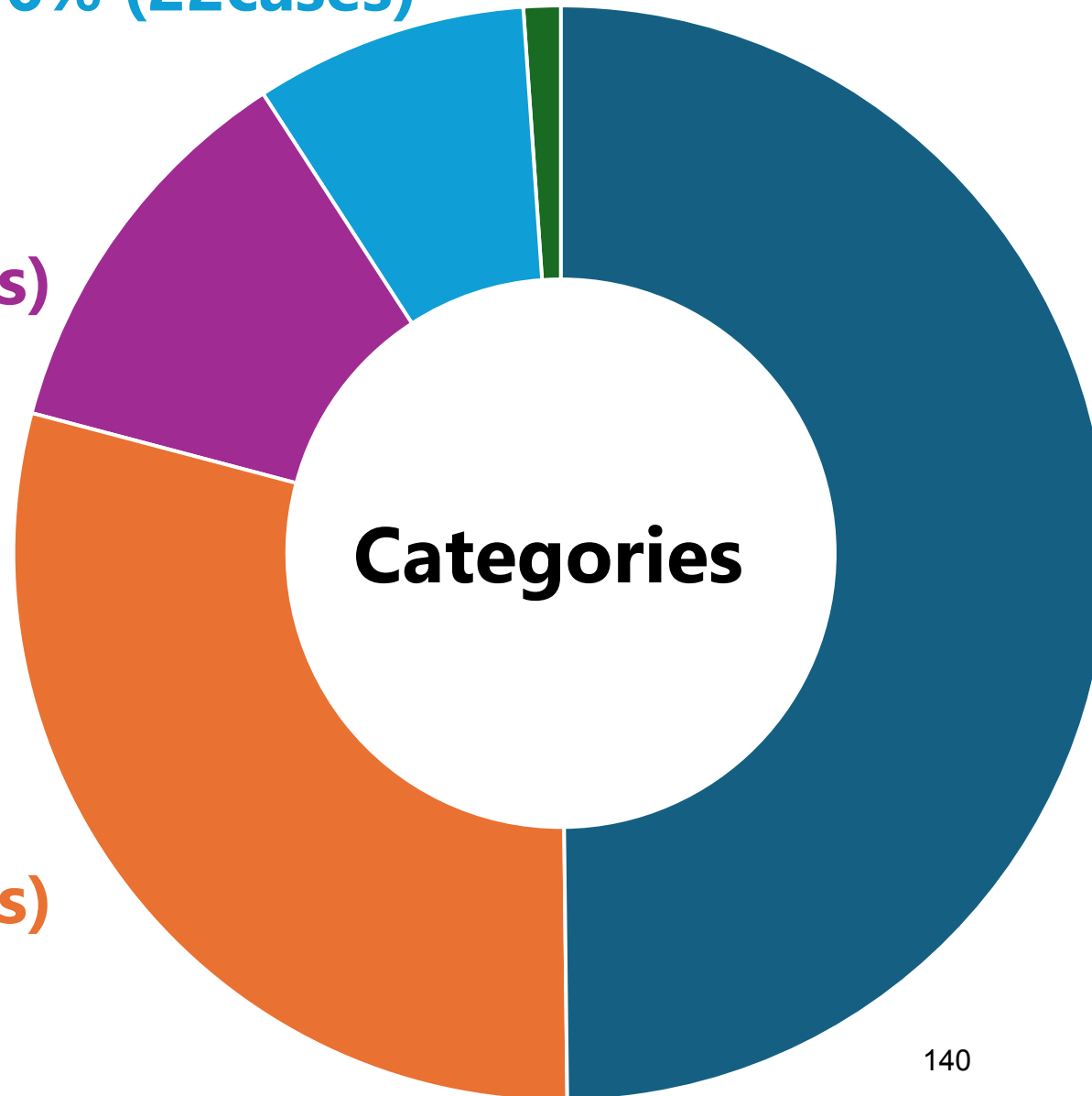
Longstanding
8.06% (22cases)

Possible
1.10% (3cases)

Others
11.7% (32cases)

Probable
29.3% (80cases)

Definite
49.8% (136cases)



Variant

Others

8.06% (22cases)

Unknown

1.10% (3cases)

14484 T>C
7.7% (21cases)

3460 G>A
0.4% (1case)

**Mitochondrial
Variant**

11778 G>A
87.9% (240cases)

※Other variants

3394 T>C

3434 A>G

3497 C>T

4171 C>A

5457 A>G

9101 T>G

12811 T>C

13501 G>A

14487 T>C

14687 C>T

Medication

Category	n
Idebenone	38
Ubidecarenone	95
Coenzyme Q10	19
ATP	11
Vitamin B	132
Vitamin C	88
isopropyl unoprostone	52
other	68
No medication	67

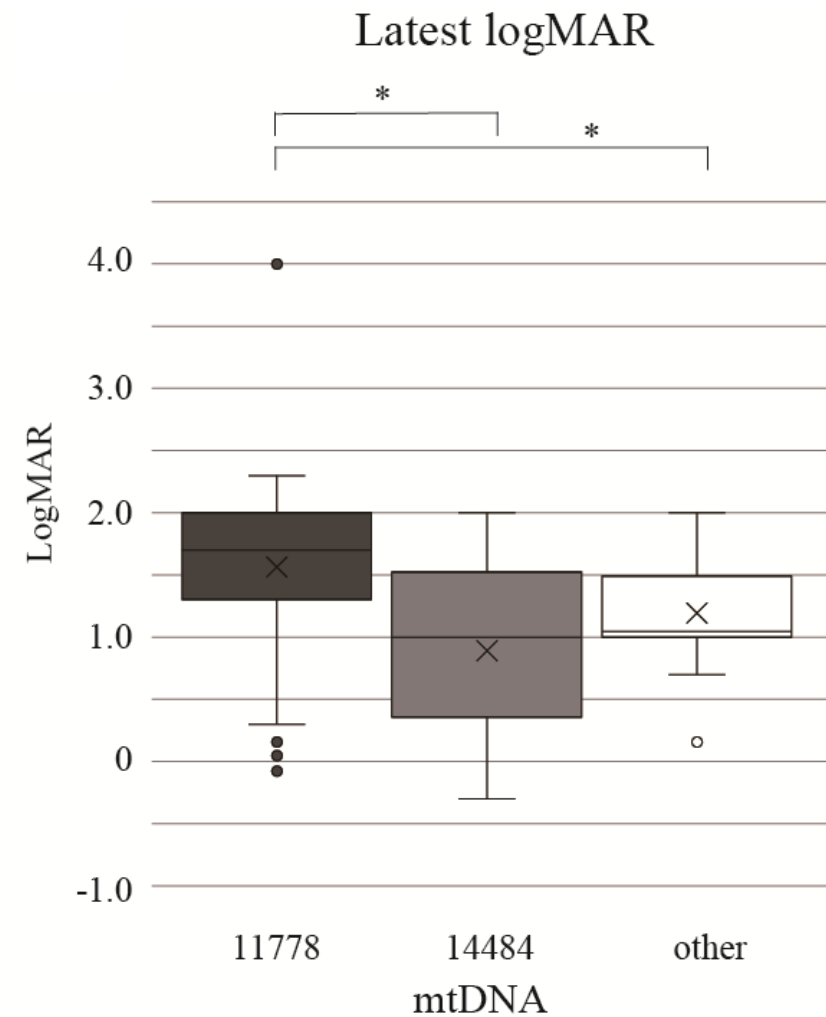
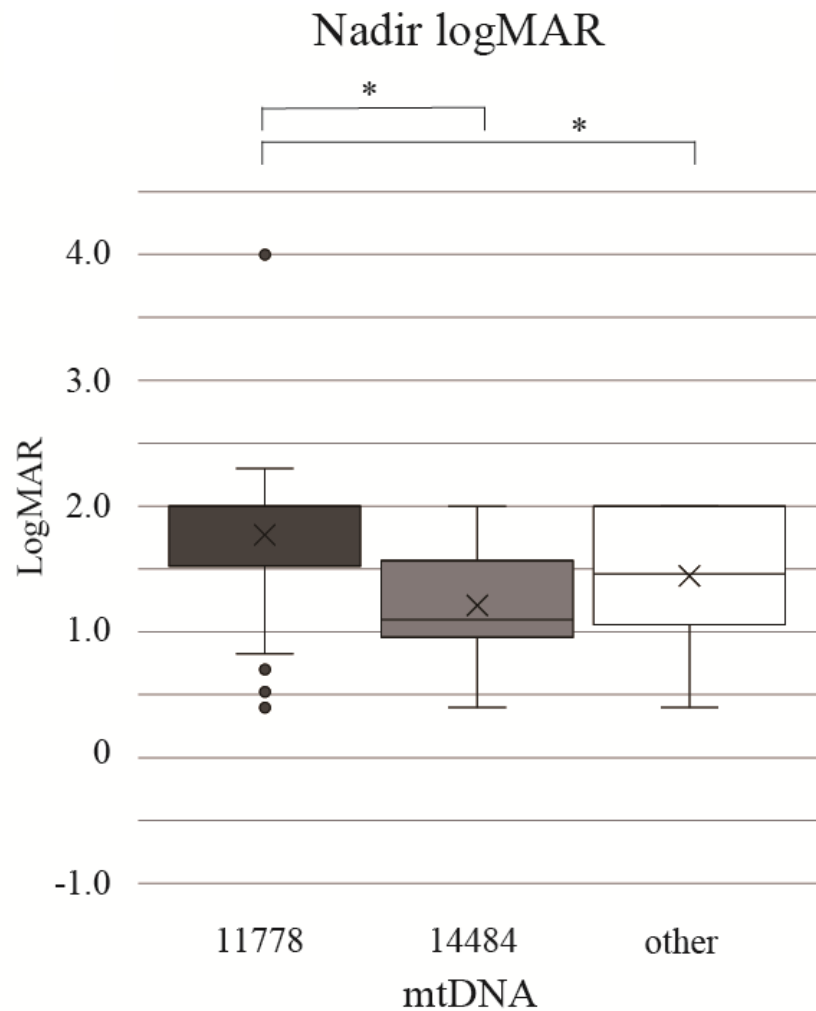
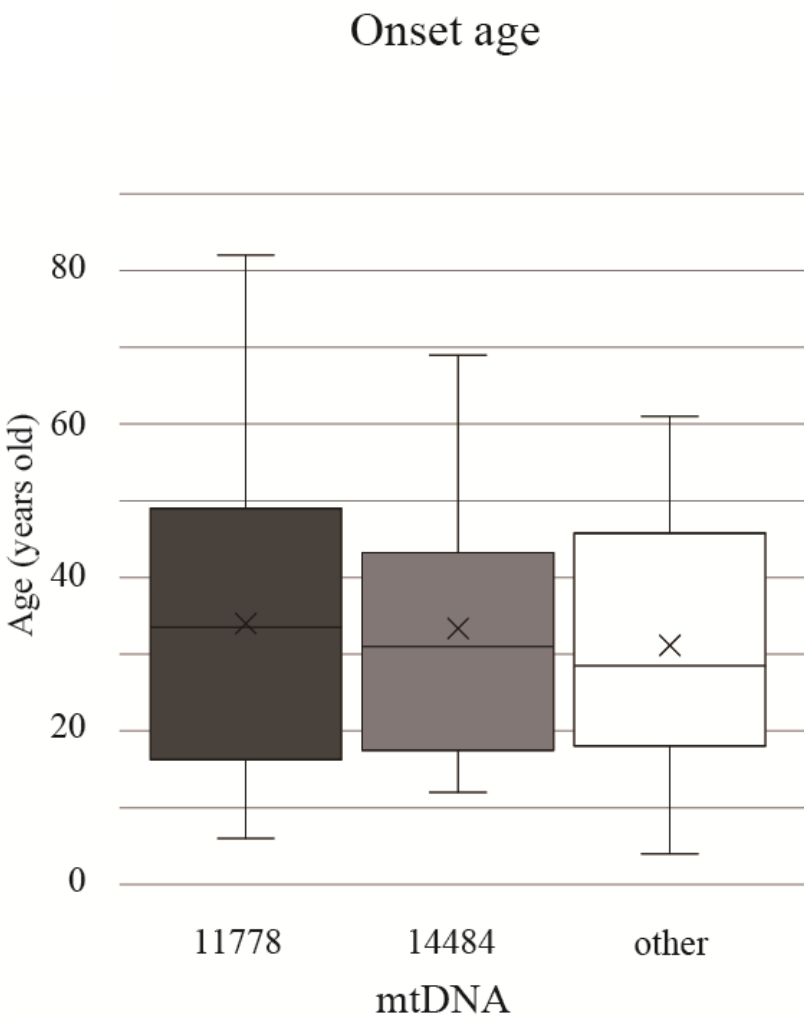
Others; Medication of glaucoma / Cyanocobalamin / Tocopherol acetate
Taurine / Medication of multiple sclerosis

Comorbid Diseases

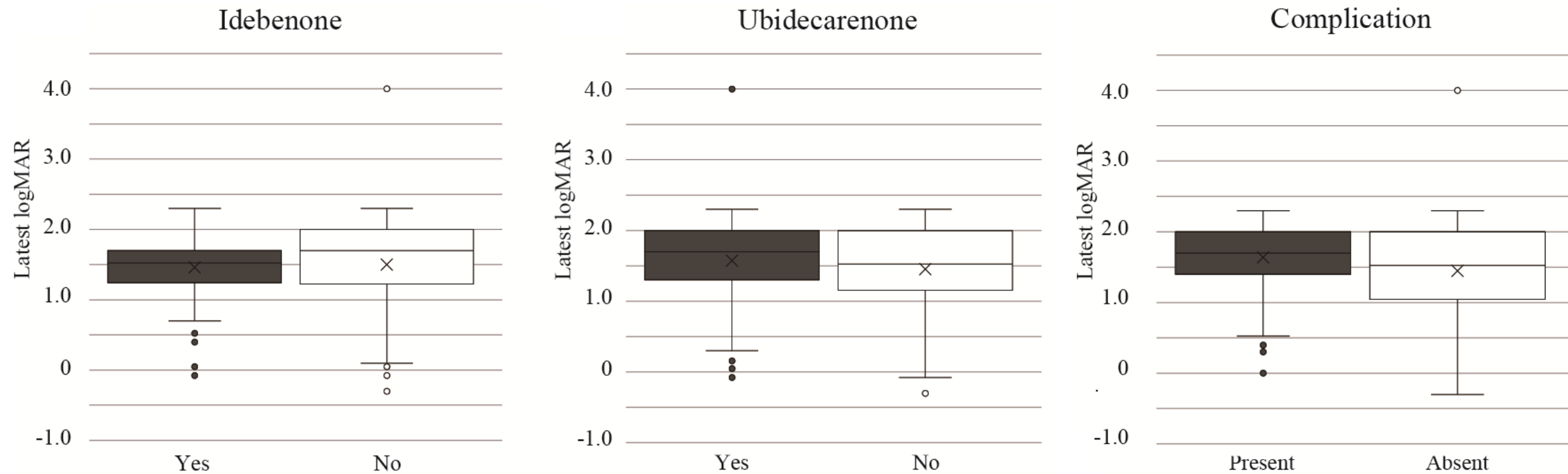
Comorbid Diseases	n
Glaucoma	17
Retinal vein occlusion	6
Multiple Sclerosis	1
MELAS	1
MERRF	0
CPEO	0
Kearns–Sayre Syndrome	0
Leigh encephalopathy	2
Diabetes Mellitus	3
Other	59
No diseases	208

Cardiovascular disease	3
Respiratory disease	3
Gastrointestinal disease	3
Renal disease	1
Metabolic disease	1
Neurological disease	11
Ophthalmological disease	21
Otorhinolaryngologic disease	2
Dermatological diseases	2
Hematological disease	1
Psychiatric disease	7
Alcohol-related disorder	4

Result : mtDNA variant and other factors



Result : Latest visual acuity and other factors



Visual acuity

146

	Median logMAR (IQR)		
	Nadir	Latest	difference
Total	1.70 (1.49, 2.00)	1.70 (1.22, 2.00)	0.000 (-0.301, 0.00)
Age			
<12yo	1.19 (1.00, 1.52)	1.00 (0.429, 1.22)	-0.199 (-0.675, 0.00)
≥12yo	2.00 (1.52, 2.00)	1.70 (1.30, 2.00)	0.00 (-0.301, 0.00)
Mutation			
mt11778 G>A	2.00 (1.52, 2.00)	1.70 (1.30, 2.00)	0.00 (-0.301, 0.00)
mt14484 T>C	1.09 (0.956, 1.57)	1.00 (0.354, 1.52)	-0.190 (-0.379, 0.00)
other	1.46 (1.06, 2.00)	1.05 (1.00, 1.49)	-0.0880 (-0.433, 0.00)
Idebenone			
Yes	1.70 (1.52, 2.00)	1.52 (1.28, 1.70)	0.00 (-0.301, 0.00)
No	1.70 (1.40, 2.00)	1.70 (1.22, 2.00)	0.00 (-0.301, 0.00)
Ubidecarenone			
Yes	2.00 (1.70, 2.00)	1.70 (1.30, 2.00)	0.00 (-0,301, 0.00)
No	1.70 (1.40, 2.00)	1.52 (1.15, 2.00)	0.00 (-0.301, 0.00)
Complication			
Present	2.00 (1.65, 2.00)	1.70 (1.40, 2.00)	0.00 (-0.301, 0.00)
Absent	1.70 (1.40, 2.00)	1.52 (1.05, 2.00)	0.00 (-0.301, 0.00)

Result : multivariate analysis

147

Coefficients:	Estimate	Std. Error	t value	Pr(> t)
(Intercept)	1.144698	0.132754	8.623	6.16e−16
Sex	0.069594	0.101260	0.687	0.4925
Age of onset	0.005978	0.002131	2.806	0.0054
Duration	−0.000182	0.003746	−0.049	0.9613
Complications	0.112099	0.081855	1.369	0.1720
mtDNA (14484)	−0.671374	0.126073	−5.325	2.16e−07
mtDNA (other)	−0.368783	0.164850	−2.237	0.0261
Idebenone use	0.036440	0.100762	0.362	0.7179
Ubidecarenone use	0.088663	0.075759	1.170	0.2429

Discussion

1. Visual Acuity
2. Male to female ratio
3. Idebenone
4. LHON plus

Discussion

Natural history of visual acuity

- CRR(clinically relevant recovery):
off-chart→on-chart or improvement in logMAR 0.2 or better
 - Natural history : 17%
 - Idebenone : 31%
 - Gene therapy : 59%
- In this study, CRR was calculated 31.8%

(Newman, N. J. et al, Surv Ophthalmol, 2024)

	Median logMAR (IQR)		
	Nadir	Latest	difference
Total	1.70 (1.49, 2.00)	1.70 (1.22, 2.00)	0.000 (-0.301, 0.00)
Age			
<12yo	1.19 (1.00, 1.52)	1.00 (0.429, 1.22)	-0.199 (-0.675, 0.00)
≥12yo	2.00 (1.52, 2.00)	1.70 (1.30, 2.00)	0.00 (-0.301, 0.00)
Mutation			
mt11778 G>A	2.00 (1.52, 2.00)	1.70 (1.30, 2.00)	0.00 (-0.301, 0.00)
mt14484 T>C	1.09 (0.956, 1.57)	1.00 (0.354, 1.52)	-0.190 (-0.379, 0.00)
other	1.46 (1.06, 2.00)	1.05 (1.00, 1.49)	-0.0880 (-0.433, 0.00)
Idebenone			
Yes	1.70 (1.52, 2.00)	1.52 (1.28, 1.70)	0.00 (-0.301, 0.00)
No	1.70 (1.40, 2.00)	1.70 (1.22, 2.00)	0.00 (-0.301, 0.00)
Ubidecarenone			
Yes	2.00 (1.70, 2.00)	1.70 (1.30, 2.00)	0.00 (-0,301, 0.00)
No	1.70 (1.40, 2.00)	1.52 (1.15, 2.00)	0.00 (-0.301, 0.00)
Complication			
Present	2.00 (1.65, 2.00)	1.70 (1.40, 2.00)	0.00 (-0.301, 0.00)
Absent	1.70 (1.40, 2.00)	1.52 (1.05, 2.00)	0.00 (-0.301, 0.00)

Discussion

Male to female ratio

- In the present study, male : female = 6.8 : 1, similar to previous studies.
- At younger than 5 years and older than 45 years, the male-to-female ratio was approximately 1:1, that is reasonable considering the effect of sex hormone.
(Poincenot, L. et al. Ophthalmology, 2020)
(Jankauskaitė, E. et al. J Appl Genet, 2020)
(Pisano, A. et al. Hum Mol Genet, 2015)
- In the latest worldwide epidemiological survey, the overall male : female = 3:1 – the authors mentioned the “**strong bias for testing man**”.

Discussion

Idebenone

- Univariate and multivariate analyses in the current study **did not reveal beneficial effect** of idebenone (IDEBPRO™) in the visual outcomes in the registered patients.
- The reason for the present result may be due to short-term duration of IDEBPRO™ medication.
- Another possible reason may be that IDEBPRO™ is not an authentic medication but a supplement, so that the magnitude of action as idebenone may be weak.

Discussion

LHON plus

- LHON was associated with increased mortality and incidence of several disorders including stroke, demyelinating disorder, dementia, and epilepsy.
(Vestergaard N., IOVS, 2017)
- This survey may not have picked up enough comorbidities.

Conclusion

- In Japan, most of LHON patients do not recover at all from their nadir visual acuity.
- Younger age and mitochondrial variants other than m.11778G>A were associated with better visual outcomes.
- This survey will be continued in the future, and more cases will be analyzed comprehensively.

Acknowledgement

Funding: grant-in-aid from the Ministry of Health, Labour and Welfare (23FC1043).

Institutes registered LHON cases (in random order/without honorifics)

Mineo Ozaki (Ozaki Eye Hospital)	Satoshi Ueki (Niigata University)
Yuka Sogabe (Mitoyo General Hospital)	Masakazu Takayama
Sinji Ohkubo (Ohkubo Eye Clinic)	(Hamamatsu University School of Medicine)
Akinori Baba (The Jikei University School of Medicine)	Makoto Aihara (The University of Tokyo)
Masato Hashimoto (Nakamura Memorial Hospital)	Toru Nakazawa (Tohoku University)
Takahisa Hirokawa	Takeshi Kezuka (Tokyo Medical University)
(Osaka Medical and Pharmaceutical University)	Takao Hayashi (Teikyo University)
Takayuki Baba (Chiba University)	Hiromasa Sawamura (Teikyo University)
Masayuki Hata (Kyoto University)	Shin Morisawa (Okayama University)
Koichiro Tamura (Oita University)	Hajime Shinoda (Keio University)
Nobuo Takeda (Ishikawa Prefectural Central Hospital)	Yoko Amaya (Fukui Prefectural Hospital)
Tomoyuki Maekubo (Miyake Eye Hospital)	Yoshiaki Shimada (Fujita Health University)
Tomomi Higashide (Kanazawa University)	Ryoma Yasumoto (Kitazato University Hospital)
Kiyotaka Nakamagoe (University of Tsukuba)	Fumio Takano (Kobe University)
Toshiyuki Yokoyama (Juntendo University Nerima Hospital)	

Administrative support: Chiaki Saito (The Japanese Neuro-Ophthalmology Society)

Case Report

Leber Hereditary Optic Neuropathy “Plus” with the m.14487 T>C Mutation as the Causality of Hemidystonia: A Case Report

Fumio Takano^a Kaori Ueda^a Norio Chihara^b Mina Arai^a
Mari Sakamoto^a Takuji Kurimoto^c Yuko Yamada-Nakanishi^a
Makoto Nakamura^a

^aDivision of Ophthalmology, Department of Surgery, Kobe University Graduate School of Medicine, Kobe, Japan; ^bDivision of Neurology, Department of Internal Medicine, Kobe University Graduate School of Medicine, Kobe, Japan; ^cKurimoto Eye Clinic, Osaka, Japan

Keywords

Leber hereditary optic neuropathy plus · Rare mitochondrial point mutation · Dystonia

Abstract

Introduction: Leber hereditary optic neuropathy (LHON) complicated with extraocular symptoms is called LHON plus. We describe a case of LHON plus with a rare mutation, which also caused dystonia. **Case Presentation:** An 18-year-old male patient developed symptoms of dystonia at the age of 15 years. Two years later, he noticed decreased visual acuity and central scotoma in the left eye. One month later, the same symptoms occurred in the right eye. Although the optic discs in both eyes revealed mildly redness and edematous change, no abnormal findings were detected on fluorescence fundus angiography and orbital magnetic resonance imaging. Mitochondrial deoxyribonucleic acid (mtDNA) sequencing detected the m.14487 T>C mutation. From clinical course and fundus findings, the case was diagnosed LHON. The optic nerve gradually atrophied and central scotoma remained. **Conclusion:** The m.14487 T>C mutation is one of the causative mutations in patients with dystonia or Leigh encephalopathy and a minor mutation in patients with LHON. However, in the present case, ocular symptoms were more severe than systematic symptoms and the disease course was consistent with LHON. For the above reasons, this case can be diagnosed as LHON plus. Whole mtDNA sequencing is important in diagnosing LHON if none of the three major mutations are detected.

© 2024 The Author(s).
Published by S. Karger AG, Basel

Correspondence to:
Kaori Ueda, kueda@med.kobe-u.ac.jp

Introduction

Leber hereditary optic neuropathy (LHON) is an acute or subacute optic neuropathy caused by point mutations in mitochondrial genes, characterized by decreased visual acuity and central scotoma. Typical LHON is caused by mitochondrial deoxyribonucleic acid (mtDNA) point mutation, followed by mitochondrial dysfunction in retinal ganglion cells [1]. One of three major mutations, m.3460 G>A, m.11778 G>A, or m.14484 T>C, is detected in over 90% of LHON cases, and less than 10% of the point mutations have detected outside of these regions [1].

Some LHON cases complicated by systemic disease are referred to as LHON “plus.” Mitochondrial diseases are expected to be related with high-energy requirement tissues, such as heart, brain, or muscles [2]. Previous nationwide survey also reported that cerebrovascular or cardiovascular diseases were more likely to be complicate by LHON [3]. In this report, we describe a case of LHON with dystonia and the rare m.14487 T>C mutation. The CARE Checklist has been completed by the authors for this case report, attached as online supplementary material (for all online suppl. material, see <https://doi.org/10.1159/000542202>).

Case Presentation

An 18-year-old male developed right-sided dystonia symptoms around the age of 15 years. At the age of 16 years, the patient underwent a thorough examination at the Division of Neurology in Kobe University Hospital to determine the cause of his symptoms. Clinical examination revealed right arm rigidity, right hand dominant bilateral postural fine regular tremor in the hands, and right foot inward turning posture when walking. Cerebrospinal fluid analysis showed the following: normal cell count, total protein, and glucose concentration; IgG index of 0.61 (normal); and no cerebrospinal fluid-specific oligoclonal bands. Serum lactic acid and pyruvate levels were 13.5 mg/dL (normal range: 3–17 mg/dL) and 1.25 mg/dL (normal range: 0.3–0.94 mg/dL), respectively. Galactocerebrosidase enzyme levels in lymphocytes and serum levels of very long-chain fatty acids were normal. The patient also had low levels of circulating ceruloplasmin (17.2 g/dL, normal range: 21–37 mg/dL), but normal levels of urinary copper (16 µg/L, normal range: <36 µg/L). Intracranial magnetic resonance imaging (MRI) revealed white matter lesions with high-intensity T2-weighted signals and partial low-intensity T1-weighted signals in the left putamen to the cerebral peduncle (shown in Fig. 1). An ophthalmologic examination revealed no abnormalities in visual function. At that point, the cause of patient's dystonia symptoms and the intracranial MRI lesion had not been determined.

One year and 8 months later, the patient experienced decreased visual acuity in the left eye and visited the ophthalmologist again. The patient had no history of ocular trauma, smoking, drinking, or drug use and no change in dystonia symptoms before or after visual impairment. The patient's older brother also had mild dystonia symptoms, but there were no family histories, including ophthalmologic disease. Decimal visual acuity was RV = 1.0 ($1.0 \times S + 5.00D$), LV = 0.2 ($0.2 \times S + 5.00D$), respectively. The light reflex was prompt and complete in both eyes without relative afferent pupillary defect. The critical flicker frequency was 36.0 Hz in the right eye and 28.5 Hz in the left eye. The visual field showed a small central scotoma in the left eye (shown in Fig. 2a). The optic discs were mildly hyperemic and edematous in both eyes, and the peripapillary capillaries exhibited mild telangiectasia (shown in Fig. 2b). Fundus fluorescein angiography showed no abnormal findings, including leakage of fluorescein from optic disc (shown in Fig. 2c) which suggested no inflammatory findings in the optic disc or retina. All blood test results were within reference ranges. Orbital and intracranial magnification MRI showed no lesions in the visual pathway. One month after the onset of symptoms

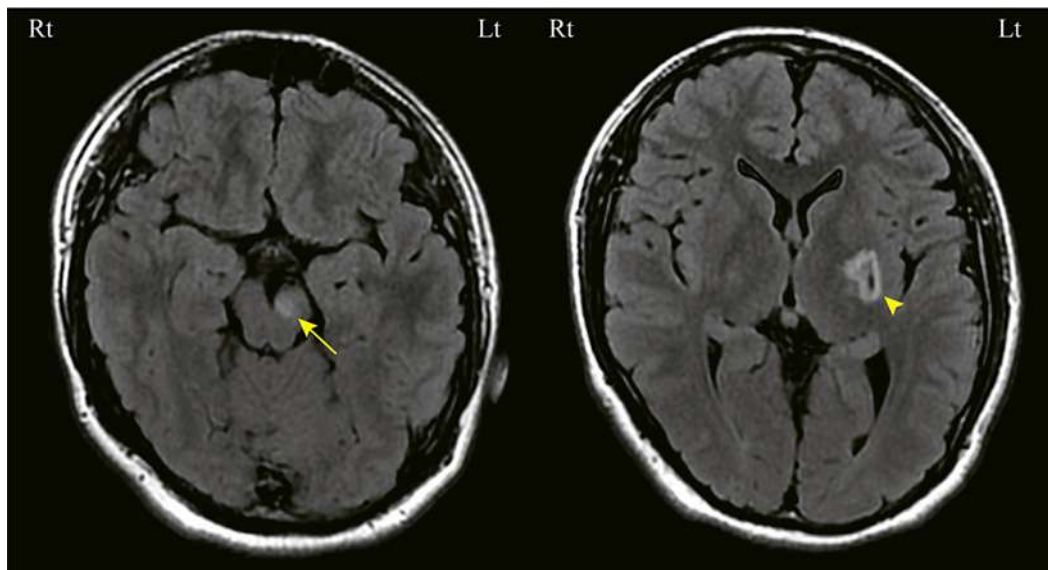


Fig. 1. Head magnetic resonance imaging during a close examination for dystonia. White lesions were detected from the left putamen to the cerebral peduncle (arrow, arrowhead, FLAIR image).

in the left eye, similar symptoms, decreased visual acuity and central scotoma, appeared in the right eye. LHON was suspected from the clinical course and results of examinations. As three major points of mutations, m.3460 G>A, m.11778 G>A, and m.14484 T>C, were negative, the entire mitochondrial DNA sequence was performed to search for rare mutations. The m.14487 T>C mutation (91% of heteroplasmy) was detected, which was a causative mutation of dystonia and Leigh encephalopathy. About 1 year after the onset of the ophthalmologic symptoms, the patient's optic nerves completely atrophied in both eyes (shown in Fig. 3a, b). His symptoms stabilized with decimal visual acuities of RV = 0.04 ($0.07 \times S + 5.50D$) and LV = 0.08 ($0.09 \times S + 4.50D$) with central scotoma in both eyes (shown in Fig. 3c), as well as dystonia symptoms did not exacerbate overtime.

Discussion

In this case, the patient developed from dystonia, leading to the diagnosis of LHON plus. Although this is a rare case, we believe it is a very educational case to consider the differential disease of dystonia.

As whole sequencing of mitochondrial gene mutations becomes more widespread, the number of reported cases of rare mutations, such as the present case, will increase. Several LHON cases with rare mutations have been reported [4]. The m.14487 T>C is a known causative mutation for Leigh encephalopathy and dystonia [5–7]. On the other hand, few papers reported this mutation point as the rare mutation of LHON [8]. Optic atrophy in Leigh's encephalopathy is thought to progress slowly in both eyes simultaneously, whereas optic nerve lesions or symptoms in typical LHON cases develop rapidly in one eye at a time with the interval of several weeks. In cases of Leigh encephalopathy with severe systemic symptoms, it may be difficult to follow up visual function in some cases, and when such cases are complicated by optic atrophy, it is difficult to distinguish them from LHON. However, in the present case, the systemic symptoms were mild and stabilized, which enabled the ophthalmological follow-up. In addition, the clinical course of the disease helped distinguish between these two

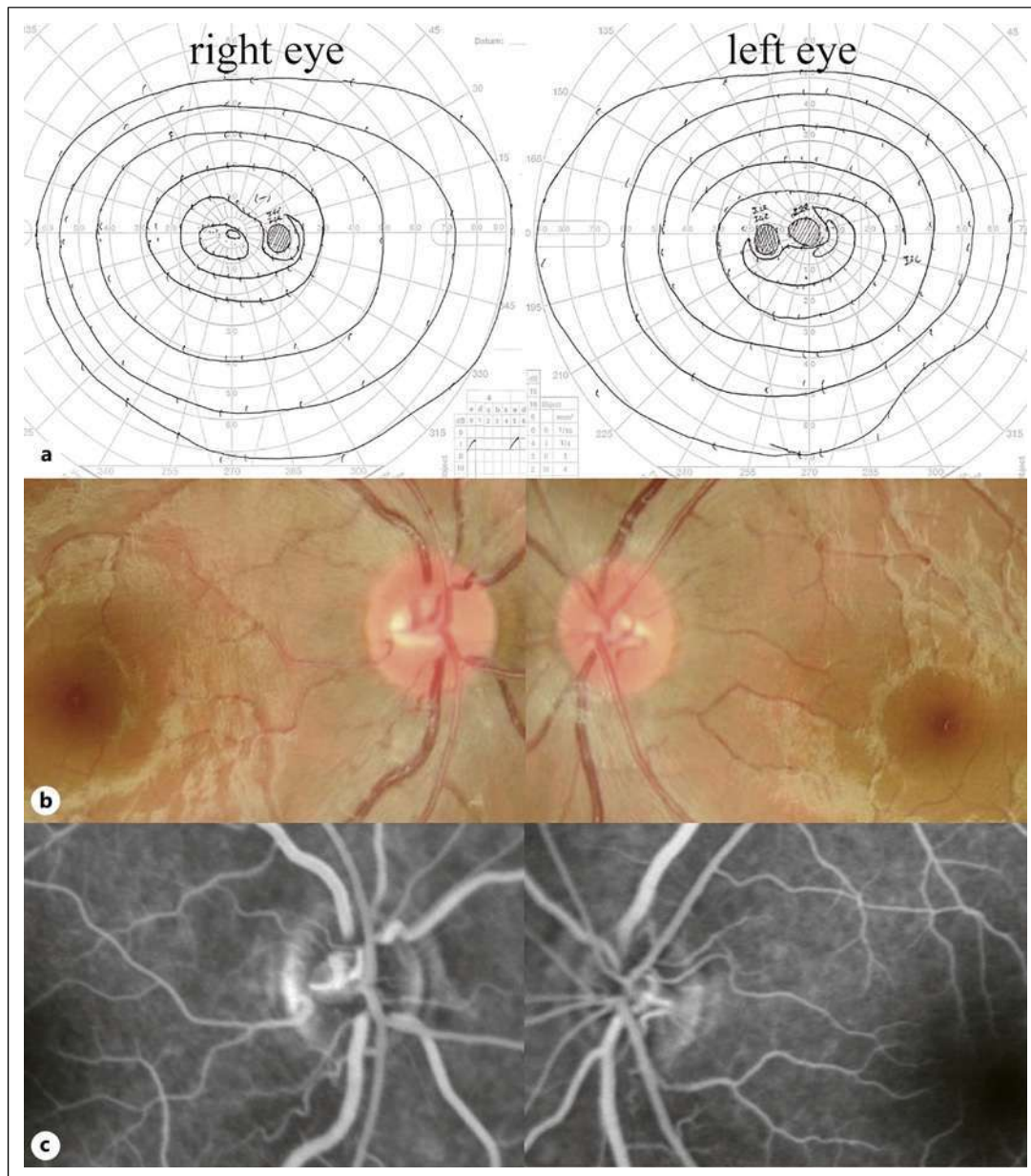


Fig. 2. Ophthalmologic findings immediately after the onset of LHON. **a** The visual field shows a left central scotoma. **b** The optic disc is hyperemic with telangiectasia. **c** Fluorescein fundus fluorescence angiography shows no leakage of fluorescence in either eye.

diseases. The ophthalmological symptoms developed in one eye, followed by the other eye after an interval of 1 month, and the patient showed no relative afferent pupillary defect, which was characteristic in LHON. The fundus image revealed characteristic mild papilledema without leakage of fluorescein, which was also typical finding in LHON. The m.14487 T>C mutation is unique in that the mutation content is 91%, which is close to homoplasmy. High mutation rate is usually related to the severity of the disorder, and this case had only mild dystonia and ocular symptoms. A detailed examination of the right-sided dystonia symptoms and the left putamen region on the MRI did not reveal any alternative diagnoses, including cerebral infarction or other metabolic abnormalities.

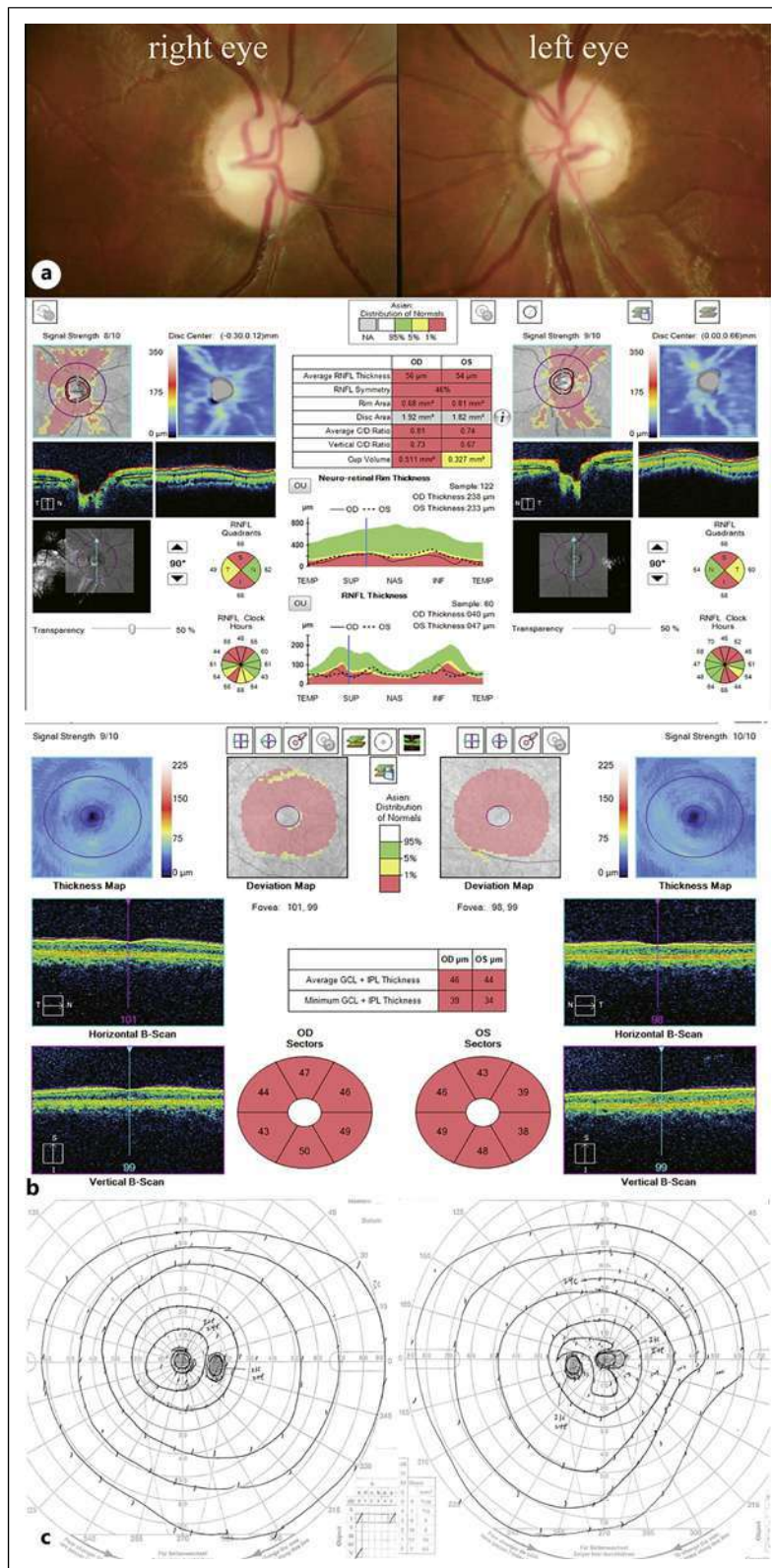


Fig. 3. Chronic phase, 1 year after the onset of the case. **a** The optic disc became atrophic in both eyes. **b** OCT showed thinning of the inner layer of the retina. **c** Central scotoma remained in both eyes.

LHON combined with systemic disease is referred to as LHON “plus.” Most patients with LHON only develop visual dysfunction because LHON mainly affects the retinal ganglion cells. However, in a nationwide survey conducted in Denmark, patients with LHON had a higher incidence of central/peripheral nerve disease, cardiovascular disease and alcohol-related disorders as LHON plus, and a significantly increased mortality rate [3]. LHON itself is not associated with mortality, but it can have serious life-threatening effects depending on the complicating disease as LHON plus. The widespread use of whole sequencing will increase the detection of rare mutations in mitochondrial genes, such as this case.

Statement of Ethics

Written informed consent was obtained from the patient and parent for publication of all clinical course and data. This report does not include any identifying information of the patient. This case report was conducted in accordance with the Declaration of Helsinki. Ethical approval is not required for this study in accordance with local or national guidelines.

Conflict of Interest Statement

The authors have no conflicts of interest.

Funding Sources

This case was not received any funding support.

Author Contributions

F.T., K.U., N.C., M.A., and M.S. examined the patients. K.U. wrote the manuscript. N.C., M.A., M.S., T.K., and Y.Y.N. reviewed and edited the manuscript. M.N. supervised the cases.

Data Availability Statement

All data generated or analyzed during this study are included in this article. Further inquiries can be directed to the corresponding author.

References

- 1 Meyerson C, Van Stavern G, McClelland C. Leber hereditary optic neuropathy: current perspectives. Clin Ophthalmol. 2015;9:1165–76. <https://doi.org/10.2147/OPTH.S62021>
- 2 Casanova A, Wevers A, Navarro-Ledesma S, Pruimboom L. Mitochondria: it is all about energy. Front Physiol. 2023;14:1114231. <https://doi.org/10.3389/fphys.2023.1114231>
- 3 Vestergaard N, Rosenberg T, Torp-Pedersen C, Vorum H, Andersen CU, Aasbjerg K. Increased mortality and comorbidity associated with leber's hereditary optic neuropathy: a nationwide cohort study. Invest Ophthalmol Vis Sci. 2017;58(11):4586–92. <https://doi.org/10.1167/iovs.17-21990>
- 4 Nakamura M, Mimura O, Wakakura M, Inatani M, Nakazawa T, Shiraga F. [Designation criteria for Leber's hereditary optic neuropathy]. Nippon Ganka Gakkai Zasshi. 2015;119(5):339–46.

- 5 Tarnopolsky M, Meaney B, Robinson B, Sheldon K, Boles RG. Severe infantile leigh syndrome associated with a rare mitochondrial ND6 mutation, m.14487T>C. *Am J Med Genet.* 2013;161a(8):2020–3. <https://doi.org/10.1002/ajmg.a.36000>
- 6 Leshinsky-Silver E, Shuvalov R, Inbar S, Cohen S, Lev D, Lerman-Sagie T. Juvenile Leigh syndrome, optic atrophy, ataxia, dystonia, and epilepsy due to T14487C mutation in the mtDNA-ND6 gene: a mitochondrial syndrome presenting from birth to adolescence. *J Child Neurol.* 2011;26(4):476–81. <https://doi.org/10.1177/0883073810384615>
- 7 Spyropoulos A, Manford M, Horvath R, Alston CL, Yu-Wai-Man P, He L, et al. Near-identical segregation of mtDNA heteroplasmy in blood, muscle, urinary epithelium, and hair follicles in twins with optic atrophy, ptosis, and intractable epilepsy. *JAMA Neurol.* 2013;70(12):1552–5. <https://doi.org/10.1001/jamaneurol.2013.4111>
- 8 Eckenweiler M, Catarino CB, Gallenmueller C, Klopstock T, Lagrèze WA, Korinthenberg R, et al. Mitochondrial DNA mutation 14487T>C manifesting as Leber's hereditary optic neuropathy. *J Neurol.* 2015;262(12):2776–9. <https://doi.org/10.1007/s00415-015-7955-5>

厚生労働科学研究費補助金（難治性疾患政策研究事業）
分担研究報告書

自己免疫網膜症に関する研究

研究分担者	九州大学・医学研究院・教授 園田 康平 弘前大学・医学研究科・教授 上野 真治
研究協力者	北海道大学・医学研究院・診療講師 安藤 亮 神戸大学・医学研究科・講師 楠原 仙太郎 九州医療センター・医長 長谷川 英一

自己免疫網膜症（Autoimmune retinopathy: AIR）は、網膜細胞を標的とする自己免疫反応による網膜症であり、広義には癌随伴網膜症（CAR）やメラノーマ随伴網膜症（MAR）も含まれる。AIR では網膜細胞が進行性に障害され著しい視機能障害をおこすが、診断基準やバイオマーカーが確立されておらず、日常の眼科診療で診断に苦慮することも多い。そこで本研究班では令和5年度より新たに AIR グループを立ち上げ、日本における AIR の実態調査や診療ガイドライン作成などを行うことを計画した。本年度は、全国 90 施設に送付した AIR に関するアンケート調査の結果をまとめたので報告する。

A. 研究目的

自己免疫網膜症（Autoimmune retinopathy: AIR）は、網膜細胞を標的とする自己免疫反応による網膜症であり、広義には癌随伴網膜症（CAR）やメラノーマ随伴網膜症（MAR）も AIR に含まれる。AIR では網膜細胞が障害されて著しい視機能障害をおこすが、診断基準やバイオマーカーが確立されておらず、日常の眼科診療では診断に苦慮することが多い

AIR の治療に関しても、ステロイドや免疫抑制剤などが有効であるという報告はあるが、標準となる治療法やガイドラインは確立されていない。

そこで本研究班では、令和5年度より新たに AIR グループ（G10）を立ち上げ、日本における AIR の実態調査、診療ガイドラ

イン作成などを行い、指定難病に該当すればその申請も行う予定である。

2 年目である本年の目的は、本邦における AIR の診断治療の現状調査と診断基準作成に向けて行なった全国アンケート調査の結果を報告することである。

B. 研究方法

全国 90 施設に AIR に関するアンケートを送付し、最終的に 28 施設から以下の質問に対する回答が得られた。

Q1：AIR、癌関連網膜症（CAR）、メラノーマ関連網膜症（MAR）の患者数（疑いを含む）とそのうち診断4項目（A：視覚機能異常を引き起こす明らかな原因がない、B：網膜電図異常がある、C：視機能低下を説明できる眼底病変や網膜変性・ジストロ

フィーがない、D: 明らかな眼内炎症がない) を満たす患者数。

Q2: 診断に必須と考えている項目。

Q3: 治療方法。

Q4: 抗網膜抗体の検査方法と、抗体の意義についての考え。

(倫理面への配慮)

今回の研究に関しては患者の個人情報はいずれも匿名化し、倫理面に十分配慮して行った。

C. 研究結果

アンケート調査の結果、回答が得られた AIR の合計患者数は 185 名であり、そのうち CAR が 83 名 (44.9%)、MAR が 3 名

(1.6%) であった。そのうち、4 項目 (A: 視覚機能異常を引き起こす明らかな原因がない、B: 網膜電図異常がある、C: 視機能低下を説明できる眼底病変や網膜変性・ジストロフィーがない、D: 明らかな眼内炎症がない) を全て満たしたのは 121 名

(65.4%) であった。

診断に必須と考える項目の上位 2 位は、B: 網膜電図異常、C: 視覚機能異常を引き起こす明らかな原因がないこと、であった。AIR の治療方法に関しては、ステロイド内服治療が最も多かった。抗網膜抗体検査は、リカバリン抗体など企業への依頼が最も多く、20 施設であった。抗網膜抗体の有無の結果は参考程度に捉える施設が多いという結果であった。

G. 研究発表

1. 論文発表

1) Saito M, Mitamura M, Fukutsu K, Zhenyu D, Ando R, Kase S, Katsuta S, Ishida

D. 考察

AIR の診断基準に関しては、海外では Fox の診断基準 (Am J Ophthalmol 2016) があり、専門家のコンセンサスに基づいている。この基準は、特に非腫瘍性 (non-paraneoplastic) 型 AIR の診断に用いられており、以下の 5 つの診断要件がある。

- (1) 視覚機能異常の明確な原因がないこと
- (2) 網膜電図 (ERG) 異常の存在
- (3) 血清中の抗網膜抗体の存在
- (4) 眼底所見に異常がないこと
- (5) 明らかな炎症がないこと

このほかに補助診断基準もある。

今後はこの Fox の診断基準を参考にし、日本の実態に合わせた AIR の診断基準を作成し、日本における患者数調査を行っていく予定である。

また、本研究は AMED (「自己免疫網膜症を対象とした多施設共同研究による診断・治療エビデンスの創出」: 研究代表 楠原仙太郎) との横断的共同研究も行なっており、オールジャパンでの AIR の研究体制を構築している。

E. 結論

今回、初めて日本における AIR の患者数調査と意識調査をおこなった。今後、より詳細な調査と検討をおこないながら、診断基準を作成したい。

F. 健康危険情報 : なし

- S. Retinal Arteriovenous Information Improves the Prediction Accuracy of Deep Learning-Based baPWV Index From Color Fundus Photographs. *Invest Ophthalmol Vis Sci*. 2025 Feb 3;66(2):63.
- 2) Fukui C, Yamana S, Xue Y, Shirane M, Tsutsui H, Asahara K, Yoshitomi K, Ito T, Lestari T, Hasegawa E, Yawata N, Takeda A, Sonoda KH, Shibata K. Functions of mucosal associated invariant T cells in eye diseases. *Front Immunol*. 2024 Feb 19;15:1341180.
- 3) Sotani Y, Imai H, Yamada H, Miki A, Kusuhara S, Nakamura M. High Intraocular Concentration of Fibrinogen Regulates Retinal Function Via the ICAM-1 Pathway. *Invest Ophthalmol Vis Sci*. 2024 Nov 4;65(13):34.
- 4) Kominami T, Ueno S, Ota J, Inooka T, Oda M, Mori K, Nishiguchi KM. Classification of fundus autofluorescence images based on macular function in retinitis pigmentosa using convolutional neural networks. *Jpn J Ophthalmol*. 2025 Mar;69(2):236-244.

2. 学会発表

- 1) 安藤亮、長谷川英一、楠原仙太郎、園田康平、近藤峰生. 自己免疫網膜症に関する日本国内調査：アンケート結果報告. 第78回日本臨床眼科学会. 11月16日 2024年, 京都.

H. 知的財産権の出願・登録状況

1. 特許取得 なし
2. 実用新案登録 なし
3. その他 なし

厚生労働科学研究費補助金（難治性疾患政策研究事業）
分担研究報告書

日本における遺伝性網膜ジストロフィに対する遺伝学的検査および
遺伝子治療の運用体制構築に関する研究

研究分担者 名古屋大学・医学系研究科・教授 西口 康二
宮崎大学・医学部・教授 池田 康博
三重大学大学・医学系研究科・眼科学・教授 近藤 峰生
京都大学・医学研究科・教授 辻川 明孝
国立病院機構東京医療センター・視覚研究部・部長 角田 和繁
研究協力者 神戸アイセンター・副センター長 前田 亜希子
京都大学・医学系研究科・特定講師 三宅 正裕

研究要旨

令和 5 年（2023 年）に遺伝性網膜ジストロフィ（IRD）に対する遺伝学的検査および遺伝子治療が保険収載された。これらを適正に運用するため、令和 6 年度に我々は以下の 2 つの取り組みを行なった。(1)IRD および日本人患者の特性を考慮した遺伝学的検査解釈のガイドライン「Specification of variant interpretation guidelines for inherited retinal dystrophy in Japan」を作成し、4 月に発出した。また、バリエントリストの内容を更新する会議を月 1 回程度行い、バリエントリストの Ver.2 を日本網膜硝子体学会のホームページに公開した。(3)ルクスターナによる遺伝子治療に関しては、令和 6 年度末までに行われた治療症例に対して治療内容と経過について報告および検討会を開催した。

A. 研究目的

令和 5 年度（2023 年度）に遺伝性網膜ジストロフィ（IRD）に対する遺伝学的検査が保険適応となった。また両アレル性 RPE65 遺伝子変異による遺伝性網膜ジストロフィに対する遺伝子治療も承認された。しかし、当時本邦においてこれらの検査および治療に関する運用に関しては全く整備されていない状況であった。

本研究グループでは、これらの運用体制を整備し、円滑な遺伝学的検査および遺伝

子治療の運用体制を構築することを目的とする。

具体的には、(1)遺伝学的検査に関しては、IRD および日本人患者の特性を考慮したバリエント解釈のガイドラインを作成して発出する。また、中央判定委員会においてバリエントリストの内容の更新を進め、遺伝学的検査の質の均てん化を推進する。(2)遺伝子治療に関しては、ルクスターナを用いた RPE65 網膜ジストロフィに対する遺伝子治療の質の向上を目的として、治療の内

容や経過に関する報告・検討会を開催する。

B. 研究方法

(1) 遺伝学的検査で得られた結果を解釈する際には、米国医遺伝学会による ACGM のバリエント解釈ガイドラインが国際的に広く用いられている。しかし、より標準化された診断基準を確保するためには、日本人の遺伝的背景の特徴に基づく追加的な指針が必要である。そこで、IRD の特徴や日本人における疾患頻度などを考慮したガイドラインを専門家集団により作成する。

また、IRD 原因遺伝子のバリエントリストに関しては、およそ月 1 回のペースでバリエントリストの更新に関する会議を Web とメールで進める。

(2) 令和 6 年度末の時点で行われたルクスターナ治療に関する報告会を Web 会議で開催し、必要に応じて「ルクスターナ注 適正使用指針」の留意事項に追加または変更を加える。

また、原因遺伝子のバリエントリストに関しては、およそ月 1 回のペースでバリエントリストの作成と更新を進める。

(倫理面への配慮)

今回の調査研究に関しては、主に遺伝学的検査および遺伝子治療のガイドラインや運用に関する議論が中心である。しかし倫理面や個人情報には十分配慮して行った。

C. 研究結果

(1) 日本人における IRD の疾患頻度、対立遺伝子頻度、現型および遺伝子型の特徴を考慮したバリエント解釈のガイドライン

「Specification of variant interpretation guidelines for inherited retinal dystrophy in Japan」を作成し、2024 年 7 月に JJ0 から発出された。このガイドラインは、データベースの使用、LOF バリエントの評価、アミノ酸残基の影響の分析、計算予測ツールの適用、機能研究の検討、変異ホットスポットの同定、分離データの評価、de novo 発生の評価、対立遺伝子データの分析、表現型情報の使用など、バリエント解釈の多面的な側面をカバーした内容となっている。

原因遺伝子のバリエントリストに関しては、Web およびメール会議により作成したバリエントリストの Ver. 2 を JRVS のホームページに公開した。現在新しい Ver. 3 の公開に向けて準備を進めている。

(2) 令和 7 年 2 月 19 日にこれまでのルクスターナ遺伝子治療の報告会が Web 会議形式で開催された。東京医療センターから 2 例、神戸アイセンターから 2 例の治療内容と経過について報告があり、審議が行われた。

審議された内容は、(1) 片眼のみの治療の可能性について、(2) GP で中心部に視野が検出されない症例の治療に関して、(3) 投与間隔の延長の可能性について、(4) OCT 上の十分な残存網膜外層構造の判断基準について、また(5)網膜下注射に際して自動注入装置を使用することを認める要望、などの内容であった。

今後も継続して検討会を行い、必要であれば「ルクスターナ注 適正使用指針」の留意事項に追加または変更を検討する予定である。

D. 考察

この研究班より発出された遺伝学的検査解釈の新たなガイドラインは、ACMG ガイドラインのデザインを IRD や日本人の状況に適合させるための適切な修正が加えられている。本ガイドラインは、日本で IRD の診断および治療に携わる眼科医および臨床遺伝医にとって、標準化された枠組みを提供する貴重な資料となりうると考えられた。

ルクスターナ治療に関しては、現時点ではまだ治療例数は少ないが、治療の適応、手術内容、術後経過などを検討し、今後治

療のガイドラインを改変する必要があるかどうかについて今後も定期的に検討する予定である。

E. 結論

今回我々が行った IRD に対する遺伝学的検査および遺伝子治療の適切な運用体制構築に関する試みは、今後の日本における IRD 診療の重要な基盤になると考えられた。

F. 健康危険情報

なし

G. 研究発表

1. 論文発表

- 1) Fujinami K, Nishiguchi KM, Oishi A, Akiyama M, Ikeda Y; Research Group on Rare, Intractable Diseases (Ministry of Health, Labour, Welfare of Japan). Specification of variant interpretation guidelines for inherited retinal dystrophy in Japan. Jpn J Ophthalmol. 2024 Jul;68(4):389-399.
- 2) Goto K, Koyanagi Y, Akiyama M, Murakami Y, Fukushima M, Fujiwara K, Iijima H, Yamaguchi M, Endo M, Hashimoto K, Ishizu M, Hirakata T, Mizobuchi K, Takayama M, Ota J, Sajiki AF, Kominami T, Ushida H, Fujita K, Kaneko H, Ueno S, Hayashi T, Terao C, Hotta Y, Murakami A, Kuniyoshi K, Kusaka S, Wada Y, Abe T, Nakazawa T, Ikeda Y, Momozawa Y, Sonoda KH, Nishiguchi KM. Disease-specific variant interpretation highlighted the genetic findings in 2325 Japanese patients with retinitis pigmentosa and allied diseases. J Med Genet. 2024 Jun 20;61(7):613-620.
- 3) Quinodoz M, Kaminska K, Cancellieri F, Han JH, Peter VG, Celik E, Janeschitz-Kriegl L, Schärer N, Hauenstein D, György B, Calzetti G, Hahaut V, Custódio S, Sousa AC, Wada Y, Murakami Y, Fernández AA, Hernández CR, Minguez P, Ayuso C, Nishiguchi KM, Santos C, Santos LC, Tran VH, Vaclavik V, Scholl HPN, Rivolta C. Detection of elusive DNA copy-number variations in hereditary disease and cancer through the use of noncoding and off-target sequencing reads. Am J Hum Genet. 2024 Apr 4;111(4):701-713.
- 4) Natsume K, Kominami T, Goto K, Koyanagi Y, Inooka T, Ota J, Kawano K, Yamada

- K, Okuda D, Yuki K, Nishiguchi KM, Ushida H. Phenotypic variability of RP1-related inherited retinal dystrophy associated with the c.5797 C > T (p.Arg1933*) variant in the Japanese population. Sci Rep. 2024 Oct 27;14(1):25669.
- 5) Fukushima M, Tao Y, Shimokawa S, Zhao H, Shimokawa S, Funatsu J, Hisai T, Okita A, Fujiwara K, Hisatomi T, Takeda A, Ikeda Y, Sonoda KH, Murakami Y. Comparison of Microperimetry and Static Perimetry for Evaluating Macular Function and Progression in Retinitis Pigmentosa. Ophthalmol Sci. 2024 Jul 20;4(6):100582.
- 6) Hiraoka M, Urakawa Y, Kawai K, Yoshida A, Hosakawa J, Takazawa M, Inaba A, Yokota S, Hirami Y, Takahashi M, Ohara O, Kurimoto Y, Maeda A. Copy number variant detection using next-generation sequencing in EYS-associated retinitis pigmentosa. PLoS One. 2024 Jun 24;19(6):e0305812.
- 7) Ueno S, Hayashi T, Tsunoda K, Aoki T, Kondo M. Nationwide epidemiologic survey on incidence of macular dystrophy in Japan. Jpn J Ophthalmol. 2024 May;68(3):167-173.
- 8) Ikeda HO, Hasegawa T, Abe H, Amino Y, Nakagawa T, Tada H, Miyata M, Oishi A, Morita S, Tsujikawa A. Efficacy and Safety of Branched Chain Amino Acids on Retinitis Pigmentosa: A Randomized, Double-Blind, Placebo-Controlled Clinical Trial. Transl Vis Sci Technol. 2024 Aug 1;13(8):29.

2. 学会発表

- 1) Nishiguchi KM. Future of genomic medicine for inherited retinal degeneration. Fuji Retina. Tokyo, March 30, 2025.
- 2) 西口康二 網膜遺伝子治療の展望 第49回日本外科系連合学会学術集会. 東京, 2024/06/06.
- 3) 西口康二 網膜疾患に対する AAV 遺伝子治療のイマとミライ 第63回日本網膜硝子体学会総会. 大阪, 2024/12/7.

H. 知的財産権の出願・登録状況

1. 特許取得 なし
2. 実用新案登録 なし
3. その他 なし



GUIDELINE

Specification of variant interpretation guidelines for inherited retinal dystrophy in Japan

Kaoru Fujinami¹ · Koji M Nishiguchi² · Akio Oishi³ · Masato Akiyama⁴ · Yasuhiro Ikeda⁵ · Research Group on Rare, Intractable Diseases (Ministry of Health, Labour, Welfare of Japan)

Received: 23 October 2023 / Accepted: 12 December 2023 / Published online: 30 July 2024
© Japanese Ophthalmological Society 2024

Abstract

Accurate interpretation of sequence variants in inherited retinal dystrophy (IRD) is vital given the significant genetic heterogeneity observed in this disorder. To achieve consistent and accurate diagnoses, establishment of standardized guidelines for variant interpretation is essential. The American College of Medical Genetics and Genomics/Association for Molecular Pathology (ACMG/AMP) guidelines for variant interpretation serve as the global “cross-disease” standard for classifying variants in Mendelian hereditary disorders. These guidelines propose a systematic approach for categorizing variants into 5 classes based on various types of evidence, such as population data, computational data, functional data, and segregation data. However, for clinical genetic diagnosis and to ensure standardized diagnosis and treatment criteria, additional specifications based on features associated with each disorder are necessary. In this context, we present a comprehensive framework outlining the newly specified ACMG/AMP rules tailored explicitly to IRD in the Japanese population on behalf of the Research Group on Rare and Intractable Diseases (Ministry of Health, Labour and Welfare of Japan). These guidelines consider disease frequencies, allele frequencies, and both the phenotypic and the genotypic characteristics unique to IRD in the Japanese population. Adjustments and modifications have been incorporated to reflect the specific requirements of the population. By incorporating these IRD-specific factors and refining the existing ACMG/AMP guidelines, we aim to enhance the accuracy and consistency of variant interpretation in IRD cases, particularly in the Japanese population. These guidelines serve as a valuable resource for ophthalmologists and clinical geneticists involved in the diagnosis and treatment of IRD, providing them with a standardized framework to assess and classify genetic variants.

Keywords ACMG/AMP guidelines · Genetic diagnosis · Inherited retinal dystrophy · Japanese · Variant interpretation

The advent of gene therapy as a potential treatment for inherited retinal dystrophy (IRD), aimed at targeting the underlying causative gene or disease variant, has sparked global

Corresponding author: Koji Nishiguchi

✉ Koji M Nishiguchi
kmn@med.nagoya-u.ac.jp

Kaoru Fujinami
k.fujinami@ucl.ac.uk

Akio Oishi
akio.oishi@nagasaki-u.ac.jp

Masato Akiyama
akiyama.masato.588@m.kyushu-u.ac.jp

Yasuhiro Ikeda
ymocl@med.miyazaki-u.ac.jp

² Department of Ophthalmology, Nagoya University
Graduate School of Medicine, 65 Tsurumai, Showa-ku,
Nagoya 466-8550, Japan

³ Department of Ophthalmology and Visual Sciences,
Graduate School of Biomedical Sciences, Nagasaki
University, Nagasaki 852-8501, Japan

⁴ Department of Ocular Pathology and Imaging Science,
Graduate School of Medical Sciences, Kyushu University,
Fukuoka 812-8582, Japan

⁵ Department of Ophthalmology, Faculty of Medicine,
University of Miyazaki, Miyazaki 889-1692, Japan

¹ Laboratory of Visual Physiology, Division of Vision
Research, National Institute of Sensory Organs, NHO Tokyo
Medical Center, Tokyo 152-8902, Japan

initiatives to improve precise genetic testing and diagnosis. Accurate genetic testing and diagnosis have become critical components in improving patient care and making informed therapeutic decisions. Recognizing the importance of these advancements, Japan is actively working toward incorporating genetic testing for IRD patients into investigations covered by national insurance. As part of this broader effort, the “Research on Rare and Intractable diseases, Health and Labour Sciences Research Grants,” funded by the Ministry of Health, Labour and Welfare of Japan, has been ongoing.

In December 2022, the “Guidelines for Genetic Testing in Inherited Retinal Dystrophy” were issued by an IRD working group on behalf of the Japanese Retina and Vitreous Society (available at https://www.jrvs.jp/guideline/ird_rd_guide_line.pdf). Whilst these guidelines represent a significant step toward standardized genetic testing for IRD, discrepancies in result interpretation among physicians and institutions can still arise, leading to diagnostic confusion and uncertainty in determining treatment eligibility. Therefore, establishment of uniform criteria for identifying the pathologic variants associated with IRD is crucial to facilitate consistent and accurate clinical application of genetic testing.

The current American College of Medical Genetics and Genomics (ACMG) guidelines serve as a commonly employed “cross-disease” standard for interpreting variant pathogenicity [1]. However, the lack of specificity of these guidelines has resulted in varying assessments of pathogenicity among different institutions. As a result, there is a need to develop unique criteria tailored to the disease specificity and ethnic considerations of IRD. Whilst the international group Clinical Genome Resource (ClinGen: <https://clinicalgenome.org/>), which is responsible for formulating the ACMG guidelines and others, has categorized IRD into 4 groups according to disease categories and pathologic variants, specific information pertaining to IRD has yet to be published.

To bridge these existing gaps, a task force for variant interpretation of IRD in Japan was formed within the IRD working group on behalf of the Research Group on Rare and Intractable Diseases (Ministry of Health, Labour and Welfare of Japan) with the objective of developing detailed variant interpretation guidelines specifically tailored to Japanese IRD cases. This task force adopted the ACMG guidelines as its fundamental framework and incorporated additional guidelines recognized for their cross-disease specificity [2]. The comprehensive ACMG guidelines for inherited sensorineural hearing loss (SNHL) [3], which shares some similarities with IRD, were referenced during the guideline development process to ensure alignment with the established standards. In instances where certain aspects remained ambiguous, the task force formulated its own evaluation criteria, taking into consideration the unique characteristics of IRD in the Japanese population.

After conducting 2 rounds of pilot assessments and incorporating subsequent revisions, the finalized variant interpretation guidelines in Japanese, titled “Specification of Variant Interpretation Guidelines for Japanese Inherited Retinal Dystrophy-1st draft,” were published (available at https://www.jrvs.jp/guideline/ird_acmg_guideline.pdf). These guidelines offer a comprehensive framework that integrates the fundamental principles of the ACMG guidelines, specific evaluations tailored to IRD, and considerations for the unique characteristics of the Japanese population. By combining these elements, the guidelines aim to provide a standardized and comprehensive approach to variant interpretation in the context of IRD in Japan.

Outline

The Specification of Variant Interpretation Guidelines for Japanese Inherited Retinal Dystrophy were developed on behalf of the Research Group on Rare and Intractable Diseases (Ministry of Health, Labour and Welfare of Japan) on the basis of the established framework of the ACMG guidelines (Tables 1 and 2) [1], which serve as the global standard for interpreting variants across different diseases. In addition to the ACMG guidelines, specific considerations were made for IRD by incorporating disease frequencies, allele frequencies, and phenotypic and genotypic characteristics. Modifications were implemented to adapt the ACMG guidelines design to the specific context of IRD (Table 4), as described below.

Summary of specifications

We have contributed the following recommended specifications for the ACMG/AMP rules to the Japanese IRD Variant Interpretation (J-IRD-VI) guidelines. Tables 1 and 2 provide a concise summary of the categories and criteria outlined in the ACMG guidelines, along with the corresponding criteria for verdict assessment [1]. These tables serve as a comprehensive reference for guiding the interpretation of genetic variants associated with Mendelian inherited diseases, in accordance with the ACMG guidelines. Notably, the sensorineural hearing loss (SNHL) expert panel has also provided specifications for 21 ACMG/AMP rules (Table 3), aiming to establish standardized guidelines for the clinical application of variant interpretation [3].

We recommended specifications for 18 ACMG/AMP rules (Table 4). Five rules had general recommendations on the application of the rule (PM5, PP3, BS4, BP4, BP7). Five rules had gene- or disease-based specifications (PS3, PM1,

Table 1 Summary of categories and criteria

	Categories	Criteria
1	PVS1	Null variant (nonsense, frameshift, canonical ± 1 or 2 splice sites, initiation codon, single or multiexon deletion) in a gene where loss of function (LOF) is a known mechanism of disease.
2	PS1	Same amino acid change as a previously established pathogenic variant regardless of nucleotide change.
3	PS2	De novo (both maternity and paternity confirmed) in a patient with the disease and no family history.
4	PS3	Well-established in vitro or in vivo functional studies supportive of a damaging effect on the gene or gene product.
5	PS4	The prevalence of the variant in affected individuals is significantly increased compared with the prevalence in controls.
6	PM1	Located in a mutational hot spot and/or critical and well-established functional domain (e.g., active site of an enzyme) without benign variation.
7	PM2	Absent from controls (or at extremely low frequency if recessive) in Exome Sequencing Project, 1000 Genomes Project, or Exome Aggregation Consortium.
8	PM3	For recessive disorders, detected in trans with a pathogenic variant
9	PM4	Protein length changes as a result of in-frame deletions/insertions in a non-repeat region or stop-loss variants.
10	PM5	Novel missense change at an amino acid residue where a different missense change determined to be pathogenic has been seen before.
11	PM6	Assumed de novo, but without confirmation of paternity and maternity.
12	PP1	Co-segregation with disease in multiple affected family members in a gene definitively known to cause the disease.
13	PP2	Missense variant in a gene that has a low rate of benign missense variation and in which missense variant is a common mechanism of disease.
14	PP3	Multiple lines of computational evidence support a deleterious effect on the gene or gene product (conservation, evolutionary, splicing impact, etc.)
15	PP4	Patient's phenotype or family history is highly specific for a disease with a single genetic etiology.
16	PP5	Reputable source recently reports variant as pathogenic, but the evidence is not available to the laboratory to perform an independent evaluation.
17	BA1	Allele frequency is $>5\%$ in Exome Sequencing Project, 1000 Genomes Project, or Exome Aggregation Consortium.
18	BS1	Allele frequency is greater than expected for disorder.
19	BS2	Observed in a healthy adult individual for a recessive (homozygous), dominant (heterozygous), or X-linked (hemizygous) disorder, with full penetrance expected at an early age.
20	BS3	Well-established in vitro or in vivo functional studies show no damaging effect on protein function or splicing.
21	BS4	Lack of segregation in affected members of a family.
22	BP1	Missense variant in a gene for which primarily truncating variants are known to cause disease.
23	BP2	Observed in trans with a pathogenic variant for a fully penetrant dominant gene/disorder or observed in cis with a pathogenic variant in any inheritance pattern.
24	BP3	In-frame deletions/insertions in a repetitive region without a known function.
25	BP4	Multiple lines of computational evidence suggest no impact on gene or gene product (conservation, evolutionary, splicing impact, etc.)
26	BP5	Variant found in a case with an alternate molecular basis for disease.
27	BP6	Reputable source recently reports variant as benign, but the evidence is not available to the laboratory to perform an independent evaluation.
28	BP7	A synonymous (silent) variant for which splicing prediction algorithms predict no impact to the splice consensus sequence nor the creation of a new splice site AND the nucleotide is not highly conserved.

Richards S, Aziz N, Bale S, et al. Standards and guidelines for the interpretation of sequence variants: a joint consensus recommendation of the American College of Medical Genetics and Genomics and the Association for Molecular Pathology. *Genet Med*. May 2015;17(5):405-24. Modified for the purpose

Each criterion is weighted as very strong (PVS1), strong (PS1-4), moderate (PM1-6), or supporting (PP1-5), and each benign criterion is weighted as stand-alone (BA1), strong (BS1-4), or supporting (BP1-6)

PM2, PP4, BA1). Six rules had strength-level specifications (PVS1, PS2, PM3, PM5, PM6, PP1). Two rules had both gene/disease-based specifications and strength-level specifications (BS1, BS2). No changes were recommended for 7 rules (PS1, PS4, PM4, BS3, BP2, BP3, BP5), and 2 rules were considered inapplicable (PP2, BP1).

Detailed specifications

Population database (BA1, BS1, PM2)

The thresholds for estimated allele frequency vary depending on the summed prevalence of monogenic diseases and

Table 2 Criteria for verdict assessment

Pathogenic	Criteria
1	Very Strong (PVS1) AND
	a ≥ 1 Strong (PS1–PS4) OR
	b ≥ 2 Moderate (PM1–PM6)
	c 1 Moderate (PM1–PM6) and 1 Supporting (PP1–PP5)
	d ≥ 2 Supporting (PP1–PP5)
2	≥ 2 Strong (PS1–PS4)
3	1 Strong (PS1–PS4) AND
	a ≥ 3 Moderate (PM1–PM6)
	b 2 Moderate (PM1–PM6) AND ≥ 2 Supporting (PP1–PP5)
	c 1 Moderate (PM1–PM6) AND ≥ 4 Supporting (PP1–PP5)
Likely Pathogenic	Criteria
	1 Very Strong (PVS1) AND 1 Moderate (PM1–PM6)
	1 Strong (PS1–PS4) AND 1–2 Moderate (PM1–PM6)
	1 Strong (PS1–PS4) AND ≥ 2 Supporting (PP1–PP5)
	≥ 3 Moderate (PM1–PM6) OR
	2 Moderate (PM1–PM6) AND ≥ 2 Supporting (PP1–PP5)
	1 Moderate (PM1–PM6) AND ≥ 4 Supporting (PP1–PP5)
Benign	Criteria
	1 Stand-Alone (BA1)
	≥ 2 Strong (BS1–BS4)
Likely Benign	
	1 Strong (BS1–BS4) and 1 Supporting (BP1–BP7)
	≥ 2 Supporting (BP1–BP7)

If the other criteria are not met, or if the criteria for pathological and benign are conflicting, the variant is classified as Uncertain Significance (VUS)

Richards S, Aziz N, Bale S, et al. Standards and guidelines for the interpretation of sequence variants: a joint consensus recommendation of the American College of Medical Genetics and Genomics and the Association for Molecular Pathology. *Genet Med*. May 2015;17(5):405–24. Modified for the purpose

Table 3 Specifications for genetic sensorineural hearing loss (SNHL)

Categories	Contents
PS1, PP3, BS4, BP4, BP5	Establishment of general recommendation rules
PS3, PM1, PM2, PP4, BA1, BS4, BP2	Detailed settings for gene and disease entity
PVS1, PS2, PM3, PM5, PM6, PP1, BS3	Detailed strength level settings
PS4, BS1, BS2	Detailed settings for genes, disease entity, and strength levels
PM4, BP3, BP7,	No changes
PP2, PP5, BP1, BP6	Removed from the criteria
Verdict assessment	Modification
Likely pathogenic	PVS1 and PM2_Supporting = likely pathogenic
Likely benign	BS1 without valid conflicting evidence

Oza AM, DiStefano MT, Hemphill SE, et al. Expert specification of the ACMG/AMP variant interpretation guidelines for genetic hearing loss. *Hum Mutat*. Nov 2018;39(11):1593–1613

the inheritance pattern, including autosomal dominant (AD), autosomal recessive (AR), and X-linked inheritance. The estimated disease prevalence of IRD in Japan is approximately 1 in 4000–8000 live births. This prevalence is lower

than that of SNHL, which is estimated to occur in 1 in 300–500 live births [3].

For the pathogenicity classification criteria, the J-IRD-VI guidelines define allele frequencies of <0.00001 for

Table 4 Summary of specifications for inherited retinal dystrophy in Japan

	Categories	Specifications/applied rules	Comments
1	PVS1	ClinGen SVI Recommendation (PVS1, PVS1 strong/moderate/supporting)	For splice site alteration, canonical splice site (+/-2bp) is the main indication.
2	PS1	No change	No change
3	PS2	SVI Recommendation for De Novo Criteria (PS2 & PM6) - Version 1.1 (Very strong/strong/moderate/supporting)	Indicated when the phenotype and genotype of the parents are identified
4	PS3	Added some identified functional changes as PS3_moderate.	Mini gene assay and zebrafish model studies showing phenocopy (strong) or functional characteristics (moderate) are applicable.
5	PS4	No change	Ancestry matched cohorts (N>20000) are preferred.
6	PM1	No change	RP1 (amino acid 650-780), CRX cone-rod homeobox protein (39-99), PRPH2 D2 Loop (123-265)
7	PM2	Allele frequency for recessive diseases<0.00002. Allele frequency for dominant diseases<0.00001.	gnomAD, HGVD, Tommo8.3k JPN
8	PM3	SVI Recommendation for (PM3) - Version 1.1 (moderate)	Pathogenic and likely pathogenic are considered according to the SNHL specification.
9	PM4	No change	Exon that deletes the entire Exon falls under the PVS1 category and is therefore not applicable.
10	PM5	Likely pathogenic variants or VUS are also included in the analysis, using a point system of 0.5 supporting 1.0 moderate, assuming 0.5 for 1 VUS and 1.0 for 1 pathogenic variant.	Partially modified. Higher conservation should be considered.
11	PM6	SVI Recommendation for De Novo Criteria (PS2 & PM6) - Version 1.1 (Very strong/strong/moderate/supporting)	Indicated when the phenotype and genotype of the parents are identified.
12	PP1	Application of SNHL point system (Strong/moderate/supporting)	Indicated when phenotype and genotype are identified
13	PP2	Removal	Removed due to variable gene size, etc.
14	PP3	REVEL scores ≥ 0.7 or damaging splice sight alteration predicted by software.	REVEL, MaxEntScan, Human Splice Finder, Splicing AI.
15	PP4	Modified (definitions for particular genes)	SAG/GRK1, CYP4V2, NR2E3/NRL.
16	PP5	Modified (suggestions for reliable resources)	Peer-reviewed publications, ClinVAR minor (criterion provided).
17	BA1	Allele frequency for recessive diseases>0.01 Allele frequency for dominant diseases>0.0003.	gnomAD, HGVD, Tommo8.3k JPN. Variants for which sufficient evidence has been established for other items may be excluded
18	BS1	Allele frequency for recessive diseases $0.001 < <0.01$ Allele frequency for dominant diseases $0.0006 < <0.0003$	gnomAD, HGVD, Tommo8.3k JPN. Variants for which sufficient evidence has been established for other items may be excluded
19	BS2	SVI Recommendation for (PM3) - Version 1.1 (moderate)	Pathogenic and likely pathogenic are considered according to the SNHL specification. Not indicated for adult-onset retinal dystrophies such as RP.
20	BS3	No change	Indicated when phenotype and genotype are identified. Not indicated for adult-onset retinal dystrophies such as RP.
21	BS4	Application of SNHL point system (Strong/moderate/supporting)	
22	BP1	Removal	
23	BP2	No change	
24	BP3	No change	
25	BP4	REVEL scores ≤ 0.15 or no damaging splice sight alteration predicted by software	REVEL, MaxEntScan, Human Splice Finder, Splicing AI.
26	BP5	No change	
27	BP6	No change	Peer-reviewed publications, ClinVAR minor (criterion provided).
28	BP7	No splice sight alteration	Mainly for variants +/- 10bp from exon edge, MaxEntScan, Human Splice Finder, and Splicing AI are applied.

Sequence Variant Interpretation General Recommendations for Using ACMG/AMP Criteria are provided by Clinical Genome Resource (ClinGen): <https://clinicalgenome.org/working-groups/sequence-variant-interpretation/>

Oza AM, DiStefano MT, Hemphill SE, et al. Expert specification of the ACMG/AMP variant interpretation guidelines for genetic hearing loss. Hum Mutat. Nov 2018;39(11):1593-1613

Specifications for SNHL was applied/modified for PS2, PM6, PP1, PP2, PP3, BP1, and BP4

AD-IRD and of <0.00002 for AR-IRD as the thresholds for the PM2 criterion. For the BA1 criterion, the allele frequency threshold is >0.0003 for AD-IRD and >0.001 for AR-IRD.

Despite these thresholds, pathologic variants with high allele frequencies (eg, NM_001142800.2(EYS):c.2528G>A (p.Gly843Glu)) have been reported [4–7]. Therefore, variants that have sufficient evidence established under other criteria may be excluded from further consideration on the basis of allele frequency alone. Additionally, the frequency of the underlying disease can vary significantly depending on the specific phenotype and gene involved.

The gnomAD database (<https://gnomad.broadinstitute.org/>) was used as a reference for global allele frequencies. Additionally, for calculating Japanese-specific allele frequencies, the Human Genetic Variation Database (HGVD, <https://www.hgvd.genome.med.kyoto-u.ac.jp/>) and TomoJPN database (Tohoku Medical Megabank Organization, <https://www.megabank.tohoku.ac.jp/>) were used. The criteria for this item are considered met when the respective databases satisfy the specified threshold conditions.

Loss of function variants (PVS1, PVS1_Strong, PVS1_Moderate, PVS1_Supporting)

The determination of loss of function (LOF) variants in the J-IRD-VI guidelines is guided by a flowchart based on the recommendations for interpreting the LOF PVS1 ACMG/AMP variant criterion (Fig. 1) [2]. The strength of evidence for LOF variants may vary depending on the specific type of variant and the presence or absence of residual protein.

For splice site variants, the canonical splice site (+/– 2 bp) is primarily considered. However, other splice site variants can be evaluated if functional and other evidence supporting their impact on splicing exist. The inclusion of functional and other evidence allows for a comprehensive assessment of the variant's effect on splice site functionality. Detailed predicted and observed impacts of variants on splicing and recommendations have been recently published by the ClinGen Sequence Variant Interpretation (SVI) Splicing Subgroup [8].

Variants affecting the same amino acid residue (PS1, PM5)

The ACMG guidelines assign strong evidence (PS1) or moderate evidence (PM5) of pathogenicity when established pathologic variants are found at the same amino acid residue [1].

Whilst the strength level for PS1 remains unchanged, the evaluation method of the J-IRD-VI guidelines for PM5 includes variants previously classified as “likely pathogenic” or “variant of unknown significance (VUS).” To incorporate

these variants, 1 VUS will be assigned 0.5 points, and 1 pathogenic/likely pathogenic variant will be assigned 1.0 point. A total score of 0.5 points represents supporting evidence, whilst a score of 1.0 or more indicates moderate evidence.

Additionally, evolutionary conservation is a crucial factor in the evaluation process. Regions with a notably low evolutionary conservation score (below 0.3 as determined by UCSC, phyloP, phastCons scores, etc: <https://genome.ucsc.edu/>) will not be considered for pathogenicity, whilst detailed calibration of the PhyloP for missense variant pathogenicity classification and ClinGen recommendations have been recently published [9].

Computational predictive tools (PP3, BP4, BP7)

The ACMG guidelines include multiple prediction software for variant evaluation [1]. However, for the evaluation of missense variants in accordance with the guidelines for SNHL, the REVEL (Rare Exome Variant Ensemble Learner) tool, which provides comprehensive evaluation, was adopted [3].

The cutoff value for the REVEL score is taken from previous reports, with a score of 0.15 or less considered supporting evidence (BP4) and a score of 0.7 or higher considered strong evidence (PP3) [10]. Detailed calibration of REVEL scores for missense variant pathogenicity classification and ClinGen recommendations for PP3/BP4 criteria have recently been published [9].

For the prediction of splice site changes, a comprehensive assessment is made when any of the following 3 software criteria are met: MaxEntScan (<https://www.ncbi.nlm.nih.gov/refseq/>) score (diff) greater than 3 [11], or Human Splice Finder (<http://umd.be/Redirect.html>) or Splicing AI (<https://asia.ensembl.org/index.html>) scores (delta) greater than 0.8 (high precision). These criteria provide evidence to support the prediction of splice site changes. Detailed predicted and observed impacts of variants on splicing and recommendations have been recently published by the ClinGen SVI Splicing Subgroup [8].

Functional studies (PS3, BS3)

Transgenic animal models that demonstrate the reproduction of the retinal phenotype (phenocopy) associated with a specific gene variant are considered strong evidence. Functional analysis using established experimental systems, such as mini gene assays or zebrafish models, can provide valuable insights into gene function. If such functional analysis demonstrates that a variant leads to a change in gene function, it is considered moderate evidence in support of its pathogenicity.

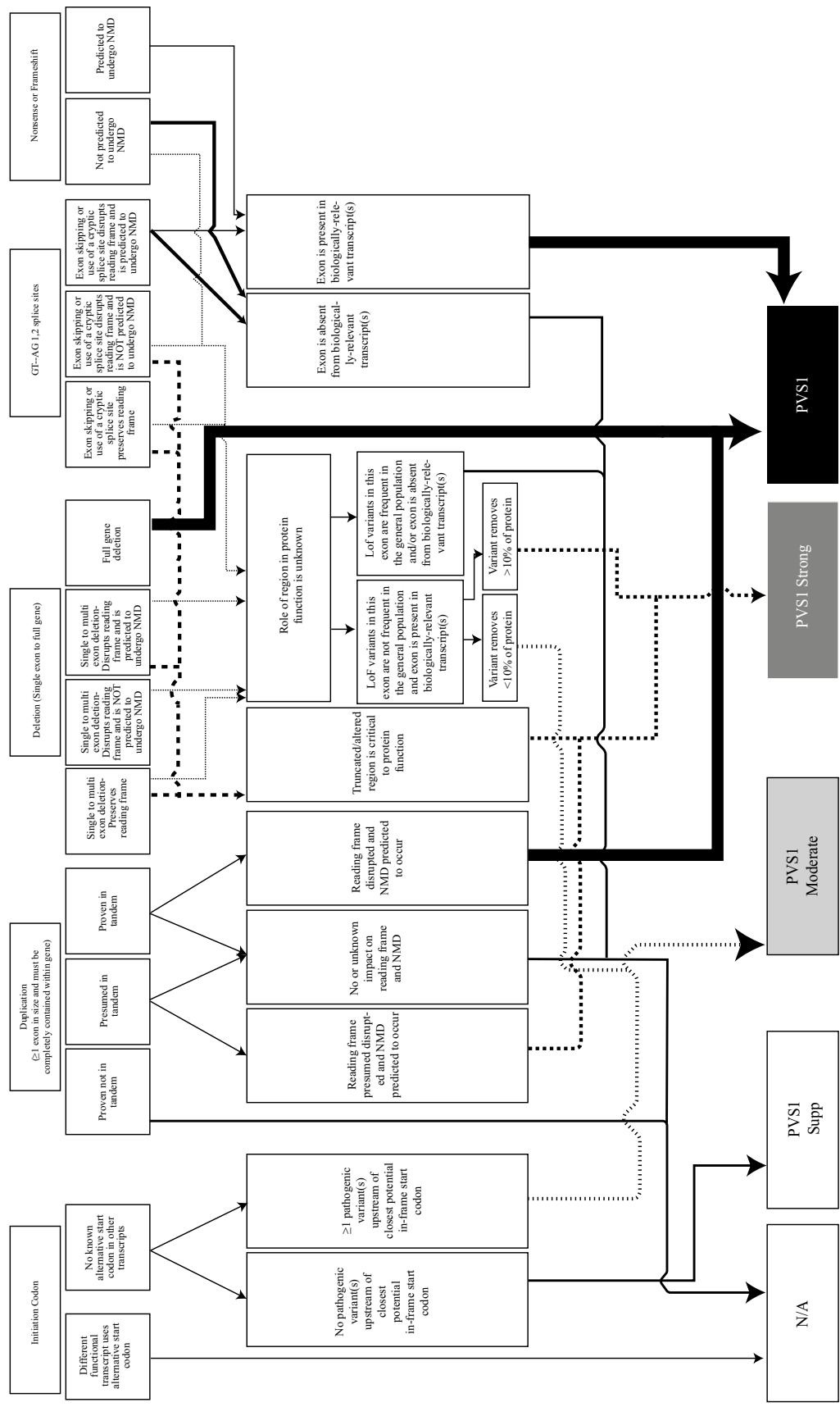


Fig. 1 Evaluation of loss of function variants (PVS1 workflow). *NMD* indicates nonsense-mediated decay, *LOF* loss of function. This diagram has been modified for the specific purpose of the Japanese Inherited Retinal Dystrophy Variant Interpretation (J-IRD-VI) guidelines, using the original publication as a foundation. About Tayoun AN, Pesaran T, DiStefano MT, Oza A, Rehm HL, Biesecker L, et al; ClinGen Sequence Variant Interpretation Working Group (ClinGen SVI). Recommendations for interpreting the loss of function PVS1 ACMG/AMP variant criterion. Hum Mutat. 2018;39:1517–24

Table 5 General recommendations for segregation scoring

	Supporting	Moderate	Strong
Likelihood	4:1	16:1	32:1
LOD Score	0.6	1.2	1.5
Autosomal dominant threshold	2 affected segregations	4 affected segregations	5 affected segregations
Autosomal recessive threshold	See Table 6	See Table 6	See Table 6

Oza AM, DiStefano MT, Hemphill SE, et al. Expert specification of the ACMG/AMP variant interpretation guidelines for genetic hearing loss. *Hum Mutat* 2018;39:1593-1613

Strande NT, Riggs ER, Buchanan AH, et al. Evaluating the Clinical Validity of Gene-Disease Associations: An Evidence-Based Framework Developed by the Clinical Genome Resource. *Am J Hum Genet.* Jun 1 2017;100(6):895-906

Table 6 Segregation scoring for autosomal recessive diseases

		Unaffected recessive segregations					
		0	1	2	3	4	5
Affected segregations	0	<0.5	<0.5	<0.5	<0.5	<0.5	0.62
	1	0.6	0.73	0.85	0.98	1.1	1.23
	2	1.2	1.33	1.45	1.58	1.7	1.83
	3	1.81	1.93	2.06	2.18	2.31	2.43
	4	2.41	2.53	2.66	2.78	2.91	3.03
	5	3.01	3.14	3.26	3.39	3.51	3.63

Oza AM, DiStefano MT, Hemphill SE, et al. Expert specification of the ACMG/AMP variant interpretation guidelines for genetic hearing loss. *Hum Mutat* 2018;39:1593-1613

Mutational hot spots or functional domains (PM1)

In manifest AD retinitis pigmentosa (AD-RP), amino acids 650-780 of the *RPI* gene have been identified as mutational hot spots [12, 13]. Similarly, in manifest IRD (AD-IRD), amino acids 39-99 of the *CRX* gene are recognized as mutational hot spots [14–16]. Furthermore, in AD-IRD, amino acids 123-265 of the *PRPH2* gene, which constitute the D2 loop, are considered to be a functional domain within this category [17, 18].

Segregation data (PP1, PP1_moderate, PP1_strong, BS4)

Intrafamilial cosegregation data are evaluated according to the guidelines for SNHL, which differentiate between AD and AR inheritance (Tables 5 and 6) [19]. The evidence is weighted according to the guidelines, taking into account the phenotype (the observed clinical manifestation) within a given family. Three levels of evidence are established according to the number and likelihood of consanguineous matches between the phenotype and genotype. However, it is important to note that the BS4 criterion does not apply to phenotypes, genes, or variants that are expected to manifest in adulthood. The focus is on the evaluation of cosegregation data for early-onset or pediatric-onset diseases rather than adult-onset conditions.

Table 7 General recommendations for de novo scoring

Supporting (PS2_Supporting or PM6_Supporting)	Moderate (PS2_Moderate or PM6)	Strong (PS2 or PM6_Strong)	Very Strong (PS2_VeryStrong or PM6_VeryStrong)
0.5 points	1.0 points	2.0 points	4.0 points

Oza AM, DiStefano MT, Hemphill SE, et al. Expert specification of the ACMG/AMP variant interpretation guidelines for genetic hearing loss. *Hum Mutat* 2018;39:1593-1613

De novo occurrence (PS2, PS2_very strong, PS2_moderate, PS2_supporting, PM6)

In the ACMG guidelines, when the maternity and paternity of a de novo variant are unconfirmed, the PM6 criterion is applied [1]. However, for the J-IRD-VI guidelines, if paternity and maternity have been confirmed, the PS2 criterion is applicable (Table 7).

In the SNHL guidelines, a weighted point system is employed to account for phenotypic/genotypic specificity. Furthermore, additional points can be added on the basis of the number of originators involved in the inheritance pattern (Table 8).

Table 8 Phenotypic consistency for de novo scoring

Phenotypic consistency	Points per proband	
	Confirmed de novo	Assumed de novo
Phenotype highly specific for gene	2	1
Phenotype consistent with gene but not highly specific	1	0.5
Phenotype consistent with gene but not highly specific and high genetic heterogeneity	0.5	0.25
Phenotype not consistent with gene	0	0

Oza AM, DiStefano MT, Hemphill SE, et al. Expert specification of the ACMG/AMP variant interpretation guidelines for genetic hearing loss. *Hum Mutat* 2018;39:1593-1613

Table 9 General recommendations for classification/zygosity of other variant

Supporting (PM3_Supporting)	Moderate (PM3)	Strong (PM3_Strong)	Very Strong (PM3_VeryStrong)
0.5 points	1.0 points	2.0 points	4.0 points

Oza AM, DiStefano MT, Hemphill SE, et al. Expert specification of the ACMG/AMP variant interpretation guidelines for genetic hearing loss. *Hum Mutat* 2018;39:1593-1613

Allelic data (PM3, BS2)

In the ACMG guidelines, moderate evidence is defined as an allelic variant of the variant under evaluation in the case of a latent genetic disease [1]. For AR-IRD, the identification of a pathogenic variant at the allele of the variant under evaluation (ie, compound heterozygosity) is considered moderate evidence.

The SNHL guidelines provide specific criteria for variant evaluation. These guidelines consider the presence or absence of allele information (phase information) for the identified pathologic variant and the number of originators (ie, family members) in whom the pathologic variant has been identified. Points are assigned on the basis of this information. If the variant under evaluation is homozygous, points are assigned according to family history. The strength of the evidence is determined by the cumulative points (Tables 9 and 10). However, in the BS2 criterion, if the phenotype, gene, or variant is expected to manifest in adulthood or cause adult-onset disease, the item is not applicable to evaluation purposes.

Phenotypic data (PP4, BP5)

The ACMG guidelines define a gene as providing supporting evidence when a specific phenotype is associated with a disease caused by a single responsible gene and when a variant is identified in that gene that matches the

Table 10 Classification/zygosity of other variant for scoring

Classification/zygosity of other variant	Points per proband	
	Known in trans	Phase unknown
Pathogenic/Likely pathogenic	1	0.5
Homozygous occurrence (Max points from homozygotes=1.0)	0.5	NA
Rare uncertain significance variant on other allele, or homozygous occurrence due to consanguinity, (max point= 0.5)	0.25	NA

Oza AM, DiStefano MT, Hemphill SE, et al. Expert specification of the ACMG/AMP variant interpretation guidelines for genetic hearing loss. *Hum Mutat* 2018;39:1593-1613

phenotype [1]. These J-IRD-VI guidelines do not limit the specific phenotype to a single responsible gene but consider specific genes to provide evidence of a phenotypic association.

Examples of gene-phenotype associations considered supporting evidence include the following: (1) *SAG/GRK1* and Oguchi disease: the presence of a prominent golden reflex seen circumferentially and an electronegative waveform with a severely reduced b-wave and milder reduction of the a-wave in a dark-adapted bright flash electroretinogram [20, 21]. (2) *CYP4V2* and Bietti crystalline corneoretinal dystrophy: the presence of diffuse crystalline deposits scattered throughout the retina, followed by progressive atrophy of the retinal pigment epithelium (RPE), choriocapillaris, and neuroretina [22]. (3) *NR2E3* and enhanced S-cone syndrome: pathognomonic electrophysiologic features, such as a slow rod-like response that appears to have a similar waveform under both scotopic and photopic conditions [23, 24]. These associations between specific genes and phenotypes are considered supporting evidence in the evaluation process.

Reputable source (PP5, BP6)

In the ACMG guidelines, if a variant under evaluation has been previously reported as pathogenic by a reputable source, it is considered supporting evidence [1]. Specifically, the J-IRD-VI guidelines define a pathologic variant as one that has been reported by a reliable source and meets the evaluation criteria provided in ClinVar (<https://www.ncbi.nlm.nih.gov/clinvar/>). However, variants reported in sources such as HMGD (<http://www.hgmd.cf.ac.uk/>), where the criteria for evaluating pathogenicity are not specified, are not applicable to the J-IRD-VI guidelines.

Discussion

The “Specification of Variant Interpretation Guidelines for Japanese Inherited Retinal Dystrophy” provides detailed specifications for interpreting genetic variants in Japanese patients with IRD. These guidelines play a critical role in ensuring accurate diagnosis and treatment decisions by providing standardized criteria. By integrating the ACMG framework and incorporating disease-specific considerations and ethnic factors unique to the Japanese population, these guidelines address the specific challenges associated with IRD in Japan.

The guidelines cover multiple aspects of variant interpretation, including the use of population databases, assessment of LOF variants, analysis of amino acid residue impact, application of computational predictive tools, consideration of functional studies, identification of mutational hotspots, evaluation of segregation data, assessment of de novo occurrences, analysis of allelic data, use of phenotypic information, and reliance on reputable sources. This comprehensive approach ensures that all relevant factors are considered during the variant interpretation process, leading to consistent and accurate results.

However, the guidelines also have certain limitations that should be addressed. One limitation is the lack of gene/disease-specific information, such as prevalence, allele frequency, functional assessment, mutational hotspots, allelic data, and phenotypic data. These missing data points could significantly enhance the quality and specificity of the guidelines. To overcome this limitation, efforts should be made to gather and store detailed data for specific genes and diseases, allowing for more precise variant interpretation and better-informed treatment decisions.

Periodic revisions of the guidelines will be necessary to keep pace with the rapid advancements in genome analysis technology and data science. The field of genomic diagnosis and treatment is continually evolving, and as new knowledge and technologies emerge, the guidelines must

be updated to reflect the latest standards and practices. In fact, the ACMG guidelines themselves are currently undergoing a revision process, highlighting the need for ongoing refinement and improvement.

Another important consideration is the availability of experimental data to support variant interpretation. Whilst the guidelines emphasize the use of reputable sources and databases, there is a need for robust experimental studies and in silico molecular genetic analyses to improve the accuracy of clinical effect and pathogenicity assessment for each variant. Access to comprehensive experimental data would strengthen the guidelines and enhance their clinical utility.

The role of genomic diagnosis and treatment is expected to expand as genome analysis technology and data science continue to advance. These guidelines aim to optimize the efficiency and uniformity of variant evaluation in IRD, with the ultimate goal of widespread genetic diagnosis for IRD patients in Japan.

Acknowledgment We express our gratitude to the working group for inherited retinal dystrophy, representing the Japanese Retina and Vitreous Society, for their valuable contributions to the development of the Japanese Inherited Retinal Dystrophy Variant Interpretation guidelines. Their dedication and expertise have played a significant role in advancing the field of genetic testing and diagnosis for inherited retinal dystrophy in Japan.

Yoshihiro Hotta, Department of Ophthalmology, Hamamatsu University School of Medicine, Shizuoka, Japan; Hiroyuki Kondo, Department of Ophthalmology, University of Occupational and Environmental Health, Fukuoka, Japan; Akiko Maeda, Department of Ophthalmology, Kobe City Eye Hospital, Hyogo, Japan; Masahiro Miyake, Kyoto University Graduate School of Medicine, Kyoto, Japan; Mineo Kondo, Department of Ophthalmology, Mie University Graduate School of Medicine, Mie, Japan; Taiji Sakamoto, Kagoshima University Graduate School of Medical and Dental Sciences, Kagoshima, Japan

Yoshihiro Hotta, Hiroyuki Kondo, Akiko Maeda, Masahiro Miyake, Mineo Kondo, Taiji Sakamoto

Funding This study is funded by Research on Rare and Intractable Diseases, Health and Labour Sciences Research Grants (grant number: JPMH23FC1043) from the Ministry of Health, Labour and Welfare of Japan and by the Practical Research Project for Rare/Intractable Diseases (grant number: JP23ek0109632) from the Japan Agency for Medical Research and Development, Japan. Role of the funder/sponsor: the funding sources had no role in the design and conduct of the study; collection, management, analysis, and interpretation of the data; preparation, review, or approval of the manuscript; or decision to submit the manuscript for publication.

Declarations

Conflicts of interest K. Fujinami, None; K. Nishiguchi, None; A. Oishi, Grants or contracts to the author's institution (Alcon, AMO), Payment or honoraria for lectures, presentations, speakers bureaus, manuscript writing or educational events (Bayer, Santen, Chugai, Novartis, Senju, HOYA, Kowa, Amgen); M. Akiyama, Advisory board on genetic testing system (Sysmex); Y. Ikeda, Advisory board on genetic testing system (Sysmex).

References

- Richards S, Aziz N, Bale S, Bick D, Das S, Gastier-Foster J, et al. ACMG laboratory quality assurance committee. standards and guidelines for the interpretation of sequence variants: a joint consensus recommendation of the American college of medical genetics and genomics and the association for molecular pathology. *Genet Med*. 2015;17:405–24.
- Abou Tayoun AN, Pesaran T, DiStefano MT, Oza A, Rehm HL, Biesecker L, et al. ClinGen sequence variant interpretation working group (ClinGen SVI) recommendations for interpreting the loss of function PVS1 ACMG/AMP variant criterion. *Hum Mutat*. 2018;39:1517–24.
- Oza AM, DiStefano MT, Hemphill SE, Cushman BJ, Grant AR, Siegert RK, et al. Expert specification of the ACMG/AMP variant interpretation guidelines for genetic hearing loss. *Hum Mutat*. 2018;39:1593–613.
- Iwanami M, Oishi A, Ogino K, Seko Y, Nishida-Shimizu T, Yoshimura N, et al. Five major sequence variants and copy number variants in the EYS gene account for one-third of Japanese patients with autosomal recessive and simplex retinitis pigmentosa. *Mol Vis*. 2019;25:766–79.
- Nishiguchi KM, Miya F, Mori Y, Fujita K, Akiyama M, Kamatani T, et al. A hypomorphic variant in EYS detected by genome-wide association study contributes toward retinitis pigmentosa. *Commun Biol*. 2021;4:140.
- Numa S, Oishi A, Higasa K, Oishi M, Miyata M, Hasegawa T, et al. EYS is a major gene involved in retinitis pigmentosa in Japan: genetic landscapes revealed by stepwise genetic screening. *Sci Rep*. 2020;10:20770.
- Yang L, Fujinami K, Ueno S, Kuniyoshi K, Hayashi T, Kondo M, et al. Genetic spectrum of EYS-associated retinal disease in a large Japanese cohort: identification of disease-associated variants with relatively high allele frequency. *Sci Rep*. 2020;10:5497.
- Walker LC, Hoya M, Wiggins GAR, Lindy A, Vincent LM, Parsons MT, et al. Using the ACMG/AMP framework to capture evidence related to predicted and observed impact on splicing: recommendations from the ClinGen SVI splicing subgroup. *Am J Hum Genet*. 2023;110:1046–67.
- Pejaver V, Byrne AB, Feng BJ, Pagel KA, Mooney SD, Karchin R, et al. Calibration of computational tools for missense variant pathogenicity classification and ClinGen recommendations for PP3/BP4 criteria. *Am J Hum Genet*. 2022;109:2163–77.
- Ioannidis NM, Rothstein JH, Pejaver V, Middha S, McDonnell SK, Baheti S, et al. REVEL: an ensemble method for predicting the pathogenicity of rare missense variants. *Am J Hum Genet*. 2016;99:87785.
- Xiang J, Peng J, Baxter S, Peng Z. AutoPVS1: an automatic classification tool for PVS1 interpretation of null variants. *Hum Mutat*. 2020;4:1488–98.
- Verbakel SK, van Huët RAC, den Hollander AI, Geerlings MJ, Kersten E, Klevering BJ, et al. Macular dystrophy and cone-rod dystrophy caused by mutations in the *RPL* gene: extending the *RPL* disease spectrum. *Invest Ophthalmol Vis Sci*. 2019;60:1192–203.
- Liu Q, Collin RW, Cremers FP, den Hollander AI, van den Born LI, Pierce EA. Expression of wild-type Rpl protein in *Rpl* knock-in mice rescues the retinal degeneration phenotype. *PLoS One*. 2012;7:e43251.
- Nishiguchi KM, Kunikata H, Fujita K, Hashimoto K, Koyanagi Y, Akiyama M, et al. Association of CRX genotypes and retinal phenotypes confounded by variable expressivity and electronegative electroretinogram. *Clin Exp Ophthalmol*. 2020;48:644–57.
- Fujinami-Yokokawa Y, Fujinami K, Kuniyoshi K, Hayashi T, Ueno S, Mizota A, et al. Clinical and genetic characteristics of 18 patients from 13 Japanese families with CRX-associated retinal disorder: identification of genotype-phenotype association. *Sci Rep*. 2020;10:9531.
- Huang L, Xiao X, Li S, Jia X, Wang P, Guo X, et al. CRX variants in cone-rod dystrophy and mutation overview. *Biochem Biophys Res Commun*. 2012;426:498–503.
- Reeves MJ, Goetz KE, Guan B, Ullah E, Blain D, Zein WM, et al. Genotype-phenotype associations in a large *PRPH2*-related retinopathy cohort. *Hum Mutat*. 2020;41:1528–39.
- Oishi A, Fujinami K, Mawatari G, Naoi N, Ikeda Y, Ueno S, et al. Genetic and phenotypic landscape of *PRPH2*-associated retinal dystrophy in Japan. *Genes (Basel)*. 2021;12:1817.
- Strande NT, Riggs ER, Buchanan AH, Ceyhan-Birsoy O, DiStefano M, Dwight SS, et al. Evaluating the clinical validity of gene-disease associations: an evidence-based framework developed by the clinical genome resource. *Am J Hum Genet*. 2017;100:895–906.
- Nishiguchi KM, Ikeda Y, Fujita K, Kunikata H, Akiho M, Hashimoto K, et al. Phenotypic features of Oguchi disease and retinitis pigmentosa in patients with S-antigen mutations: a long-term follow-up study. *Ophthalmology*. 2019;126:1557–66.
- Miyake Y, Horiguchi M, Suzuki S, Kondo M, Tanikawa A. Electrophysiological findings in patients with Oguchi's disease. *Jpn J Ophthalmol*. 1996;40:511–9.
- Murakami Y, Koyanagi Y, Fukushima M, Yoshimura M, Fujiwara K, Akiyama M, et al. Genotype and long-term clinical course of Bietti crystalline dystrophy in Korean and Japanese patients. *Ophthalmol Retina*. 2021;5:1269–79.
- de Carvalho ER, Robson AG, Arno G, Boon CJF, Webster AA, Michaelides M. Enhanced S-cone syndrome: spectrum of clinical, imaging, electrophysiologic, and genetic findings in a retrospective case series of 56 patients. *Ophthalmol Retina*. 2021;5:195–214.
- Mears AJ, Kondo M, Swain PK, Takada Y, Bush RA, Saunders TL, et al. Nrl is required for rod photoreceptor development. *Nat Genet*. 2001;29:447–52.

Publisher's Note Springer Nature remains neutral with regard to jurisdictional claims in published maps and institutional affiliations.

rs #	Chr	Position	(GR Allele	Allele	Gene syml	Pathogenic/Likely pa	Nucleotide change	Amino acid change	Transcript ID	J-IRD-VI criteria
rs756649389	1	9972074	A	G	NMNAT1	Pathogenic	c.1A>G	p.M1V	NM_022787	PVS1, PM2, PP5, PM3
rs748902766	1	9972126	A	G	NMNAT1	Pathogenic	c.53A>G	p.N18S	NM_022787	PM1,PM2, PM3, PP3, PP5, PP3
rs763325435	1	9975672	C	T	NMNAT1	Pathogenic	c.196C>T	p.R66W	NM_022787	PM1,PM2, PM3, PP3, PP5, PP3
	1	9978227	g.9978227_9		NMNAT1	Pathogenic	c.299+2452_*275del		NM_022787	PVS1, PM3
	1	9979705	g.9979705_9		NMNAT1	Pathogenic	c.300-1326_*13512del		NM_022787	PVS1, PM3
	1	9982508	GG	G	NMNAT1	Pathogenic	c.648del	p.W216*	NM_022787	PVS1, PM2, PM3
rs375110174	1	9982570	C	T	NMNAT1	Pathogenic	c.709C>T	p.R237C	NM_022787	PM1,PM2, PM3, PP3, PP5, PS3, PP3
	1	26460115	C	T	DHDDS	Likely Pathogenic	c.736C>T	p.(Gln246*)	NM_205861	PVS1_Strong, PM2
rs121917745	1	68429835	G	A	RPE65	Pathogenic	c.1543C>T	p.(Arg515Trp)	NM_000329	PS1, PM3_Very Strong, PP3
rs281865520	1	68438248	T	TT	RPE65	Pathogenic	c.1067dupA	p.(Asn356Lysfs*9)	NM_000329	PVS1_Very Strong, PM3_Moderate, PP5
rs2100817136	1	68438287	A	C	RPE65	Pathogenic	c.1028T>G	p.(Leu343*)	NM_000329	PVS1_Very Strong, PM2, PM3_Moderate
rs61752877	1	68444656	G	A	RPE65	Pathogenic	c.370C>T	p.(Arg124*)	NM_000329	PVS1_Very Strong, PM3, PP5
s7596 90120	1	68444794	C	T	RPE65	Likely Pathogenic	c.355G>A	p.(Cys112Tyr)	NM_000329	PS3_moderate, PM2, PM3_Supporting, PP3
	1	68446772	A	AA	RPE65	Likely Pathogenic	c.183_184insT	p.(Asp62*)	NM_000329	PVS1_Very Strong, PM2
	1	68446778	G	C	RPE65	Pathogenic	c.177C>G	p.(His59Gln)	NM_000329	PS3, PM2, PM3, PP3
rs368088025	1	68446825	G	A	RPE65	Pathogenic	c.130C>T	p.(Arg44*)	NM_000329	PVS1_Very Strong, PM3_Strong, PP5
rs61751281	1	68446837	C	T	RPE65	Likely Pathogenic	c.118G>A	p.(Gly40Ser)	NM_000329	PP1_Supporting, PP3, PP5, PM5, PM3_Moderate
rs866809120	1	68448668	TCAA	T	RPE65	Pathogenic	c.46_49del	p.(Phe16Lysfs*14)	NM_000329	PVS1_Very Strong, PM2, PM3_Moderate
rs61753045	1	93997981	G	T	ABCA4	Pathogenic	c.6609C>A	p.(Tyr2203Ter)	NM_000350.3	PVS1, PM2, PM3, PP5
rs61750654	1	94000870	G	A	ABCA4	Pathogenic	c.6445C>T	p.(Arg2149Ter)	NM_000350.3	PVS1, PM3, PP5
rs61750648	1	94001072	G	A	ABCA4	Likely Pathogenic	c.6316C>T	p.(Arg2106Cys)	NM_000350.3	PM3_Strong, PM5, PP3, PP5
	1	94001098	G	A	ABCA4	Likely pathogenic	c.6290C>T	p.(Pro2097Leu)	NM_000350.3	PM2, PM3_strong, PP3, PP5
rs61751383	1	94005500	G	A	ABCA4	Pathogenic	c.6088C>T	p.(Arg2030Ter)	NM_000350.3	PVS1, PM3, PP5
rs61750639	1	94007710	C	T	ABCA4	Pathogenic	c.5929G>A	p.(Gly1977Ser)	NM_000350.3	PM3_Verystrong, PP3, PP5
	1	94011262	C	A	ABCA4	Likely pathogenic	c.5584G>T	p.(Gly1862Cys)	NM_000350.3	PM2, PM3_moderate, PP3, PP5
rs62642576	1	94011319	G	A	ABCA4	Pathogenic	c.5527C>T	p.(Arg1843Trp)	NM_000350.3	PM3_Verystrong, PP3, PP5
rs62642562	1	94011334	G	C	ABCA4	Pathogenic	c.5512C>G	p.(His1838Asp)	NM_000350.3	PM3_Verystrong, PP3, PP5
	1	94014541	A	G	ABCA4	Pathogenic	c.5460+2T>C		NM_000350.3	PVS1, PM2, PM3_moderate
	1	94014601	AAC	A	ABCA4	Likely Pathogenic	c.5400_5401del	p.(Phe1801HisfsTer16	NM_000350.3	PVS1, PM2

rs760549861	1	94014685	G	A	ABCA4	Pathogenic	c.5318C>T	p.(Ala1773Val)	NM_000350.3	PM2, PM3_Verystrong, PP3, PP5
rs776757706	1	94014688	C	T	ABCA4	Pathogenic	c.5315G>A	p.(Trp1772Ter)	NM_000350.3	PVS1, PM2, PM3_moderate, PP5
rs61750157	1	94021391	C	T	ABCA4	Likely Pathogenic	c.4867G>A	p.(Gly1623Ser)	NM_000350.3	PM2, PM3_moderate, PM5_moderate, PP3, PP5
rs61750153	1	94021871	A	G	ABCA4	Likely Pathogenic	c.4748T>C	p.(Leu1583Pro)	NM_000350.3	PM3_strong, PP3, PP5
rs61750147	1	94029521	C	T	ABCA4	Likely Pathogenic	c.4463G>A	p.(Cys1488Tyr)	NM_000350.3	PM2, PM3_moderate, PM5_moderate, PP3, PP4
rs61750146	1	94029522	A	G	ABCA4	Pathogenic	c.4462T>C	p.(Cys1488Arg)	NM_000350.3	PM2, PM3_Verystrong, PM5, PP3, PP5
rs200967229	1	94030427	C	T	ABCA4	Likely Pathogenic	c.4352+1G>A		NM_000350.3	PVS1_moderate, PM3_Strong, PP5
rs61750142	1	94030452	C	T	ABCA4	Pathogenic	c.4328G>A	p.(Arg1443His)	NM_000350.3	PM3_Verystrong, PM5, PP3, PP5
rs61750138	1	94030991	C	A	ABCA4	Pathogenic	c.4253+5G>T		NM_000350.3	PM2, PM3_Verystrong, PP5
rs763267492	1	94042802	G	A	ABCA4	Likely Pathogenic	c.3287C>T	p.(Ser1096Leu)	NM_000350.3	PM3_Strong, PP3, PP5.
rs201855602	1	94043470	G	A	ABCA4	Pathogenic	c.3056C>T	p.(Thr1019Met)	NM_000350.3	PM3_Strong, PM2, PM5_supporting, PP3, PP5
rs201471607	1	94046943	T	C	ABCA4	Pathogenic	c.2894A>G	p.(Asn965Ser)	NM_000350.3	PM3_Verystrong, PM5_moderate, PP3, PP5
rs575453437	1	94060674	C	T	ABCA4	Likely Pathogenic	c.2023G>A	p.(Val675Ile)	NM_000350.3	PS3_Moderate, PM3_moderate, PP3, PP5
rs61749418	1	94062581	C	T	ABCA4	Likely Pathogenic	c.1933G>A	p.(Asp645Asn)	NM_000350.3	PM3_moderate, PM5_moderate, PP3, PP5
rs61751385	1	94063110	A	C	ABCA4	Pathogenic	c.1760+2T>G		NM_000350.3	PVS1, PM3_Verystrong, PP5
	1	94078699	G	C	ABCA4	Pathogenic	c.1247C>G	p.(Ser416Ter)	NM_000350.3	PVS1, PM2, PM3_Supporting
	1	94080477	C	T	ABCA4	Pathogenic	c.1099+1G>A		NM_000350.3	PVS1, PM2, PM3_moderate
rs794727903	1	94080697	G	A	ABCA4	Pathogenic	c.880C>T	p.(Gln294Ter)	NM_000350.3	PVS1, PM2, PM3_moderate, PP5
	1	94103013	A	C	ABCA4	Likely Pathogenic	c.570+2T>G		NM_000350.3	PVS1, PM2
	1	94103032	G	A	ABCA4	Pathogenic	c.553C>T	p.(Gln185Ter)	NM_000350.3	PVS1, PM2, PM3_moderate
rs62654395	1	94111546	C	T	ABCA4	Likely Pathogenic	c.194G>A	p.(Gly65Glu)	NM_000350.3	PM3_Strong, PP3, PP5
	1	94113041	C	T	ABCA4	Pathogenic	c.92G>A	p.(Trp31Ter)	NM_000350.3	PVS1, PM2, PM3_moderate
	1	150343307	A	G	PRPF3	Pathogenic	c.1283-2A>G		NM_004698	PVS1_Moderate, PM2, PP5
	1	197268414	T	C	CRB1	Likely pathogenic	c.2T>C	p.M1?	NM_201253	PVS1_Verystrong, PM2
	1	197328434	A	AT	CRB1	Likely pathogenic	c.84dupT	p.K29*	NM_201253	PVS1_Verystrong, PM2
	1	197329003	GGTA/	G	CRB1	Pathogenic	c.652+3_652+6delAAGT		NM_201253	PVS1_Strong, PM3_Strong, PM2
	1	197329004	G	T	CRB1	Likely pathogenic	c.652+1G>T		NM_201253	PVS1_Strong, PM2, PM3_supporting
	1	197421079	GA	G	CRB1	Likely pathogenic	c.1045delA	p.N418Ifs*34	NM_201253	PVS1_Verystrong, PM2
rs114342808	1	197421404	C	T	CRB1	Likely pathogenic	c.1576C>T	p.R526X	NM_201253	PVS1_Verystrong, PM3
	1	197421516	GC	G	CRB1	Likely pathogenic	c.1482delC	p.S563Rfs*10	NM_201253	PVS1_Verystrong, PM2

rs267598278	1	197421741	C	T	CRB1	Likely pathogenic	c.1913C>T	p.S638L	NM_201253	PM3_Strong, PM5, PP1, PP5
rs150412614	1	197427555	C	T	CRB1	Likely pathogenic	c.2230C>T	p.R744X	NM_201253	PVS1_VeryStrong, PM3, PP1, PP5
rs767648174	1	197427633	G	A	CRB1	Likely pathogenic	c.2308G>A	p.G770S	NM_201253	PM3_Strong, PM5, PP3, PP5
rs752377040	1	215634578	A	G	USH2A	Likely Pathogenic	c.15178T>C	p.Ser5060Pro	NM_206933	PM5, PM3_VeryStrong,
	1	215648540	C	A	USH2A	Likely Pathogenic	c.14570G>T	p.Gly4857Val	NM_206933	PM5, PM2, PM3_Strong
rs527236125	1	215648660	C	T	USH2A	Likely Pathogenic	c.14450G>A	p.Gly4817Glylu	NM_206933	PS1, PM2, PP5
rs397517990	1	215650648	C	T	USH2A	Likely Pathogenic	c.14287G>A	p.Gly4763Arg	NM_206933	PS1, PM2, PM3_Moderate, PP5
	1	215650729	CT	C	USH2A	Likely Pathogenic	c.14205delA	p.Glu4736Lysfs*10	NM_206933	PVS1_VeryStrong, PM2
	1	215670970	A	T	USH2A	Likely Pathogenic	c.14133+2T>A		NM_206933	PVS1_VeryStrong, PM2
	1	215671095	G	T	USH2A	Likely Pathogenic	c.14010C>A	p.Tyr4670*	NM_206933	PVS1_VeryStrong, PM2
	1	215671100	AC	A	USH2A	Likely Pathogenic	c.14004delG	p.Leu4668Phefs*10	NM_206933	PVS1_VeryStrong, PM2
rs527236124	1	215671258	C	A	USH2A	Likely Pathogenic	c.13847G>T	p.Gly4616Val	NM_206933	PM5, PM3_Strong, PP1, PP5
	1	215671270	CA	C	USH2A	Likely Pathogenic	c.13834delT	p.Cys4612Alafs*22	NM_206933	PVS1_VeryStrong, PM2
	1	215674282	CC	C	USH2A	Likely Pathogenic	c.13628delG	p.Gly4544Valfs*6	NM_206933	PVS1_VeryStrong, PM2
rs527236127	1	215674445	C	T	USH2A	Likely Pathogenic	c.13466G>A	p.Gly4489Asp	NM_206933	PS1, PM2, PP5
	1	215674519	C	T	USH2A	Likely Pathogenic	c.13392G>A	p.Trp4464*	NM_206933	PVS1_VeryStrong, PM2
rs139474806	1	215674572	T	C	USH2A	Likely Pathogenic	c.13339A>G	p.Met4447Val	NM_206933	PM5, PM3_VeryStrong,
	1	215674608	TT	T	USH2A	Likely Pathogenic	c.13302delA	p.Lys4435Asnfs*26	NM_206933	PVS1_VeryStrong, PM2
	1	215674707	G	A	USH2A	Pathogenic	c.13204C>T	p.Gln4402*	NM_206933	PVS1_VeryStrong, PM2, PM3_Supporting
rs768161313	1	215674795	CATTT	C	USH2A	Likely Pathogenic	c.13112_13115del	p.Gln4371Argfs*19	NM_206933	PVS1_VeryStrong, PM3_Moderate, PP5
rs527236137	1	215674901	G	A	USH2A	Pathogenic	c.13010C>T	p.Thr4337Met	NM_206933	PS1, PM3_Strong, PP1, PP5
rs397517982	1	215675172	C	T	USH2A	Likely Pathogenic	c.12739G>A	p.Gly4247Arg	NM_206933	PS1, PM2, PP3, PP5
	1	215675203	A	T	USH2A	Likely Pathogenic	c.12708T>A	p.Cys4236*	NM_206933	PVS1_VeryStrong, PM2
	1	215675464	C	T	USH2A	Likely Pathogenic	c.12447G>A	p.Trp4149*	NM_206933	PVS1_VeryStrong, PM2
	1	215675494	AC	A	USH2A	Likely Pathogenic	c.12416delG	p.Gly4139Valfs*28	NM_206933	PVS1_VeryStrong, PM2
	1	215680217	G	A	USH2A	Likely Pathogenic	c.12226C>T	p.Gln4076*	NM_206933	PVS1_VeryStrong, PM2
rs527236138	1	215680275	C	T	USH2A	Likely Pathogenic	c.12168G>A	p.Trp4056*	NM_206933	PVS1_VeryStrong, PM2
	1	215680364	G	A	USH2A	Pathogenic	c.12079C>T	p.Gln4027*	NM_206933	PVS1_VeryStrong, PM2, PP1, PP5
	1	215728283	TAG	T	USH2A	Pathogenic	c.11811_11812del	p.Tyr3938Argfs*8	NM_206933	PVS1_VeryStrong, PM2, PM3_Supporting
	1	215759735	C	T	USH2A	Pathogenic	c.11156G>A	p.Arg3719His	NM_206933	PM5, PM3_VeryStrong, PP1, PP5
	1	215759735	C	T	USH2A	Pathogenic	c.11156G>A	p.Arg3719His	NM_206933	PM5, PM3_VeryStrong, PP1, PP5

	1	215779842	C	A	USH2A	Likely Pathogenic	c.10939+1G>T		NM_206933	PVS1_VeryStrong, PM2
rs527236119	1	215782779	T	C	USH2A	Likely Pathogenic	c.10544A>G	p.Asp3515Gly	NM_206933	PS1, PM2, PM3_Moderate
	1	215782808	AGG	A	USH2A	Pathogenic	c.10513_10514del	p.Pro3505Tyrfs*9	NM_206933	PVS1_VeryStrong, PM2, PM3_Supporting
rs549931193	1	215782825	G	A	USH2A	Pathogenic	c.10498C>T	p.Gln3500*	NM_206933	PVS1_VeryStrong, PM2, PM3_Supporting
	1	215786700	TATG/	T	USH2A	Likely Pathogenic	c.10353_10356del	p.His3452Glnfs*4	NM_206933	PVS1_VeryStrong, PM2
rs111033263	1	215799066	A	G	USH2A	Pathogenic	c.9799T>C	p.Cys3267Arg	NM_206933	PS1, PM3_Supporting, PP3, PP5
rs527236118	1	215799114	A	G	USH2A	Likely Pathogenic	c.9751T>C	p.Cys3251Arg	NM_206933	PS1, PM2, PP1, PP5
rs760225886	1	215816996	C	T	USH2A	Pathogenic	c.9570+1G>A		NM_206933	PVS1_VeryStrong, PM3_Strong, PP5
	1	215817118	C	T	USH2A	Likely Pathogenic	c.9449G>A	p.Trp3150*	NM_206933	PVS1_VeryStrong, PM2
	1	215837990	C	A	USH2A	Likely Pathogenic	c.9371+1G>T		NM_206933	PVS1_VeryStrong, PM2
	1	215844293	C	A	USH2A	Likely Pathogenic	c.9258+1G>T		NM_206933	PVS1_VeryStrong, PM3_Moderate, PP5
rs2102821808	1	215844383	CATAC	C	USH2A	Pathogenic	c.9165_9168del	p.Ile3055Metfs*2	NM_206933	PVS1_VeryStrong, PM2, PP5
rs527236120	1	215867169	AC	A	USH2A	Likely Pathogenic	c.8682delG	p.Arg2894Serfs*23	NM_206933	PVS1_VeryStrong, PM2, PP5
rs397518039	1	215877882	T	C	USH2A	Pathogenic	c.8559-2A>G		NM_206933	PVS1_Moderate, PM3_VeryStrong, PP1, PP5
	1	215878929	CC	C	USH2A	Likely Pathogenic	c.8392delG	p.Gly2799Valfs*31	NM_206933	PVS1_VeryStrong, PM2
rs201863550	1	215879068	C	T	USH2A	Pathogenic	c.8254G>A	p.Gly2752Arg	NM_206933	PS1, PM3_VeryStrong, PP1, PP5
	1	215888437	CG	C	USH2A	Likely Pathogenic	c.8211delC	p.Asp2738Metfs*31	NM_206933	PVS1_VeryStrong, PM2
	1	215888765	TG	T	USH2A	Likely Pathogenic	c.7883delC	p.Pro2628Glnfs*13	NM_206933	PVS1_VeryStrong, PM2
	1	215888989	G	A	USH2A	Pathogenic	c.7660C>T	p.Gln2554*	NM_206933	PVS1_VeryStrong, PM2, PM3_Moderate
	1	215934664	G	A	USH2A	Likely Pathogenic	c.7252C>T	p.Gln2418*	NM_206933	PVS1_VeryStrong, PM2
	1	215934705	GG	C	USH2A	Likely Pathogenic	c.7210_7211delinsG	p.Pro2404Valfs*9	NM_206933	PVS1_VeryStrong, PM2
rs199840367	1	215970645	C	A	USH2A	Likely Pathogenic	c.6937G>T	p.Gly2313Cys	NM_206933	PM5, PM3_Moderate, PP5
rs55958016	1	216000489	C	T	USH2A	Pathogenic	c.6399G>A	p.Trp2133*	NM_206933	PVS1_VeryStrong, PM2, PM3_Moderate, PP1, PP5
	1	216046521	T	A	USH2A	Likely Pathogenic	c.6235A>T	p.Lys2079*	NM_206933	PVS1_VeryStrong, PM2
rs1053812278	1	216070216	AG	A	USH2A	Pathogenic	c.5933delC	p.Pro1978Leufs*6	NM_206933	PVS1_VeryStrong, PM2, PM3_Supporting
	1	216070283	CTT	C	USH2A	Likely Pathogenic	c.5865_5866del	p.Ser1956Cysfs*16	NM_206933	PVS1_VeryStrong, PM2
rs751130485	1	216072910	G	A	USH2A	Likely Pathogenic	c.5836C>T	p.Arg1946*	NM_206933	PVS1_VeryStrong, PM3_Moderate, PP5
	1	216078095	C	A	USH2A	Likely Pathogenic	c.5566G>T	p.Glu1856*	NM_206933	PVS1_VeryStrong, PM2
	1	216078265	TTTCC	T	USH2A	Likely Pathogenic	c.5391_5395del	p.Asn1797Lysfs*4	NM_206933	PVS1_VeryStrong, PM2
	1	216078266	TT	T	USH2A	Likely Pathogenic	c.5394delA	p.Lys1799Serfs*18	NM_206933	PVS1_VeryStrong, PM2
rs770329105	1	216078332	G	A	USH2A	Pathogenic	c.5329C>T	p.Arg1777Trp	NM_206933	PS1, PM3_Supporting, PP5
	1	216084706	AG	A	USH2A	Pathogenic	c.5158delC	p.Leu1720*	NM_206933	PVS1_VeryStrong, PM2, PP5
rs754768875	1	216086749	G	A	USH2A	Pathogenic	c.4957C>T	p.Arg1653*	NM_206933	PVS1_VeryStrong, PM3_Moderate, PP5
	1	216175245	CACTT	C	USH2A	Likely Pathogenic	c.4630_4633del	p.Lys1544Valfs*25	NM_007123	PVS1_VeryStrong, PM2
	1	216175299	T	C	USH2A	Likely Pathogenic	c.4580A>G	p.Tyr1527Cys	NM_007123	PM2, PM3_VeryStrong,
	1	216175430	GATT	C	USH2A	Likely Pathogenic	c.4431_4448del	p.Ile1478_Ile1483del	NM_007123	PM4, PM2, PM3_Moderate
rs527236136	1	216198428	AT	A	USH2A	Pathogenic	c.3967delA	p.Met1323*	NM_007123	PVS1_VeryStrong, PM2, PP5
	1	216198461	GC	G	USH2A	Likely Pathogenic	c.3934delG	p.Ala1312Profs*6	NM_007123	PVS1_VeryStrong, PM2
	1	216198504	GA	G	USH2A	Pathogenic	c.3891delT	p.Gln1298Argfs*12	NM_007123	PVS1_VeryStrong, PM2, PP5

rs527236135	1	216199719	TG	T	USH2A	Likely Pathogenic	c.3718delC	p.Gln1240Argfs*7	NM_007123	PVS1_VeryStrong, PM2
	1	216199839	CCTT	C	USH2A	Likely Pathogenic	c.3596_3598del	p.Glu1199del	NM_007123	PM4, PM2, PM3_Supporting
	1	216200086	AT	A	USH2A	Pathogenic	c.3351delA	p.Tyr1118Ilefs*20	NM_007123	PVS1_VeryStrong, PM2, PM3_Supporting
	1	216231963	G	A	USH2A	Likely Pathogenic	c.2983C>T	p.Gln995*	NM_007123	PVS1_VeryStrong, PM2, PP5
	1	216246741	G	A	USH2A	Likely Pathogenic	c.2653C>T	p.His885Tyr	NM_007123	PM5, PM3_Moderate, PP1, PP3
	1	216246784	G	T	USH2A	Pathogenic	c.2610C>A	p.Cys870*	NM_007123	PVS1_VeryStrong, PM3_Moderate, PP5
	1	216247207	G	T	USH2A	Pathogenic	c.2187C>A	p.Cys729*	NM_007123	PVS1_VeryStrong, PM3_Moderate, PP5
	1	216289328	A	T	USH2A	Pathogenic	c.1923T>A	p.Cys641*	NM_007123	PVS1_VeryStrong, PM2, PP5
	1	216289338	CAAA	C	USH2A	Likely Pathogenic	c.1908_1912del	p.Asp636Glu*5	NM_007123	PVS1_VeryStrong, PM2
	1	216289339	AACA	A	USH2A	Pathogenic	c.1907_1911del	p.Asp636Valfs*5	NM_007123	PVS1_VeryStrong, PM2, PM3_Supporting
rs534534437	1	216289375	G	A	USH2A	Pathogenic	c.1876C>T	p.Arg626*	NM_007123	PVS1_VeryStrong, PM3_Supporting, PP5
	1	216292174	C	T	USH2A	Likely Pathogenic	c.1840+1G>A		NM_206933	PVS1_Strong, PM2
	1	216292222	AAGT	A	USH2A	Likely Pathogenic	c.1774_1792del	p.Pro592Serfs*38	NM_007123	PVS1_VeryStrong, PM2
	1	216292286	A	G	USH2A	Likely Pathogenic	c.1729T>C	p.Cys577Arg	NM_007123	PM5, PM2, PM3_Supporting, PP3
	1	216292292	AAG	A	USH2A	Likely Pathogenic	c.1721_1722del	p.Pro574Leufs*22	NM_007123	PVS1_VeryStrong, PM2
	1	216292372	T	G	USH2A	Pathogenic	c.1645-2A>C		NM_206933	PVS1_VeryStrong, PM2, PM3_Supporting
	1	216323633	C	T	USH2A	Likely Pathogenic	c.1391G>A	p.Arg464His	NM_007123	PS1, PM3_Moderate, PP5
	1	216323634	G	A	USH2A	Likely Pathogenic	c.1390C>T	p.Arg464Cys	NM_007123	PP5, PM2, PM3_Supporting
	1	216324229	C	A	USH2A	Likely Pathogenic	c.1267G>T	p.Gly423*	NM_007123	PVS1_VeryStrong, PM2
	1	216327619	G	A	USH2A	Pathogenic	c.820C>T	p.Arg274*	NM_007123	PVS1_VeryStrong, PM2, PP5
rs111033280	1	216327637	C	T	USH2A	Pathogenic	c.802G>A	p.Gly268Arg	NM_007123	PS1, PM3_Supporting, PP3, PP5
	1	216365052	C	G	USH2A	Likely Pathogenic	c.685G>C	p.Gly229Arg	NM_007123	PS1, PP3, PP5
	1	216418675	C	A	USH2A	Pathogenic	c.490G>T	p.Val164Phe	NM_007123	PS1, PM3_Supporting, PP1, PP5
	2	29070736	G	A	PCARE	Pathogenic	c.3526C>T	p.Q1176X	NM_00102988	PVS1, PM2, PM3_Supporting
	2	29070902	ATG	A	PCARE	Pathogenic	c.3358_3360delinsT	p.H1120Ffs*12	NM_00102988	PVS1, PM2, PM3
	2	29070946	C	A	PCARE	Likely Pathogenic	c.3316G>T	p.E1106X	NM_00102988	PVS1, PM2
	2	29071274	G	GG	PCARE	Pathogenic	c.2988delinsCA	p.T997Hfs*110	NM_00102988	PVS1, PM2, PM3_Supporting
	2	29072170	T	A	PCARE	Likely Pathogenic	c.2092A>T	p.K698X	NM_00102988	PVS1, PM2
	2	29073437	G	GA	PCARE	Pathogenic	c.825delinsTC	p.S276Qfs*35	NM_00102988	PVS1, PM2, PM3_Supporting
	2	29073690	A	AAGC	PCARE	Pathogenic	c.572delinsAGGCTTAC	p.L191Qfs*15	NM_00102988	PVS1, PM2, PM3_Supporting
rs2063893838	2	29073692	A	C	PCARE	Pathogenic	c.570T>G	p.Y190X	NM_00102988	PVS1, PM2, PM3_Supporting
	2	29073693	TA	T	PCARE	Pathogenic	c.568_569delinsA	p.Y190Ifs*66	NM_00102988	PVS1, PM2, PM3_Supporting
	2	29073865	C	A	PCARE	Pathogenic	c.397G>T	p.E133X	NM_00102988	PVS1, PM2, PM3_Supporting
	2	96279487	CT	C	SNRNP20C	Likely pathogenic	c.5096delA	p.(Glu1699fs)	NM_014014	PVS1,PM2
	2	96293088	G	A	SNRNP20C	Likely pathogenic	c.2044C>T	p.Pro682Ser	NM_014014	PS1,PM2,PP3,PP5
	2	96293090	C	T	SNRNP20C	Likely pathogenic	c.2042G>A	p.(Arg681His)	NM_014014	PM2, PM5, PP3, PP5
	2	96293091	G	A	SNRNP20C	Likely pathogenic	c.2041C>T	p.(Arg681Cys)	NM_014014	PM2, PM5, PP3, PP5
	2	98396166	AGA	A	CNGA3	Likely Pathogenic	c.997_998del	p.D333Lfs*35	NM_001298	PVS1、PM2
	2	111929283	AG	G	MERTK	Pathogenic	c.225_226delinsG	p.G76Efs*3	NM_006343	PVS1,PM2,PM3,PP5

rs527236134	2	111929428	C	T	MERTK	Pathogenic	c.370C>T	p.Q124X	NM_006343	PVS1,PM2,PM3_Supporting
	2	112019512	C	T	MERTK	Pathogenic	c.2179C>T	p.R727X	NM_006343	PVS1, PM2, PM3, PP1_Moderate, PP5
	2	181566095	AC	A	CERKL	Likely Pathogenic	c.639delG	p.(Ser214HisfsTer36)	NM_00103031	PVS1, PM3_supporting
rs746595127	2	181603865	C	T	CERKL	Pathogenic	c.453G>A	p.(Trp151Ter)	NM_00103031	PVS1, PM3_supporting, PP5
rs587777209	2	233328488	C	T	SAG	Pathogenic	c.523C>T	p.R175X	NM_000541	PVS1,PM3,PP4
	2	233328600	CT	C	SAG	Pathogenic	c.636delT	p.L213Sfs*14	NM_000541	PVS1,PM2,PM3_Supporting、PP4
rs397514681	2	233335029	C	T	SAG	Pathogenic	c.874C>T	p.R292X	NM_000541	PVS1,BA1(AD_gene),PP4,PM3_Supporting
	2	233335079	AA	A	SAG	Pathogenic	c.924_925delinsA	p.N309Tfs*12	NM_000541	PVS1,PM2,PM3、PP4
	3	101229408	ATC	A	IMPG2	Likely Pathogenic	c.3603_3604del	p.Gln1201Hisfs*3	NM_016247	PVS1_VeryStrong, PM2
rs267606875	3	101232917	C	A	IMPG2	Likely Pathogenic	c.3097G>T	p.Glu1033*	NM_016247	PVS1_VeryStrong, PM2
	3	101242820	G	A	IMPG2	Pathogenic	c.2890C>T	p.Arg964*	NM_016247	PVS1_VeryStrong, PM3_Supporting, PP5
	3	101243615	G	A	IMPG2	Pathogenic	c.2716C>T	p.Arg906*	NM_016247	PVS1_VeryStrong, PM3_Strong, PP5
rs267606876	3	101246000	GT	G	IMPG2	Likely Pathogenic	c.1344delA	p.Glu448Aspfs*11	NM_016247	PVS1_VeryStrong, PM2
	3	101246082	C	T	IMPG2	Pathogenic	c.1263G>A	p.Trp421*	NM_016247	PVS1_VeryStrong, PM2, PM3_Supporting, PP5
	3	101319593	TA	T	IMPG2	Likely Pathogenic	c.324delT	p.Phe108Leufs*31	NM_016247	PVS1_VeryStrong, PM2
rs587783011	3	101319825	GGTT	G	IMPG2	Likely Pathogenic	c.89_92del	p.Gln30Profs*5	NM_016247	PVS1_VeryStrong, PM2
	3	121772605	T	TCT	IQCB1	Likely pathogenic	c.1522_1523dup	p.(Ala509LysfsTer3)	NM_00102357	PVS1_strong,PM3_supporting,PP5
	3	121788368	C	T	IQCB1	Pathogenic	c.1194G>A	p.(Trp398Ter)	NM_00102357	PVS1,PM2,PP5
rs1948821736	3	121790112	G	A	IQCB1	Pathogenic	c.1090C>T	p.(Arg364Ter)	NM_00102357	PVS1,PM3_supporting,PP5,
rs727503968	3	129528777	A	G	RHO	Pathogenic	c.44A>G	p.N15S	NM_000539	PP5_Strong, PM5_Strong, PP3_Strong, PM1_Moderate, I
rs104893786	3	129528783	C	T	RHO	Pathogenic	c.50C>T	p.(Thr17Met)	NM_000539	PS3, PM2, PM5_Supporting, PM1_Strong, PP5
	3	129528801	C	T	RHO	Likely Pathogenic	c.68C>T	p.P23L	NM_000539	PS3_Moderate, PM2, PM5, PP1, PP3
rs28933394	3	129528906	C	G	RHO	Likely Pathogenic	c.173C>G	p.T58R	NM_000539	PM2, PM5_Supporting, PM1_Strong, PP3, PP5
rs527236101	3	129528913	C	A	RHO	Pathogenic	c.180C>A	p.Y60X	NM_000539	PVS1_Very Strong, PP5_Very Strong, PM2_Supporting
	3	129528929	A	T	RHO	Pathogenic	c.196A>T	p.K66X	NM_000539	PVS1, PM2, PP5
rs1057521112	3	129528996	T	C	RHO	Likely Pathogenic	c.263T>C	p.(Leu88Pro)	NM_000539	PS3_Moderate, PM2, PP1_Moderate, PP5
rs759945007	3	129529035	G	A	RHO	Likely Pathogenic	c.302G>A	p.G101E	NM_000539	PP3_Strong, PM1_Moderate, PM5_Moderate, PM2_Sup
rs104893773	3	129529049	G	A	RHO	Pathogenic	c.316G>A	p.G106R	NM_000539	PS3_Moderate, PM5_Strong, PM1_Strong, PP5
	3	129530891	G	T	RHO	Likely Pathogenic	c.377G>T	p.W126L	NM_000539	PM1_Moderate, PP3_Moderate, PM2_Supprrting, PP5_Si
rs104893775	3	129530917	C	T	RHO	Pathogenic	c.403C>T	p.R135W	NM_000539	PM2, PM5, PM1_Strong, PP3, PP5
rs104893793	3	129531005	C	T	RHO	Likely Pathogenic	c.491C>T	p.A164V	NM_000539	PS3_Moderate, PM5, PP1, PP5
	3	129531015	C	G	RHO	Pathogenic	c.501C>G	p.C167W	NM_000539	PM1_Strong, PM5_Strong, PP3_Strong, PP5_Strong, PM:
	3	129531026	C	T	RHO	Pathogenic	c.512C>T	p.P171L	NM_000539	PS3_Moderate, PM2, PM5, PM1_Strong, PP3, PP5
rs775557680	3	129532261	G	A	RHO	Likely Pathogenic	c.541G>A	p.E181K	NM_000539	PS3_Moderate, PM2, PM5_Supporting, PP1, PP3, PP5
rs527236100	3	129532282	G	A	RHO	Likely Pathogenic	c.562G>A	p.G188R	NM_000539	PS3_Moderate, PM2, PM5, PP1_Moderate, PP3
rs104893779	3	129532288	G	A	RHO	Likely Pathogenic	c.568G>A	p.D190N	NM_000539	PS3_Moderate, PM5, PM1_Strong, PP5
rs104893777	3	129532289	A	G	RHO	Likely Pathogenic	c.569A>G	p.D190G	NM_000539	PS3_Moderate, PM2, PM5, PP1
rs373974298	3	129532298	C	A	RHO	Likely Pathogenic	c.578C>A	p.T193K	NM_000539	PS3_Moderate, PM2, PM5, PP1
	3	129532754	T	A	RHO	Likely Pathogenic	c.918T>A	p.Y306X	NM_000539	PVS1_Strong, PM2

	3	129533606	A	G	RHO	Likely Pathogenic	c.937-2A>G		NM_000539	PVS1_Strong, PM2, PP5
	3	129533619	C	A	RHO	Likely Pathogenic	c.948C>A	p.(Cys316*)	NM_000539	PVS1_Strong, PM2
rs104893778	3	129533701	C	T	RHO	Pathogenic	c.1030C>T	p.Q344X	NM_000539	PVS1_Strong, PS3, PM2, PM1_Strong, PP5
rs29001637	3	129533710	C	T	RHO	Pathogenic	c.1039C>T	p.P347S	NM_000539	PS3, PM2, PM5, PM1_Strong
rs29001566	3	129533711	C	T	RHO	Pathogenic	c.1040C>T	p.P347L	NM_000539	PS3, PM2, PM5, PM1_Strong, PP5
	3	150972454	A	G	CLRN1	Pathogenic	c.253+2T>C	p.?	NM_174878	PVS1_Very Strong, PM2, PM3, PP3
	4	653926	C	G	PDE6B	Pathogenic	c.786C>G	p.(Tyr262Ter)	NM_000283.4	PVS1, PM2, PM3_Supporting
rs527236090	4	655939	G	C	PDE6B	Likely Pathogenic	c.993-1G>C		NM_000283.4	PVS1_Moderate, PM2, PM3
rs527236089	4	659018	G	C	PDE6B	Pathogenic	c.1467+1G>C		NM_000283.4	PVS1, PM2, PP5
	4	660575	G	A	PDE6B	Likely Pathogenic	c.1576G>A	p.(Glu526Lys)	NM_000283.4	PM2, PM3_moderate, PP3, PP5
rs527236088	4	660603	T	A	PDE6B	Pathogenic	c.1604T>A	p.(Ile535Asn)	NM_000283.4	PM3_Verystrong, PP1_Moderate, PP3, PP5
rs121918581	4	662188	C	T	PDE6B	Pathogenic	c.1669C>T	p.(His557Tyr)	NM_000283.4	PM3_Verystrong, PM5, PP3, PP5
rs761619791	4	662231	C	T	PDE6B	Likely Pathogenic	c.1712C>T	p.(Thr571Met)	NM_000283.4	PM2, PM3_Strong, PP3
rs373037737	4	663803	C	T	PDE6B	Pathogenic	c.1954C>T	p.(Gln652Ter)	NM_000283.4	PVS1, PM3, PP1, PP5
rs970990957	4	667898	C	T	PDE6B	Pathogenic	c.2395C>T	p.(Arg799Ter)	NM_000283.4	PVS1, PM2, PM3, PP1, PP5
rs1553901823	4	16000495	C	T	PROM1	Likely Pathogenic	c.1578+1G>A		NM_006017.3	AR PVS1, PP5
rs137853006	4	16013299	G	A	PROM1	Pathogenic	c.1117C>T	p.(Arg373Cys)	NM_006017.3	PS3, PP1_strong, PP5
	4	47936421	C	G	CNGA1	Likely Pathogenic	c.2061G>C	p.X687Tyr	NM_00114256	PS1, PM4, PM2
	4	47937064	AC	A	CNGA1	Likely Pathogenic	c.1417delG	p.Val473Tyrfs*17	NM_00114256	PVS1_Strong, PM2, PP1
rs369717052	4	47937224	G	A	CNGA1	Likely Pathogenic	c.1258C>T	p.Arg420*	NM_00114256	PVS1_Strong, PM2, PP5
	4	47940761	A	T	CNGA1	Pathogenic	c.652+2T>A	splicing	NM_00114256	PM2, PP3
rs749012133	4	47949866	AG	A	CNGA1	Pathogenic	c.253delC	p.Leu85Phefs*4	NM_00114256	PVS1_VeryStrong, PP1, PP5
	4	47951385	AT	A	CNGA1	Likely Pathogenic	c.191delA	p.Tyr64Leufs*25	NM_00114256	PVS1_VeryStrong, PM2
rs527236058	4	47951397	AC	A	CNGA1	Pathogenic	c.179delG	p.Gly60Valfs*29	NM_00114256	PVS1_VeryStrong, PP1, PP5
rs199476187	4	186194568	G	A	CYP4V2	likely pathogenic	c.283G>A	p.G95R	NM_207352	PM3_Verystrong, PP1, PP3, PP4, PP5
rs199476190	4	186197044	T	G	CYP4V2	likely pathogenic	c.518T>G	p.L173W	NM_207352	PM3_Strong, PP1, PP3, PP4, PP5, BS1
rs369063468	4	186198976	C	T	CYP4V2	Pathogenic	c.694C>T	p.R232X	NM_207352	PVS1, PM3, PP4, PP5
	4	186201223	GC	G	CYP4V2	likely pathogenic	c.868_869delinsG	p.S292Pfs*13	NM_207352	PVS1, PM2
rs199476198	4	186205232	G	A	CYP4V2	Pathogenic	c.1020G>A	p.W340X	NM_207352	PVS1, PM3_Strong, PP4, PP5
	4	186205269	A	GA	CYP4V2	Pathogenic	c.1057delinsGA	p.K353Efs*6	NM_207352	PVS1, PM2, PM3_Supporting, PP4
rs199476183	4	186208863	A	G	CYP4V2	Pathogenic	c.1091-2A>G		NM_207352	PVS1_Moderate, PM3_Strong, PP5, PP3
	4	186209164	T	C	CYP4V2	likely pathogenic	c.1297T>C	p.F433L	NM_207352	PM2, PM3, PP3, PP4
rs753942596	5	149884549	G	A	PDE6A	Pathogenic	c.1957C>T	p.(Arg653Ter)	NM_000440.3	PVS1, PM3_supporting, PP5
rs759589388	5	149895227	G	A	PDE6A	Pathogenic	c.1684C>T	p.(Arg562Trp)	NM_000440.3	PS3, PM3, PM5_Supporting, PP3, PP5
	6	10803832	C	T	MAK	Pathogenic	c.551G>A	p.W184X	NM_00124295	PVS1, PM2, PM3_Supporting
	6	10813662	C	GC	MAK	likely Pathogenic	c.340delinsGC	p.A116Gfs	NM_00124295	PVS1, PM3
rs775334320	6	35503627	G	A	TULP1	Likely pathogenic	c.1255C>T	p.(Arg419Trp)	NM_003322	PM2, PM3, PP1_Moderate, PP3
rs200769197	6	35503636	G	A	TULP1	Likely pathogenic	c.1246C>T	p.(Arg416Cys)	NM_003322	PM3_Strong, PM5_Supporting, PP1_Moderate, PP3
rs766181526	6	35503808	C	T	TULP1	Likely pathogenic	c.1153G>A	p.(Gly385Arg)	NM_003322	PS1,PM2,PP3,PP5

rs121909076	6	35503816	A	G	TULP1	Pathogenic	c.1145T>C	p.(Phe382Ser)	NM_003322	PS4, PM3, PM1_Strong, PP3
	6	35512858	G	A	TULP1	Likely pathogenic	c.3G>A	p.M1?	NM_003322	PVS1,PM2
	6	42178373	T	A	GUCA1A	Pathogenic	c.295T>A	p.Y99N	NM_00138491	PM2,PP3, PP5, PM5_Strong, PP3_Strong, PM1_Moderate
	6	42178374	A	C	GUCA1A	Pathogenic	c.296A>C	p.Y99S	NM_00138491	PM2, PP3, PP5,PM5_Strong, PM1_Moderate, PP3_Moderate
rs121434631	6	42179248	C	T	GUCA1A	Pathogenic	c.451C>T	p.L151F	NM_00138491	PM2, PP5,PP5_Very Strong, PM1_Moderate, PM2_Supporting
	6	42704365	C	A	PRPH2	Likely pathogenic	c.828G>T	p.E276D	NM_000322	PS3, PM2, PM5, PP3
	6	42704445	A	C	PRPH2	Likely pathogenic	c.748T>G	p.C250G	NM_000322	PM1_Strong, PM1, PM2, PM5, PP3
rs61755816	6	42704461	G	T	PRPH2	Pathogenic	c.732C>A	p.N244K	NM_000322	PM1_Strong, PS3_Moderate, PM2, PM5
	6	42704485	G	C	PRPH2	Pathogenic	c.708C>G	p.Y236X	NM_000322	PVS1_Verystrong, PM2, PP5,
	6	42704529	A	C	PRPH2	Likely pathogenic	c.664T>G	p.C222G	NM_000322	PM1, PM2, PM5, PP3, PS2_supporting
	6	42704546	G	C	PRPH2	Pathogenic	c.647C>G	p.P216R	NM_000322	PS1, PM1, PM2, PM5, PP5
rs61755806	6	42704546	G	A	PRPH2	Pathogenic	c.647C>T	p.P216L	NM_000322	PM1_Strong, PS3_Moderate, PM1, PM2, PM5, PP5,
	6	42704549	T	G	PRPH2	Pathogenic	c.644A>C	p.N215T	NM_000322	PS1, PM1, PM2, PM5
rs61755800	6	42704559	T	C	PRPH2	Likely pathogenic	c.634A>G	p.S212G	NM_000322	PM1, PM2, PM5, PP3, PP5
	6	42704560	G	C	PRPH2	Pathogenic	c.633C>G	p.F211L	NM_000322	PS1, PM1, PM2, PM5, PP3
	6	42704561	A	AT	PRPH2	Likely pathogenic	c.631_632insA	p.F211Yfs*7	NM_000322	PVS1_Verystrong, PM2
rs61755798	6	42704564	G	A	PRPH2	Pathogenic	c.629C>T	p.P210L	NM_000322	PS3, PM1, PM2, PM5, PP3, PP5
rs62645931	6	42704604	T	C	PRPH2	Likely pathogenic	c.589A>G	p.K197E	NM_000322	PM1, PM2, PM5, PP1_Moderate, PP5, BP4
rs61755792	6	42721821	G	A	PRPH2	Pathogenic	c.514C>T	p.R172W	NM_000322	PS3, PM1_Strong, PM2, PM5, PP5
rs527236098	6	42721836	C	T	PRPH2	Likely pathogenic	c.499G>A	p.G167S	NM_000322	PM1, PM2, PM5, PP3, PP5
	6	42721926	C	G	PRPH2	Pathogenic	c.409G>C	p.G137R	NM_000322	PS1, PM1, PM2, PM5
rs527236067	6	63720652	TTAGT	TT	EYS	Likely Pathogenic	c.9374_9379delinsAA	p.I3127Nfs*2	NM_00114280	PM2, PM3_Strong
	6	63721170	A	G	EYS	Likely Pathogenic	c.8861T>C	p.F2954S	NM_00114280	PM2, PM3, PM5, PP1_Moderate, PP3
	6	63721226	G	T	EYS	Pathogenic	c.8805C>A	p.Y2935*	NM_00114280	PM3_Verystrong, PP5, PP1_Moderate, BS1
	6	63721226	G	C	EYS	Likely Pathogenic	c.8805C>G	p.Y2935*	NM_00114280	PM2, PM3_Strong
rs1299355731	6	63726602	TTTTT	TTTTT	EYS	Likely Pathogenic	c.8145_8150delinsAAA	p.K2717Rfs*24	NM_00114280	PVS1_Strong, PM2, PM3
	6	63726609	G	A	EYS	Pathogenic	c.8143C>T	p.R2715*	NM_00114280	PVS1, PM3, PP5
rs751629543	6	63726614	TGAA	T	EYS	Likely Pathogenic	c.8133_8137delCTTTC	p.F2712fs	NM_00114280	PVS1_Strong, PM3, PP5
rs184722374	6	63726645	C	A	EYS	Pathogenic	c.8107G>T	p.E2703*	NM_00114280	PSV1_Verystrong, PM3_Strong, PP5, BS1
	6	63762577	C	-	EYS	Likely Pathogenic	c.7955delG	p.C2652Lfs*30	NM_00114280	PVS1_Moderate, PM2, PM3
rs527236066	6	63762613	C	T	EYS	Pathogenic	c.7919G>A	p.W2640*	NM_00114280	PVS1, PM3_Verystrong, PM1_Strong, PP5
	6	63762629	T	TG	EYS	Likely Pathogenic	c.7902dupC	p.N2635fs	NM_00114280	PVS1, PM2
	6	63778066	GGA	G	EYS	Likely Pathogenic	c.7836_7837delTC	p.P2613fs	NM_00114280	PVS1, PM2
	6	63778082	G	A	EYS	Pathogenic	c.7822C>T	p.Q2608*	NM_00114280	PVS1, PM2, PM3_Supporting
	6	63778097	C	A	EYS	Likely Pathogenic	c.7807G>T	p.G2603*	NM_00114280	PVS1, PM2
	6	63788161	CTG	C	EYS	Pathogenic	c.7665_7666delCA	p.Y2555fs	NM_00114280	PVS1, PM2, PM3
	6	63788212	CC	C	EYS	Likely Pathogenic	c.7616delG	p.G2539Efs*14	NM_00114280	PVS1, PM2
	6	63788218	G	-	EYS	Likely Pathogenic	c.7610delC	p.P2538Qfs*15	NM_00114280	PVS1_Moderate, PM2, PM3
	6	63788250	C	A	EYS	Pathogenic	c.7579-1G>T		NM_00114280	PVS1, PM2, PM3

rs1311193836	6	63789144	C	G	EYS	Pathogenic	c.7492G>C	p.A2498P	NM_001142801 PM3_Verystrong, PP3, PP5
	6	63806208	T	TA	EYS	Pathogenic	c.7392dupT	p.T2465fs	NM_001142801 PVS1, PM2, PM3_Supporting, PP5
	6	63806267	TGGA	TA	EYS	Likely Pathogenic	c.7331_7334delinsTA	p.F2444Lfs*16	NM_001142801 PVS1, PM2
	6	63806274	C	A	EYS	Likely Pathogenic	c.7327G>T	p.E2443*	NM_001142801 PVS1, PM2
	6	63806318	G	T	EYS	Pathogenic	c.7283C>A	p.S2428*	NM_001142801 PVS1, PM2, PM3
rs758899480	6	63864185	C	T	EYS	Pathogenic	c.7228+1G>A		NM_001142801 PVS1, PM3_Strong, PP5
rs527236069	6	63984389	CA	C	EYS	Pathogenic	c.7048delT	p.C2350fs	NM_001142801 PVS1, PM2, PM3_Supporting
	6	63984409	C	CGA	EYS	Pathogenic	c.7028_7029insTC	p.C2344fs	NM_001142801 PVS1, PM2, PM3_Supporting
	6	63984436	G	T	EYS	Likely Pathogenic	c.7002C>A	p.C2334*	NM_001142801 PVS1, PM3
rs1060499783	6	63984462	G	A	EYS	Pathogenic	c.6976C>T	p.R2326*	NM_001142801 PVS1, PM3_Supporting, PP5
	6	63984542	GCTTT	G	EYS	Likely Pathogenic	c.6868_6896delinsC:p.	p.P2290Qfs*12	NM_001142801 PVS1, PM2
	6	63999115	GG	G	EYS	Pathogenic	c.6793_6794delinsC	p.P2265Qfs*46	NM_001142801 PVS1, PM2, PM3
rs752953889	6	64066348	TA	T	EYS	Pathogenic	c.6714delT	p.I2239fs	NM_001142801 PVS1, PM3_Strong, PP5
	6	64081864	A	G	EYS	Pathogenic	c.6563T>C	p.I2188T	NM_001142801 PM3_Verystrong, PM5_Supporting, PP5
rs527236068	6	64081870	C	T	EYS	Pathogenic	c.6557G>A	p.G2186E	NM_001142801 PM3_Verystrong, PP5, PP1
	6	64081886	TTTTT	TTTT	EYS	Likely Pathogenic	c.6537_6541delinsAAA	p.T2181Qfs*4,	NM_001142801 PVS1, PM2
rs749909863	6	64230600	C	T	EYS	Pathogenic	c.6416G>A	p.C2139Y	NM_001142801 PM3_Verystrong, PM5, PP3, BS1
	6	64436254	G	T	EYS	Pathogenic	c.5847C>A	p.Y1949*	NM_001142801 PVS1, PM2, PM3, PP5
	6	64436266	C	G	EYS	Likely Pathogenic	c.5836-1G>C		NM_001142801 PVS1, PM2
	6	64436267	T	C	EYS	Pathogenic	c.5836-2A>G		NM_001142801 PVS1, PM2, PM3
	6	64439195	AAAA/	AAAA/	EYS	Pathogenic	c.5797_5802delinsTTTT	p.I1935Yfs*6	NM_001142801 PVS1, PM2, PP1
	6	64439203	C	A	EYS	Pathogenic	c.5794G>T	p.G1932*	NM_001142801 PVS1, PM2, PM3
	6	64590337	G	-	EYS	Likely Pathogenic	c.5530del	p.P1844Lfs*35	NM_001142801 PVS1_Moderate, PM2, PM3
	6	64590361	C	A	EYS	Pathogenic	c.5506G>T	p.E1836*	NM_001142801 PVS1, PM2, PM3_Supporting, PP1_Moderate
	6	64590664	ACA	A	EYS	Pathogenic	c.5201_5203delinsT	p.F1735Qfs*6	NM_001142801 PVS1, PM2, PM3_Supporting, PP1
	6	64590698	C	CA	EYS	Pathogenic	c.5168dupT	p.L1723fs	NM_001142801 PVS1, PM2, PM3
rs1766380760	6	64590709	C	CT	EYS	Likely Pathogenic	c.5157dupA	p.E1720fs	NM_001142801 PVS1, PM2
	6	64590781	C	A	EYS	Pathogenic	c.5086G>T	p.E1696X	NM_001142801 PVS1, PM2, PM3
	6	64590840	G	C	EYS	Pathogenic	c.5027C>G	p.S1676*	NM_001142801 PVS1, PM2, PM3
rs527236074	6	64590853	G	A	EYS	Pathogenic	c.5014C>T	p.Q1672*	NM_001142801 PVS1, PM2, PM3_Strong
rs527236065	6	64590909	C	CT	EYS	Pathogenic	c.4957dupA	p.S1653fs	NM_001142801 PVS1, PM3_Verystrong, PM1_Strong, PP5, BS1
	6	64590955	TTTTT	TTTT	EYS	Pathogenic	c.4908_4912delinsAAA	p.R1638Efs*41	NM_001142801 PVS1, PM2, PM3_Supporting
	6	64591008	G	C	EYS	Likely Pathogenic	c.4859C>G	p.S1620*	NM_001142801 PVS1, PM2
rs768092887	6	64591309	CT	C	EYS	Pathogenic	c.4557delA	p.A1520fs	NM_001142801 PVS1, PM2, PM3_Supporting
rs1428994453	6	64591415	C	T	EYS	Pathogenic	c.4452G>A	p.W1484*	NM_001142801 PVS1, PM2, PP5
	6	64591465	CCTCT	CCTCT	EYS	Pathogenic	c.4395_4402delinsTCA	p.D1468Vfs*13	NM_001142801 PVS1, PM2, PM3
	6	64591479	CTA	CA	EYS	Pathogenic	c.4385_4387delinsTG	p.S1462Lfs*16	NM_001142801 PVS1, PM2, PM3
	6	64591844	AGA	AA	EYS	Pathogenic	c.4021_4023delinsTT	p.S1341Ffs*11	NM_001142801 PVS1, PM2, PM3_Supporting
	6	64591854	CTG	C	EYS	Likely Pathogenic	c.4011_4012delCA	p.H1337fs	NM_001142801 PVS1, PM2

	6	64593256	TAA	T	EYS	Likely Pathogenic	c.3736_3737delTT	p.L1246fs	NM_001142801 PVS1, PM2
	6	64617507	C	A	EYS	Likely Pathogenic	c.3595G>T	p.E1199*	NM_001142801 PVS1, PM2
	6	64617529	C	T	EYS	Pathogenic	c.3573G>A	p.W1191X	NM_001142801 PVS1, PM3_Supporting, PP5
	6	64813380	G	T	EYS	Pathogenic	c.3441C>A	p.C1147*	NM_001142801 PVS1, PM2, PM3_Supporting
	6	64813471	CT	C	EYS	Likely Pathogenic	c.3349delA	p.S1117fs	NM_001142801 PVS1, PM2
	6	64821643	ACATT	A	EYS	Likely Pathogenic	c.3227_3243+1delGTA	p.C1076fs	NM_001142801 PVS1, PM2
rs1300490966	6	64821644	C	T	EYS	Pathogenic	c.3243+1G>A		NM_001142801 PVS1, PM2, PM3, PP5
	6	64886696	C	T	EYS	Likely Pathogenic	c.2992+1G>A		NM_001142801 PVS1, PM2
rs878853349	6	64902131	CAT	C	EYS	Pathogenic	c.2826_2827delAT	p.V944fs	NM_001142801 PVS1, PM2, PM3, PP5
rs74419361	6	64912597	C	T	EYS	Pathogenic	c.2528G>A	p.G843E	NM_001142801 PS3_Moderate, PM3_Verystrong, PM5, PP3, BA1
	6	64912603	T	TT	EYS	Pathogenic	c.2522delinsAA	p.Y841*	NM_001142801 PVS1, PM2, PM3
	6	64912638	GAT	GT	EYS	Likely Pathogenic	c.2484_2486delinsAC	p.I829Pfs*39	NM_001142801 PVS1, PM2
rs371032798	6	64945794	G	A	EYS	Pathogenic	c.2380C>T	p.R794*	NM_001142801 PVS1, PM2, PP5
	6	64945814	GT	G	EYS	Likely Pathogenic	c.2359delA	p.T787fs	NM_001142801 PVS1, PM2
	6	64945834	G	T	EYS	Pathogenic	c.2340C>A	p.C780*	NM_001142801 PVS1, PM2, PM3_Supporting
	6	64945856	TT	TTT	EYS	Likely Pathogenic	c.2317_2318delinsAAA	p.N773Kfs*2	NM_001142801 PVS1, PM2
rs752736741	6	64997581	C	T	EYS	Pathogenic	c.2259+1G>A		NM_001142801 PVS1, PM3_Strong, PM1_Strong, PP5
	6	65295862	C	A	EYS	Pathogenic	c.2023+1G>T		NM_001142801 PVS1, PM2, PM3
rs527236072	6	65334996	C	A	EYS	Pathogenic	c.1750G>T	p.E584*	NM_001142801 PVS1, PM2, PM3_Strong
	6	65335116	CACTC	CAA	EYS	Likely Pathogenic	c.1624_1630delinsTTG	p.S543Kfs*62	NM_001142801 PVS1, PM2
	6	65344143	A	ACTTT	EYS	Pathogenic	c.1493_1494insAAAG	p.D498fs	NM_001142801 PVS1, PM2, PM3
	6	65344144	TCAAT	T	EYS	Likely Pathogenic	c.1487_1492delTTATT	p.V496_I497del	NM_001142801 PM2, PM3, PM4
	6	65344144	TCAAT	CTTTT	EYS	Pathogenic	c.1485_1493delinsCG	p.V496Efs*13	NM_001142801 PVS1, PM2, PM3
	6	65353618	C	T	EYS	Pathogenic	c.1300-1G>A		NM_001142801 PVS1, PM, PM3
	6	65384385	C	A	EYS	Pathogenic	c.1299+1G>T		NM_001142801 PVS1, PM2, PM3, PP5
	6	65384424	TCA	TA	EYS	Pathogenic	c.1259_1261delinsTA	p.N421Mfs*8	NM_001142801 PVS1, PM2, PM3
rs764163418	6	65384473	G	GT	EYS	Pathogenic	c.1211dupA	p.N404fs	NM_001142801 PVS1, PM3_Strong, PP5
rs1195522061	6	65405173	C	T	EYS	Pathogenic	c.1056+1G>A		NM_001142801 PVS1, PM2, PP5
	6	65405287	CA	C	EYS	Pathogenic	c.942delT	p.A315fs	NM_001142801 PVS1, PM3_Verystrong
	6	65494706	C	T	EYS	Likely Pathogenic	c.705G>A	p.W235*	NM_001142801 PVS1, PM2
	6	65494707	C	T	EYS	Pathogenic	c.704G>A	p.W235X	NM_001142801 PVS1, PM2, PM3
	6	65494779	C	T	EYS	Likely Pathogenic	c.632G>A	p.C211Y	NM_001142801 PM3_Strong, PM5_Supporting, PP1
	6	65494804	G	A	EYS	Pathogenic	c.607C>T	p.Q203*	NM_001142801 PVS1, PM2, PP5
rs780433094	6	65494883	TTCC	T	EYS	Pathogenic	c.525_527delGGA	p.E176del	NM_001142801 PM3_Verystrong, PM4, PP5, BS1
	6	65494961	TG	T	EYS	Likely Pathogenic	c.449delC	p.T150fs	NM_001142801 PVS1, PM2
	6	65495000	AT	A	EYS	Pathogenic	c.410delA	p.N137fs	NM_001142801 PVS1, PM2, PM3_Supporting
rs786205652	6	65495231	CA	C	EYS	Likely Pathogenic	c.179delT	p.L60fs	NM_001142801 PVS1, PM2
	6	65495293	CAT	C	EYS	Likely Pathogenic	c.116_117delAT	p.Y39fs	NM_001142801 PVS1, PM2
rs137853113	7	23140784	C	T	KLHL7	Pathogenic	c.458C>T	p.A153V	NM_001031711 PS3_Moderate, PM2, PP1_Strong, PP3, PP5

	7	33095292	TTTTC -	RP9	Likely pathogenic	c.603_607delGAAAA	p.K202Efs*13	NM_203288	PVS1, PM2
	7	128393029	C A	IMPDH1	Pathogenic	c.1449-1G>T		NM_00114257	PVS1_VeryStrong, PM2, PP3
	7	128395237	G T	IMPDH1	Likely Pathogenic	c.969C>A	p.Tyr323*	NM_00114257	PVS1_VeryStrong, PM2
	7	128395237	GTAC TT	IMPDH1	Likely Pathogenic	c.966_969delinsAA	p.Tyr323Lysfs*4	NM_00114257	PVS1_VeryStrong, PM2
	7	128395238	TAC T	IMPDH1	Likely Pathogenic	c.966_967del	p.Tyr323Glnfs*4	NM_00114257	PVS1_VeryStrong, PM2
	7	128398520	T C	IMPDH1	Likely Pathogenic	c.638A>G	p.Lys213Arg	NM_00114257	PM5, PM2, PP3, PP5
	7	128398543	GTTC G	IMPDH1	Likely Pathogenic	c.612_614del	p.Lys204del	NM_00114257	PM5, PM4, PM2, PP3, PP5
rs121912550	7	128398557	C T	IMPDH1	Likely Pathogenic	c.601G>A	p.Asp201Asn	NM_00114257	PS1, PP3, PP5
rs121912552	7	128398562	C G	IMPDH1	Likely Pathogenic	c.596G>C	p.Arg199Pro	NM_00114257	PS1, PM2, PP3, PP5
	7	128409350	GT G	IMPDH1	Likely Pathogenic	c.162delA	p.Glu54Aspfs*27	NM_00110260	PVS1_VeryStrong, PM2
	8	10622619	G A	RP1L1	Likely Pathogenic	c.583C>T	p.(Gln195Ter)	NM_178857.6	PVS1, PM2
	8	10622799	G A	RP1L1	Likely Pathogenic	c.403C>T	p.(Gln135Ter)	NM_178857.6	PVS1, PM2
	8	10622805	C A	RP1L1	Likely Pathogenic	c.397G>T	p.(Glu133Ter)	NM_178857.6	PVS1, PM2
	8	10623177	G A	RP1L1	Likely Pathogenic	c.25C>T	p.(Gln9Ter)	NM_178857.6	PVS1, PM2
	8	54621418	GC G	RP1	Likely pathogenic	c.458delC	p.(Pro153fs)	NM_006269	PVS1,PM2
	8	54621424	C CA	RP1	Pathogenic	c.458dup	p.(Arg154fs)	NM_006269	PVS1,PM2,PP5
rs527236105	8	54622149	TG T	RP1	Pathogenic	c.650delG	p.(Gly217fs)	NM_006269	PVS1_Strong, PM2, PM3_Supporting
	8	54624883	A AA	RP1	Likely pathogenic	c.1001dupA	p.(Met335fs)	NM_006269	PVS1_Strong, PM2, PM3
rs765129639	8	54625379	CAT C	RP1	Pathogenic	c.1498_1499delAT	p.(Met500fs)	NM_006269	PVS1_Strong, PM3_Strong, PP5
	8	54625863	G T	RP1	Likely pathogenic	c.1981G>T	p.(Glu661*)	NM_006269	PVS1_Strong, PM1, PM2, PP1
rs1365669334	8	54625902	A AA	RP1	Pathogenic	c.2025dup	p.(Ser676fs)	NM_006269	PVS1,PM1,PM2,PP5
rs104894082	8	54625911	C T	RP1	Pathogenic	c.2029C>T	p.(Arg677*)	NM_006269	PVS1_Strong, PM1, PM2, PM1_Strong, PP5
rs878853328	8	54625914	C T	RP1	Likely pathogenic	c.2032C>T	p.(Gln678*)	NM_006269	PVS1_Strong, PM1
	8	54625947	C T	RP1	Likely pathogenic	c.2065C>T	p.(Gln689*)	NM_006269	PVS1_Strong, PM1, PM2
rs1554519555	8	54626101	C G	RP1	Pathogenic	c.2219C>G	p.Ser740Ter	NM_006269	PVS1,PS1,PM1,PM2,PP5
	8	54626259	AG G	RP1	Likely pathogenic	c.2377delA	p.(Arg793fs)	NM_006269	PVS1,PM2
	8	54626439	A T	RP1	Likely pathogenic	c.2557A>T	p.(Lys853*)	NM_006269	PVS1, PM2
	8	54626439	GT T	RP1	Likely pathogenic	c.2557A >T	p.(Lys853*)	NM_006269	PVS1,PM2
	8	54626473	TAAC T	RP1	Likely pathogenic	c.2592_2596delAACTT	p.(Thr865fs)	NM_006269	PVS1_Strong, PM2
	8	54626476	CT C	RP1	Likely pathogenic	c.2597delT	p.(Leu866fs)	NM_006269	PVS1_Strong, PM2
	8	54626481	A T	RP1	Likely pathogenic	c.2599A>T	p.(Lys867*)	NM_006269	PVS1, PM2
rs1449723475	8	54626489	G GA	RP1	Likely pathogenic	c.2613dupA	p.(Arg872fs)	NM_006269	PVS1_Strong, PP1, PP5
	8	54626881	GT T	RP1	Likely pathogenic	c.2999delG	p.(Gly1000fs)	NM_006269	PVS1,PM2
rs1337293997	8	54627551	C A	RP1	Likely pathogenic	c.3669C>A	p.(Cys1223*)	NM_006269	PVS1_Strong, PM2
rs769601671	8	54627719	TT T	RP1	Pathogenic	c.3843delT	p.Pro1282fs	NM_006269	PVS1,PM2,PP5
rs762951570	8	54628077	TG T	RP1	Likely pathogenic	c.4196delG	p.(Cys1399fs)	NM_006269	PVS1_Strong, PM3, PP5
	8	54628282	CT T	RP1	Likely pathogenic	c.4400delC	p.(Ser1467fs)	NM_006269	PVS1,PM2
	8	54628473	AGG G	RP1	Likely pathogenic	c.4591_4592delAG	p.(Arg1531s)	NM_006269	PVS1,PM2
rs118031911	8	54629679	C T	RP1	Pathogenic	c.5797C>T	p.(Arg1933*)	NM_006269	PVS1_Strong, PM3_Verystrong, PM1_Strong, BS1

rs775367880	8	54630060	GA	G	RP1	Pathogenic	c.6181delA	p.(Ile2061fs)	NM_006269	PVS1_Moderate, PS4, PM3_Strong
	9	2717939	G	A	KCNV2	Pathogenic	c.200G>A	p.(Trp67Ter)	NM_133497.4	PVS1, PM2, PM3_moderate
NA	9	2718258	C	CG	KCNV2	Pathogenic	c.520dup	p.(Asp174GlyfsTer198	NM_133497.4	PVS1, PM2, PM3_moderate
rs751600925	9	2718268	T	C	KCNV2	Likely Pathogenic	c.529T>C	p.(Cys177Arg)	NM_133497.4	PM3_strong, PP3, PP5
	9	2718356	G	C	KCNV2	Likely Pathogenic	c.617G>C	p.(Arg206Pro)	NM_133497.4	PM2, PM3_moderate, PP3, PP5
rs202200956	9	2718670	G	C	KCNV2	Likely Pathogenic	c.931G>C	p.(Gly311Arg)	NM_133497.4	PM2, PM3_strong, PP5
rs149648640	9	2729470	G	A	KCNV2	Likely Pathogenic	c.1381G>A	p.(Gly461Arg)	NM_133497.4	PM3_strong, PP3, PP5
rs527236116	9	32541967	GTCTC	G	TOPORS	Likely Pathogenic	c.2554_2557del	p.(Glu852GlnfsTer13)	NM_005802.5	PVS1_strong, PM2, PP5
	9	32541985	CG	C	TOPORS	Likely Pathogenic	c.2539del	p.(Arg847AspfsTer19)	NM_005802.5	PVS1_Strong, PM2
rs869312183	9	32541986	G	A	TOPORS	Likely Pathogenic	c.2539C>T	p.(Arg847Ter)	NM_005802.5	PVS1_strong, PM2, PP5
	10	47348828	CCTGC	C	RBP3	Pathogenic	c.345_349del	p.(Trp116AlafsTer7)	NM_002900.3	PVS1, PM2, PM3_moderate
rs1480910058	10	47349116	G	A	RBP3	Pathogenic	c.632G>A	p.(Trp211Ter)	NM_002900.3	PVS1, PM2, PM3_moderate
rs727502919	10	71615617	G	T	CDH23	Likely pathogenic	c.945+1G>T		NM_001171931	PVS1_moderate, PM2, PP3, PP5
	10	71725506	CG	C	CDH23	Likely pathogenic	c.3566delG	p.S1190Afs*5	NM_001171931	PVS1_Very Strong, PM2
	10	71785696	TTC	T	CDH23	Likely pathogenic	c.5779_5780del	p.S1927Cfs*16	NM_022124	PVS1_Very Strong, PM2
	10	71788938	A	G	CDH23	Pathogenic	c.5821-2A>G		NM_022124	PVS1_Very Strong, PM2, PP3
	10	93612940	A	AG	PDE6C	Likely Pathogenic	c.215delinsAG	p.T75Hfs*20	NM_006204	PVS1_Very Strong, PM2_Supporting, PP3
	10	93621931	G	C	PDE6C	Likely Pathogenic	c.724-1G>C		NM_006204	PVS1_Very Strong, PM2_Supporting, PP3
	10	93635497	ACT	A	PDE6C	Likely Pathogenic	c.1270_1272delinsA	p.L425Hfs*12	NM_006204	PVS1_Very Strong, PM2_Supporting
rs752963712	10	93640953	G	A	PDE6C	Likely Pathogenic	c.1771G>A	p.E591K	NM_006204	PP3_Strong, PM1_Supporting, PM2_Supporting
rs776912070	10	93659118	C	T	PDE6C	Likely Pathogenic	c.2159C>T	p.T720M	NM_006204	PM1_Supporting, PP5_Moderate, PM2_Supporting, PP3
	10	93659159	CAA	C	PDE6C	Likely Pathogenic	c.2200_2202delins	p.Q736Gfs*8	NM_006204	PVS1_Very Strong, PM2_Supporting
rs281865214	11	61951879	C	T	BEST1	Likely pathogenic	c.73C>T	p.R25W	NM_004183	PS1, PM2, PP1_Supporting, PP3, PP5
rs281865221	11	61955194	C	A	BEST1	Likely pathogenic	c.240C>A	p.F80L	NM_004183	PM5_Supporting, PM2, PP1_Supporting, PP3, PP5
rs1555098634	11	61955195	G	T	BEST1	Likely pathogenic	c.241G>A	p.V81M	NM_004183	PM2+PP3+PP5
	11	61955948	G	C	BEST1	Likely pathogenic	c.478G>C	p.A160P	NM_004183	PS1, PM3_Supporting, PP3, PP5
rs200277476	11	61956946	C	T	BEST1	Pathogenic	c.584C>T	p.A195V	NM_004183	PM3_Verystrong, PP3, PP5, BS1
rs281865239	11	61957403	G	A	BEST1	Likely pathogenic	c.653G>A	p.R218H	NM_004183	PS1, PM3_Supporting, PM5, PP1_Supporting, PP3, PP5
rs372989281	11	61958194	C	T	BEST1	Pathogenic	c.763C>T	p.R255W	NM_004183	PM3_Verystrong, PP1, PP3, PP5
rs281865267	11	61959548	G	C	BEST1	Likely pathogenic	c.918G>C	p.E306D	NM_004183	PM5_Supporting, PM2, PP1_Supporting, PP3
	11	77160272	C	A	MYO7A	Likely Pathogenic	c.1190C>A	p.(Ala397Asp)	NM_000260	PM2, PM3, PM5, PP3, PP5
	11	77162124	G	C	MYO7A	Likely Pathogenic	c.1348G>C	p.(Glu450Gln)	NM_000260	PM2, PP3, PM3, PM5
	11	77162253	C	T	MYO7A	Pathogenic	c.1477C>T	p.(Gln493*)	NM_000260	PVS1_Very Strong, PM2, PM3, PP5
	11	77166073	C	T	MYO7A	Pathogenic	c.1708C>T	p.(Arg570*)	NM_000260	PVS1_Very Strong, PM2, PM3, PM5, PP5
	11	77184716	G	A	MYO7A	Likely Pathogenic	c.3503+1G>A		NM_000260	PVS1_Very Strong, PM2
rs111033214	11	77189348	G	A	MYO7A	Likely Pathogenic	c.3508G>A	p.(Glu1170Lys)	NM_000260	PM3, PM5_Moderate, PP3, PP5
	11	77198535	CTG	C	MYO7A	Likely Pathogenic	c.4483_4484del	p.(Trp1495Aspfs*8)	NM_000260	PVS1_Very Strong, PM2
	11	77198563	C	T	MYO7A	Likely Pathogenic	c.4510C>T	p.(Gln1504*)	NM_000260	PVS1_Very Strong, PM2
	11	77205461	G	C	MYO7A	Likely Pathogenic	c.5481-1G>C		NM_000260	PVS1_Moderate, PM2, PM3, PP5

rs773945008	11	77211206	C	T	MYO7A	Likely Pathogenic	c.6106C>T	p.(Gln2036*)	NM_000260	PVS1_Very Strong, PM2
	11	77211303	TTA	T	MYO7A	Likely Pathogenic	c.6204_6205del	p.(Ile2069Profs*6)	NM_000260	PVS1_Very Strong, PM2
	11	77211904	G	A	MYO7A	Pathogenic	c.6321G>A	p.(Trp2107*)	NM_000260	PVS1_Very Strong, PM2, PM3, PP5
	12	88055647	T	A	CEP290	Likely pathogenic	c.6889A>T	p.(Lys2297Ter)	NM_025114.4	PVS1,PM2
rs752197734	12	88068657	A	T	CEP290	Likely pathogenic	c.6012-12T>A		NM_025114.4	PM3_Strong,PP3,PP5
	12	88071383	AA	A	CEP290	Pathogenic	c.5924del	p.(Leu1975TrpfsTer15	NM_025114.4	PVS1,PM2,PM3_supporting
	12	88071848	T	A	CEP290	Pathogenic	c.5788A>T	p.(Lys1930Ter)	NM_025114.4	PVS1,PM2,PM3,PP5
	12	88080205	CTA	C	CEP290	Likely pathogenic	c.5201_5202del	p.(Leu1734CysfsTer11	NM_025114.4	PVS1,PM2
rs781670422	12	88092781	C	A	CEP290	Pathogenic	c.3361G>T	p.(Glu1121Ter)	NM_025114.4	PVS1,PM2,PM3_supporting
	12	88109164	TT	T	CEP290	Pathogenic	c.2390del	p.(Lys797SerfsTer2)	NM_025114.4	PVS1,PM3,PP5
	12	88111786	T	TTGA	CEP290	Likely pathogenic	c.2124_2125insGGCTT	p.(Thr709GlyfsTer10)	NM_025114.4	PVS1,PM2
	12	88115144	TCT	T	CEP290	Pathogenic	c.1864_1865del	p.(Asp622PhefsTer5)	NM_025114.4	PVS1,PM2,PP5
rs587783009	12	88118482	C	T	CEP290	Pathogenic	c.1711+1G>A		NM_025114.4	PVS1,PM3,PP5
rs760415289	12	88118549	G	A	CEP290	Pathogenic	c.1645C>T	p.(Arg549Ter)	NM_025114.4	PVS1,PM3,PP5
rs137852835	12	88130324	G	A	CEP290	Pathogenic	c.613C>T	p.(Arg205Ter)	NM_025114.4	PVS1,PM2,PP5
	12	88130376	T	TAA	CEP290	Likely pathogenic	c.560_561insTT	p.(Asp188Ter)	NM_025114.4	PVS1,PM2
	12	88139531	C	A	CEP290	Pathogenic	c.214G>T	p.(Glu72Ter)	NM_025114.4	PVS1,PM2,PM3,PP5
	12	89421235	C	T	POC1B	Likely Pathogenic	c.1355G>A	p.(Arg452Gln)	NM_172240.3	PM3_verystrong, PP5
rs200082142	12	89466815	G	T	POC1B	Likely Pathogenic	c.987C>A	p.(Tyr329Ter)	NM_172240.3	PVS1, PM3_moderate
	12	89492051	C	G	POC1B	Likely Pathogenic	c.337G>C	p.(Asp113His)	NM_172240.3	PM2, PP1_moderate, PM3_moderate, PP3
	13	113671641	CT	C	GRK1	Pathogenic	c.971delT	p.L324Rfs*62	NM_002929	PVS1,PM3_Supporting, PP4
	13	113735078	GCC	G	GRK1	Pathogenic	c.1408_1409del	p.P471Ffs*28	NM_002929	PVS1,PM2,PM3_Supporting, PP4
rs554396590	14	21303542	C	T	RPGRIP1	Pathogenic	c.799C>T	p.(Arg267Ter)	NM_020366.4	PVS1,PM3,PP5
rs763671264	14	21320072	GG	G	RPGRIP1	Pathogenic	c.1363del	p.(Glu455LysfsTer2)	NM_020366.4	PVS1,PM2,PP5
	14	21320178	G	T	RPGRIP1	Pathogenic	c.1467+1G>T		NM_020366.4	PVS1,PM2,PM3,PP5
rs776963292	14	21321929	C	T	RPGRIP1	Pathogenic	c.1687C>T	p.(Arg563Ter)	NM_020366.4	PVS1,PM2,PP5
	14	21325310	GC	AA	RPGRIP1	Pathogenic	c.2294_2295delinsAA	p.(Cys765Ter)	NM_020366.4	PVS1,PM2,PM3_supporting
rs1429786931	14	21326017	C	T	RPGRIP1	Pathogenic	c.2554C>T	p.(Arg852Ter)	NM_020366.4	PVS1,PM2,PP5
rs587783012	14	21345144	CCGA	C	RPGRIP1	Pathogenic	c.3565_3571del	p.(Arg1189GlyfsTer7)	NM_020366.4	PVS1,PM3,PP5
	14	24082697	G	A	NRL	Likely Pathogenic	c.152C>T	p.P51L	NM_00135476	PS3_Moderate, PM2, PM5, PP1_Moderate, PP3, PP5
	14	24082700	G	A	NRL	Likely Pathogenic	c.149C>T	p.S50L	NM_00135476	PS3_Moderate, PM2, PM1_Strong, PP3
	14	67725206	C	A	RDH12	Likely pathogenic	c.295C>A	p.L99I	NM_152443	PM3_Strong, PM5, PP1_Moderate, PP5, BS1
rs28940315	14	67729286	TC	T	RDH12	Likely pathogenic	c.759delC	p.F254Lfs*24	NM_152443	PVS1_Strong, PM2, PP5
	14	67729293	T	TA	RDH12	Likely pathogenic	c.761_762insA	p.F254Lfs*19	NM_152443	PVS1_Strong, PM2
	14	88426705	G	A	SPATA7	Pathogenic	c.845+1G>A		NM_018418.5	PVS1,PM2,PM3_Supporting
	14	88437565	C	T	SPATA7	Likely pathogenic	c.1183C>T	p.(Arg395Ter)	NM_018418.5	PVS1_strong,PM3,PP5
rs928368462	14	88839563	C	T	TTC8	Likely Pathogenic	c.226C>T	p.Q76X	NM_198309	PVS1,PM3_Supporting
rs763706390	14	88841049	A	ATA	TTC8	Pathogenic	c.312delinsATA	p.A105*	NM_198309	PVS1,PM2,PM3_Supporting
	15	71811506	C	T	NR2E3	Likely pathogenic	c.142C>T	p.R48C	NM_014249	PM1,PM2, PM3, PP1

rs544807110	15	71811515	G	A	NR2E3	Likely pathogenic	c.151G>A	p.G51R	NM_014249	PP5, PM1,PM2, PM3
rs121912631	15	71811530	G	A	NR2E3	Pathogenic	c.166G>C	p.G56R	NM_014249	PS1, PP3, PP5, PM1,PM2
rs767304567	15	71811586	C	G	NR2E3	Likely pathogenic	c.222C>G	p.S74R	NM_014249	PM1,PM2, PM3, PP3
rs104894492	15	71811590	C	T	NR2E3	Pathogenic	c.226C>T	p.R76W	NM_014249	PP5, PM1, PM5, PP3, PM2, PM3
rs775720634	15	71811809	C	T	NR2E3	Pathogenic	c.289C>T	p.R97C	NM_014249	PM1,PM2, PM3, PP3, PM5, PP5
rs766096417	15	71811831	G	A	NR2E3	Pathogenic	c.311G>A	p.R104Q	NM_014249	PP5, PM1, PM5, PP3, PM2, BP6, PM3
rs776270511	15	71811957	G	A	NR2E3	Pathogenic	c.352G>A	p.V118M	NM_014249	PM1,PM2, PM3, PP3, PP5
rs527236086	15	71811969	C	T	NR2E3	Likely pathogenic	c.364C>T	p.R122C	NM_014249	PM1,PM2, PM3, PP3, PP5
	15	71813560	AT	-	NR2E3	Pathogenic	c.919_920delAT	p.I307Lfs*33	NM_014249	PVS1, PM2, PM3
	15	71814017	C	G	NR2E3	Likely pathogenic	c.1000C>G	p.R334G	NM_014249	PM1,PM2, PM3, PP3, PP5, PP4, BP4
rs750931603	15	71814065	C	T	NR2E3	Pathogenic	c.1048C>T	p.Q350*	NM_014249	PVS1, PP5, PM2, PM3
rs28933990	15	89210794	G	A	RLBP1	Likely Pathogenic	c.700C>T	p.(Arg234Trp)	NM_000326	PM3, PM5,PP3, PP5
	16	57904843	G	GT	CNGB1	Likely Pathogenic	c.2524_2525insA	p.(Thr842AsnfsTer10)	NM_001297.5	PVS1, PM2, PM3_supporting
	16	57960027	G	A	CNGB1	Likely Pathogenic	c.622C>T	p.(Gln208Ter)	NM_001297	PVS1, PM2
	17	1650808	A	C	PRPF8	likely pathogenic	c.7002T>G	p.Y2334X	NM_006445	PVS1_Moderate, PM2
	17	1650849	G	A	PRPF8	Pathogenic	c.6961C>T	p.Q2321X	NM_006445	PVS1_Moderate, PS3_Moderate, PM2
	17	1650881	C	A	PRPF8	likely pathogenic	c.6929G>T	p.R2310M	NM_006445	PS1, PM2, PP3
	17	1650882	T	C	PRPF8	Pathogenic	c.6928A>G	p.R2310G	NM_006445	PS3_Moderate, PM2, PM5, PP3, PP5
rs121434236	17	1650884	T	C	PRPF8	Pathogenic	c.6926A>G	p.H2309R	NM_006445	PS1, PM2, PM6, PP3, PP5
	17	1650909	G	A	PRPF8	likely pathogenic	c.6901C>T	p.P2301S	NM_006445	PM2, PM5, PP3, PP5
	17	1651183	G	A	PRPF8	likely pathogenic	c.6778C>T	p.Q2260X	NM_006445	PVS1, PM2
	17	1655347	CACTT	C	PRPF8	likely pathogenic	c.5986_5987+2delinsA	p.N1996Vfs*2	NM_006445	PVS1, PM2
	17	8003212	GGT	G	GUCY2D	Likely pathogenic	c.167_168del	p.V56Gfs*262	NM_000180	PVS1_Verystrong, PM2
	17	8012607	G	GT	GUCY2D	Pathogenic	c.2113+1G>GT		NM_000180	PVS1_Verystrong, PM2, PM3_moderate
rs61750173	17	8014701	G	A	GUCY2D	Likely pathogenic	c.2513G>A	p.R838H	NM_000180	PM2, PM5, PS2_supporting, PP3, PP5, PP1_supporting
rs1598150793	17	8014986	G	T	GUCY2D	Likely pathogenic	c.2704G>T	p.V902L	NM_000180	PM2, PM5, PP3, PS2_supporting
rs527236092	17	76540143	T	C	PRCD	Pathogenic	c.2T>C	p.M1?	NM_00107762	PVS1_Moderate, PM3_Strong, PP1_Moderate, PP5
rs527451635	17	76540193	C	T	PRCD	Pathogenic	c.52C>T	p.R18X	NM_00107762	PVS1, PM3_Supporting, PM1_Strong, PP5
rs387907268	17	76540205	C	T	PRCD	Pathogenic	c.64C>T	p.R22X	NM_00107762	PVS1, PM3, PM1_Strong, PP5, PP3
rs779066277	17	76540216	G	A	PRCD	Pathogenic	c.74+1G>A		NM_00107762	PVS1, PM3, PP5
	17	81528553	C	T	FSCN2	Likely pathogenic	c.22C>T	p.(Gln8*)	NM_00107718	PVS1_Very Strong, PM2
	17	81535050	AG	A	FSCN2	Likely pathogenic	c.827-1delG		NM_00107718	PVS1_Very Strong, PM2
	19	32676474	G	T	RGS9BP	Pathogenic	c.211G>T	p.E71X	NM_207391	PVS1, PM2, PM3_Supporting
rs749738655	19	47836260	C	T	CRX	Likely pathogenic	c.118C>T	p.(Arg40Trp)	NM_000554.6	PM1,PM2,PM5,PP3,PP5
rs104894672	19	47836263	C	T	CRX	Likely pathogenic	c.121C>T	p.(Arg41Trp)	NM_000554.6	PS3_moderate,PM1,PP1_moderate,PP3,PP5
rs863224863	19	47836266	G	A	CRX	Likely pathogenic	c.124G>A	p.(Glu42Lys)	NM_000554.6	PM1,PM2,PP3,PP5
rs1437021651	19	47836269	C	T	CRX	Likely pathogenic	c.127C>T	p.(Arg43Cys)	NM_000554.6	PM1,PM2,PM5,PP3,PP5
rs771736389	19	47836270	G	A	CRX	Likely pathogenic	c.128G>A	p.(Arg43His)	NM_000554.6	PM1,PM2,PM5,PP3,PP5
rs104894673	19	47839335	C	T	CRX	Likely pathogenic	c.268C>T	p.(Arg90Trp)	NM_000554.6	PS3_moderate,PM1,PM5_supporting,PP3

	19	47839500	CC	C	CRX	Likely pathogenic	c.434del	p.(Pro145LeufsTer42)	NM_000554.6	PVS1_strong,PM2,PM6_supporting
rs1968169100	19	47839656	CC	C	CRX	Likely pathogenic	c.590del	p.(Pro197ArgfsTer22)	NM_000554.6	PVS1_strong,PM2,PP5
rs281865516	19	47839681	CC	C	CRX	Likely pathogenic	c.615del	p.(Ser206ProfsTer13)	NM_000554.6	PVS1_strong,PM2
	19	47839705	CC	C	CRX	Likely pathogenic	c.639del	p.(Tyr214IlefsTer5)	NM_000554.6	PVS1_strong,PM2
	19	47839794	G	T	CRX	Likely pathogenic	c.727G>T	p.(Gly243Ter)	NM_000554.6	PVS1_strong,PM2,PP1_supporting
	19	54118396	C	T	PRPF31	Likely Pathogenic	c.118C>T	p.(Gln40Ter)	NM_015629.4	PVS1, PM2
	19	54121886	G	T	PRPF31	Likely Pathogenic	c.265G>T	p.(Glu89Ter)	NM_015629.4	PVS1, PM2
	19	54121925	G	T	PRPF31	Likely Pathogenic	c.304G>T	p.(Glu102Ter)	NM_015629.4	PVS1, PM2
	19	54121931	G	T	PRPF31	Likely Pathogenic	c.310G>T	p.(Glu104Ter)	NM_015629.4	PVS1, PM2
	19	54122496	G	C	PRPF31	Likely Pathogenic	c.323-1G>C		NM_015629.4	PVS1, PM2
	19	54123465	CAG	C	PRPF31	Likely Pathogenic	c.433_434del	p.(Ser145ProfsTer8)	NM_015629.4	PVS1, PM2
rs527236094	19	54123783	G	T	PRPF31	Likely Pathogenic	c.562G>T	p.(Glu188Ter)	NM_015629.4	PVS1, PM2
rs144738703	19	54123836	C	G	PRPF31	Likely Pathogenic	c.615C>G	p.(Tyr205Ter)	NM_015629.4	PVS1, PM2
	19	54128159	T	TG	PRPF31	Pathogenic	c.1033dupG	p.(Ala345GlyfsTer130)	NM_015629.4	PVS1, PM2, PP5
rs868538598	19	54128187	C	T	PRPF31	Pathogenic	c.1060C>T	p.(Arg354Ter)	NM_015629.4	PVS1, PM2, PP5
NA	19	54128371	GG	G	PRPF31	Pathogenic	c.1142del	p.(Gly381GlufsTer32)	NM_015629.4	PVS1, PM2, PP5
NA	19	54129064	A	AAG	PRPF31	Likely Pathogenic	c.1154_1155insAG	p.(Asp386GlyfsTer28)	NM_015629.4	PVS1, PM2
rs527236096	20	63995027	G	C	PRPF6	Likely Pathogenic	c.550G>C	p.D184H	NM_012469	PM2, PP3, PP3_Strong, PM5_Moderate, PM2_Supportin
	20	64016827	G	A	PRPF6	Likely Pathogenic	c.1629G>A	p.W543*	NM_012469	PVS1, PM2
NA	NA	38297392	CAA	C	RPGR	Likely Pathogenic	c.1304_1305delTT	p.(Leu435ArgfsTer17)	NM_000328.3	PVS1, PM2
rs104894929	X	18642012	A	G	RS1	Likely Pathogenic	c.667T>C	p.(Cys223Arg)	NM_000330.4	PM2, PP3,PP5, PM5
rs281865361	X	18642054	G	A	RS1	Likely Pathogenic	c.625C>T	p.(Arg209Cys)	NM_000330.4	PM2, PP3,PP5, PM5
rs104894930	X	18642071	G	A	RS1	Likely Pathogenic	c.608C>T	p.(Pro203Leu)	NM_000330.4	PM2, PP3,PP5, PM5
rs281865358	X	18642080	C	T	RS1	Likely Pathogenic	c.599G>A	p.(Arg200His)	NM_000330.4	PM2, PP3,PP5, PM5
rs281865357	X	18642081	G	A	RS1	Likely Pathogenic	c.598C>T	p.(Arg200Cys)	NM_000330.4	PM2, PP3,PP5, PM5
rs281865355	X	18642089	C	T	RS1	Likely Pathogenic	c.590G>A	p.(Arg197His)	NM_000330.4	PM2, PP3,PP5, PM5
rs281865355	X	18642089	C	G	RS1	Likely Pathogenic	c.590G>C	p.(Arg197Pro)	NM_000330.4	PM2, PM5, PP1_Supporting, PP3
rs281865354	X	18642090	G	A	RS1	Likely Pathogenic	c.589C>T	p.(Arg197Cys)	NM_000330.4	PM2, PP3,PP5, PM5
	X	18642098	A	AG	RS1	Likely Pathogenic	c.580_581insC	p.(Ile194Thrfs*70)	NM_000330.4	PSV1_Strong, PM2
rs61753174	X	18642105	G	A	RS1	Likely Pathogenic	c.574C>T	p.(Pro192Ser)	NM_000330.4	PM2, PP3,PP5, PM5
rs61753171	X	18642135	G	A	RS1	Likely Pathogenic	c.544C>T	p.(Arg182Cys)	NM_000330.4	PM2, PP3,PP5, PM5
	X	18642157	C	T	RS1	Likely Pathogenic	c.523-1G>A		NM_000330.4	PSV1, PM2
rs281865348	X	18644429	C	T	RS1	Likely Pathogenic	c.522+1G>A		NM_000330.4	PSV1, PM2
rs61753166	X	18644463	C	T	RS1	Likely Pathogenic	c.489G>A	p.(Trp163*)	NM_000330.4	PSV1_Strong, PM2
rs61752159	X	18644530	C	T	RS1	Likely Pathogenic	c.422G>A	p.(Arg141His)	NM_000330.4	PM2, PP3,PP5, PM5
rs281865345	X	18647191	C	T	RS1	Likely Pathogenic	c.326G>A	p.(Gly109Glu)	NM_000330.4	PM2, PP3, PM5, PP5
rs61752068	X	18647212	C	T	RS1	Likely Pathogenic	c.305G>A	p.(Arg102Gln)	NM_000330.4	PM2, PP3, PM5, PP5
rs61752067	X	18647213	G	A	RS1	Likely Pathogenic	c.304C>T	p.(Arg102Trp)	NM_000330.4	PM2, PP3,PP5, PM5
rs61752064	X	18647229	C	T	RS1	Likely Pathogenic	c.288G>A	p.(Trp96*)	NM_000330.4	PSV1_Very Strong, PM2

	X	18647231	AC	A	RS1	Likely Pathogenic	c.285delG	p.(Trp96Glyfs*30)	NM_000330.4	PSV1_Very Strong, PM2
rs61752062	X	18647241	C	G	RS1	Likely Pathogenic	c.276G>C	p.(Trp92Cys)	NM_000330.4	PM2, PP3, PP5, PM5
rs61752061	X	18647250	A	T	RS1	Likely Pathogenic	c.267T>A	p.(Tyr89*)	NM_000330.4	PSV1_Very Strong, PM2
rs61752060	X	18647251	T	C	RS1	Likely Pathogenic	c.266A>G	p.(Tyr89Cys)	NM_000330.4	PM2, PP3, PP5, PM5
rs61750459	X	18647255	G	A	RS1	Likely Pathogenic	c.262C>T	p.(Gln88*)	NM_000330.4	PSV1_Very Strong, PM2
	X	18647321	GA	G	RS1	Likely Pathogenic	c.195delT	p.(His66Thrfs*60)	NM_000330.4	PSV1_Very Strong, PM2
	X	18647331	T	TA	RS1	Likely Pathogenic	c.185_186insT	p.(Glu62Aspfs*24)	NM_000330.4	PSV1_Very Strong, PM2
rs281865332	X	18672068	T	C	RS1	Likely Pathogenic	c.1A>G	p.(Met1Val)	NM_000330.4	PSV1_Very Strong, PM2
rs771214648	X	38285819	TTC	T	RPGR	Likely Pathogenic	c.3178_3179del	p.(Glu1060ArgfsTer18)	NM_00103485	PVS1_moderate, PP1_moderate, PM2, PP5
rs1601917999	X	38285893	CCT	C	RPGR	Likely Pathogenic	c.3104_3105del	p.(Glu1035GlyfsTer43)	NM_00103485	PVS1_moderate, PP1_moderate, PM2, PP5
	X	38285906	CT	C	RPGR	Likely Pathogenic	c.3092del	p.(Glu1031GlyfsTer58)	NM_00103485	PVS1_moderate, PP1_moderate, PM2, PP5
	X	38286000	TCC	T	RPGR	Likely Pathogenic	c.2997_2998del	p.(Glu1000GlyfsTer78)	NM_00103485	PVS1_moderate, PP1_moderate, PM2, PP5
NA	X	38286373	C	CT	RPGR	Likely Pathogenic	c.2625dup	p.(Gly876ArgfsTer203)	NM_00103485	PVS1_moderate, PP1_moderate, PM2, PP5
	X	38286562	C	A	RPGR	Likely Pathogenic	c.2437G>T	p.(Glu813Ter)	NM_00103485	PVS1_Strong, PM2
rs398122960	X	38286592	CCT	C	RPGR	Likely Pathogenic	c.2405_2406del	p.(Glu802GlyfsTer32)	NM_00103485	PVS1_strong, PM2, PP5
rs2067187618	X	38286738	TCTCC	T	RPGR	Likely Pathogenic	c.2257_2260del	p.(Gly753LysfsTer61)	NM_00103485	PVS1_strong, PM2, PP5
rs1555961852	X	38286761	TTC	T	RPGR	Likely Pathogenic	c.2236_2237del	p.(Glu746ArgfsTer23)	NM_00103485	PVS1_strong, PM2, PP5
	X	38286845	GC	G	RPGR	Likely Pathogenic	c.2153del	p.(Gly718AlafsTer97)	NM_00103485	PVS1_strong, PM2
	X	38286918	T	TTCTC	RPGR	Likely Pathogenic	c.2073_2080dup	p.(Lys694ArgfsTer6)	NM_00103485	PVS1_strong, PM2, PP5
	X	38286992	C	T	RPGR	Likely Pathogenic	c.2007G>A	p.(Trp669Ter)	NM_00103485	PVS1_Strong, PM2
	X	38286996	TG	T	RPGR	Likely Pathogenic	c.2002del	p.(His668ThrfsTer29)	NM_00103485	PVS1_strong, PM2
rs527236108	X	38287018	C	A	RPGR	Likely Pathogenic	c.1981G>T	p.(Glu661Ter)	NM_00103485	PVS1_strong, PM2
NA	X	38287889	A	AATG	RPGR	Likely Pathogenic	c.1724_1725insGCATG	p.(Ile576HisfsTer13)	NM_000328.3	PVS1, PM2
NA	X	38287892	C	CAT	RPGR	Likely Pathogenic	c.1721_1722insAT	p.(Thr575Ter)	NM_000328.3	PVS1, PM2
NA	X	38287921	G	A	RPGR	Likely Pathogenic	c.1693C>T	p.(Gln565Ter)	NM_000328.3	PVS1, PM2
	X	38287972	C	A	RPGR	Likely Pathogenic	c.1642G>T	p.(Glu548Ter)	NM_000328.3	PVS1, PM2
	X	38290964	G	A	RPGR	Likely Pathogenic	c.1567C>T	p.(Gln523Ter)	NM_000328.3	PVS1, PM2
	X	38290970	G	A	RPGR	Likely Pathogenic	c.1561C>T	p.(Gln521Ter)	NM_000328.3	PVS1, PM2
	X	38298967	G	A	RPGR	Pathogenic	c.1234C>T	p.(Arg412Ter)	NM_000328.3	PVS1, PM2, PP5
	X	38299066	C	A	RPGR	Likely Pathogenic	c.1135G>T	p.(Glu379Ter)	NM_00103485	PVS1, PM2
rs527236109	X	38299113	A	ACTAC	RPGR	Pathogenic	c.1084_1087dup	p.(Val363GlyfsTer15)	NM_00103485	PVS1, PM2, PP5
	X	38299124	A	T	RPGR	Likely Pathogenic	c.1077T>A	p.(Cys359Ter)	NM_000328.3	PVS1, PM2
rs2067498092	X	38301373	T	C	RPGR	Pathogenic	c.935-2A>G		NM_000328.3	PVS1, PM2, PP5
	X	38304635	C	T	RPGR	Likely Pathogenic	c.934G>A	p.(Asp312Asn)	NM_000328.3	PVS1, PM2
rs527236111	X	38304673	TAA	T	RPGR	Likely Pathogenic	c.894_895del	p.(Ser298ArgfsTer47)	NM_00103485	PVS1, PM2
	X	38310765	C	A	RPGR	Likely Pathogenic	c.628G>T	p.(Glu210Ter)	NM_000328.3	PVS1, PM2
rs62638646	X	38318828	C	A	RPGR	Pathogenic	c.469+1G>T		NM_000328.3	PVS1, PM2, PP5
rs1601974881	X	38318907	GAA	G	RPGR	Pathogenic	c.389_390del	p.(Phe130SerfsTer4)	NM_000328.3	PVS1, PM2, PP5
	X	46837128	A	T	RP2	likely pathogenic	c.28A>T	p.K10X	NM_006915	PVS1, PM2

	X	46837187	G	A	RP2	likely pathogenic	c.87G>A	p.W29X	NM_006915	PVS1, PM2
	X	46837203	GTAA	G	RP2	Pathogenic	.		NM_006915	PVS1_Moderate, PM2, PP3
	X	46853573	G	A	RP2	likely pathogenic	c.200G>A	p.C67Y	NM_006915	PS3_Moderate, PM2, PP3
	X	46853589	CT	C	RP2	likely pathogenic	c.216_217delinsC	p.Y73Ifs*18	NM_006915	PVS1, PM2
	X	46853668	A	AG	RP2	likely pathogenic	c.295delinsAG	p.S99Rfs*25	NM_006915	PVS1, PM2
	X	46853725	C	T	RP2	likely pathogenic	c.352C>T	p.R118C	NM_006915	PS1, PM2, PP3, PP5
rs28933687	X	46853726	G	A	RP2	Pathogenic	c.353G>A	p.R118H	NM_006915	PS3_Moderate, PM2, PM5, PP3, PP5
	X	46853753	TC	T	RP2	likely pathogenic	c.380_381delinsT	p.L129Cfs*27	NM_006915	PVS1, PM2
rs1924904597	X	46853782	ATT	—	RP2	likely pathogenic	c.409_411del	p.I137del	NM_006915	PS3_Moderate, PM2, PM4, PP5
	X	46854046	CG	C	RP2	likely pathogenic	c.673_674delinsC	p.G226Vfs*12	NM_006915	PVS1, PM2
	X	46860019	CAAA	C	RP2	likely pathogenic	c.800_804delinsC	p.E269Cfs*3	NM_006915	PVS1, PM2
	X	49209387	GA	G	CACNA1F	Likely pathogenic	c.4860del	p.L1621Cfs*139	NM_005183	PVS1_Verystrong, PM2
rs782740998	X	49211947	G	A	CACNA1F	Pathogenic	c.4084C>T	p.R1362X	NM_005183	PVS1_Verystrong, PM2, PP5
rs1252151297	X	49215479	C	A	CACNA1F	Pathogenic	c.3334G>T	p.E1112X	NM_005183	PVS1_Verystrong, PM2, PS2_supporting
rs122456135	X	49219344	G	A	CACNA1F	Likely pathogenic	c.2683C>T	p.R895X	NM_005183	PVS1_Verystrong, PM2
	X	49223006	TG	T	CACNA1F	Likely pathogenic	c.2040del	p.K681Sfs*28	NM_005183	PVS1_Verystrong, PM2
	X	49230905	T	TAC	CACNA1F	Likely pathogenic	c.465_466insGT	p.S156Vfs*48	NM_005183	PVS1_Verystrong, PM2
	X	49231796	GGTT	G	CACNA1F	Likely pathogenic	c.149_156del	p.R50Pfs*65	NM_005183	PVS1_Verystrong, PM2
	X	85873173	A	G	CHM	Likely Pathogenic	c.1649T>C	p.(Leu550Pro)	NM_000390.4	PM2, PM5_Supporting, PP3, PP5
	X	85878981	A	T	CHM	Likely Pathogenic	c.1593T>A	p.(Tyr531Ter)	NM_000390.4	PVS1, PM2
	X	85894260	C	A	CHM	Likely Pathogenic	c.1438G>T	p.(Glu480Ter)	NM_000390.4	PVS1, PM2
	X	85901099	G	T	CHM	Likely Pathogenic	c.1334C>A	p.(Ser445Ter)	NM_000390.4	PVS1, PM2
	X	85956239	GT	G	CHM	Pathogenic	c.1079delA	p.(Asn360ThrfsTer49)	NM_000390.4	PVS1, PM2, PP5
	X	85956285	G	C	CHM	Likely Pathogenic	c.1034C>G	p.(Ser345Ter)	NM_000390.4	PVS1, PM2
NA	X	85957977	T	A	CHM	Likely Pathogenic	c.820-2A>T		NM_000390.4	PVS1, PM2
rs527236048	X	85958872	G	A	CHM	Pathogenic	c.808C>T	p.(Arg270Ter)	NM_000390.4	PVS1, PM2, PP5
rs886041179	X	85958881	G	A	CHM	Pathogenic	c.799C>T	p.(Arg267Ter)	NM_000390.4	PVS1, PM2, PP5
rs886041178	X	85958923	G	A	CHM	Pathogenic	c.757C>T	p.(Arg253Ter)	NM_000390.4	PVS1, PM2, PP5
rs2147675545	X	85963750	GT	G	CHM	Pathogenic	c.616dupA	p.(Thr206AsnfsTer17)	NM_000390.4	PVS1, PM2, PP5
rs886041177	X	85963840	CCT	C	CHM	Pathogenic	c.525_526del	p.(Glu177LysfsTer6)	NM_000390.4	PVS1, PM2, PP5
rs886041176	X	85964048	CCTG	C	CHM	Pathogenic	c.315_318del	p.(Ser105ArgfsTer20)	NM_000390.4	PVS1, PM2, PP5
rs774941511	X	85978893	T	C	CHM	Pathogenic	c.190-2A>G		NM_000390.4	PVS1, PM2, PP5
NA	X	85981786	C	T	CHM	Pathogenic	c.140G>A	p.(Trp47Ter)	NM_000390.4	PVS1, PM2, PP5